STRESS INDUCED LIPID ENHANCEMENT IN MICROALGAE: *Scenedesmus* sp.

Ph.D. Thesis

By

VISHAL ANAND

DEPARTMENT OF BIOSCIENCES AND BIOMEDICAL ENGINEERING

INDIAN INSTITUTE OF TECHNOLOGY INDORE

MARCH 2021

STRESS INDUCED LIPID ENHANCEMENT IN MICROALGAE: *Scenedesmus* sp.

A THESIS

Submitted in partial fulfillment of the
requirements for the award of the degree
of
DOCTOR OF PHILOSOPHY

by

VISHAL ANAND

DEPARTMENT OF BIOSCIENCES AND BIOMEDICAL ENGINEERING
INDIAN INSTITUTE OF TECHNOLOGY INDORE

MARCH 2021

INDIAN INSTITUTE OF TECHNOLOGY INDORE

CANDIDATE'S DECLARATION

I hereby certify that the work which is being presented in the thesis entitled **STRESS INDUCED LIPID ENHANCEMENT IN MICROALGAE: *Scenedesmus* sp.** in partial fulfillment of the requirements for the award of the degree of **DOCTOR OF PHILOSOPHY** and submitted in the **DEPARTMENT OF BIOSCIENCES AND BIOMEDICAL ENGINEERING, Indian Institute of Technology Indore**, is an authentic record of my own work carried out during the time period from July 2016 to March 2021 under the supervision of Dr. Kiran Bala, Associate professor, IIT Indore.

The matter presented in this thesis has not been submitted by me for the award of any other degree to this or any other institute.

Vishal Anand (16/07/2021)

Signature of the student with date
(Vishal Anand)

This is to certify that the above statement made by the candidate is correct to the best of my knowledge.

July 16, 2021
Signature of Thesis Supervisor with date

(Dr. Kiran Bala)

VISHAL ANAND has successfully given his/her Ph.D. Oral Examination held on July 16, 2021.

Dr SOMADITYA SEN
2021 July 16th

Signature of Chairperson (OEB)
Date:

Signature of External Examiner
Date: 16th July, 2021

Signature(s) of Thesis Supervisor
Date: July 16, 2021

Signature of PSPC Member #1
Date: 16.07.2021

Signature of PSPC Member #2
Date: 16/07/2021

Signature of Convener, DPGC
Date: 16/07/2021

Debasis Nayak
16.07.2021
Signature of Head of Department
Date:

ACKNOWLEDGEMENTS

I would like to thank all who have made a contribution to this project: completing a Ph.D. is not an individual endeavor, but the product of years of work by an unseen team.

Firstly, I would like to express my sincere gratitude to my supervisor Dr. Kiran Bala, who believed in my abilities and gave me the incredible opportunity to work under her supervision. I am extremely grateful to her for all the supports over the past few years and devoting countless time for insightful discussions and suggestions. I am thankful for the motivation and patience that kept me being productive and focused during challenging period.

I am sincerely grateful to my PSPC members Dr. Prashant Kodgire and Dr. Sampak Samanta, who helped me by providing guideline and feedback to focus my work towards Ph.D. thesis. I would also like to thank Head of the Department, Dr. Debasis Nayak, for his suggestions and unwavering supports. I am grateful to all faculty members of BSBE for their direct or indirect supports in my research work. Prof. Neelesh Jain, officiating Director, Indian Institute of Technology Indore, has been a constant source of motivation, assistance, and support to me in every way.

I would like to thank Ministry of Education, Government of India, New Delhi, for providing financial support to do research work.

I am also thankful to all the staff members of BSBE who directly or indirectly provided support to carry out my research work. Specifically, my sincere regards to Mr. Gaurav Singh, Mr. Murphy Bhaskar Ganveer, and Mr. Arif Patel for their assistance and support.

I would like to acknowledge sophisticated instrumentation centre (SIC), IIT Indore for providing access to instruments for measurements and

sample analysis. I would also like to express my gratitude to whole IITI community for their continuous assistance and support.

I would like to also thank to all my dear friends (Mr. Deshmukh Suchit Ashokrao, Mr. Mrinal Kashyap, Ms. Atreyee Ghosh, Mr. Arjun Meda, Ms. Kanchan Samadhiya, Ms. Rimjhim Sangtani, Ms. Palak Saket, Mr. Rahul Chouhan) in Algal EcoTechnology & Sustainability Group, IIT Indore and all the friends from around the world who have joined me along this journey inside and outside the academic world. Special thanks to my IIT friends: Mr. Ankit Jaiswal, Mr. Anubhav Tamrakar, Mr. Pranav, and Mr. Rajarshi Roy for sharing the greatest memories in Indore, for the smiles and comforting words during the course of my Ph.D.

Last but not least, my deepest love and gratitude is for my father Late Sri Birender Kumar and my mother Ms. Rita Sinha whom I owe absolutely everything: thanks for your infinite love and support, hard work, and sacrifices. Thanks to my beloved siblings Dr. Vikash Anand, Dr. Chetna Sinha, Dr. Dhirendra Sinha, Ms. Vandana Sinha, Mr. Prashant Sinha, Ms. Archana Sinha, for being my motivation and unconditional love. I would like to acknowledge Navish Anand Sinha, Vihaan Sinha, Akshara Sinha, Dhriti Sinha for their unconditional love. Thank you all for your love and blessings.

VISHAL ANAND

DEDICATION

THIS THESIS IS DEDICATED TO MY FATHER

SYNOPSIS

Introduction:

Microalgae are the photosynthetic autotrophs that can survive in fresh as well as marine water. These photosynthetic organisms can be eukaryotic or prokaryotic (cyanobacteria) (Li et al., 2008). It is believed that approx. 50,000 species have been explored till-date which can survive in diverse environmental conditions (Richmond, 2004), confirming enormous diversity within the group. These organisms can capture sunlight and convert the solar energy into efficacious products such as lipids (glycerophospholipids and triacylglycerols), carbohydrates, proteins, etc. These are also defined as oleaginous microorganisms due to their lipid accumulation potential, which is almost 15-20% higher as compared land based oleaginous crops (Aratboni et al., 2019). Their lipid content under various environmental perturbations such as salinity, pH, light, and nutrients, can be increased upto 70% of algal dry cell weight (DCW) (Fan et al., 2014; Donot et al., 2014). Because of their speedy growth rate, high CO_2 fixation rate, no competition for arable land, and less impact on freshwater resources, these can cement their position in the run of a suitable candidate to produce renewable energy and can be considered as a sustainable feedstock for energy demands.

Moreover, the algal cultivation is not restricted to any climatic, seasonal or geographical variation and can be cultivated even in wastewater or saline water (Ochsenreitheri et al., 2016). Despite being a good storehouse of lipids, mass production of algal biodiesel is bounded because of high production cost, low yield of lipids, and lack of efficient harvesting and extraction steps (Zhao et al., 2019). Therefore, to make algal biodiesel commercially applicable and economically viable, it is indeed imperative to optimize certain crucial factors pertaining to algal lipid accumulation (Ruiz et al., 2016).

In the recent decade, multiple studies have reported various strategies and approaches to incite lipid biosynthesis in microalgae cells. These

strategies include harmonizing light intensity in cultures, CO_2 concentration and temperature, coaxing nutrient starvation in the culture, implementing stress via potentially toxic metals or high salinity condition or peroxide addition. Also, the ongoing research have however provided a track advancing towards lipid accumulation but the specificity related with the strength of strain assortment and familiarization with the site-specific and other culture conditions often makes the process inappropriate specific to a location.

In the current study, to understand the impact of chronic/acute stress factors such as salinity, nutrients, and hydrogen peroxide on *Scenedesmus* sp., the work was divided into two parts: (1) long-term study and (2) short-term study. The growth profile, pigment content, biomolecular transitions, biochemical composition, and fatty acid methyl ester profile are some of the important parameters evaluated to monitor the impact of strong and mild agents.

Objectives:

A. Long term:

1. **To monitor the impacts of different salts at varying concentrations on growth profile and biochemical composition of *Scenedesmus* sp.**
2. **To study the effect of sodium chloride under nutrients replete/deplete conditions**

B. Short term:

3. **To understand algal behavior in two stage approach with hydrogen peroxide under nitrate and phosphate variations**
4. **Multicomponent exposure – To monitor the impact of hydrogen peroxide, sodium chloride, nitrate and phosphate**

The thesis consists of seven chapters, which include a general introduction of microalgae, algal lipids, and biofuels derived from microalgae, followed by the implementation of different strategies for enhancement of lipids accumulated in the *Scenedesmus* sp. such as

exposure to different salts, nitrate, phosphate, and hydrogen peroxide. Further, several biochemical and instrumental analyses were performed to validate and confirm the lipid accumulation potential of *Scenedesmus* sp.

Thesis chapters contribution:

In **Chapter 1** (General Introduction), the basics of algae, algae-derived lipids, types of biofuels produced, and different strategies employed for lipid enhancement has been discussed. The recent advances in the area of lipid enhancement have also been included, which elaborates the study's current scenario, followed an insight into the fatty acid methyl ester profiling and its relevance towards fuel properties.

In **Chapter 2**, the overall experimental approach and different methods/protocols employed for estimating growth profile, biochemical composition, and fatty acid methyl esters (FAME) are described briefly. In addition to quantitative analysis, the qualitative analysis is further described: primarily the biomolecular transition analysis (FTIR) and confocal microscopy. The analysis of stress biomarkers to identify stress tolerance capacity of *Scenedesmus* sp. was also discussed briefly. The variables and ranges followed in this thesis are represented as follows:

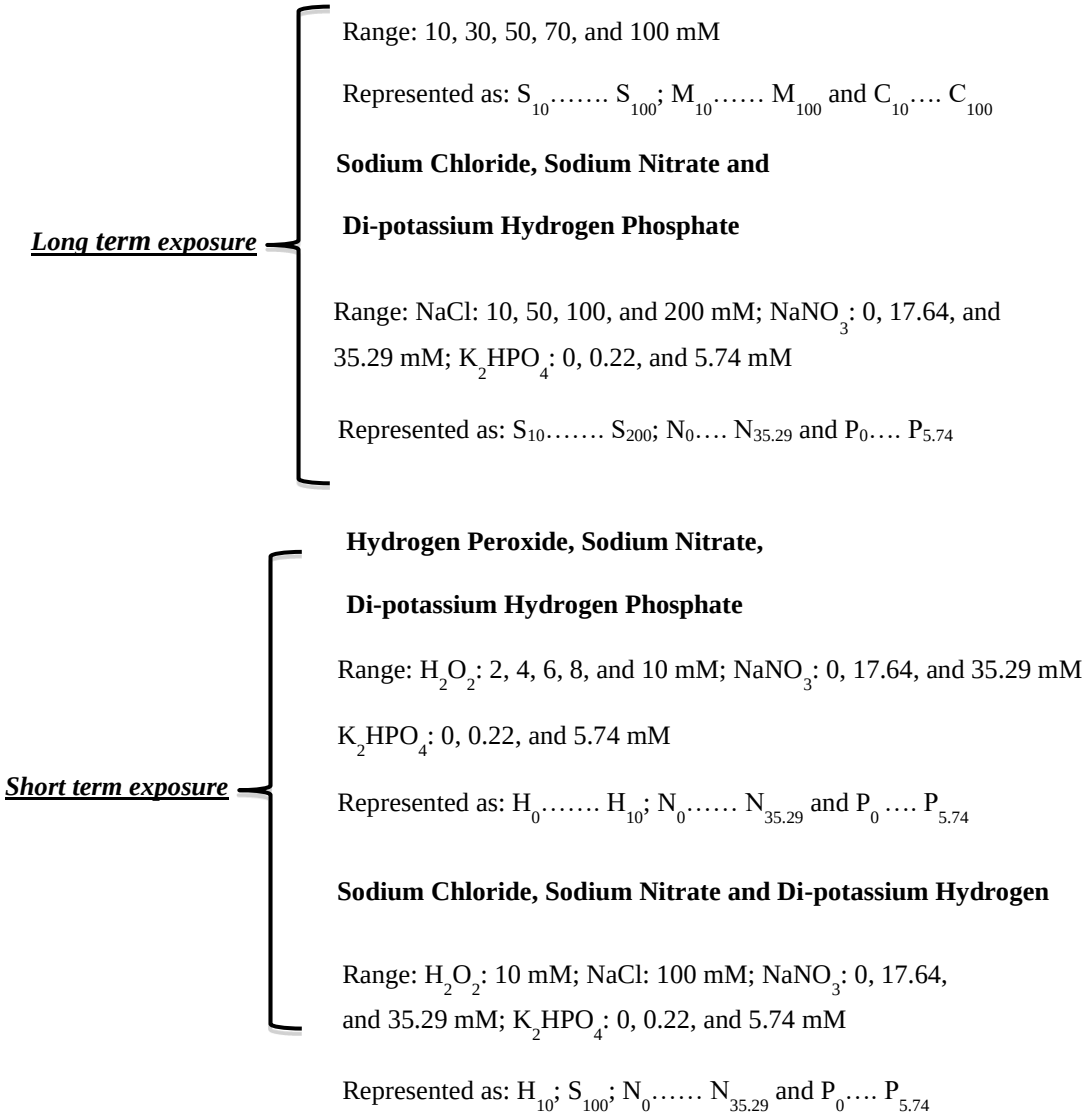

In **Chapter 3**, we report the impact of varying concentrations of different salts such as sodium chloride, magnesium chloride and calcium chloride (represented with codes as S, M and C, respectively) on growth as well as biochemical profile of *Scenedesmus* sp. studied at different time periods (5, 10 and 15 days). At 100 mM (Table 1) salt exposure on 15th day, higher biomass and chlorophyll content was observed for NaCl as compared to $CaCl_2$ and $MgCl_2$. Additionally, maximum lipid content (Table 1) was observed to be accumulated at NaCl (100 mM) supplementation. Moreover, the important fatty acids (oleic, palmitic, stearic, linolenic, and linoleic acid) influencing the biodiesel properties were the major constituents of fatty acid methyl ester profiling done through gas chromatography, which was utilized further for computation of various fuel properties such as cetane

number (CN), iodine value (IV), saponification value (SV) etc. Stress biomarker analysis, confocal microscopy, scanning electron microscopy, and FTIR also validated the lipid accumulation in *Scenedesmus* sp. The variance and statistical relationship between different variables under all the treatments were analyzed by principal component analysis (PCA). Conclusively, 100 mM NaCl was observed to perform well for the accumulation of lipids without much compromising the biomass.

Table 1. Impact on algal profile under different salts treatment at varying concentrations.

Salt (mM)	Biomass Concentration (µg/mL)	Lipid Content (%)	Chlorophyll Concentration (µg/mL)
$\mathbf{S_{10}}$	1076.3±27.9	10.5±0.6	20.5±1.3
$\mathbf{S_{30}}$	1043.8±13.0	10.2±0.5	17.3±0.3
$\mathbf{S_{50}}$	998.7±25.2	13.0±0.2	15.7±0.3
$\mathbf{S_{70}}$	973.9±12.7	15.9±0.6	14.5±0.2
$\mathbf{S_{100}}$	804.3±39.5	19.7±0.4	13.7±0.6
$\mathbf{M_{10}}$	725.0±32.8	12.4±0.8	15.4±0.9
$\mathbf{M_{30}}$	653.0±60.9	12.7±0.3	12.5±0.4
$\mathbf{M_{50}}$	581.1±20.7	10.3±0.4	9.8±0.4
$\mathbf{M_{70}}$	508.7±21.2	18.2±0.3	9.3±0.5
$\mathbf{M_{100}}$	485.3±13.6	17.9±1.9	8.8±0.2
$\mathbf{C_{10}}$	924.3±13.2	7.3±0.2	17.0±0.5
$\mathbf{C_{30}}$	768.6±24.0	9.6±0.1	16.2±0.3
$\mathbf{C_{50}}$	731.7±11.3	11.9±0.2	14.3±0.7
$\mathbf{C_{70}}$	652.6±8.2	10.9±0.7	12.7±0.2
$\mathbf{C_{100}}$	598.0±11.8	13.4±0.8	11.8±0.1

In **Chapter 4**, along with the exposure of salt stress in varying concentrations, the impact of different concentrations of critical nutrients such as nitrate and phosphate on the lipid accumulation potential of *Scenedesmus* sp. was analyzed. Table 2 represent the algal behavior observed at varying sodium chloride under nutrients. It was observed that at $N_{17.64}P_{0.22}$ and $N_{17.64}P_{5.74}$, biomass decreased with

increasing salt exposure; however, at $N_{35.29}P_{0.22}$ and $N_{17.64}P_0$, biomass increases till S_{50} and thereby decreases afterward.

Table 2. Effect on algal profile at sodium chloride under replete/ deplete nutrients condition

Combination	Biomass concentration (µg/mL)	Lipid Content (%)	Chlorophyll concentration (µg/mL)
$S_0N_0P_0$	545.7±5.4	20.3±0.7	5.7±0.2
$S_{100}N_0P_0$	727.4±21.7	19.1±0.4	4.3±0.1
$S_{10}N_{17.64}P_{0.22}$	792.3±6.1	7.6±1.3	9.6±0.2
$S_{50}N_{17.64}P_{0.22}$	791.5±9.5	7.3±0.7	8.7±0.2
$S_{100}N_{17.64}P_{0.22}$	704.7±24.2	9.0±0.6	8.2±0.1
$S_{200}N_{17.64}P_{0.22}$	631.0±10.6	8.5±0.8	8.1±0.0
$S_0N_0P_{0.22}$	397.7±8.8	25.3±2.4	5.7±0.0
$S_{10}N_0P_{0.22}$	426.1±5.3	14.7±1.1	5.6±0.1
$S_{50}N_0P_{0.22}$	522.6±24.2	17.7±0.6	6.3±0.1
$S_{100}N_0P_{0.22}$	537.0±22.3	38.5±3.4	6.2±0.1
$S_{200}N_0P_{0.22}$	489.4±8.8	35.6±1.6	4.8±0.1
$S_0N_{35.29}P_{0.22}$	706.9±3.3	6.6±1.5	9.5±0.1
$S_{10}N_{35.29}P_{0.22}$	714.0±19.7	6.7±0.9	8.4±0.1
$S_{50}N_{35.29}P_{0.22}$	751.2±13.5	5.7±0.2	6.6±0.2
$S_{100}N_{35.29}P_{0.22}$	614.7±29.9	9.0±0.8	5.1±0.1
$S_{200}N_{35.29}P_{0.22}$	558.3±11.2	8.5±0.8	5.1±0.1
$S_0N_{17.64}P_0$	516.8±17.1	10.8±0.2	8.3±0.0
$S_{10}N_{17.64}P_0$	630.8±11.0	8.2±1.5	7.1±0.1
$S_{50}N_{17.64}P_0$	714.2±12.9	9.0±1.2	7.4±0.1
$S_{100}N_{17.64}P_0$	635.9±15.0	12.9±1.3	7.8±0.0
$S_{200}N_{17.64}P_0$	595.3±6.2	9.9±1.3	6.1±0.1
$S_0N_{17.64}P_{5.74}$	663.5±13.4	8.0±0.9	7.0±0.1
$S_{10}N_{17.64}P_{5.74}$	581.5±10.6	10.5±0.8	6.5±0.1
$S_{50}N_{17.64}P_{5.74}$	568.2±30.8	8.6±0.8	6.3±0.1
$S_{100}N_{17.64}P_{5.74}$	569.3±22.4	6.3±0.3	7.3±0.1
$S_{200}N_{17.64}P_{5.74}$	468.9±37.4	11.0±1.3	6.2±0.1

$S_{100}N_0P_{0.22}$ was determined to accumulate maximum total lipids as compared to other variables and concentrations studied. C18:0 and C18:1 fatty acid was also observed higher for $S_{100}N_0P_{0.22}$, and the

presence of stress was validated through ROS accumulation. In the present study, it was also observed that the cumulative effect of sodium chloride and phosphate in the absence of nitrate leads to the accumulation of twice the amount of lipid compared to the independent effect of sodium chloride obtained from the previous chapter.

In **Chapter 5,** the short-term stress exposure to Hydrogen peroxide (Table 3) was studied along with the nutrients owing to the fact that H_2O_2 has substantial impact on algal cell growth, and its long-term exposure leads to cell deterioration. *Scenedesmus* sp. subjected to synergized varying nitrate and phosphate concentrations (N_0P_0, $N_{17.64}P_{0.22}$, $N_0P_{0.22}$, $N_{35.29}P_{0.22}$, $N_{17.64}P_0$, and $N_{17.64}P_{5.74}$) for 48 hours in first stage (Fig. 1) along with the induction of different H_2O_2 concentrations for 24 hours in second stage, exhibited decrease in biomass and chlorophyll content with increase in H_2O_2 concentrations (0 mM, 2 mM, 4 mM, 6 mM, 8 mM, and 10 mM). Under this multicomponent variation of hydrogen peroxide, nitrate and phosphate, lipid accumulation was found to be highest in the algal cells cultivated in $H_{10}N_0P_{0.22}$ conditions. It was also observed that in the nitrate and phosphate deprived media, without the induction of H_2O_2, algal cells accumulated more lipid content as compared to algal cells grown in H_2O_2 (10 mM) induced media.

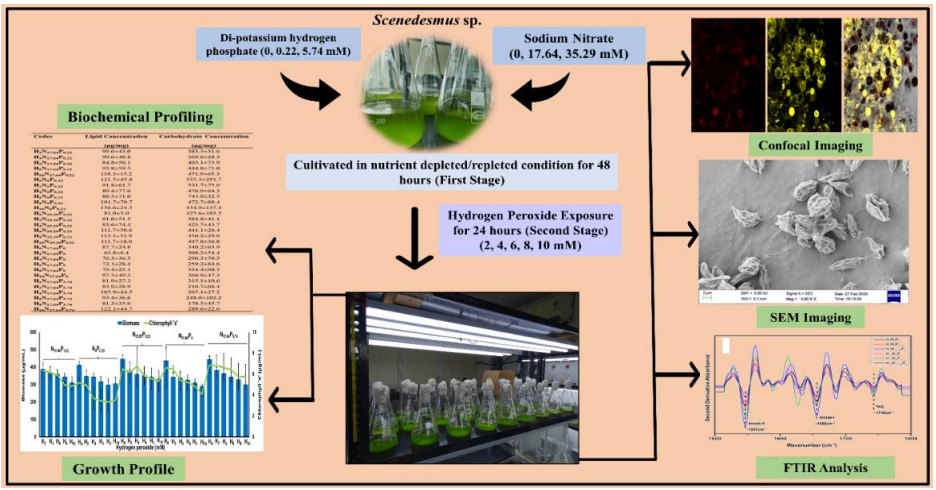

Figure 1. Impact of nutrients variation in first stage (48hrs) and addition of hydrogen peroxide in second stage (24hrs).

Table 3. Algal profile in two stage approach with hydrogen peroxide under nitrate and phosphate variation

Combination	Biomass concentration (µg/mL)	Lipid Content (%)	Chlorophyll concentration (µg/mL)
$H_0N_0P_0$	329.9±29.9	14.5±3.3	5.1±0.6
$H_{10}N_0P_0$	286.9±12.0	13.9±3.8	2.9±0.0
$H_0N_0P_{0.22}$	412.6±18.2	12.1±4.5	5.1±0.4
$H_2N_0P_{0.22}$	347.7±31.9	9.1±6.1	4.9±0.5
$H_4N_0P_{0.22}$	345.7±19.6	8.9±7.7	3.6±1.0
$H_6N_0P_{0.22}$	317.5±28.2	8.6±7.1	3.4±1.0
$H_8N_0P_{0.22}$	297.8±36.0	10.1±7.0	3.3±0.9
$H_{10}N_0P_{0.22}$	305.5±38.3	15.6±2.4	3.4±0.1
$H_2N_{17.64}P_{0.22}$	388.9±24.8	9.9±4.3	6.3±0.7
$H_4N_{17.64}P_{0.22}$	368.9±33.7	9.9±4.0	6.1±0.5
$H_6N_{17.64}P_{0.22}$	361.8±25.0	8.4±5.6	5.9±0.3
$H_8N_{17.64}P_{0.22}$	346.0±20.1	9.3±5.9	4.9±0.3
$H_{10}N_{17.64}P_{0.22}$	310.7±31.4	11.8±1.5	4.8±0.4
$H_0N_{35.29}P_{0.22}$	447.2±22.4	8.1±0.5	6.4±0.7
$H_2N_{35.29}P_{0.22}$	379.8±9.9	9.1±5.1	6.1±0.9
$H_4N_{35.29}P_{0.22}$	359.3±5.0	8.3±7.4	6.7±1.8
$H_6N_{35.29}P_{0.22}$	353.4±7.3	11.1±5.0	5.8±0.8
$H_8N_{35.29}P_{0.22}$	343.6±4.2	11.3±5.1	5.5±1.0
$H_{10}N_{35.29}P_{0.22}$	331.8±9.9	11.1±1.8	5.3±0.9
$H_0N_{17.64}P_0$	438.0±66.9	8.7±2.4	6.6±1.9
$H_2N_{17.64}P_0$	343.5±21.3	6.1±0.6	6.4±0.2
$H_4N_{17.64}P_0$	339.0±28.9	7.6±3.6	5.4±0.8
$H_6N_{17.64}P_0$	327.1±12.7	7.2±2.8	5.2±0.7
$H_8N_{17.64}P_0$	309.8±21.5	7.9±2.5	4.8±0.5
$H_{10}N_{17.64}P_0$	291.5±7.6	9.7±4.9	4.0±0.1
$H_0N_{17.64}P_{5.74}$	444.6±21.2	8.1±2.7	6.8±0.7
$H_2N_{17.64}P_{5.74}$	383.4±13.2	8.3±2.8	6.8±0.9
$H_4N_{17.64}P_{5.74}$	364.8±26.1	10.5±4.4	6.6±1.3
$H_6N_{17.64}P_{5.74}$	345.9±25.1	9.3±3.6	6.4±1.1
$H_8N_{17.64}P_{5.74}$	329.2±12.9	8.1±3.5	5.7±1.2
$H_{10}N_{17.64}P_{5.74}$	300.4±52.5	12.2±4.4	5.7±1.2

In **Chapter 6**, to investigate further in two stage process, the cumulative effect of sodium chloride, hydrogen peroxide along with variable levels of nitrate and phosphate is studied on lipid accumulation (Table 4) potential of *Scenedesmus* sp. It was observed that the presence of 10 mM H_2O_2 at all the sodium chloride-nitrate-phosphate combinations, as well as that of 100 mM NaCl at all hydrogen peroxide-nitrate-phosphate combinations, exhibited decrease in biomass and chlorophyll content as compared to the media deprived of H_2O_2 and NaCl. The highest lipid content (Table 4) was observed in $S_{100}H_{10}N_{35.29}P_{5.74}$. It was also observed that when *Scenedesmus* sp. was cultivated in media composed of 10 mM H_2O_2 at all SNP combinations as well as in the presence of 100 mM NaCl at all HNP combinations exhibited high lipid accumulation as compared to algal cells cultivated in the media deprived of H_2O_2 and NaCl. The accumulation of C20:0 fatty acid was increased exceptionally when the algal cells were subjected to short term stress exposure as compared to the long-term stress exposure. In a nutshell, the presence of H_2O_2 or that of NaCl tends to produce considerable amount of stress onto the algal cells, leading to the accumulation of high FAME content. The importance of the presence of nitrate in comparison to that of phosphate can also be summarized from the results obtained.

In summary, *Scenedesmus* sp. was subjected to various stress players in the chronological order of the experiments performed, the combinations in Tables 5 and 6 were determined to perform well and accumulate a considerable amount of lipids without much compromising the biomass. It can be concluded from the results obtained that the presence of mild as well as potent inducing agents, such as NaCl and H_2O_2, contribute significantly to the accumulation of lipids. Additionally, the significance of the absence of nitrate for the accumulation of algal lipids can also be summarized.

Table 4. Multi-component exposure: Sodium chloride, Hydrogen peroxide, nitrate, and phosphate

Combination	Biomass concentration (µg/mL)	Lipid Content (%)	Chlorophyll concentration (µg/mL)
$S_0H_{10}N_{17.64}P_{0.22}$	310.7±31.4	11.8±1.5	3.7±0.7
$S_0H_0N_0P_{0.22}$	412.6±18.2	12.1±4.5	5.1±0.4
$S_0H_{10}N_0P_{0.22}$	305.5±38.3	15.6±2.4	3.4±0.1
$S_0H_0N_{35.29}P_{0.22}$	447.2±22.4	8.1±0.5	6.4±0.7
$S_0H_{10}N_{35.29}P_{0.22}$	331.8±9.9	11.1±1.8	5.3±0.9
$S_0H_0N_{17.64}P_0$	438.0±66.9	8.7±2.4	6.6±1.9
$S_0H_{10}N_{17.64}P_0$	296.9±11.2	9.7±4.9	4.0±0.1
$S_0H_0N_0P_0$	329.9±29.9	14.5±3.3	5.1±0.6
$S_0H_{10}N_0P_0$	286.9±12.0	13.9±3.8	2.9±0.0
$S_0H_0N_{35.29}P_0$	449.5±4.1	10.4±0.8	4.2±0.1
$S_0H_{10}N_{35.29}P_0$	291.5±7.6	17.1±1.7	3.1±0.1
$S_0H_0N_{17.64}P_{5.74}$	444.6±21.2	8.1±2.7	6.8±0.7
$S_0H_{10}N_{17.64}P_{5.74}$	300.4±52.5	12.2±4.4	5.7±1.2
$S_0H_0N_0P_{5.74}$	451.0±3.0	13.9±0.6	4.6±0.3
$S_0H_{10}N_0P_{5.74}$	318.2±2.5	17.0±1.1	4.1±0.2
$S_0H_0N_{35.29}P_{5.74}$	411.9±5.9	11.1±0.7	2.7±0.5
$S_0H_{10}N_{35.29}P_{5.74}$	263.7±4.0	20.3±2.2	2.6±0.3
$S_{100}H_0N_{17.64}P_{0.22}$	419.1±2.4	11.4±2.8	3.6±0.3
$S_{100}H_{10}N_{17.64}P_{0.22}$	280.4±16.1	16.5±2.2	3.4±0.2
$S_{100}H_0N_0P_{0.22}$	390.8±8.0	15.5±1.6	3.7±0.1
$S_{100}H_{10}N_0P_{0.22}$	320.2±4.9	19.2±1.1	2.6±0.2
$S_{100}H_0N_{35.29}P_{0.22}$	402.1±5.1	12.0±0.8	2.4±0.2
$S_{100}H_{10}N_{35.29}P_{0.22}$	318.5±2.9	12.9±1.4	2.2±0.1
$S_{100}H_0N_{17.64}P_0$	384.9±2.4	14.0±2.8	3.3±0.1
$S_{100}H_{10}N_{17.64}P_0$	288.5±4.9	16.5±2.2	2.1±0.1
$S_{100}H_0N_0P_0$	321.1±6.4	14.4±1.6	3.0±0.1
$S_{100}H_{10}N_0P_0$	278.1±8.0	20.7±1.1	2.0±0.1
$S_{100}H_0N_{35.29}P_0$	437.3±10.6	10.8±0.8	3.2±0.1
$S_{100}H_{10}N_{35.29}P_0$	316.7±3.1	14.0±1.1	2.2±0.1
$S_{100}H_0N_{17.64}P_{5.74}$	365.5±4.2	18.0±2.1	2.9±0.2
$S_{100}H_{10}N_{17.64}P_{5.74}$	256.3±3.1	22.2±1.3	2.4±0.3
$S_{100}H_0N_0P_{5.74}$	326.8±7.7	16.6±1.1	3.1±0.1
$S_{100}H_{10}N_0P_{5.74}$	289.4±2.8	21.3±0.4	2.4±0.3
$S_{100}H_0N_{35.29}P_{5.74}$	298.6±2.5	16.9±1.1	3.2±0.1
$S_{100}H_{10}N_{35.29}P_{5.74}$	254.6±2.6	22.6±1.6	2.7±0.1

Table 5. Summary-Long term exposure

Combination	Biomass Concentration (µg/mL)	Lipid Content (%)
$S_{100}N_{17.64}P_{0.22}$	804.3±39.5	18.4±0.4
$S_{100}N_{0}P_{0.22}$	537.0±22.3	38.5±3.4

Table 6. Summary-Short term exposure

Combination	Biomass Concentration (µg/mL)	Lipid Content (%)
$S_{0}H_{10}N_{0}P_{0.22}$	305.5±38.3	15.6±2.4
$S_{100}H_{10}N_{0}P_{0.22}$	320.2±4.9	19.2±1.1
$S_{100}H_{10}N_{35.29}P_{5.74}$	254.6±2.6	22.6±1.6

Conclusions:

- After long term exposure, the total lipid content increased upto 18.4 and 38.5% at $S_{100}N_{17.64}P_{0.22}$ and $S_{100}N_{0}P_{0.22,}$ along with biomass accumulation of 804.3 and 537 µg/mL, respectively.
- After short term exposure, the total lipid content increased upto 15.6, 19.2 and 22.6% at $S_{0}H_{10}N_{0}P_{0.22,}$ $S_{100}H_{10}N_{0}P_{0.22,}$ and $S_{100}H_{10}N_{35.29}P_{5.74}$ along with biomass accumulation of 305, 320, and 254 µg/mL, respectively.

It is concluded that, after long-term exposure to varying salts, NaCl at 100 mM ($S_{100}N_{17.64}P_{0.22}$) significantly enhanced lipid content which is further enhanced ($S_{100}N_{0}P_{0.22}$) at 100 mM NaCl in the absence of nitrate (N_0) with optimal phosphate ($P_{0.22}$) concentration. However, under short-term exposure increase in lipid accumulation was monitored but less than long term exposure. Therefore, all the strategies adopted to enhance the lipid accumulation in the algal cells acknowledge the appreciable potential of *Scenedesmus* sp., which needs to be explored and exploited further for sustainable large-scale lipid production.

References

Aratboni, H. A., Rafiei, N., Garcia-Granados, R., Alemzadeh, A., & Morones-Ramírez, J. R. (2019). Biomass and lipid induction strategies in microalgae for biofuel production and other applications. Microbial Cell Factories, 18(1), 1-17.

Bellou, S., Triantaphyllidou, I. E., Aggeli, D., Elazzazy, A. M., Baeshen, M. N., & Aggelis, G. (2016). Microbial oils as food additives: recent approaches for improving microbial oil production and its polyunsaturated fatty acid content. Current Opinion in Biotechnology, 37, 24-35.

Ratledge, C. (2015). Single cell oils for the 21st century. Single Cell Oils: Microbial and Algal Oils, 3.

Fan, J., Cui, Y., Wan, M., Wang, W., & Li, Y. (2014). Lipid accumulation and biosynthesis genes response of the oleaginous *Chlorella pyrenoidosa* under three nutrition stressors. Biotechnology for Biofuels, 7(1), 1-14.

Ji, X. J., Ren, L. J., Nie, Z. K., Huang, H., & Ouyang, P. K. (2014). Fungal arachidonic acid-rich oil: research, development and industrialization. Critical Reviews in Biotechnology, 34(3), 197-214.

Li, Y., Horsman, M., Wu, N., Lan, C. Q., & Dubois-Calero, N. (2008). Biofuels from microalgae. Biotechnology Progress, 24(4), 815-820.

Ochsenreither, K., Glück, C., Stressler, T., Fischer, L., & Syldatk, C. (2016). Production strategies and applications of microbial single cell oils. Frontiers in Microbiology, 7, 1539.

Richmond, A. (Ed.). (2004). Handbook of microalgal culture: biotechnology and applied phycology (Vol. 577). Oxford: Blackwell Science.

Ruiz, J., Olivieri, G., De Vree, J., Bosma, R., Willems, P., Reith, J. H., ... & Barbosa, M. J. (2016). Towards industrial products from microalgae. Energy & Environmental Science, 9(10), 3036-3043.

Xie, D., Jackson, E. N., & Zhu, Q. (2015). Sustainable source of omega-3 eicosapentaenoic acid from metabolically engineered *Yarrowialipolytica*: from fundamental research to commercial production. Applied Microbiology and Biotechnology, 99(4), 1599-1610.

Zhao, Y., Wang, H. P., Han, B., & Yu, X. (2019). Coupling of abiotic stresses and phytohormones for the production of lipids and high-value by-products by microalgae: A review. Bioresource Technology, 274, 549-556.

LIST OF PUBLICATIONS

(A) Publications from Ph.D. thesis

1. **Anand, V**., Kashyap, M., Sharma, M. P., & Bala, K. (2021). Impact of hydrogen peroxide on microalgae cultivated in varying salt-nitrate-phosphate conditions. Journal of Environmental Chemical Engineering, 105814. (IF: 5.9)
2. **Anand, V**., Kashyap, M., Ghosh, A., Samadhiya, K., & Kiran, B. (2021). A strategy for lipid production in *Scenedesmus* sp. by multiple stresses induction. Biomass Conversion and Biorefinery, 1-11. (IF: 4.9)
3. **Anand, V**., Kashyap, M., Ghosh, A., & Kiran, B. (2020) Spectroscopic insights exploring triacylglyceride accumulation in *Scenedesmus* sp. via biomolecular transitions. Bioresource Technology Report, 12, 100593. (Elsevier)
4. **Anand, V**., Kashyap, M., Samadhiya, K., Ghosh, A., & Kiran, B. (2019). Salinity driven stress to enhance lipid production in *Scenedesmus vacuolatus*: A biodiesel trigger? Biomass and Bioenergy, 127, 105252. (IF: 5.0)
5. **Anand, V**., Kashyap, M., Samadhiya, K., & Kiran, B. (2019). Strategies to unlock lipid production improvement in algae. International Journal of Environmental Science and Technology, 16(3), 1829-1838. (IF: 2.8)
6. **Anand, V**., Kashyap, M., Ghosh, A., & Kiran, B. Multiple stress inducers to impact algae biodiesel properties: Effect of Hydrogen peroxide exposure under nutrients depleted/repleted conditions. (Submitted: Environmental Science and Pollution Research)

(B) Publications apart from thesis

1. Kashyap, M., Samadhiya, K., Ghosh, A., **Anand, V**., Lee, H., Sawamoto, N., ... & Bala, K. (2021). Synthesis, characterization and application of intracellular Ag/AgCl nanohybrids biosynthesized in *Scenedesmus* sp. as neutral lipid inducer and antibacterial agent. Environmental Research, 201, 111499. (IF: 6.4)
2. Kashyap, M., **Anand, V**., Ghosh, A., & Kiran, B. (2021). Superintending *Scenedesmus* and *Chlorella* sp. with lead and cobalt tolerance governed via stress biomarkers. Water Supply. (IF: 0.9)
3. Ghosh, A., Sangtani, R., **Anand, V**., Kashyap, M., & Kiran, B. (2021). Synergistic dynamics of critical cofactors effectuates fuel relevant metabolic profile of *Scenedesmus* sp.: Targeting cleaner energy production. Journal of Cleaner Production, 297, 126640. (IF: 9.2)
4. Ghosh, A., Samadhiya, K., Kashyap, M., **Anand, V.**, Sangwan, P., & Kiran, B. Response surface optimization of nutrients for improved FAME profile in *Scenedesmus vacuolatus*. Environmental Science and Pollution Research. pp 1-13. (IF: 4.2)
5. Kashyap, M., Samadhiya, K., Ghosh, A., **Anand, V.**, Shirage, P.M., & Kiran, B. Screening of microalgae for biosynthesis and optimization of Ag/AgCl nano hybrids having antibacterial effect. RSC Advances, 2019, 9-25583-25591. (IF: 3.3)
6. Samadhiya, K., Ghosh, A., Kashyap, M., **Anand, V.**, & Kiran, B. Bioprospecting of native algal strains with unique lipids, proteins and carbohydrates signatures: A Time dependent study. (Journal Environmental Progress & Sustainable Energy: Under Review).

TABLE OF CONTENT

LIST OF FIGURES

LIST OF TABLES

NOMENCALTURE

EPA	Eicosapentaenoic acid
PUFA	Polyunsaturated fatty acid
PI	Photosynthesis-irradiance
PBR	Photobioreactors
TAGs	Triacylglycerides
FAME	Fatty acid methyl ester
FA	Fatty acid
ACCase	Acetyl-CoA carboxylase
NADPH	Nicotinamide adenine dinucleotide phosphate
TCA	Tricarboxylic acid cycle
SPV	Sulpho-phospho-vanillin
OD	Optical density
DCW	Dry cell weight
SFA	Saturated fatty acid
NCIM	National Collection of Industrial Microorganisms
NCL	National Chemical Laboratory
BG-11	Blue Green-11 media
ROS	Reactive oxygen species
SOD	Superoxide dismutase
CAT	Catalase
APX	Ascorbate peroxidase
GPX	Glutathione peroxidase

APX	Ascorbate peroxidase
TCA	Tricarboxylic acid
IV	Iodine value
CN	Cetane number
SV	Saponification value
DUm	Degree of unsaturation
SCSF	Straight-chain saturation factor
PCA	Principal component analysis

ACRONYMS

GC-FID	Gas Chromatography-Flame ionization detector
FTIR	Fourier-transform infrared spectroscopy
SEM	Scanning electron microscope
UV-Vis	Ultraviolet visible spectroscopy

CHAPTER 1

Chapter 1

1 Introduction

1.1 Microalgae

Microalgae are multicellular or unicellular photosynthetic organisms that can live in various environments (Chisti, 2007; Ogburn and Vogt, 2017). The microalgae scale ranges from a few micrometres (µm) to a few hundred micrometres (µm). They are found in various diverse forms such as clusters or chains; and also occur in filamentous forms. These different forms of algae mainly depend on species and habitats (Abomohra et al., 2017; Moreno-Garrido, 2008). Microalgae are thallophytes, which means they are non-vascular plants and, unlike terrestrial plants, lack leaves, roots, and stems. Like terrestrial plants, they also have chlorophyll as the primary photosynthetic pigment (Vonshak and Maske, 1982). In addition to chlorophyll, accessory pigments like carotenoids, phycobilins etc. are also found in these species. Algae are a rich source of lipids/oils and carbohydrates, which enable these species to be suitable contender for the fabrication of renewable energy sources.

1.2 Classification of microalgae

Microalgae are categorised into the following classifications which is based on their abundance (i) Diatoms (Bacillariophyceae), (ii) Green algae (Chlorophyceae), (iii) Golden-Brown Algae, (iv) Prymnesiophytes, (v) Eustigmatophytes, (vi) Cyanobacteria (Cyanophyceae).

(i) Diatoms: Diatoms, the most familiar algal species, include about thousands of known species occurring in both fresh and salty water (phytoplanktons) (Sheehan et al., 1998). Diatoms are found on a solid surface. Fucoxanthin and β-carotene are the most common pigments present in diatoms, which covers chlorophyll ‘a’ and chlorophyll ‘c’ pigments, making diatoms golden-brown in color apparency. Centrals

and Pennates, are the primary group of diatoms being identified by radial and bilateral symmetry (Tomaselli, 2004). Cell wall of these species are primarily comprised of lipids, chrysolaminarin (β-1, 3) and polymerized silicate (Sheehan et al., 1998).

(ii) Green Algae: This is the prevalent consortium of algae. Around 8000, green microalgae species have been identified till date, and almost all are found in freshwater (Neenan, 1986; Sheehan et al., 1998). Like terrestrial plants, green microalgae are also found with chlorophyll 'a' and chlorophyll 'b' as primary pigment associated with several carotenoids, which empower them to adapt under stress conditions (Tomaselli, 2004). Energy molecule such as lipid and starch are the stored energy sources that help species to survive under unfavorable environmental conditions. It has been found that lipid synthesis and its accumulation can be enhanced in green microalgae under nitrogen-deficiency (Sheehan et al., 1998). Since green algae have a high oil storing capacity; these are a point of attraction towards the synthesis/extraction of renewable energy. Amongst various green microalgal species, *Chlorella* and *Chlamydomonas* are the two species, which are most studied. This class is considered precedents of higher plants (Sheehan et al., 1998).

(iii) Golden-Brown Algae: These are also called as chrysophytes. Similar to diatoms, they also constitute fucoxanthin and β-carotene as the primary pigments. These are mostly present in oligotrophic water where the amount of nutrients in water is low with less plant habitation. Approximately 1000 species have been identified (Sheehan et al., 1998; Tomaselli, 2004). Primarily stored macromolecules in golden brown algae are chrysolaminarinis and lipids (Sheehan et al., 1998).

(iv) Prymnesiophytes: These are tiny unicellular flagellate algae and are found in the ocean (planktonic algae) (Tomaselli, 2004). These are also known as haptophytes and have approximately 500 in number have been found (Sheehan et al., 1998). They are also composed of fucoxanthin like chrysophytes and diatoms, giving color to the cells.

They are also composed of chrysolaminarin and lipids as the major stored products (Sheehan et al., 1998).

(v) Eustigmatophytes: These are a small group of eukaryotic microalgae, which include marine, freshwater and soil-living species. These are coccoid in shape with a cell wall composed of polysaccharides. The marine species of this class include *Nannochloropsis,* which contain high amounts of eicosapentaenoic acid (EPA). These are also a useful resource for polyunsaturated fatty acid (PUFA) (Tomaselli, 2004).

(vi) Cyanobacteria: These are a well-known group with over 2000 identified species containing chlorophyll 'a' (Tomaselli, 2004). It is named so because of the chlorophyll covering pigmentation of phycocyanin and phycoerythrin (Tomaselli, 2004). They have bacterial similarity in cell morphology as they are devoid of chloroplast and nucleus (Sheehan et al., 1998; Neenam, 1986).

1.3 Photochemical reactions in microalgae

Photosynthesis is a chemical reaction where light energy is captured by green plant or microalgae and converted into energy-rich compounds (starch/carbohydrate) and oxygen. In this process, light energy is captured to convert carbon dioxide (CO_2) into glucose and oxygen. Glucose, directly or indirectly obtained by photosynthesis, is the energy source of all earth organisms' growth and metabolism (Richmond, 2004). Chlorophyll 'a' is the primary pigment that absorbs light/solar energy to carry out photosynthesis, and the amount of pigment present plays a significant part in photosynthesis (MacIntyre et al., 2002). Accumulation of desired products and by-products is also pigment concentration dependent (Su et al., 2008).

Marine phytoplankton performs fifty percent of total photosynthesis taking place on earth (Rubio et al., 2003). Photosynthetic activity along with growth profile are mostly dependent on light availability. Amount of light absorbed by the algal cell cultivated in a photobioreactor or

open pond system depends upon the light intensity, culture density, cell pigmentation etc. Photosynthesis-irradiance (PI) curve shows the relationship with the amount of light energy captured for photosynthesis. Moreover, this curve also predicts culture performance (Rubio et al., 2003).

1.4 Conditions for growth of microalgae

Physiological behavior and biochemical composition of microalgae are regulated through the specific growth rate, culture media, and other environmental conditions, including life span/cycle of the species (Richmond, 1986). Besides this, temperature, light, carbon dioxide, nutrients availability, pH, etc. are involved in biochemical composition and growth profile (Zhu et al., 1997; Tzovenis et al., 1997).

For large-scale activities, suitable bioreactors with specific designs and optimized conditions are essential, making it possible to turn these scientific discoveries into an economical product. At present, algal biomass production cost is more expensive than growing crops. However, full utilization of freely available solar energy can further control production costs.

The cultivation condition is the important factor influencing the attributes of microalgae. The four primary forms of cultivation are heterotrophic, mixotrophic, photoautotrophic and photoheterotrophic.

Photoautotrophic microalgae, similar to other photosynthetic plants, uses carbon dioxide and sunlight to perform metabolic activity. Various photoautotrophic microalgae species, such as *Chlorella* sp., *Monallanthus salina*, *Botryococcus braunii*, *Chlorella zofingiensis*, *Dunaliella primolecta*, *Desmodesmus brasiliensis*, *Chlorella vulgaris*, *Neochloris oleoabundans* and *Scenedesmus obliquus*, have been noticed to improve and increase oil content under photoautotrophic cultivation (Chisti, 2007; Rodolfi et al., 2009; Kiran et al., 2014).

In place of carbon dioxide and sunlight, heterotrophic species consume organic carbon as energy source present in the media composition. Modifying cultivation conditions or applying genetic engineering enables autotrophic microalgae to be transformed into heterotrophic microalgae. For example, *P. tricornutum* also known as obligate photoautotroph has recently been grown heterotrophically by the insertion of a Glut 1 gene which is responsible for encoding the protein of glucose transporter (Glut1) (Zaslavskaia et al., 2001).

Mixotrophic algae can use heterotrophic (organic compounds) and autotrophic (sunlight and carbon dioxide), depending upon the substrates, organic nutrients, and light intensity present.

Photoheterotrophs species are also known as metabolic photoorganotrophs, consuming sunlight and organic molecules as energy and carbon sources. Specific light-regulated metabolites may be increased by photoheterotrophic cultivation (Tomčala et al., 2017). The critical variation stuck between photoheterotrophic and mixotrophic microalgae depend upon the utilization of energy: both light and organic molecules can be consumed by mixotrophic algae as an energy supplier, while photoheterotrophic microalgae need light as an energy source.

1.5 Microalgae cultivation systems

Different types of cultivation systems for microalgae have their own advantages. Cultivation system's choice relies upon cost, eventual outcome, supplements source, and CO_2 capturing capacity. Open cultivation system and closed cultivation system are the two types of system used for microalgae cultivation (Suali and Sarbatly, 2012). Open system for cultivation is a very old technique and used for mass scale cultivation since 1950s. Lakes, counterfeit lakes, tidal ponds are a few examples of open cultivation system. In contrast, the photobioreactors (PBRs) chamber like tubular PBR, column PBR and Flat PBR are the few examples of closed cultivation system of microalgae. These PBRs are configured to overcome the issues with

lake systems like contamination, biomass harvesting, and maintenance of environmental conditions viz. temperature, pH, CO_2 bubbling etc. (Bahadar and Khan, 2013).

Additionally, exhaust fumes might be captured from a power plant, giving different characteristic preferences for the usage of closed photobiorectors (PBRs) (Zimmerman et al., 2011). Various kinds of PBRs have arrived in the market (Table 1.1). In any case, if the operating cost of closed PBRs is more generous than open lake systems, however, the stresses over the possibility of scaling up, PBRs still exist (Janssen et al., 2003).

Table 1.1: Various algae culture system with advantages and limitations

Algal culture system		Advantages	Limitations
Open Cultivation system  Example: Natural pond, raceway pond, circular pond, inclined system		Low energy input, Utilization of barren land, Easy to clean and maintain, Economical reliable	Low biomass productivity Inefficient mixing Low mass transfer rate Chance of high contamination Consume lot of space
Closed cultivation system	Column PBR 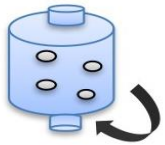	Low energy consumption Readily tempered High mass transfer Good mixing	Expensive compared to open ponds Difficult to scaleup Maintenance of temperature is difficult
	Tubular PBR 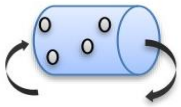	Less chances of co-contamination Proper illumination	Fouling Wall growth of algae takes place easily Difficult to maintain pH, dissolved O_2 and CO_2.
	Flat PBR 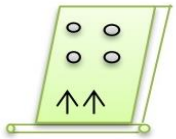	Low-cost maintenance, good productivity Proper illumination Low power consumption	Cells grow on the wall Less control of culture temperature Requirement of many sections for large scale

(Dragone et al., 2010; Tan et al., 2018; Bilad et al., 2014)

1.6 Algal biomass harvesting

Pilot-scale production of biofuels involves a sufficient accumulation of algal biomass. Low biomass concentration is caused by restricted light penetration and small microalgal cell size, which ultimately increases the cost and energy consumption of the harvesting process (Reitan et al., 1994). In addtion, these processes may also be affected due to the high division time. Some commonly used harvesting techniques includes air-flotation, auto-flotation, centrifugation, electrophoresis, flocculation, filtration, and ultrafiltration. Method selection primarily depends on the desired outcome and the subsequent processes. Although bulk harvesting and thickening, is a dual process—removing microalgae biomass from the large culture condition is called bulk culturing. Based upon the initial biomass obtained and the method used, such as flotation, gravity sedimentation, or flocculation, the total solid matter can reach 2–7 percent (Brennan and Owende, 2010). The slurry content is further increased in the thickening phase through filtration, ultrasonic aggregation, and centrifugation. The thickening technique consumes high amount of energy in comparison to bulk harvesting process (Brennan and Owende, 2010). Harvesting microalgal species is a downstream process that involves gathering and extracting algal biomass from the cultivation medium (Dragone et al., 2010). Table 1.2 summarizes various types of harvesting methods along with their benefits and drawbacks. These strategies need to be monitored closely to economically reap algae cells, which are regarded as primary necessities in organizing a profitable industry based on algal biofuels.

Table 1.2: Harvesting processes employed for microalgal biomass.

Harvesting technique	Benefits	Drawbacks
Auto and bioflocculation	Economical method Accepts reprocessing Time saving Non-destructive	Alterations in cellular structure Risk of microbiological infection
Chemical coagulation/ flocculation	Quick and consecutive method No energy needs	Chemical flocculants are uneconomical harmful to algal biomass. Reprocessing of grwoth medium is restricted
Centrifugation	Rapid approach High recovery proficiencies Appropriate for almost all microalgal species	Costly method High energy constraints Only suitable for high-value goods High shear forces cause cell damage.
Electrical based processes	Applied to a wide variety of microalgal species Least requirement of chemical flocculants	Inadequately distributed High energy and equipment cost
Flotation	Possible for large range harvesting Cost effective method Low space requirements Rapid working times	It almost always necessitates the use of chemical flocculants. Impossible for marine microalgae
Filtration	Excessive improvement in productivities It allows the split of shear sensitive species	The prospect of fouling/clogging raises operating expenses Membranes needed frequent washing Membrane replacement and pumping are the two most important related costs.
Centrifugation	Time saving Suitable for all kind of species	Uneconomical for large scale High consumption of electricity

(Barros et al., 2015, Abdelaziz et al., 2013; Singh & Patidar, 2018)

1.7 Microalgae lipid biomolecules – bioenergy feedstocks

Lipids are generally water-insoluble macromolecules, soluble in a nonpolar solvent such as alcohol, chloroform, benzene, ether etc. These are the primary constituents of almost all organisms' cell wall and play a vital part in metabolic functions. Polar and nonpolar are the two types of lipids found. Glycosylglycerides and phosphoglycerides

are the prime examples of polar lipids whereas wax, fatty acid, hydrocarbon, steryl ester and sterols are various nonpolar lipids (Gunstone and Harwood, 2007). Lipids such as sterols, glycosyl-glycerides, and phosphoglycerides are the important constituents of biological membranes. By acting as a matrix for various metabolic processes, they serve as porous wall to provide permeability restrictions between cells and organs. TAGs (triacylglycerols) are neutral lipids processed as lipid bodies in the thylakoid membrane under adverse conditions. These lipid bodies are the feedstocks for producing alternative renewable energy sources, whereas structural lipids are the major component of membranes such as phospholipids and glycolipids. These TAGs are catabolized to produce energy during nutrient deprivation (Gurr et al., 2002). Thus these two leading groups of algal lipids enable the species to survive in an adverse environmental condition.

TAGs are the most common type of nonpolar lipid in algae, accounting for 20 to 50 percent of the lyophilized biomass or dry cell weight (Brennan and Owende, 2010). Thus, algae containing high contents of TAGs can be utilized as feedstock for bioenergy production. Algae exhibit a high growth rate compared to plants, with a doubling time of 1-6 days, associated with more biomass accumaltion along with increase in lipid production. Oil content of microalgae are more (10 to 20 times) than terriestrail crops (Chisti, 2007). Algae can be cultivated either in municipal/household wastewater or grown in saline, brackish and coastal seawater. Since algae are efficient consumers of nitrate or phosphate as nutrients source for their growth and development, cultivating algae in wastewater can control the water pollution or can be used as wastewater treatment strategy. Additionally, microalgae are eukaryotic photosynthetic organisms that capture light and CO_2 to produce energy molecules and can be powerfully utilized to fix CO_2 in flue gases from industries—capturing environmental CO_2 results in diminishing global warming.

Furthermore, algae do not compete for environments where food crops are grown (Chisti, 2008). Microalgal biofuel is a renewable fuel source that belongs to the third and fourth generation of biofuel feedstocks which can help fight fossil fuel depletion for energy demand. An overview of the algae-based biofuels production process is represented in figure 1.1. Biodiesel production as a feedstock, algae have a significant outcome in the renewable energy sector compared to plants, as it needs less area for cultivation and more biomass generation. All these advantages make algae a suitable candidate compared to land plants/crops to target biofuels and other essential metabolites.

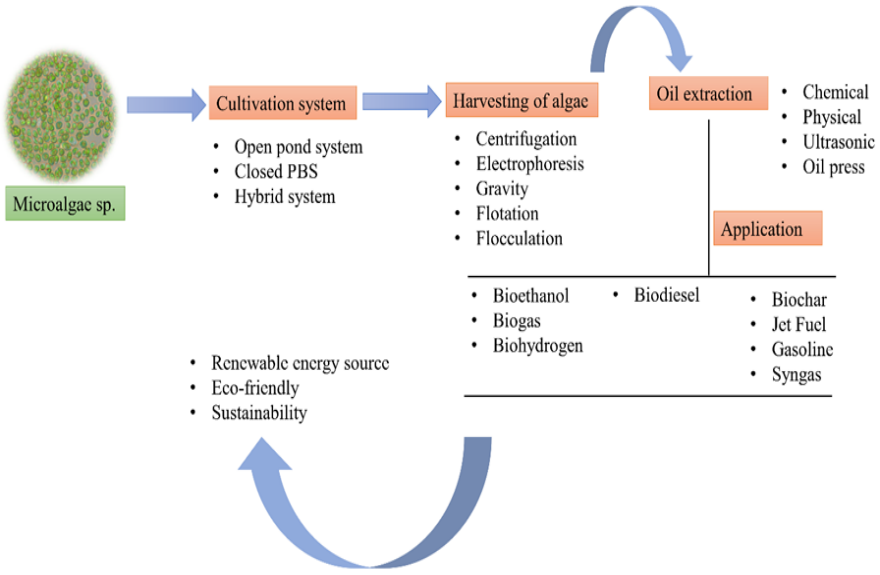

Figure 1.1: Schematic representation of microalgae towards biofuels production and sustainability.

1.8 History of lipid manipulation in algae

Microalgae are the pivotal for sustainable lipid production and its subsequent conversion to biodiesel. Numerous algae species have been tested for high oil/lipid content in addition to terrestrial plants (Griffiths, and Harrison, 2009; Sheehan et al., 1998; Gouveia and Oliveira, 2009). Although microalgae, even with a proper culturing condition such as sufficient nutrient treatment, accumulate less oil quantity, account 60% for commercial exploitation (Jorquera et al.,

2010; Gouveia and Oliveira, 2009). Therefore, various other strategies have been exploited in many ways for successful biodiesel production.

Different methods have been identified for lipid enhancement in microalgae. Amongst various strategies to enhance lipid content, environmental manipulation is regarded as a effortless engineering process (Courchesne et al., 2009), while genetic engineering level are complicated and tough process (Sheehan et al., 1998). However, nutrients poor condition, high salinity, and CO_2 aeration are employed continuously to microalgae for high lipid synthesis (Chiu et al., 2009; Takagi and Yoshida, 2006). Amongst all these, nitrogen/nitrate deprivation is a highly applied approach to increase lipid accumulation— in most of the studies, single stress at a single point of time is applied. However, Pal et al. (2011) explored the effects of different stresses (nitrogen deprivation, salinity, and light intensity) on *Nannochloropsis* sp. and observed a sharp decline in total lipid productivity at high-level of salt and light intensity under nitrogen depletion in comparison to control conditions. Thus, it was suggested that nitrogen deficiency might not be the most acceptable procedure of inducing high lipid production when talking in terms of lipid productivity. It was also concluded that decrease in overall lipid productivities is due to nutrient deficiency and reduction in algal biomass, which can utilize this nitrogen for growth and TAGs synthesis. Salama et al. (2013) cultivated freshwater *Chlamydomonas mexicana* in different salt concentrations and observed a major rise in lipid percent at 0.05 M sodium chloride (NaCl), thus concluding osmotic stress-triggered lipid synthesis in microalga. But stress conditions providing high lipid accumulation also severely affect cell's ability to increase its population. Microalgae growth is restricted under stress because carbon flux changes its path from photosynthesis fixation of carbon towards starch and fatty acid production (Li et al., 2011). To understand the correlation between lipid productivity and growth rate of microalga, Adams et al. (2013) conducted a study by treating algae sp. under high and low nitrogen stress, discovering

specific reactions in distinct species due to stress sensitivity. However, nitrogen deprivation being one of the major outbreaks for lipid induction, results in decline of photosynthetic activity-due to the incapability of cells to synthesize proteins without a nitrogen source (Johnson and Alric, 2013). Photosynthesis impediment is a rate-determining step for high lipid yield because more extensive accessibility of incorporated or fixed carbon provides a better reserve for lipid storage. Research is moving towards monitoring the cell pathways in finding a path for lipid production without decrease in photosynthetic activity.

1.9 Biosynthesis of lipids in microalgae

The major portion of algal biomass is composed of lipids. Microalgae consist of different kinds of lipids, such as polar, nonpolar, phospholipid, and glycolipids. Amongst which nonpolar lipids (neutral lipids) are the backbone for biodiesel production. These neutral lipids undergo transesterification reaction to generate FAME, which is a generic term of biodiesel. Biosynthesis of TAGs or fatty acid in microalgae occurs similar to terrestrial crops (Maity et al., 2014; Hulatt et al., 2017). Three major steps involved in FA synthesis are: (1) the rate-determining step in which formulation of malonyl- CoA occur due to carboxylation of acetyl-CoA; (2) elongation of acyl chain; and (3) and last is TAGs formation (Nobusawa et al., 2017; Sakthivel, 2011).

Lipid synthesis occurs in the plastid, where pyruvate, a glycolysis product, is converted to acetyl Co-A. This pathway's main enzyme in lipid synthesis is acetyl Co-A carboxylase, which produce malonyl Co-A. This conversion process is irreversible and is considered as a rate-determining step. Biotin is an important molecule required for the function of ACCase enzyme (Roessler et al., 1994). Condensation, reduction, and dehydration are the three main steps in fatty acid chain synthesis. Fatty acid synthase (FAS) enzyme enables the reactions to generate C16:0 or C18:0. Now, this C18:0 is processed into C18:1 by Δ-9 stearoyl ACP desaturase enzyme (Slabas and

Fawcett, 1992). The termination of chain elongation is another essential step in lipid synthesis. Acyl-ACP thioesterase and Acyl-transferase are the two critical enzymes responsible termination step in fatty acid synthesis. These enzymes plays a different role in lipid synthesis; for example, thioesterase is involved in TAGs formation from free fatty acids, which is important energy storage molecule in microalgae while glycolipids are produced from acyl-transferase. Fat A and Fat B, two forms of thioesterase found in plastids, selectively convert FA-ACPs to free fatty acids. Unsaturated fatty acids are associated with Fat A, while saturated fatty acids are associated with Fat B (Sivakumar et al., 2012).

Several desaturases are involved in fatty acid synthesis known as desaturation steps, whose identification depends upon the position of carbon where they introduced, such as Δ-6, Δ-12, Δ-15. The three enzymes; FAD3 (Δ-15), FAD2 (DΔ12), and SAD (DΔ9), are responsible for PUFAs generations. The endoplasmic reticulum is the site for PUFA synthesis (Wallis et al., 2002). However, biodiesel is produced from TAGs in algal cells through the Kennedy pathway or the PCDAG pathway. Two powerful enzymes, DGAT and PGAT, are necessary for the pathway to function (Merchant et al., 2012).

Enzymes like elongases and synthetases are required during lipid synthesis, which occurs in the presence of NADPH as it requires a lot of energy. The operation of malate enzyme transforms malate and pyruvate into NADPH, a light-dependent process. The enzymes activity involved in lipid synthesis was investigated for light concerning, and was discovered that during the dark time, citrate is formed from acetyl Co-A with the help of ATP-citrate lyase, lowering the NADPH production and fatty acid synthesis in microalgae (Bellou and Aggelis, 2013). Mühlroth et al. (2013) discovered that genes which are involved in fatty acid synthesis as well as in tricarboxylic acid cycle (TCA cycles) are expressed together, and metabolites produced during TCA cycle can also be utilized for fatty acid biosynthesis. TAGs biosynthesis and stability within the cells are needed for lipid accumulation. CHT7 encourages TAGs aggregation in *Chlamydomonas* under nitrogen-

deprived environemt and retains high levels of TAGs for up to 48 hours after nitrogen repletion. Following improved cell growth in nutrients sufficient environment, it also downregulates genes associated with cellular quiescence (Tsai et al., 2014). Furthermore, the modified transcriptional regulator helps in efficient carbon partitioning for fatty acid synthesis alongwith enhanced biomass accumulation (Chen et al., 2018).

1.10 Lipids mapping and quantification

To achieve higher lipid productivity, there is need to know the pathways and factors affecting lipid biosynthesis, which can be unfolded nowadays through dedicated studies. The exact knowledge and detailed composition of lipids are necessary to target specific products such as biofuels, PUFA etc.

Extracting lipids from cells is a challenge in itself because methods used for extraction can influence the yield and nature. After extraction, lipids are converted into fatty acid methyl esters to prevent oxidation. Folch et al. (1957) and Bligh and dyer (1959) are the most accepted and widely used methods for extraction of lipids. In recent years, various other methods have also been derived. For example, one-step rapid extraction method has been optimized showing five folds higher yield as compared to conventional methods (Axelsson and Gentili 2014). Solvents play an important role in the process of lipid extraction. Generally, a mixture of polar and nonpolar solvents is used to extract high amount of lipids from cells such as hexane, chloroform, chloroform–methanol in different ratios. For example, mixture of chloroform–methanol (2:1) after ultra-sonication gave 19% yield (Dos Santos et al. 2015). Supercritical carbon dioxide extraction pressurized liquid extraction and sonication are different approaches, which can also be used for efficient lipid extraction from microalgae.

Gravimetric is the most commonly used method which is able to depict the quantity of lipids extracted but not the quality of lipids such as carbon chain length, degree of unsaturation, etc. In this method,

large quantity of sample is required for accurate and reliable results. The gravimetric method has been overcome by colorimetric approaches such as sulpho-phospho-vanillin (SPV) method, which is able to detect lower concentrations of lipids even from wet algae. SPV reagent does not react with carbohydrate, protein or glycerol, which makes it more reliable (Byreddy et al., 2016). Fluorescence techniques such as fluorescent dye (Nile red) staining of lipid droplets in algal cells have also been evolved with time. Nile red is fluorescence dye, which binds specifically to polar and nonpolar lipid bodies. It gives yellow fluorescence when bound to neutral lipids like TAGs and red fluorescence when bound to phospholipids. This method is used to visualize lipid bodies inside algal cells. Size of lipid bodies can also be measured using confocal microscopy. Optical density of 0.8 to 1 is considered best for NR analysis as high O.D. results in fluorescence quenching (Gusbeth et al., 2016). Another limitation is photooxidization of dyes, due to which properties of lipids like degree of saturation, melting temperature etc. cannot be predicted. To overcome these limitations, researchers have come up with another noninvasive technique i.e. in vivo analysis of cells using Raman spectroscopy. It enables us to quantify lipid bodies as well as unsaturation, chain length, Tm, etc. Single-cell laser-trapping Raman spectroscopy (LTRS), coherent antistroke Raman scattering (CARS), surface-enhanced Raman spectroscopy (SERS), resonance Raman spectroscopy (RRS) and confocal Raman spectroscopy (CRM) are few variants of Raman spectroscopy used for lipid analysis (Sharma et al., 2015). Beside above-mentioned methods, various spectroscopic methods such as NIR, FTIR, MRS, NMR etc. can also be used for lipid detection as well as quantification in vivo (Yan et al., 2015).

GC–MS is most commonly used technique to identify different fatty acids. Diverse ionic liquid columns have been tested for separation of FAMEs and FAEEs for better peak resolution and retention time, which was not achieved using normal polyethylene glycol (PEG) column. Cis and trans isoforms of fatty acids were also

resolved using ionic columns (Weatherly et al., 2016). FI-MS analysis assist in interpreting PUFA from biodiesel FAs. During GC analysis, a vacuum UV detector was also tested in place of FID for deconvoluted FAs, which were co-eluting for rapid differentiation between cis and trans isoforms of the FAs (Fan et al., 2016; Furuhashi et al., 2016).

On top of that, thin-layer chromatography (TLC) has also been used to implement high determination for different classes of lipids. In a recent survey, $AgNO_3$ and urea coated plates were used to distinct branched and unbranched chain fatty acids leading to improved resolution than normal TLC or GC method (Yan et al., 2015). HPLC is also used in lipidome studies. In chromerid algae, more than 250 analytes were separated and identified using Orbitrap mass analyzer (Jouhet et al., 2017). A variant of HPLC i.e. UPLC, helped in identification of lipids in *Chlamydomonas* sp. (Tomčala et al., 2017; Sharma et al., 2015). Integrated chromatography–mass spectrophotometry are hyphenated techniques which are always better than independent versions for the quantitative scanning of all existing fatty acids in sample, whereas it does not identify lipid class to which fatty acids are associated. Development of highly sophisticated instruments has led to the development of new approaches for lipid research. Area of lipidomics has taken its height with the development of various ionization techniques such as electrospray ionization, desorption electrospray ionization and matrix-assisted laser desorption ionization (EI) (Lingwood et al., 2011). Mass spectrometers with different analyzers like Orbitrap, quadrupole (Q) and time of flight (TOF) can be used for the analysis of polar lipids. These efforts collectively added momentum to the field of lipidomics. Based on the functional group/structural features, lipids are identified by MS in positive or negative mode. For example, neutral lipids are always identified as positive mode which means as a protonated molecule $[M+H]^+$, ammonium adducts $[M+NH_4]^+$ or alkali cations [Na^+or Li^+], $[M+Na]^+$ whereas SQDGs are mainly detected as negative ions [M-H] (Gonen et al., 2005).

Each MS configuration has its own advantages and disadvantages whether it is of high resolution like quadrupole time of flight (Q-TOF), MALDI-TOF or low-resolution techniques such as triple quadrupole, ion trap, Fourier transform ion cyclotron resonance mass spectrometry (FTICR-MS) in terms of functions, scanning speed and peak resolution. Lipids can further be explored using either electrospray ionization (ESI)-QQQ-MS or ESI-QTOF-MS or shotgun-MS approach.

Collision-induced dissociation produces fragments of different lipid classes having diverse characteristics, which can be identified through neutral loss or precursor ion scanning after infusing directly. In this, the lipid of certain interest is added as internal standard to lipid extracts of biological samples (Han and Gross, 2005).

Tandem mass spectroscopy is a vital part of shotgun lipidomics and generates high mass accuracy and high mass resolutions in the form of peaks. Quadrupole-time-of-flight instrument can also play a significant role for lipid profiling of any specific lipid class extracted from sample of interest (Krank et al., 2007; Roessler et al., 2007).

Microalgae synthesizes insignificant quantities of TAGs under favorable environmental conditions, but under unfavorable environmental conditions, their physical or chemical stimuli gets activated and significantly induce TAGs synthesis. Nutrient starvation (such as nitrogen or phosphorus deficiency), pH, and salinity are chemical stress inducer molecules, whereas temperature and light intensity are physical paramters for inducing stress (Hu et al., 2008).

1.11 Strategies for lipid induction in microalgae

Biochemical engineering, genetic engineering, and transcriptomic engineering are three techniques that could theoretically be used to enhance lipid content in algae. Traditional approaches for channelling metabolic flux and assessing factors that depict a significant role in all of these steps and thus leading to an increased

lipid accumulation along with the synthesis of some other beneficial products. Long-term perspectives include genetic and transcriptomic engineering. Scientific community has taken note of omics and has given it much publicity. There is lot to learn from the omics approach. In addition to metabolomics, transcriptomics, genomics, and proteomics; lipidomics has gained much attention. For system biology research, lipidomics is a must-have method. Exploring algae metabolic pathways for improved lipid accumulation, extensive assessement of desired molecules, and molecular profiling of TAGs are some of the critical challenges for considering algae as a better option for biofuel production. For future application as a final marketable commodity, maximising biomass development and recovering secondary metabolite is essential. Furthermore, the integration of various strategies is necessary for the optimization and enhancement of algal systems. It is important to emphasise that incorporating these systems will assist and complement research on microalgal applications. To resolve and develop algal structures, people working in physiology, chemistry, biology, and engineering must collaborate. Improved in lipid productivity and techniques to support analysis and production, committed research and development will revolutionise the algal lipid sector.

As we know, microalgae can survive in diverse and extreme environments because they are found in enormous diversity and are inbuilt with a typical form of cellular lipids, which acts as a shield against adverse conditions (Sato et al., 2000). Many reports are available in terms of microalgal lipid metabolism (Schuhmann et al. 2012; Anand et al., 2019). Few microalgae species constitute 5-20 percent lipid content per dry cell weight (DCW) with a large biomass under normal growth conditions. However, under adverse or unfavorable environmental conditions, these species modify their lipid biosynthesis metabolic pathway to enhance the synthesis of neutral lipids and accumulate higher lipids (20–50% DCW). This accumulation

of neutral lipids enables microalga to prevail under adverse environmental condition.

In contempt of the fact that microalgae are regarded as a suitable feedstock for biofuel processing, commercialization has proven difficult. The major bottleneck for the commercialization of algae-based biofuels is low lipid productivity and high principal costs. High amount of lipid content in microalgae either in the laboratory or outdoor conditions can be achieved through stress induction. In the sense of biodiesel, polar lipid, especially in the form of TAGs, are suitable (Miao and Wu 2006; Hu et al., 2008). Quantity of TAGs depends upon genetic constituents, which eventually controls their metabolic functions. Much research has been carried out on increasing the synthesis of neutral lipids or FAs in microalgae species. The most common approach for increasing lipid synthesis in microalgae includes salinity, pH, light intensity and duration, temperature, heavy metals, nutrients (nitrogen and phosphorus), and other chemicals stimuli. In the following sections, effect of various TAGs initiation methods on different microalgae species is evaluated.

1.11.1 Nutrients hunger condition

Carbon, nitrogen, sulfur, and phosphorus etc. are macronutrients, whereas cobalt, manganese, iron, copper and zinc etc. are micronutrients required for the growth of microalgae. Nutrient availability affects microalgae development and proliferation considerably with wide-ranging effects on lipids and FAs composition. These nutrients such as nitrogen, phosphorus etc. plays an essential role in cellular function. For example, nitrogen is an essential constituent and considered as building block of proteins, Deoxyribonucleic acid (DNA), and Ribonucleic acid (RNA). Nutrients deficiency leads to programmed cell death, as it slowly and steadily declines the cell number or cell growth. In such condition, these species alter their metabolic pathway and activate the biosynthesis pathway of fatty acids, unless sufficient carbon dioxide (CO_2) and light are present for

photosynthesis to be carried out (Thompson, 1996). TAGs production under adverse environmental condition may perhaps provide a shielding system for microalga. Energy providing molecule such as nicotinamide adenine dinucleotide phosphate and adenosine triphosphate are synthesized during normal photosynthesis and are utilized for generating biomass, leaving ATP as ADP (Adenosine diphosphate) and $NADP^+$ (Nicotinamide adenine dinucleotide phosphate) as electron acceptor molecule for photosynthesis. However, under nutrients deficiency, when the cell growth and proliferation get reduced, the major electron acceptor for photosynthesis, $NADP^+$ is reduced. It is well established that photosynthesis is primarily regulated by light energy and cannot be stopped entirely. The situation where photosynthesis ultimately stops lead to programmed cell death, where organelle gets damaged (Zhu, 2000). Although a pool of NADPH is being generated under diminished photosynthesis and under such conditions, these NADPH are utilized for fatty acid biosynthesis leading to enhanced production or accumulation of fatty acid and recycle $NADP^+$ (Sato et al., 2000; Banerjee et al., 2017).

Mutlifarious studies have been performed to spike TAGs accumulation in microalgae when nutrients are scarce. Green alga, *Chlamydomonas moewusii*, when cultivated under nutrients deprived condition, resulted in increased Oleic (C18:1) and Palmitoleic (C16:1) acid accumulation with a decrease in PUFA such as α-Linolenic (C18:3) acid (Arisz et al., 2000). Diatom, *Stephanodiscus minutulus*, cultivated under nitrate or phosphate limitation with a modified media with silicon showed increase in TAGs accumulation with decrease in polar lipids (Lynn et al., 2000). A common observation was made for enhanced lipid production mainly neutral lipids or TAGs under nitrogen-depleted condition in many microalgae species (Yeh and Chang, 2011; Praveenkumar et al., 2012; Hsieh and Wu, 2009). Hu et al. (2006) performed a series of experiments on several green microalgae, cyanobacteria, and diatoms under nitrogen deficiency and came to a common conclusion showing enhanced lipid production.

Nitrogen is the only extremely vital nutrient influencing lipid metabolism in algae. Rodolfi et al. (2009) conducted a detailed study of lipid production under nitrogen and phosphorus starvation on several green microalgae, diatoms, eustigmatophyte, red algae and prymnesiophytes. He also conducted a study on large-scale production of biomass alongwith lipids. However, *Phaeodactylum tricornutum* was observed with a slight boost in TAGs and 69 to 75% enhancement in total lipids and 6 to 8 percent in phospholipids under lower nitrogen conditions (Alonso et al., 2000). Likewise, many other studies have been conducted for lipid enhancement in different microalgae. *Scenedesmus* sp. showed 30 and 53 percent increment under nitrogen and phosphorus deficiency, and *Chlorella vulgaris* had shown 40 percent increment in lipid synthesis under low nitrogen treatment (Xin et al., 2010; Illman et al., 2000). Table 1.3 represent some of the studies that were carried out in different microalgae species under varying nutrients condition. It also revealed that nitrogen starvation not only deals with FA synthesis but also influences pigment composition. Solovchenko et al. (2008) performed a study on *Parietochloris incise* cultivated in nitrogen depleted condition, showing a significant boost in carotenoids and chlorophyll ratio.

Similar to nitrogen, phosphorus has also been tested for lipid enhancement in different microalgae. Reitan et al. (1994) showed increased lipid accumulation under phosphorus limitation in *P. tricornutum*, *Pavlova lutheri*, *Chaetoceros* sp. and *Isochrysis galbana,* although reduced lipid content observed for *Tetraselmis* sp., and *Nannochloris atomus*. Another observation is increased palmitic (C16:0) and oleic (C18:1) acid with a decrease in C20:5ω3, C22:6ω3 and C18:4ω3 PUFA.

Increased level of PUFA [sulfoquinovosyl diacylglycerols (SQDG), phosphatidylcholine (PC), monogalactosyldiacylglycerol (MGDG), and digalactosyldiacylglycerol (DGDG)] has been observed in *Chlorella kessleri* under phosphorus limitation condition (El-Sheek and Rady, 1995).

Based on a literature survey, it was revealed that the nitrogen limitation condition is highly practised and most extensively operated in nearly all microalgae species to target renewable fuels compared to other nutrient stress conditions. Nitrogen limitation severely impacts growth and is considered as an essential nutrient. It is comparatively simple to utilize and monitor nitrate stress on algae i.e. by withdrawing the nitrogen supply from the growth media and monitoring its impact on growth. All the microalgae species investigated so far have successfully enhanced TAGs synthesis under different nutrients stress condition. Therefore, nitrogen starvation/limitation is the most effective way of increasing lipid synthesis. Nevertheless, excessive lipid accumulation under nitrogen stress might encounter a steady drop in growth rates with low cell number.

Omics can also help to solve the problems related to lipid enhancement. Limitations can be overcome by studying the metabolism pathways. These pathways are interdependent and have positive or negative effect on each other. In a transcriptomic study, *P. tricornutum* showed co-expression of 106 genes related to TCA cycle and PUFA synthesis (Mühlroth et al., 2013). This knowledge helps us in diversion of carbon partitioning more toward lipid synthesis. Proteomics can also help in studying the activity of different enzymes, proteins and transcription factors. Transcription factors play major role in regulation of gene expression of various enzymes responsible for metabolite production. N^- and N^+ cultures of *N. gladiana* revealed 20 TFs which were affecting the carbon partitioning into lipid. Mutants of TFs were developed using CRISPR-Cas9, and they showed 40–50% lipid carbon partitioning as compared to WT 20% (Ajjawi et al., 2017). Isoforms of various enzymes and their effects can be studied using omics techniques.

Radakovits et al. (2010) analyzed manipulation in various pathway levels for improved biofuels production from microalga, which consists of avoidance of lipid catabolism and constraining

metabolic pathways, lipid biosynthesis, leading to the production of another vitality compounds such as starch.

The above approach for lipid enhancement observed to be effective in boosting lipid content inside cells. A report concluded by Li et al. (2010) states that starch synthesis pathways can be blocked by deactivating ADP-glucose phosphorylase in *C. reinhardtii* and thus diverting photosynthetic carbon flux towards TAGs synthesis, which results in 10-fold enhancement of TAGs accumulation. A parallel study performed by Wang et al. (2009) showed that inhibiting starch synthesis in *C. reinhardtii*, increases lipid synthesis at nitrogen depleted condition by 15 to 30-fold in wild type species as compared to a starch-less mutant. It was surprising that these mutants now need stress to stimulate lipid synthesis, but then again demonstrated that carbon flux could effectively divert high TAGs accumulation inside cells. The question still persists in stimulating TAGs biogenesis under normal environment condition.

1.11.2 Temperature stress

Growth condition is an essential factor which generally determines the synthesis of biomolecules. It is a well-known fact that variations in culture environment switch biosynthetic pathway towards lipid synthesis rather than carbohydrate synthesis. Beside nutrients variation, temperature also has an impact on lipid synthesis in microalgae. Fatty acid improvement in microalgae at varying temperature was examined long before (Aaronson, 1973; Norman and Thompson, 1985). Significant temporary changes observed in growth profile due to temperature variations. Typical temperature differences or unexpected temperature changes due to any reason also changes the production efficiency of microalgae. It has been observed that microalgae cells get well acclimatized to 30 and 35°C after 15^{th} and 30^{th} generation and reach upto 40°C at 135^{th} generation (Huertas et al., 2011).

Table 1.3: Different types of nutrient stress to induce lipids in microalgae (N= Nitrogen, P= Phosphorus)

Strain	Nutrients Stress	Change in lipid accumulation/profile	References
Chlorella vulgaris	N limitation	Total lipid increased by 16.41 percent	Converti et al., 2009
Chlamydomonas reinhardtii	N limitation	Enhanced total lipids (lipid: amide ratio)	Dean et al., 2010
Phaeodactylum tricornutum	N limitation	TAG level increased from 69 to 75 percent	Alonso et al., 2000
Chlorella sp.	N limitation	Lipid productivity of 53.96±0.63 mg/L/d	Praveenkumar et al., 2012
Nannochloropsis oculata	N limitation	Total lipid increased by 15.31 percent	Converti et al., 2009
Chlorella sp.	Urea limitation	increased productivity of 0.124 g/ L/d	Converti et al., 2009
Scenedesmus sp.	N & P limitation	Increase in TAGs	Gardner et al., 2011
Phaeodactylum tricornutum	P limitation	Increase in total lipids high content of 16:0 and 18:1	Reitan et al., 1994
Scenedesmus sp.	N & P starvation	Lipids increased 30 and 53%, respectively	Xin et al., 2010

Fatty acid produced by microalgae and its composition is certainly affected by temperature differences (Guschina and Harwood 2006; Morgan-Kiss et al., 2006). Biomass is also affected under varied temperature alongwith reduction in the ratio of PUFA to SFA (Renaud

et al., 2002). Few studies showing data for different microalgal species with lipid induction under varying temperature are represented in Table 1.4. Lipid content of *Nannochloropsis oculata* increased from 7.9 to 14.9 percent (1.8-fold) with temperature rise from 20 to 25°C; however, a decrease in growth rate was observed (Converti et al., 2009). Higher temperature is found linked with increase in protein content in *Isochrysis galbana* with a decrease in lipids and carbohydrates (Lynch and Thompson, 1982). Lipid profile is also found to be affected with time period and cell growth. In *Dunaliella salina*, decrease in neutral lipids observed alongwith an increase in phospholipids and glycols under temperature variations (Lynch and Thompson, 1982). Many reports revealed an increase in SFA with increased temperature whereas increased PUFA with decrease in temperature in different cyanobacteria and microalgae (Murata et al., 1975; Sato and Murata, 1980). Accumulation of lipids modifies/protects or drives membranes' physical properties so that microalgae can perform a regular activity such as photosynthesis, ion exchange, and respiratory process etc. (Somerville, 1995). Membrane lipids showed change in structure with temperature shift resulting in increased PUFA synthesis (Callow, 1999).

Polyunsaturated fatty acid can’t be firmly packed as contains multiple double/triple bonds. Hence the flexibility of membranes containing PUFA is enhanced. Higher temperature resulted in decreased PUFA in *Botryococcus braunii* and *Chlorella vulgaris* (Sushchik et al., 2003), while *Nannochloropsis salina* showed high lipid content and growth rate with rise in temperature (Boussiba et al., 1987). McLarnon-Riches et al. (1998) detected an increase in oleate with a decrease in stearidonic and linoleate acid in green algae, *Selenastrum capricornutum* during drop of temperature from 25 to 10°C. The impact of temperature on lipid synthesis varies from species to species. As noticed, in nearly all microalgae species at a minimal temperature, high lipid synthesis occurs while having slight impacts on carbohydrate synthesis because carbon flux gets diverted from

carbohydrate to protein synthesis. The study also rationalized that temperature fluctuation or reduced temperature showed a high impact on amino acid (AA) and putative osmolyte biosynthesis. Hence, glycolysis is an intermediate step towards the synthesis of acetyl CoA's precursors, guiding the synthesis of comparatively more FA than usual (Wang et al., 2016).

Various researchers have observed impacts of a decrease in temperature on lipid accumulation. For example, *Scenedesmus* sp. showed 2.5-fold increment in lipid content when the temperature dropped from 25 to 20°C with a loss of 8 percent in growth rate (Xin et al., 2011). Converti et al. (2009) had also observed the same trend where *Chlorella vulgaris* found to show 2.5-fold increase in lipid content when the temperature of culture media decreased from 30 to 25°C without affecting its biomass or growth rate. *Chlorella sorokiniana* when cultivated at low temperature (18°C) increased lipid content with a decline in growth rate with increased lipid productivity of 30 mg/L/d at 26°C (Wang et al., 2016). To improve harmful impacts of low temperature on lipid synthesis, Wang et al. (2016) performed an experiment where media was mixed with Glycine betaine (GBT), a quaternary ammonium compound during early growth phase. It was concluded that the addition of GBT might improve the growth rate, biomass productivity, lipid content and lipid productivity of *C. sorokiniana* by facilitating carbon flux both at the ideal temperature (26°C) and at sub-optimal temperature (18°C). Hence proved that low temperature naturally reduces the carboxylase activity resulting in high energy supply with no change in the light intensity. Maxwell et al. (1994) conducted a study where *Chlorella vulgaris* got acclimatized and could enhance its biomass at 5°C with minimal chlorophyll content. A similar trend was observed for a diatom, *Dunaliella salina* (Kró et al., 1997) and *Dunalliella tertiolecta* (Levasseur et al., 1990). Although, *Skeletonema costatum* showed different reaction where chlorophyll content increases with lowering down of temperature.

Table 1.4: Lipid content in microalgae at varying temperatures

Microalgae	Varying temperature	Changes under stress	Reference
Chaetoceros sp.	At 25°C	Lipid content increases by 16.8 percent	Renaud et al., 2002
Nannochloropsis oculata	Increase from 20°C to 25°C	Lipid production enhanced by 14.92%	Converti et al., 2009
Chlorella ellipsoidea	Reducing temperature	Unsaturated fatty acid increases by 2 times	Joh et al., 1993
Dunaliella salina	Change of temperature from 30°C to 12°C	Increase in unsaturated lipids	Thompson., 1996
Selenastrum capricornutum	Temperature from 25°C to 10°C	Increase in oleate fatty acid	McLarnon-Riches et al., 1998
Phaeodactylum tricornutum	Shift of temperature from 25°C to 10°C for 12 hrs	High yield of PUFA and EPA	Jiang & Gao., 2004
Spirulina platensis, Chlorella vulgaris, Botryococcus braunii	Increase in temperature	Saturated FAs increased	Sushchik et al., 2003
Nannochloropsis salina	Increase in temperature	Increase in total lipids	Boussiba et al., 1987
Rhodomonas sp., *Cryptomonas* sp., *Isochrysis* sp.	Range of 27 °C to 30 °C	Lipid production increased by 15.5, 12.7, and 21.7% respectively	Renaud et al., 2002

Effect of temperature on lipid synthesis or its accumulation depends on distinct species. After a literature survey, in almost all species of cyanobacteria or green microalgae, low-temperature is found to trigger lipid accumulation. Besides high lipid accumulation at lower

temperature, there seems insignificant impact on carbohydrate synthesis. As a consequence of this study, it was justified that the putative osmolyte and amino acid biosynthesis get reduced as the temperature decline. Therefore, glycolysis mediates a significant role of acetyl-CoA precursor, leading to more FA synthesis. Merely a constrained data is accessible on this issue, and that too most of the work was performed at a laboratory scale where required temperature maintenance is possible. At present, for the commercialization of algal biofuels, temperature-induced lipid production at large-scale farming seems to be not much studied. But it has been found that lipid profiles are affected at different temperatures due to which biodiesel properties would also change.

1.11.3 Salinity induced lipid enhancement

Another environmental factor that influences algae growth and productivity is salinity. Excessive salinity raises extracellular osmotic pressure, causing stress in algal cells, which can be observed through physiological and biochemical processes. Once microalgae are exposed to different salts at different concentrations, restoration of turgor pressure, control of ion uptake/export through the cell membrane, and accumulation of osmo-protecting solutes and stress proteins become active.. Multiple changes occur at morphological, physiological, and even molecular levels under salinity amended culture media. Salinity induced media enables algae species to change their metabolic pathway for their survival.

Under high salts exposure usually microalgae, cyanobacteria or diatoms reduces their cell size-because of impact on cell division, which ultimately ceases cells motility and prompts colony formation in such species (Fakhry and Maghraby, 2015; Hema et al., 2007; Khona et al., 2016; Nakamura et al., 1975; Neelam, and Subramanyam, 2013). The impact of salt on microalgae species can be observed easily through the growth profile, for example, *Chlamydomonas reinhardtii* showed slow growth rate under high salt concentration when compared

to untreated (control) condition as indicated through optical density (OD) i.e. same OD at 750 nm took more time to reach under salt exposure. It has been further observed that cells were compact and in dividing stage as seen under microscope at all the ranges of salt concentrations (Talebi et al., 2013). *Chlorella emersonii*, *Chlorella vulgaris*, *Chlorella salina* and *Scenedesmus opoliensis* showed a negative effect on growth under various salt treatment (Demetriou et al., 2007). Figure 1.3 delivers a brief of adaptation reactions when algae cells are subjected to hypersaline conditions.

When cells are exposed to unfavourable environmental conditions, number of events occur in the interior and exterior of the cells. Some species e.g. *Chlamydomonas* are subjected to adverse environments, enters into a transient phase called “palmelloid”. Beside this there occur numerous structural changes such as (i) gathering of cells i.e. grouping of cells at least two cells per group, (ii) improved excretion of exopolysaccharide (EPS), (iii) loss of flagella which stop cells motility (iv) thick membrane shared by EPS surrounding the cells and (v) stiffening of cell walls. The palmelloids or colony formation around the cells expands gradually till 24 hrs after exposure to high salt concentration. Neutral lipids are the remarkably efficient resources of stored energy. These lipids act as a shield for sensitive inner organs and hormones and are essential structural elements for most cellular membranes (Singh et al., 2002). The mechanism of stress tolerance generally depends upon the structure of phospholipid bilayers. Under salinity stress, lipid and fatty acid composition alter membrane fluidity and permeability, assisting algal species in bearing and adapting to changing conditions.

Lipids are rich in hydrogen bonds, which are prime accused of oxidative reactions. Salinity stress also causes osmotic pressure difference within microalgae cells. This osmotic pressure difference causes change in metabolic pathway and compel them to adapt to these new environmental conditions (Kan et al., 2012; Richmond, 2017)— such metabolic modifications caused by salt treatment result in

considerable increase in the lipid content. Besides increasing lipid content, it has also been found that salt concentration variations also affect the lipid composition (Sharma et al., 2012).

There are many examples (Table 1.5) showing microalgae cultivated under different salts with varying concentrations for lipid enhancement. Amongst which *Dunaliella* species represent the finest example of algae, which can survive at an elevated concentration of salts. The *Dunaliella* species can multiply at the saturation range of almost all salt concentrations and enable these species as a preferred contender to study the impacts of salinity stress on microalgae (Azachi et al., 2002; Xu and Beardall, 1997). In an experiment, *Dunaliella salina* was cultured in NaCl incorporated media and observed a significantly high ratio of monounsaturated fatty acid (MUFA) in 3.5 M of NaCl as compared to 0.5 M (Azachi et al., 2002). Additional supplement of NaCl (2.0 M) during the cultivation of *Dunaliella tertiolecta* caused a rise in intracellular lipids and TAGs (Xu and Beardall, 1997). As the salt concentration increases from 0.4 M to 4 M, the percent of total SFA and MUFA increases with decrease in PUFA in *Dunaliella* sp. (Xu and Beardall, 1997). The study mentioned above was further confirmed by Chen et al. (2008), where they concluded that when salt concentration increases from 10 to 20 g/L, both neutral lipids as well as polar lipids enhanced sharply, whereas neutral lipids accumulation dropped at and above 30 g/L. Cells exposed to high concentrations of salt results in increased accumulation of FA both SFA and MUFA.

The type of salt exposed to microalgae generates stress which has its own effect on algal cells. For example, in the study conducted by Srivastava and Goud (2017), *Desmodesmus* GS12 (KR905187) and *Chlorella sorokiniana* CG12(KR905186) were cultivated in NaCl, $MgCl_2$, KCl, and $CaCl_2$. Lipid production increased in both GS12 (44.97%) and CG12 (40.02%) upon treatment with $CaCl_2$, revealing Ca^{2+} as an essential element in cell signaling and its role in lipid synthesis. A similar work was carried out by Anand et al. (2019), in

which *Scenedesmus vacuolatus* was cultivated in NaCl, $MgCl_2.6H_2O$ and $CaCl.2H_2O$ in the concentration range of 10, 30, 50, 70 and 100 mM. It was concluded that NaCl has the least impact on biomass accumulation as compared to other salts studied. NaCl and $MgCl_2.6H_2O$ showed high accumulation of neutral lipids as indicated through Nile red fluorescence intensity. Besides this, increased SFA with decrease in PUFA was also observed. Other studies on *Botryococcus braunii* (Rao et al., 2007), *Cladophora Vagabunda* (Elenkov et al., 1996), *Desmodesmus abundans* (Xia, et al., 2014), *Scenedesmus obliquus* and *Chlamydomonas Mexicana* (Salama et al., 2013) also indicated an increase in saturated fatty acid (SFA) rather than polyunsaturated fatty acid (PUFA).

1.11.4 Effect of pH and potentially toxic metals

Acidity or basicity of culture media is an added component that specifically alters the microalga growth profile and its composition. Accessibility and addition of heavy metals or microelements such as iron, manganese, cobalt, and carbon also affect pH value, ultimately affecting the growth rate and fatty acid composition (Cheng and He, 2014). Table 1.6. represents summary of few studies carried on different algal species under varying pH to enhance lipid accumulation. pH of the microalgae culture system rises during daytime due to photosynthesis and uptake of CO_2, and just opposite phenomena occur at night showing decrease in pH level due to respiration. CO_2 or any other carbon source in culture media is one of the main reasons behind rise in pH level (Havlik et al., 2013).

Table 1.5: Lipid accumulation in microalgae at varying salt and pH expsoure

Microalgae	Salt treatment	Lipid profile after treatment	Reference
Dunaliella salina	29 to 205 g/L sodium chloride	Improved C18 FA	Azachi et al., 2002
Dunaliella tertiolecta	29 g/L to 58 g/L sodium chloride	Enhanced lipid content and TAG accumulation	Takagi & Yoshida., 2006
Dunaliella sp.	sodium chloride treatment from 23 to 234 g/L	Increased total FA and monounsaturated FA	Xu &Beardall., 1997
Nitzschia laevis	Sodium chloride cocentration from 10 to 20 g/L	Increased unsaturated FA	Chen et al., 2008
Crythecodinium cohnii ATCC 30556	Sodium chloride at 9 g/L	Rise in DHA and total FA content	Jiang & Chen., 1999
Schizochytrium limacinum	Salt concentration (9 to 36 g/L) and at a temperature range of 16–30°C	Rise in C15:0 and C17:0 occus	Zhu et al., 2007
Unidentified Chlamydomonas sp.	Low pH	Increased in saturated fatty acid	Tatsuzawa et al., 1996
Chlorella sp.	alkaline pH	Increased TAGs	Guckert& Cooksey., 1990

SFA were found to be produced in high amounts with decrease in glycolipids under alkaline pH in microalgae. Such treatment condition hardly depends upon the availability of nitrogen or carbon levels. A decrease in total lipids with rise in SFA (C16:0) and MUFA (C18:1) was observed by Guckert et al. in 1990. Thus, high or low pH variation may result in high SFA production in membrane signifying an adaptive response to reduce membrane fluidity. *Tetraselmis*, *Isochrysis* and *Nannochloropsis* can be sustained within the pH range of 6.75–

7.25 with CO_2 injections, while control condition reaches the pH of 8.25 within 15 days (Abu-Rezq et al., 1999). Different species might have different responses at varying pH values. However, the most appropriate pH value for microalgae growth lies in the range of 7–9. The ideal pH range for microalgae cell density varies by strain and is very small.

Lipid synthesis is also considerably harm by the pH value. It was analyzed that high lipid accumulation occurs in the pH range of 7-9.5 in most microalgae species. Rai et al. (2015) claimed 23 percent improvement in lipid content at pH 8 with highest biomass at pH 7 in *Chlorella* sp. Similarly, Zhang et al. (2014) examined high lipid content at an initial pH of 7.0. However, TGAs significantly enhanced up to 63.0 percent at pH of 5.0, and the highest biomass was produced at pH 9. Although the fatty acid synthesis enhanced significantly with pH, the total TAGs and biomass production did not alter considerably at varying pH (5-9) range.

Besides pH, trace metals concentration also significantly alters the cell density, carbohydrates and lipid concentration in various algal species. However, as claimed by various studies, it can be finalized that heavy metals' efficiency depends on their content in the media compostion, their co-operative interaction or opposed impacts with other environmental factors and species type. Many studies were showing the effect of heavy metals on lipid content in various microalgae species. Liu et al. (2008) cultivated *Scenedesmus* in an iron incorporated media showing 28.2 percent lipid enhancement while magnesium mixed with calcium and EDTA in culture media showed a 29.7 percent increase in lipid content. *Chlorella vulgaris* upon treatment with iron showed enhanced lipid content up to 56.6 percent (Einicker-Lamas et al., 1996). In addition to iron, there are few other potentially toxic metals such as zinc, cadmium and copper which enhanced the lipid content in *Euglena gracilis* (Einicker-Lamas et al., 2002). Li et al. (2013) observed high biomass (6.47 g/L) and lipid content (5.78 g/L) in *Chlorella protothecoides* upon copper treatment

and concluded that copper-induced lipid synthesis in *Chlorella* get affected both quantitatively and qualitatively.

Copper (4 mg/L) has also been observed for high production of fatty acids in *Chlorella pyrenoidosa*, *C. vulgaris*, *C. protothecoides* (Sibi et al., 2014). Heavy metals have shown a significant influence on fatty acid composition as well as in fatty acid content. Similarly, Rocchetta et al. (2006) observed increase in saturated fatty acid upon treatment with elevated concentration of heavy metals. Heavy metal treatment enables cells to accumulate more carbon from the media and deflect carbon flux to produce lipids with a high proportion of saturated fatty (C14:0, C16:0 and C18:0) acids in comparison to polyunsaturated fatty acids. In spite of that, metal treatment is not alone responsible for variation in fatty acid composition but is also influenced by other ingredients. For instance, the co-operative impact of low-CO_2 exposure along with iron when compared with elevated CO_2, showed little or negligible impact of iron on fatty acid synthesis having long carbon chain fatty acids in *Chlorella vulgaris.*

1.11.5 Light as lipid inducer

The extent of solar energy captured by the earth's atmosphere is around 3.9×10^6 Mega Joules (MJ) every year. A minor fraction of this energy is diverged into chemical energy (Sajjadi et al., 2018). Microalgae contains green pigment chlorophyll and requires light as a vital source of energy for carrying out photosynthesis. Microalgae can capture light in the wavelength range of 400–700 nm. This visible solar energy reaching earth is 43 percentof the total light energy. As a result, exposure to appropriate light intensity and light energy are the key elements that can influence or even regulate lipid and biomass production in algal species.

Another important parameter which affects both biomass and lipid production (Table 1.6) is the light and dark (L-D) cycle. These (L-D) cycle can also alter the biochemical arrangement of algal species. Consequently, variation and optimization of L-D cycles significantly

improve photosynthetic competence along with algal lipid and biomass productivity. Wahidin et al. (2013) examined high lipid content and growth rate of *Nannochloropsis* sp. with change in L-D cycle from 12:12 to18:06.

Increase in light intensity causes decrease in protein content with increased accumulation of lipids as observed in *Dunaliela tertiolecta*. However, this phenomenon exhibits up to light saturation level only (Cuhel et al., 1984). Morris et al. (1974) further concluded that *Phaeodactylum tricornutum*, a marine diatom, cultivated at low light intensity of ~400 Lux led to high protein synthesis. It was further revealed that high light intensity results in increased production polysaccharides (extracellular), while low light intensity results in higher protein synthesis (Krzemińska et al., 2014). Besides varying light intensity, presence or absence of light also plays a extensive role in growth as well as lipid profiling. *D. virdis* cultivated in the absence of light results in enhanced production of total lipids, along with decrease in TAGs, free alcohols, free FA, and sterols (Wahidin et al., 2013). In 1989, identical results were concluded by Sukenik et al. where *Nannochloropsis* sp. was cultured under low light intensity ($35\mu mol/m^2/s^1$) and found 40 percent increment in total lipids, which is composed of galactolipids as the main ingredient along with TAGs. In an earlier study, it was proved that increased light intensity causes oxidative stress leading to damage of PUFA and results in increased accumulation of TAGs (Khotimchenko and Yakovleva, 2005). High light intensity induces synthesis of C16:1 (3 trans) FA with alteration in the total content of FAs in microalgae. It was discovered that polar lipids formation generally occurs at low light intensity. High light intensity causes a rapid increase in the number of storage lipids, primarily TAGs, while lowering total polar lipid content (Pessoa, 2012).

Table 1.6: Lipid stimulation at varying light intensity

Microalgae	Irradiation	Alteration in lipid profile	Reference
Tichocarpus crinitus	Low light intensity	Enhanced TAGs	Khotimchenko&Yakovleva., 2005
Pavlova lutheri	Increased light	Improved lipid accumulation	Carvalho &Malcata., 2005
Thalassiosira pseudonana	Constant (L-D) cycle stable light at log phase	Enhanced TAGs and PUFA	Brown et al., 1996
Unidentified diatoms	Minute light (2 µmol photons $/m^2/s^1$)	Upto 50 percent increase in MGDG	Mock & Kroon., 2002
Selenastrum capricornutum	Dark condition	Upsurge in linoleate FA	MaLarnon et al., 1998
Nannochloropsis oculata	UV-A rays	Rise in PUFA, structural lipids	Srinivas & Ochs., 2012
Phaeodactylum tricornutum	UV radiation	Improved PUFA and EPA	Ling et al., 2006
Chaetoceros muelleri	UV-A rays	Enhanced monounsaturated FA	Liang et al., 2006

Every organism has an inbuilt mechanism to deal with stress conditions. Similarly, microalgal species accumulate more TAGs under excessive light stress or any other stress since they act as shields. As mentioned above, electron acceptor required for photosynthetic machinery might get damaged during stress environment. Improved fatty acid production is collected as TAGs, possibly facilitating the cells to re-create or produce its electron acceptor pool.

Ultraviolet light (215–400 nm) severely disturbs the algal metabolic system mainly by damage to the photosynthetic machinery. There are two types of UV rays (UV-B, 215-380 nm and UV-A, 380-400 nm), UV-B is more lethal and cause severe damage to cells than

UV-A radiation, even at the same intensity (Xue et al., 2005). UV-B rays directly impact cellular DNA and cause a significant injury, while UV-A has indirect effects by releasing ROS (reactive oxygen species) and free OH° (hydroxyl radicals). It was observed that UV-A rays under mild intensity could promote photosynthesis while UV-B rays even at low intensity have a lethal impact. Algae cells protect themselves from damage caused by UV radiation by synthesizing few carotenoids, pigments, or developing some protective cell wall by enhancing lipid content or through migration (Rastogi and Incharoensakdi, 2013; Tsukagoshi, 2012).

1.11.6 Hydrogen peroxide exposure

Hydrogen peroxide, a well-known oxidative stress inducer, is also used to increase lipid production in microalgae. Several studies were conducted to monitor the impact of H_2O_2 on algal biomass, lipids and FAME to understand its relevance towards biofuel production (Sivaramakrishnan and Incharoensakdi, 2017; Battah et al., 2015; Burch and Franz, 2016). Biomass production decreases with increase in the concentration of H_2O_2 as monitored by Sivaramakrishnan & Incharoensakdi (2017). This study revealed that H_2O_2 concentration greater than 3 mM had severely affected the biomass and cause a sharp decline in biomass and growth profile. A parallel examination was conducted by Yilancioglu et al. (2014), showing a decline in cell survival (20 percent) at 4 mM H_2O_2 concentration as analyzed in newly isolated strain of *Dunaliella salina* Tuz_KS_01. Treatment of cell with H_2O_2 affects the photosynthesis efficiency and growth rate of algal species. Although unlike other stress, H_2O_2 is also involved in lipid induction e.g. *Caenorhabditis elegans* and *Saccharomyces cerevisiae*; however, the mechanism behind it is still in question (Solovchenko, 2012). H_2O_2 (2 mM) treated *Scenedesmus* sp. revealed a rise in lipid content of around 55 to 60 percent of DCW (Sivaramakrishnan and Incharoensakdi, 2017). Biosynthesis of lipids requires more energy in contrast to proteins and carbohydrates synthesis. Therefore, under any stress implemented for lipid production, the electron flux is instructed

with additional electrons consumption to lessen the ROS production as a defensive mechanism (Solovchenko, 2012). Accumulation of excessive intracellular ROS in algae creates injury via damaging cellular organelle. Though, algal cells are capable of overcoming such damage through the activation of an antioxidative defence system. Kang et al. (2014) used H_2O_2 as oxidative stress inducer for lipid accumulation in *Chlorella vulgaris*. Yilancioglu et al. (2014) further concluded that oxidative stress enhances intracellular lipid accumulation by 44% with exogenous H_2O_2.

1.12 Algae biodiesel properties

As detailed above fatty acids/oil or algal lipids undergo transesterification reaction to produce biodiesel. Algae oil contains a mixture of polyunsaturated, saturated and monosaturated fatty acids, which affects biodiesel quality (Sharma et al., 2008). “Monoalkyl esters of long-chain fatty acids obtained from animal fats or organic waste, named B100,” is known as biofuels according to ASTM (ASTM D6751-08, 2008).

Despite the recent weightage giving to algae-based biodiesel as a replacement of fossil fules, there are only a few studies in the literature that identify the fuel properties of algal-derived biofuels. Biodiesel made from *Chlorella protothecoides* was stated to meet ASTM requirements by Miao et al. (2006) and Xu et al., (2006). Francisco et al. (2010) have collected biodiesel from six separate algal species and discovered that they all met European biodiesel requirements.

The composition of FAME influences the qualities of biodiesel. A careful analysis of pure compounds or mixtures of clean compounds helps us in evaluating the relationship between a property's variation and its composition (Chuck et al., 2009; Knothe, 2005). The number of double bond in fatty acid and the chain length fatty acid are the two most essential factors in deciding the fuel properties. Some of the algae-based biodiesel properties are summaried below:

The cetane (CN) number indicates a fuel's autoignition characteristics, which is primarily determined by the hydrocarbon chain. The higher the CN value, the longer the chain of hydrocarbon groups. As a result, feedstocks high in saturated fatty acids have more CN than fuels low in saturated fatty acids. The minimum standard CN value, according to ASTM and European specifications, is 47 and 51.

The amount of I_2 (iodine) that interacts with carbon-carbon double bonds decides the iodine value (IV) related to FAME unsaturation. As per the EN 14214, IV value of 120 I_2g/100g FAME is required to defend the fuel's oxidative stability. Fatty acids with several double bonds have a significant effect on oxidative stability, and IV is a degree of total unsaturation.

For all biodiesel types, specific gravity/density drop within a narrow range of 0.873–0.883 mg/m^3. A density specification of 860–900 kg/m^3 is included in the EN 14214 standard.

There are few cold flow properties which describe the biodiesl qualities at low termperaturer are pour point (PP), cloud point (CP), and cold filter plugging point (CFPP). Because of significant seasonal and regional temperature fluctuations, neither the European nor the US standards have firm requirements for these properties, even though they are essential factors in assessing biodiesel suitability.

The internal friction of one component of a fluid passing over another induces viscosity, which is a measure of resistance to liquid flow. Since it affects the efficiency of fuel injection, viscosity is a crucial property. Higher viscosity usually implies less efficient fuel atomization. (Haşimoğlu et al., 2008). The development of wide droplet sizes, low vaporisation are caused by high viscosity (Ochoterena et al., 2008; Alptekin and Canakci, 2008). As a result, there is less total combustion, more emissions, and more oil dilution..

Fuel volatility is inversely proportional to a flashpoint. The flash point's primary aim is to make sure that fatty acid methyl ester

(FAME) has been cleaned by eliminating surplus methanol, as even minute quantities of methanol residue in FAME can cause the flashpoint to drop dramatically. As per the U.S. standard and European (101°C), the minimum requirements for flashpoint is 93°C and 101°C, respectively.

Design of favored FAME profile has been investigated to optimize biodiesel performance concerning oxidative durability and cold flow (Durrett et al., 2008; Pinzi et al., 2009). The optimum composition of FAME should have comparatively minimal concentration of saturated fatty acid inorder to reduce cold flow problems, oxidative instability can be minimize at low concentration of polyunsaturated fatty acid, and high levels of monounsaturated FA. Oleic (18:1) and palmitoleic (16:1) acid provide the best harmony flanked by cold flow and oxidative stability, without much affecting cetane number (Knothe, 2009; Pinzi et al., 2009). Some laboratories are in progress to modify algal lipids composition to enhance their appropriateness as biodiesel feedstock.

1.13 Gaps in research and opportunities for investigation

Lipids quantity and quality in microalgae is dependent on various environmental factors including nutrients, salinity, temperature, heavy metals, pH, hydrogen peroxide and light exposure etc. Beside these abiotic stresses, lipid synthesis can also be improved through biotic stress. Variations in all these factors above or below optimum levels create stress, which ultimately improves lipid synthesis.

However, enhancement of lipids under stress condition simultaneously decreases biomass production, which is another important factor under consideration. Many studies considered and evaluated the impact of single component stress on lipid enhancement without giving much attention to compromised biomass. Very few reports are available where both biomass and lipid are considered together during optimization process.

High and fast stimulation of lipid biosynthesis can also be achieved through a multicomponent stress system, which may include the combined effect of various chemical or physical stresses. Besides these, the two-stage cultivation system also seems to improve lipids and biomass accumulation with stress exposure to larger number of cells in second phase. Till date various species of microalgae, diatoms or cyanobacteria are explored in context to biodiesel production. But there are many more species, which are not yet famous and known for their biodiesel production potential. Therefore, an in-depth investigation is needed to identify newer strains with high lipid storage and biomass production in context to large-scale production. Thus, to hunt suitable process parameters, it is also necessary to understand and explore various stress conditions as a farming method that will increase the desired molecule synthesis.

1.14 Hypothesis to carry out present study

Algal species are supposed to accumulate more neutral lipids under stress conditions. However, stress provided through complete removal of nutrients is not the ultimate solution, as it will adversely affect the growth of algal species. Additionally, algae have to face multicomponent exposure in the open environment which may further synergistically affect the lipid production. Even indigenously isolated algal species are supposed to perform better and get acclimatized in outdoor environment.

With these key elements, in the current study, indigenously isolated *Scenedesmus* sp. is explored and trained for enhanced lipids and biomass production potential. Higher lipid accumulation without much compromising the biomass is the main objective of this study. Different salts with varying concentrations, presence/absence of important nutrients (N and P) and hydrogen peroxide have been tried in different combinations with short- and long-term exposure strategy under mono and multi-component system. Biomass and chlorophyll accumulation were studied as growth indicators. Biochemical

composition in terms of total lipids and carbohydrates is evaluated to understand carbon channeling. Further detailed FAME profiling and its impact of biodiesel properties gave this study a novel touch/strategy to evaluate the efficiency and future aspects.

Precise aims of the current study were characterized as follows and are discussed in subsequent chapters:

1. Impact of different salts with varying concentrations on indigenously isolated microalgae, *Scenedesmus* sp.
2. Sodium chloride as lipid inducer under nutrients repleted/depleted conditions- chronic exposure to understand long-term effects.
3. Effect of Hydrogen peroxide and nutrients to understand growth behaviour and FAME profile of the studied strain- acute exposure for short-term duration.
4. Multicomponent environment to estimate biomass and lipid content of studied strain.

References

Aaronson, S. (1973). Effect of incubation temperature on the macromolecular and lipid content of the phytoflagellate *ochromonas danica* 1. Journal of Phycology, 9(1), 111-113.

Abdelaziz, A. E., Leite, G. B., & Hallenbeck, P. C. (2013). Addressing the challenges for sustainable production of algal biofuels: II. Harvesting and conversion to biofuels. Environmental Technology, 34(13-14), 1807-1836.

Abomohra, A. E. F., El-Sheekh, M., & Hanelt, D. (2017). Screening of marine microalgae isolated from the hypersaline Bardawil lagoon for biodiesel feedstock. Renewable Energy, 101, 1266-1272.

Abu-Rezq, T. S., Al-Musallam, L., Al-Shimmari, J., & Dias, P. (1999). Optimum production conditions for different high-quality marine algae. Hydrobiologia, 403, 97-107.

Adams, C., Godfrey, V., Wahlen, B., Seefeldt, L., & Bugbee, B. (2013). Understanding precision nitrogen stress to optimize the growth and lipid content tradeoff in oleaginous green microalgae. Bioresource Technology, 131, 188-194.

Ajjawi, I., Verruto, J., Aqui, M., Soriaga, L. B., Coppersmith, J., Kwok, K., ... & Carlson, T. J. (2017). Lipid production in *Nannochloropsis gaditana* is doubled by decreasing expression of a single transcriptional regulator. Nature Biotechnology, 35(7), 647-652.

Alonso Azov, Y. (1982). Effect of pH on inorganic carbon uptake in algal cultures. Applied and Environmental Microbiology, 43(6), 1300-1306.

Alonso, D. L., Belarbi, E. H., Fernández-Sevilla, J. M., Rodríguez-Ruiz, J., & Grima, E. M. (2000). Acyl lipid composition variation related to culture age and nitrogen concentration in continuous

culture of the microalga *Phaeodactylum tricornutum*. Phytochemistry, 54(5), 461-471.

Alptekin, E., & Canakci, M. (2008). Determination of the density and the viscosities of biodiesel–diesel fuel blends. Renewable Energy, 33(12), 2623-2630.

Anand, V., Kashyap, M., Samadhiya, K., Ghosh, A., & Kiran, B. (2019). Salinity driven stress to enhance lipid production in *Scenedesmus vacuolatus*: A biodiesel trigger?. Biomass and Bioenergy, 127, 105252.

Andersson, M. X., Stridh, M. H., Larsson, K. E., Liljenberg, C., & Sandelius, A. S. (2003). Phosphate-deficient oat replaces a major portion of the plasma membrane phospholipids with the galactolipid digalactosyldiacylglycerol. FEBS Letters, 537(1-3), 128-132.

Arisz, S. A., van Himbergen, J. A., Musgrave, A., van den Ende, H., & Munnik, T. (2000). Polar glycerolipids of *Chlamydomonas moewusii*. Phytochemistry, 53(2), 265-270.

ASTM D6751-08 (2008). Standard Specification for Biodiesel Fuel Blend Stock (B100) for Middle Distillate Fuels, ASTM International, West Conshohocken, PA. DOI: 10.1520/D6751-08.

Axelsson, M., & Gentili, F. (2014). A single-step method for rapid extraction of total lipids from green microalgae. PloS One, 9(2), e89643.

Azachi, M., Sadka, A., Fisher, M., Goldshlag, P., Gokhman, I., & Zamir, A. (2002). Salt induction of fatty acid elongase and membrane lipid modifications in the extreme halotolerant alga *Dunaliella salina*. Plant Physiology, 129(3), 1320-1329.

Bagnato, C., Prados, M. B., Franchini, G. R., Scaglia, N., Miranda, S. E., & Beligni, M. V. (2017). Analysis of triglyceride synthesis unveils a green algal soluble diacylglycerol acyltransferase and

provides clues to potential enzymatic components of the chloroplast pathway. BMC Genomics, 18(1), 223.

Bahadar, A., & Khan, M. B. (2013). Progress in energy from microalgae: a review. Renewable and Sustainable Energy Reviews, 27, 128-148.

Banerjee, A., Maiti, S. K., Guria, C., & Banerjee, C. (2017). Metabolic pathways for lipid synthesis under nitrogen stress in *Chlamydomonas* and *Nannochloropsis*. Biotechnology Letters, 39(1), 1-11.

Barros, A. I., Gonçalves, A. L., Simões, M., & Pires, J. C. (2015). Harvesting techniques applied to microalgae: a review. Renewable and Sustainable Energy Reviews, 41, 1489-1500.

Battah, M., El-Ayoty, Y., Abomohra, A. E. F., Abd El-Ghany, S., & Esmael, A. (2015). Effect of Mn^{2+}, Co^{2+} and H_2O_2 on biomass and lipids of the green microalga *Chlorella vulgaris* as a potential candidate for biodiesel production. Annals of Microbiology, 65(1), 155-162.

Bellou, S., & Aggelis, G. (2013). Biochemical activities in *Chlorella* sp. and *Nannochloropsis salina* during lipid and sugar synthesis in a lab-scale open pond simulating reactor. Journal of Biotechnology, 164(2), 318-329.

Bilad, M. R., Arafat, H. A., & Vankelecom, I. F. (2014). Membrane technology in microalgae cultivation and harvesting: a review. Biotechnology Advances, 32(7), 1283-1300.

Bligh, E.G., Dyer, W.J., (1959). A rapid method of total lipid extraction and purification. Canadian Journal of Biochemistry Physiology, 37(8), 911-7.

Boussiba, S., Vonshak, A., Cohen, Z., Avissar, Y., & Richmond, A. (1987). Lipid and biomass production by the halotolerant microalga *Nannochloropsis salina*. Biomass, 12(1), 37-47.

Brennan, L., & Owende, P. (2010). Biofuels from microalgae—a review of technologies for production, processing, and extractions of biofuels and co-products. Renewable and Sustainable Energy Reviews, 14(2), 557-577.

Brown, M. R., Dunstan, G. A., Norwood, S. J., & Miller, K. A. (1996). Effects of harvest stage and light on the biochemical composition of the diatom *Thalassiosira pseudonana* 1. Journal of Phycology, 32(1), 64-73.

Burch, A. R., & Franz, A. K. (2016). Combined nitrogen limitation and hydrogen peroxide treatment enhances neutral lipid accumulation in the marine diatom *Phaeodactylum tricornutum*. Bioresource Technology, 219, 559-565.

Byreddy, A. R., Gupta, A., Barrow, C. J., & Puri, M. (2016). A quick colorimetric method for total lipid quantification in microalgae. Journal of Microbiological Methods, 125, 28-32.

Callow, J. A. (1999). Advances in botanical research. Elsevier.

Carvalho, A. P., & Malcata, F. X. (2005). Optimization of ω-3 fatty acid production by microalgae: crossover effects of CO_2 and light intensity under batch and continuous cultivation modes. Marine Biotechnology, 7(4), 381-388.

Chen, G. Q., Jiang, Y., & Chen, F. (2008). Salt-induced alterations in lipid composition of diatom *Nitzschia laevis* (Bacillariophyceae) under heterotrophic culture condition 1. Journal of Phycology, 44(5), 1309-1314.

Chen, X., Hu, G., & Liu, L. (2018). Hacking an algal transcription factor for lipid biosynthesis. Trends in Plant Science, 23(3), 181-184.

Cheng, D., & He, Q. (2014). Assessment of environmental stresses for enhanced microalgal biofuel production–an overview. Frontiers in Energy Research, 2, 26.

Chisti, Y. (2007). Biodiesel from microalgae. Biotechnology Advances, 25(3), 294-306.

Chisti, Y. (2008). Biodiesel from microalgae beats bioethanol. Trends in Biotechnology, 26(3), 126-131.

Chiu, S. Y., Kao, C. Y., Tsai, M. T., Ong, S. C., Chen, C. H., & Lin, C. S. (2009). Lipid accumulation and CO_2 utilization of *Nannochloropsis oculata* in response to CO_2 aeration. Bioresource Technology, 100(2), 833-838.

Chuck, C. J., Bannister, C. D., Hawley, J. G., Davidson, M. G., La Bruna, I., & Paine, A. (2009). Predictive model to assess the molecular structure of biodiesel fuel. Energy & Fuels, 23(4), 2290-2294.

Converti, A., Casazza, A. A., Ortiz, E. Y., Perego, P., & Del Borghi, M. (2009). Effect of temperature and nitrogen concentration on the growth and lipid content of *Nannochloropsis oculata* and *Chlorella vulgaris* for biodiesel production. Chemical Engineering and Processing: Process Intensification, 48(6), 1146-1151.

Courchesne, N. M. D., Parisien, A., Wang, B., & Lan, C. Q. (2009). Enhancement of lipid production using biochemical, genetic and transcription factor engineering approaches. Journal of Biotechnology, 141(1-2), 31-41.

Cuhel, R. L., Ortner, P. B., & Lean, D. R. (1984). Night synthesis of protein by algae 1. Limnology and Oceanography, 29(4), 731-744.

Dean, A. P., Sigee, D. C., Estrada, B., & Pittman, J. K. (2010). Using FTIR spectroscopy for rapid determination of lipid accumulation in response to nitrogen limitation in freshwater microalgae. Bioresource Technology, 101(12), 4499-4507.

Demetriou, G., Neonaki, C., Navakoudis, E., & Kotzabasis, K. (2007). Salt stress impact on the molecular structure and function of the photosynthetic apparatus—the protective role of polyamines. Biochimica et Biophysica Acta (BBA)-Bioenergetics, 1767(4), 272-280.

dos Santos, R. R., Moreira, D. M., Kunigami, C. N., Aranda, D. A. G., & Teixeira, C. M. L. L. (2015). Comparison between several methods of total lipid extraction from *Chlorella vulgaris* biomass. Ultrasonics Sonochemistry, 22, 95-99.

Dragone, G., Fernandes, B. D., Vicente, A. A., & Teixeira, J. A. (2010). Third generation biofuels from microalgae.

Durrett, T. P., Benning, C., & Ohlrogge, J. (2008). Plant triacylglycerols as feedstocks for the production of biofuels. The Plant Journal, 54(4), 593-607.

Einicker-Lamas, M., Mezian, G. A., Fernandes, T. B., Silva, F. L. S., Guerra, F., Miranda, K., ... & Oliveira, M. M. (2002). *Euglena gracilis* as a model for the study of Cu^{2+} and Zn^{2+} toxicity and accumulation in eukaryotic cells. Environmental Pollution, 120(3), 779-786.

Einicker-Lamas, M., Soares, M. J., Soares, M. S., & Oliveira, M. M. (1996). Effects of cadmium on *Euglena gracilis* membrane lipids. Brazilian Journal of Medical and Biological Research= Revista brasileira de pesquisas medicas e biologicas, 29(8), 941-948.

Elenkov, I., Stefanov, K., Dimitrova-Konaklieva, S., & Popov, S. (1996). Effect of salinity on lipid composition of *Cladophora vagabunda*. Phytochemistry, 42(1), 39-44.

El-Sheek, M. M., & Rady, A. A. (1995). Effect of phosphorus starvation on growth, photosynthesis and some metabolic processes in the unicellular green alga *Chlorella kessleri*. Phyton.

Fakhry, E. M., & El Maghraby, D. M. (2015). Lipid accumulation in response to nitrogen limitation and variation of temperature in *Nannochloropsis salina*. Botanical Studies, 56(1), 6.

Fan, H., Smuts, J., Bai, L., Walsh, P., Armstrong, D. W., & Schug, K. A. (2016). Gas chromatography–vacuum ultraviolet spectroscopy for analysis of fatty acid methyl esters. Food Chemistry, 194, 265-271.

Folch, J., Lees, M., & Stanley, G. S. (1957). A simple method for the isolation and purification of total lipides from animal tissues. Journal of Biological Chemistry, 226(1), 497-509.

Francisco, E. C., Neves, D. B., Jacob-Lopes, E., & Franco, T. T. (2010). Microalgae as feedstock for biodiesel production: carbon dioxide sequestration, lipid production and biofuel quality. Journal of Chemical Technology & Biotechnology, 85(3), 395-403.

Furuhashi, T., Nakamura, T., Fragner, L., Roustan, V., Schön, V., & Weckwerth, W. (2016). Biodiesel and poly-unsaturated fatty acids production from algae and crop plants–a rapid and comprehensive workflow for lipid analysis. Biotechnology Journal, 11(10), 1262-1267.

Gardner, R., Peters, P., Peyton, B., & Cooksey, K. E. (2011). Medium pH and nitrate concentration effects on accumulation of triacylglycerol in two members of the chlorophyta. Journal of Applied Phycology, 23(6), 1005-1016.

Gilmour, D. J., & Zimmerman, W. B. (2012). Can algal biofuels play a major role in meeting future energy needs?.

Gonen, T., Cheng, Y., Sliz, P., Hiroaki, Y., Fujiyoshi, Y., Harrison, S.C., Walz, T. (2005). Lipid-protein interactions in double-layered two-dimensional AQP0 crystals. Nature, 438(7068), 633-8.

Gouveia, L., & Oliveira, A. C. (2009). Microalgae as a raw material for biofuels production. Journal of Industrial Microbiology & Biotechnology, 36(2), 269-274.

Griffiths, M. J., & Harrison, S. T. (2009). Lipid productivity as a key characteristic for choosing algal species for biodiesel production. Journal of Applied Phycology, 21(5), 493-507.

Guckert, J. B., & Cooksey, K. E. (1990). Triglyceride accumulation and fatty acid profile changes in *Chlorella* (Chlorophyta) during high Ph-induced cell cycle Inhibition 1. Journal of Phycology, 26(1), 72-79.

Gunstone, F. D., & Harwood, J. L. (2007). Lipid metabolism. In The Lipid Handbook with CD-ROM (pp. 651-716). CRC Press.

Gurr M.I., Harwood J.L., Frayn K.N. (2002) Lipid biochemistry. An Introduction, 5th edition. Blackwell, Oxford, 320 pp

Gusbeth, C. A., Eing, C., Göttel, M., Sträßner, R., & Frey, W. (2016). Fluorescence diagnostics for lipid status monitoring of microalgae during cultivation. International Journal of Renewable Energy Biofuels, 2016, 1-12.

Guschina, I. A., & Harwood, J. L. (2006). Lipids and lipid metabolism in eukaryotic algae. Progress in Lipid Research, 45(2), 160-186.

Han, X., & Gross, R. W. (2005). Shotgun lipidomics: electrospray ionization mass spectrometric analysis and quantitation of cellular lipidomes directly from crude extracts of biological samples. Mass Spectrometry Reviews, 24(3), 367-412.

Härtel, H., Dörmann, P., & Benning, C. (2000). DGD1-independent biosynthesis of extraplastidic galactolipids after phosphate deprivation in Arabidopsis. Proceedings of the National Academy of Sciences, 97(19), 10649-10654.

Haşimoğlu, C., Ciniviz, M., Özsert, İ., İçingür, Y., Parlak, A., & Salman, M. S. (2008). Performance characteristics of a low heat rejection diesel engine operating with biodiesel. Renewable Energy, 33(7), 1709-1715.

Havlik, I., Lindner, P., Scheper, T., & Reardon, K. F. (2013). On-line monitoring of large cultivations of microalgae and cyanobacteria. Trends in Biotechnology, 31(7), 406-414.

Hema, R., Senthil-Kumar, M., Shivakumar, S., Reddy, P. C., & Udayakumar, M. (2007). *Chlamydomonas reinhardtii*, a model system for functional validation of abiotic stress responsive genes. Planta, 226(3), 655-670.

Hsieh, C. H., & Wu, W. T. (2009). Cultivation of microalgae for oil production with a cultivation strategy of urea limitation. Bioresource Technology, 100(17), 3921-3926.

Hu, Q., Sommerfeld, M., Jarvis, E., Ghirardi, M., Posewitz, M., Seibert, M., & Darzins, A. (2008). Microalgal triacylglycerols as feedstocks for biofuel production: perspectives and advances. The Plant Journal, 54(4), 621-639.

Hu, Q., Zhang, C., & Sommerfeld, M. (2006,). Biodiesel from algae: lessons learned over the past 60 years and future perspectives. In Journal of Phycology (Vol. 42, pp. 12-12). 9600.

Huertas, I. E., Rouco, M., Lopez-Rodas, V., & Costas, E. (2011). Warming will affect phytoplankton differently: evidence through a mechanistic approach. Proceedings of the Royal Society B: Biological Sciences, 278(1724), 3534-3543.

Hughes, A. D., Kelly, M. S., Black, K. D., & Stanley, M. S. (2012). Biogas from Macroalgae: is it time to revisit the idea?. Biotechnology for Biofuels, 5(1), 86.

Hulatt, C. J., Wijffels, R. H., Bolla, S., & Kiron, V. (2017). Production of fatty acids and protein by *Nannochloropsis* in flat-plate photobioreactors. PloS One, 12(1), e0170440.

Illman, A. M., Scragg, A. H., & Shales, S. W. (2000). Increase in *Chlorella strains* calorific values when grown in low nitrogen medium. Enzyme and Microbial Technology, 27(8), 631-635.

Janssen, M., Tramper, J., Mur, L. R., & Wijffels, R. H. (2003). Enclosed outdoor photobioreactors: Light regime, photosynthetic efficiency, scale-up, and future prospects. Biotechnology and Bioengineering, 81(2), 193-210. ss

Jiang, H., & Gao, K. (2004). Effects of lowering temperature during culture on the production of polyunsaturated fatty acids in the marine diatom *Phaeodactylum tricornutum* (Bacillariophyceae) 1. Journal of Phycology, 40(4), 651-654.

Jiang, Y., & Chen, F. (1999). Effects of salinity on cell growth and docosahexaenoic acid content of the heterotrophic marine microalga *Crypthecodinium cohnii*. Journal of Industrial Microbiology and Biotechnology, 23(6), 508-513.

Joh, T., Yoshida, T., Yoshimoto, M., Miyamoto, T., & Hatano, S. (1993). Composition and positional distribution of fatty acids in polar lipids from *Chlorella ellipsoidea* differing in chilling susceptibility and frost hardiness. Physiologia Plantarum, 89(2), 285-290.

Johnson, X., & Alric, J. (2013). Central carbon metabolism and electron transport in *Chlamydomonas reinhardtii*: metabolic constraints for carbon partitioning between oil and starch. Eukaryotic Cell, 12(6), 776-793.

Jorquera, O., Kiperstok, A., Sales, E. A., Embiruçu, M., & Ghirardi, M. L. (2010). Comparative energy life-cycle analyses of microalgal

biomass production in open ponds and photobioreactors. Bioresource Technology, 101(4), 1406-1413.

Jouhet, J., Lupette, J., Clerc, O., Magneschi, L., Bedhomme, M., Collin, S., ... & Rebeille, F. (2017). LC-MS/MS versus TLC plus GC methods: consistency of glycerolipid and fatty acid profiles in microalgae and higher plant cells and effect of a nitrogen starvation. PLoS One, 12(8), e0182423.

Kan, G., Shi, C., Wang, X., Xie, Q., Wang, M., Wang, X., & Miao, J. (2012). Acclimatory responses to high-salt stress in *Chlamydomonas* (Chlorophyta, Chlorophyceae) from Antarctica. Acta Oceanologica Sinica, 31(1), 116-124.

Kang, N. K., Lee, B., Choi, G. G., Moon, M., Park, M. S., Lim, J., & Yang, J. W. (2014). Enhancing lipid productivity of *Chlorella vulgaris* using oxidative stress by TiO_2 nanoparticles. Korean Journal of Chemical Engineering, 31(5), 861-867.

Khona, D. K., Shirolikar, S. M., Gawde, K. K., Hom, E., Deodhar, M. A., & D'Souza, J. S. (2016). Characterization of salt stress-induced palmelloids in the green alga, *Chlamydomonas reinhardtii*. Algal Research, 16, 434-448.

Khotimchenko, S. V., & Yakovleva, I. M. (2005). Lipid composition of the red alga *Tichocarpus crinitus* exposed to different levels of photon irradiance. Phytochemistry, 66(1), 73-79.

Khozin-Goldberg, J., Lau, M. C., Smith, G. J., Vijaykrishna, D., Cary, S. C., Lacap, D. C., ... & McKay, C. P. (2011). Ancient origins determine global biogeography of hot and cold desert cyanobacteria. Nature Communications, 2(1), 1-6.

Kiran, B., Kumar, R., & Deshmukh, D. (2014). Perspectives of microalgal biofuels as a renewable source of energy. Energy Conversion and Management, 88, 1228-1244.

Knothe, G. (2005). Van Gerpen, J.. Krahl. J. Ed.

Knothe, G. (2009). Improving biodiesel fuel properties by modifying fatty ester composition. Energy & Environmental Science, 2(7), 759-766.

Krank, J., Murphy, R. C., Barkley, R. M., Duchoslav, E., & McAnoy, A. (2007). Qualitative analysis and quantitative assessment of changes in neutral glycerol lipid molecular species within cells. Methods in Enzymology, 432, 1-20.

Kró, M., Maxwell, D. P., & Huner, N. P. (1997). Exposure of *Dunaliella salina* to low temperature mimics the high light-induced accumulation of carotenoids and the carotenoid binding protein (Cbr). Plant and Cell Physiology, 38(2), 213-216.

Krzemińska, I., Pawlik-Skowrońska, B., Trzcińska, M., & Tys, J. (2014). Influence of photoperiods on the growth rate and biomass productivity of green microalgae. Bioprocess and Biosystems Engineering, 37(4), 735-741.

Levasseur, M. E., Morissette, J. C., Popovic, R., & Harrison, P. J. (1990). Effects of long term exposure to low temperature on the photosynthetic apparatus of *Dunaliella tertiolecta* (Chlorophyceae) 1. Journal of Phycology, 26(3), 479-484.

Li, Y., Han, D., Hu, G., Dauvillee, D., Sommerfeld, M., Ball, S., & Hu, Q. (2010). *Chlamydomonas* starchless mutant defective in ADP-glucose pyrophosphorylase hyper-accumulates triacylglycerol. Metabolic Engineering, 12(4), 387-391.

Li, Y., Han, D., Sommerfeld, M., & Hu, Q. (2011). Photosynthetic carbon partitioning and lipid production in the oleaginous microalga *Pseudochlorococcum* sp. (Chlorophyceae) under nitrogen-limited conditions. Bioresource Technology, 102(1), 123-129.

Li, Y., Mu, J., Chen, D., Han, F., Xu, H., Kong, F., ... & Feng, B. (2013). Production of biomass and lipid by the microalgae

Chlorella protothecoides with heterotrophic-Cu (II) stressed (HCuS) coupling cultivation. Bioresource Technology, 148, 283-292.

Liang, Y., Beardall, J., & Heraud, P. (2006). Effects of nitrogen source and UV radiation on the growth, chlorophyll fluorescence and fatty acid composition of *Phaeodactylum tricornutum* and *Chaetoceros muelleri* (Bacillariophyceae). Journal of Photochemistry and Photobiology B: Biology, 82(3), 161-172.

Lingwood, D., Binnington, B., Róg, T., Vattulainen, I., Grzybek, M., Coskun, Ü., ... & Simons, K. (2011). Cholesterol modulates glycolipid conformation and receptor activity. Nature Chemical Biology, 7(5), 260-262.

Liu, Z. Y., Wang, G. C., & Zhou, B. C. (2008). Effect of iron on growth and lipid accumulation in *Chlorella vulgaris*. Bioresource Technology, 99(11), 4717-4722.

Lynch, D. V., & Thompson, G. A. (1982). Low temperature-induced alterations in the chloroplast and microsomal membranes of *Dunaliella salina*. Plant Physiology, 69(6), 1369-1375.

Lynn, S. G., Kilham, S. S., Kreeger, D. A., & Interlandi, S. J. (2000). Effect of nutrient availability on the biochemical and elemental stoichiometry in the freshwater diatom *Stephanodiscus minutulus* (Bacillariophyceae). Journal of Phycology, 36(3), 510-522.

MacIntyre, H. L., Kana, T. M., Anning, T., & Geider, R. J. (2002). Photoacclimation of photosynthesis irradiance response curves and photosynthetic pigments in microalgae and cyanobacteria 1. Journal of Phycology, 38(1), 17-38.

Maity, J. P., Bundschuh, J., Chen, C. Y., & Bhattacharya, P. (2014). Microalgae for third generation biofuel production, mitigation of

greenhouse gas emissions and wastewater treatment: Present and future perspectives–A mini review. Energy, 78, 104-113.

Markou, G., & Nerantzis, E. (2013). Microalgae for high-value compounds and biofuels production: a review with focus on cultivation under stress conditions. Biotechnology Advances, 31(8), 1532-1542.

Maxwell, D. P., Falk, S., Trick, C. G., & Huner, N. P. (1994). Growth at low temperature mimics high-light acclimation in *Chlorella vulgaris*. Plant Physiology, 105(2), 535-543.

McLarnon-Riches, C. J., Rolph, C. E., Greenway, D. L., & Robinson, P. K. (1998). Effects of environmental factors and metals on *Selenastrum capricornutum* lipids. Phytochemistry, 49(5), 1241-1247.

Merchant, S. S., Kropat, J., Liu, B., Shaw, J., & Warakanont, J. (2012). TAG, You're it! *Chlamydomonas* as a reference organism for understanding algal triacylglycerol accumulation. Current Opinion in Biotechnology, 23(3), 352-363.

Miao, X., & Wu, Q. (2006). Biodiesel production from heterotrophic microalgal oil. Bioresource Technology, 97(6), 841-846.

Mock, T., & Kroon, B. M. (2002). Photosynthetic energy conversion under extreme conditions—II: the significance of lipids under light limited growth in Antarctic sea ice diatoms. Phytochemistry, 61(1), 53-60.

Moreno-Garrido, I. (2008). Microalgae immobilization: current techniques and uses. Bioresource Technology, 99(10), 3949-3964.

Morgan-Kiss, R. M., Priscu, J. C., Pocock, T., Gudynaite-Savitch, L., & Huner, N. P. (2006). Adaptation and acclimation of photosynthetic microorganisms to permanently cold environments. Microbiology and Molecular Biology Reviews, 70(1), 222-252.

Morris, I., Glover, H. E., & Yentsch, C. S. (1974). Products of photosynthesis by marine phytoplankton: the effect of environmental factors on the relative rates of protein synthesis. Marine Biology, 27(1), 1-9.

Mostafa, M., & Amal, A. Effect of Phosphorus Starvation on Growth, Photo-synthesis and Some Metabolic Processes in the Uni-cellular Green Alga *Chlorella kessleri*.

Mühlroth, A., Li, K., Røkke, G., Winge, P., Olsen, Y., Hohmann-Marriott, M. F., ... & Bones, A. M. (2013). Pathways of lipid metabolism in marine algae, co-expression network, bottlenecks and candidate genes for enhanced production of EPA and DHA in species of *Chromista*. Marine Drugs, 11(11), 4662-4697.

Murata, N., Troughton, J. H., & Fork, D. C. (1975). Relationships between the transition of the physical phase of membrane lipids and photosynthetic parameters in *Anacystis nidulans* and lettuce and spinach chloroplasts. Plant Physiology, 56(4), 508-517.

Nakamura, K. A. Z. U. O., Bray, D. F., & Wagenaar, E. B. (1975). Ultrastructure of *Chlamydomonas eugametos* palmelloids induced by chloroplatinic acid treatment. Journal of Bacteriology, 121(1), 338-343.

Neelam, S., & Subramanyam, R. (2013). Alteration of photochemistry and protein degradation of photosystem II from *Chlamydomonas reinhardtii* under high salt grown cells. Journal of Photochemistry and Photobiology B: Biology, 124, 63-70.

Neenan, B. (1986). Fuels from microalgae: Technology status, potential and research requirements. Solar Energy Research Institute.

Nobusawa, T., Hori, K., Mori, H., Kurokawa, K., & Ohta, H. (2017). Differently localized lysophosphatidic acid acyltransferases

crucial for triacylglycerol biosynthesis in the oleaginous alga *Nannochloropsis*. The Plant Journal, 90(3), 547-559.

Norman, H. A., & Thompson Jr, G. A. (1985). Effects of low-temperature stress on the metabolism of phosphatidylglycerol molecular species in *Dunaliella salina*. Archives of Biochemistry and Biophysics, 242(1), 168-175.

Ochoterena, R., Larsson, M., Andersson, S., & Denbratt, I. (2008). Optical studies of spray development and combustion characterization of oxygenated and Fischer-Tropsch fuels (No. 2008-01-1393). SAE Technical Paper.

Ogburn, Z. L., & Vogt, F. (2017). Microalgae as embedded environmental monitors. Analytica chimica acta, 954, 1-13.

Pal, D., Khozin-Goldberg, I., Cohen, Z., & Boussiba, S. (2011). The effect of light, salinity, and nitrogen availability on lipid production by *Nannochloropsis* sp. Applied Microbiology and Biotechnology, 90(4), 1429-1441.

Pessoa, M. F. (2012). Harmful effects of uv radiation in algae and aquatic macrophytes-areview. Emirates Journal of Food and Agriculture, 510-526.

Pinzi, S., Garcia, I. L., Lopez-Gimenez, F. J., Luque de Castro, M. D., Dorado, G., & Dorado, M. P. (2009). The ideal vegetable oil-based biodiesel composition: a review of social, economical and technical implications. Energy & Fuels, 23(5), 2325-2341.

Praveenkumar, R., Shameera, K., Mahalakshmi, G., Akbarsha, M. A., & Thajuddin, N. (2012). Influence of nutrient deprivations on lipid accumulation in a dominant indigenous microalga *Chlorella* sp., BUM11008: Evaluation for biodiesel production. Biomass and Bioenergy, 37, 60-66.

Radakovits, R., Jinkerson, R. E., Darzins, A., & Posewitz, M. C. (2010). Genetic engineering of algae for enhanced biofuel production. Eukaryotic Cell, 9(4), 486-501.

Rai, M. P., Gautom, T., & Sharma, N. (2015). Effect of salinity, pH, light intensity on growth and lipid production of microalgae for bioenergy application. OnLine Journal of Biological Sciences, 15(4), 260. DOI: 10.3844/ojbsci.2015.260.267

Ralser, M., Wamelink, M. M., Kowald, A., Gerisch, B., Heeren, G., Struys, E. A., ... & Krobitsch, S. (2007). Dynamic rerouting of the carbohydrate flux is key to counteracting oxidative stress. Journal of Biology, 6(4), 10.

Rao, A. R., Dayananda, C., Sarada, R., Shamala, T. R., & Ravishankar, G. A. (2007). Effect of salinity on growth of green alga *Botryococcus braunii* and its constituents. Bioresource Technology, 98(3), 560-564.

Rastogi, R. P., & Incharoensakdi, A. (2013). UV radiation-induced accumulation of photoprotective compounds in the green alga *Tetraspora* sp. CU2551. Plant Physiology and Biochemistry, 70, 7-13.

Reitan, K. I., Rainuzzo, J. R., & Olsen, Y. (1994). Effect of nutrient limitation on fatty acid and lipid content of marine microalgae 1. Journal of Phycology, 30(6), 972-979.

Ren, H. Y., Liu, B. F., Kong, F., Zhao, L., Xie, G. J., & Ren, N. Q. (2014). Enhanced lipid accumulation of green microalga *Scenedesmus* sp. by metal ions and EDTA addition. Bioresource Technology, 169, 763-767.

Ren, H. Y., Liu, B. F., Ma, C., Zhao, L., & Ren, N. Q. (2013). A new lipid-rich microalga *Scenedesmus* sp. strain R-16 isolated using Nile red staining: effects of carbon and nitrogen sources and initial

pH on the biomass and lipid production. Biotechnology for Biofuels, 6(1), 143.

Ren, M. L., Boeing, W. J., Dungan, B. N., Holguin, F. O., & Schaub, T. (2014). pH effects on growth and lipid accumulation of the biofuel microalgae *Nannochloropsis salina* and invading organisms. Journal of Applied Phycology, 26(3), 1431-1437.

Renaud, S. M., Thinh, L. V., Lambrinidis, G., & Parry, D. L. (2002). Effect of temperature on growth, chemical composition and fatty acid composition of tropical Australian microalgae grown in batch cultures. Aquaculture, 211(1-4), 195-214.

Richmond, A. (1986). Cell response to the environmental factors. Handbook of Microalgal Mass Culture., 69-99.

Richmond, A. (2004). Biological principles of mass cultivation. Handbook of microalgal culture: Biotechnology and Applied Phycology, 125-177.

Richmond, A. (Ed.). (2017). Handbook of microalgal mass culture (1986). CRC press.

Rocchetta, I., Mazzuca, M., Conforti, V., Ruiz, L., Balzaretti, V., & de Molina, M. D. C. R. (2006). Effect of chromium on the fatty acid composition of two strains of *Euglena gracilis*. Environmental Pollution, 141(2), 353-358.

Rodolfi, L., Chini Zittelli, G., Bassi, N., Padovani, G., Biondi, N., Bonini, G., & Tredici, M. R. (2009). Microalgae for oil: Strain selection, induction of lipid synthesis and outdoor mass cultivation in a low-cost photobioreactor. Biotechnology and Bioengineering, 102(1), 100-112.

Roessler, J. G., Thompson, B. M., McCrum, E. C., & Russell, D. W. (2007). Extraction and analysis of sterols in biological matrices by high performance liquid chromatography electrospray ionization mass spectrometry. Methods in Enzymology, 432, 145-170.

Roessler, P. G., Bleibaum, J. L., Thompson, G. A., & Ohlrogge, J. B. (1994). Characteristics of the gene that encodes acetyl-CoA carboxylase in the diatom *Cyclotella cryptica*. Annals of the New York Academy of Sciences, 721, 250.

Rubio, F. C., Camacho, F. G., Sevilla, J. F., Chisti, Y., & Grima, E. M. (2003). A mechanistic model of photosynthesis in microalgae. Biotechnology and Bioengineering, 81(4), 459-473.

Sajjadi, B., Chen, W. Y., Raman, A. A. A., & Ibrahim, S. (2018). Microalgae lipid and biomass for biofuel production: A comprehensive review on lipid enhancement strategies and their effects on fatty acid composition. Renewable and Sustainable Energy Reviews, 97, 200-232.

Sakthivel, R. (2011). Microalgae lipid research, past, present: a critical review for biodiesel production, in the future. Journal of Experimental Sciences.

Salama, E. S., Kim, H. C., Abou-Shanab, R. A., Ji, M. K., Oh, Y. K., Kim, S. H., & Jeon, B. H. (2013). Biomass, lipid content, and fatty acid composition of freshwater *Chlamydomonas mexicana* and *Scenedesmus obliquus* grown under salt stress. Bioprocess and Biosystems Engineering, 36(6), 827-833.

Sato, N., & Murata, N. (1980). Temperature shift-induced responses in lipids in the blue-green alga, *Anabaena variabilis*: the central role of diacylmonogalactosylglycerol in thermo-adaptation. Biochimica et Biophysica Acta (BBA)-Lipids and Lipid Metabolism, 619(2), 353-366.

Sato, N., Hagio, M., Wada, H., & Tsuzuki, M. (2000). Environmental effects on acidic lipids of thylakoid membranes.

Schuhmann, H., Lim, D. K., & Schenk, P. M. (2012). Perspectives on metabolic engineering for increased lipid contents in microalgae. Biofuels, 3(1), 71-86.

Sharma, K. K., Schuhmann, H., & Schenk, P. M. (2012). High lipid induction in microalgae for biodiesel production. Energies, 5(5), 1532-1553.

Sharma, S. K., Nelson, D. R., Abdrabu, R., Khraiwesh, B., Jijakli, K., Arnoux, M., ... & Jagannathan, R. (2015). An integrative Raman microscopy-based workflow for rapid in situ analysis of microalgal lipid bodies. Biotechnology for Biofuels, 8(1), 1-14.

Sharma, Y. C., Singh, B., & Upadhyay, S. N. (2008). Advancements in development and characterization of biodiesel: a review. Fuel, 87(12), 2355-2373.

Sheehan, J., Dunahay, T., Benemann, J., & Roessler, P. (1998). A look back at the US Department of Energy's aquatic species program: biodiesel from algae. National Renewable Energy Laboratory, 328, 1-294.

Sibi, G., Anuraag, T. S., & Bafila, G. (2014). Copper stress on cellular contents and fatty acid profiles in *Chlorella* species. Online Journal of Biological Sciences, 14, 209-217.

Singh, G., & Patidar, S. K. (2018). Microalgae harvesting techniques: A review. Journal of Environmental Management, 217, 499-508.

Singh, S. C., Sinha, R. P., & Hader, D. P. (2002). Role of lipids and fatty acids in stress tolerance in cyanobacteria. Acta Protozoologica, 41(4), 297-308.

Singh, S. P., & Singh, P. (2015). Effect of temperature and light on the growth of algae species: a review. Renewable and Sustainable Energy Reviews, 50, 431-444.

Sivakumar, G., Xu, J., Thompson, R. W., Yang, Y., Randol-Smith, P., & Weathers, P. J. (2012). Integrated green algal technology for bioremediation and biofuel. Bioresource Technology, 107, 1-9.

Sivaramakrishnan, R., & Incharoensakdi, A. (2017). Enhancement of lipid production in *Scenedesmus* sp. by UV mutagenesis and hydrogen peroxide treatment. Bioresource Technology, 235, 366-370.

Skrupski, B., Wilson, K. E., Goff, K. L., & Zou, J. (2013). Effect of pH on neutral lipid and biomass accumulation in microalgal strains native to the Canadian prairies and the Athabasca oil sands. Journal of Applied Phycology, 25(4), 937-949.

Slabas, A. R., & Fawcett, T. (1992). The biochemistry and molecular biology of plant lipid biosynthesis. Plant Molecular Biology, 19(1), 169-191.

Solovchenko, A. E. (2012). Physiological role of neutral lipid accumulation in eukaryotic microalgae under stresses. Russian Journal of Plant Physiology, 59(2), 167-176.

Solovchenko, A. E., Khozin-Goldberg, I., Didi-Cohen, S., Cohen, Z., & Merzlyak, M. N. (2008). Effects of light and nitrogen starvation on the content and composition of carotenoids of the green microalga *Parietochloris incisa*. Russian Journal of Plant Physiology, 55(4), 455-462.

Somerville, C. (1995). Direct tests of the role of membrane lipid composition in low-temperature-induced photoinhibition and chilling sensitivity in plants and cyanobacteria. Proceedings of the National Academy of Sciences of the United States of America, 92(14), 6215.

Srinivas, R., & Ochs, C. (2012). Effect of UV-A irradiance on lipid accumulation in *Nannochloropsis oculata*. Photochemistry and Photobiology, 88(3), 684-689.

Srivastava, G., & Goud, V. V. (2017). Salinity induced lipid production in microalgae and cluster analysis (ICCB 16-BR_047). Bioresource Technology, 242, 244-252.

Su, C. H., Fu, C. C., Chang, Y. C., Nair, G. R., Ye, J. L., Chu, I. M., & Wu, W. T. (2008). Simultaneous estimation of chlorophyll a and lipid contents in microalgae by three-color analysis. Biotechnology and Bioengineering, 99(4), 1034-1039.

Suali, E., & Sarbatly, R. (2012). Conversion of microalgae to biofuel. Renewable and Sustainable Energy Reviews, 16(6), 4316-4342.

Sukenik, A., Carmeli, Y., & Berner, T. (1989). Regulation of fatty acid composition by irradiance level in the eustigmatophyte *Nannochloropsis* sp. 1. Journal of Phycology, 25(4), 686-692.

Sushchik, N. N., Kalacheva, G. S., Zhila, N. O., Gladyshev, M. I., & Volova, T. G. (2003). A temperature dependence of the intra-and extracellular fatty-acid composition of green algae and cyanobacterium. Russian Journal of Plant Physiology, 50(3), 374-380.

Takagi, M., & Yoshida, T. (2006). Effect of salt concentration on intracellular accumulation of lipids and triacylglyceride in marine microalgae *Dunaliella* cells. Journal of Bioscience and Bioengineering, 101(3), 223-226.

Talebi, A. F., Tabatabaei, M., Mohtashami, S. K., Tohidfar, M., & Moradi, F. (2013). Comparative salt stress study on intracellular ion concentration in marine and salt-adapted freshwater strains of microalgae. Notulae Scientia Biologicae, 5(3), 309-315.

Tan, X. B., Lam, M. K., Uemura, Y., Lim, J. W., Wong, C. Y., & Lee, K. T. (2018). Cultivation of microalgae for biodiesel production: a review on upstream and downstream processing. Chinese Journal of Chemical Engineering, 26(1), 17-30.

Tatsuzawa, H., Takizawa, E., Wada, M., & Yamamoto, Y. (1996). Fatty acid and lipid composition of the acidophilic green alga *Chlamydomonas* sp. 1. Journal of Phycology, 32(4), 598-601.

Thompson Jr, G. A. (1996). Lipids and membrane function in green algae. Biochimica et Biophysica Acta (BBA)-Lipids and Lipid Metabolism, 1302(1), 17-45.

Tiwari, K., Upadhyay, D. J., Mösker, E., Süssmuth, R., & Gupta, R. K. (2015). Culturable bioactive actinomycetes from the great Indian Thar Desert. Annals of Microbiology, 65(4), 1901-1914.

Tomaselli, L. (2004). The microalgal cell. Handbook of microalgal culture: Biotechnology and Applied Phycology, 1, 3-19.

Tomčala, A., Kyselová, V., Schneedorferová, I., Opekarová, I., Moos, M., Urajová, P., ... & Oborník, M. (2017). Separation and identification of lipids in the photosynthetic cousins of Apicomplexa *Chromera velia* and *Vitrella brassicaformis*. Journal of Separation Science, 40(17), 3402-3413.

Tsai, C. H., Warakanont, J., Takeuchi, T., Sears, B. B., Moellering, E. R., & Benning, C. (2014). The protein Compromised Hydrolysis of Triacylglycerols 7 (CHT7) acts as a repressor of cellular quiescence in *Chlamydomonas*. Proceedings of the National Academy of Sciences, 111(44), 15833-15838.

Tsukagoshi, H. (2012). Defective root growth triggered by oxidative stress is controlled through the expression of cell cycle-related genes. Plant Science, 197, 30-39.

Tzovenis, I., De Pauw, N., & Sorgeloos, P. (1997). Effect of different light regimes on the docosahexaenoic acid (DHA) content of *Isochrysis aff. galbana* (clone T-ISO). Aquaculture International, 5(6), 489-507.

Vonshak, A., & Maske, H. (1982). Algae: growth techniques and biomass production. In Techniques in bioproductivity and photosynthesis. Pergamon Press, Oxford.

Wahidin, S., Idris, A., & Shaleh, S. R. M. (2013). The influence of light intensity and photoperiod on the growth and lipid content of

microalgae *Nannochloropsis* sp. Bioresource Technology, 129, 7-11.

Wallis, J. G., Watts, J. L., & Browse, J. (2002). Polyunsaturated fatty acid synthesis: what will they think of next?. Trends in Biochemical Sciences, 27(9), 467-473.

Wang, Y., He, B., Sun, Z., & Chen, Y. F. (2016). Chemically enhanced lipid production from microalgae under low sub-optimal temperature. Algal Research, 16, 20-27.

Wang, Z. T., Ullrich, N., Joo, S., Waffenschmidt, S., & Goodenough, U. (2009). Algal lipid bodies: stress induction, purification, and biochemical characterization in wild-type and starchless *Chlamydomonas reinhardtii*. Eukaryotic Cell, 8(12), 1856-1868.

Weatherly, C. A., Zhang, Y., Smuts, J. P., Fan, H., Xu, C., Schug, K. A., ... & Armstrong, D. W. (2016). Analysis of long-chain unsaturated fatty acids by ionic liquid gas chromatography. Journal of Agricultural and Food Chemistry, 64(6), 1422-1432.

Wirshing, A. (2012). Genetic engineering of Dunaliella: potential for improved biofuel production.

Xia, L., Rong, J., Yang, H., He, Q., Zhang, D., & Hu, C. (2014). NaCl as an effective inducer for lipid accumulation in freshwater microalgae *Desmodesmus abundans*. Bioresource Technology, 161, 402-409.

Xin, L., Hong-Ying, H., & Yu-Ping, Z. (2011). Growth and lipid accumulation properties of a freshwater microalga *Scenedesmus* sp. under different cultivation temperature. Bioresource Technology, 102(3), 3098-3102.

Xin, L., Hong-Ying, H., Ke, G., & Ying-Xue, S. (2010). Effects of different nitrogen and phosphorus concentrations on the growth,

nutrient uptake, and lipid accumulation of a freshwater microalga *Scenedesmus* sp. Bioresource Technology, 101(14), 5494-5500.

Xu, H., Miao, X., & Wu, Q. (2006). High quality biodiesel production from a microalga *Chlorella protothecoides* by heterotrophic growth in fermenters. Journal of Biotechnology, 126(4), 499-507.

Xu, X. Q., & Beardall, J. (1997). Effect of salinity on fatty acid composition of a green microalga from an antarctic hypersaline lake. Phytochemistry, 45(4), 655-658.

Xue, L., Zhang, Y., Zhang, T., An, L., & Wang, X. (2005). Effects of enhanced ultraviolet-B radiation on algae and cyanobacteria. Critical Reviews in Microbiology, 31(2), 79-89.

Yan, Y., Wang, X., Liu, Y., Xiang, J., Wang, X., Zhang, H., ... & Jin, Q. (2015). Combined urea-thin layer chromatography and silver nitrate-thin layer chromatography for micro separation and determination of hard-to-detect branched chain fatty acids in natural lipids. Journal of Chromatography A, 1425, 293-301.

Yeh, K. L., & Chang, J. S. (2011). Nitrogen starvation strategies and photobioreactor design for enhancing lipid content and lipid production of a newly isolated microalga *Chlorella vulgaris* ESP-31: implications for biofuels. Biotechnology Journal, 6(11), 1358-1366.

Yilancioglu, K., Cokol, M., Pastirmaci, I., Erman, B., & Cetiner, S. (2014). Oxidative stress is a mediator for increased lipid accumulation in a newly isolated *Dunaliella salina* strain. PLoS One, 9(3), e91957.

Zaslavskaia, L. A., Lippmeier, J. C., Shih, C., Ehrhardt, D., Grossman, A. R., & Apt, K. E. (2001). Trophic conversion of an obligate photoautotrophic organism through metabolic engineering. Science, 292(5524), 2073-2075.

Zhang, Q., Wang, T., & Hong, Y. (2014). Investigation of initial pH effects on growth of an oleaginous microalgae *Chlorella* sp. HQ for lipid production and nutrient uptake. Water Science and Technology, 70(4), 712-719.

Zhu, C. J., Lee, Y. K., & Chao, T. M. (1997). Effects of temperature and growth phase on lipid and biochemical composition of *Isochrysis galbana* TK1. Journal of Applied Phycology, 9(5), 451-457.

Zhu, J. K. (2000). Genetic analysis of plant salt tolerance using Arabidopsis. Plant Physiology, 124(3), 941-948.

Zhu, L., Zhang, X., Ji, L., Song, X., & Kuang, C. (2007). Changes of lipid content and fatty acid composition of *Schizochytrium limacinum* in response to different temperatures and salinities. Process Biochemistry, 42(2), 210-214.

Zimmerman, W. B., Zandi, M., Bandulasena, H. H., Tesař, V., Gilmour, D. J., & Ying, K. (2011). Design of an airlift loop bioreactor and pilot scales studies with fluidic oscillator induced microbubbles for growth of a microalgae *Dunaliella salina*. Applied Energy, 88(10), 3357-3369.

CHAPTER 2

Chapter 2

Materials and Methods

2.1 Experimental design

This chapter delineates the methodology involved for understanding the impact of varying treatments including salinity, nutrients, and oxidative stress, individually as well as an intercalated approach for achieving augmented biomass and lipid production. Different strategies were employed for achieving the research objectives, and the experiments were performed in two parts:

Long-term stress

1. *To monitor the impact of different salts at varying concentrations on growth profile and biochemical composition of Scenedesmus sp.*
2. *To study the effect of sodium chloride under nutrients replete/deplete condition*

Short-term stress

1. *To understand algal behavior in two stage approach with hydrogen peroxide under nitrate and phosphate variations*
2. *Multicomponent exposure – To analyze the effect of hydrogen peroxide, sodium chloride, nitrate and phosphate*

Schematic representation of experimental approach is represented in Figure 2.1. The outline of experiment design has been developed as research progressed, which specifies distinct culture conditions, quantitative and qualitative lipid analysis, and varying treatment framework.

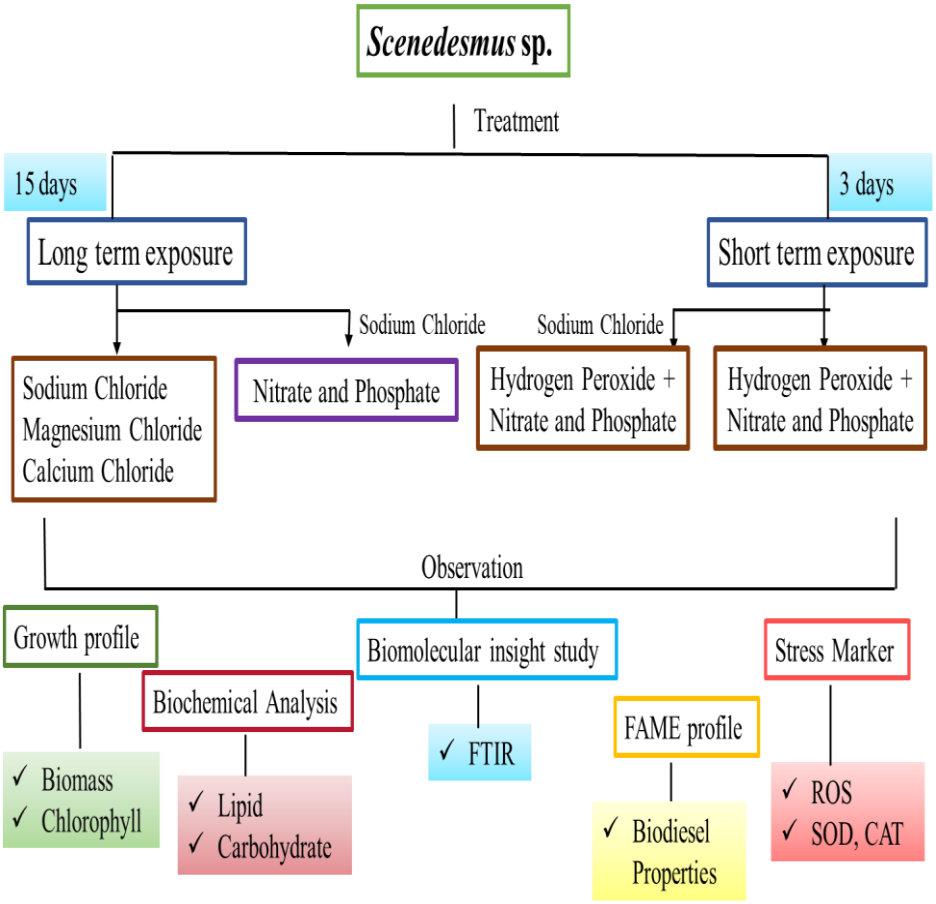

Figure 2.1: Systematic representation of comprehensive experimental framework

2.2 Microalgae collection and identification

Green eukaryotic microalgae species was isolated from domestic wastewater collected from Lal Bagh Indore, Madhya Pradesh, India. The strain was identified as *Scenedesmus vacuolatus*/sp. (Figure 2.2). by the National Collection of Industrial Microorganisms (NCIM), National Chemical Laboratory (NCL), Pune, India, using 18s rRNA and ITS rRNA gene sequencing.

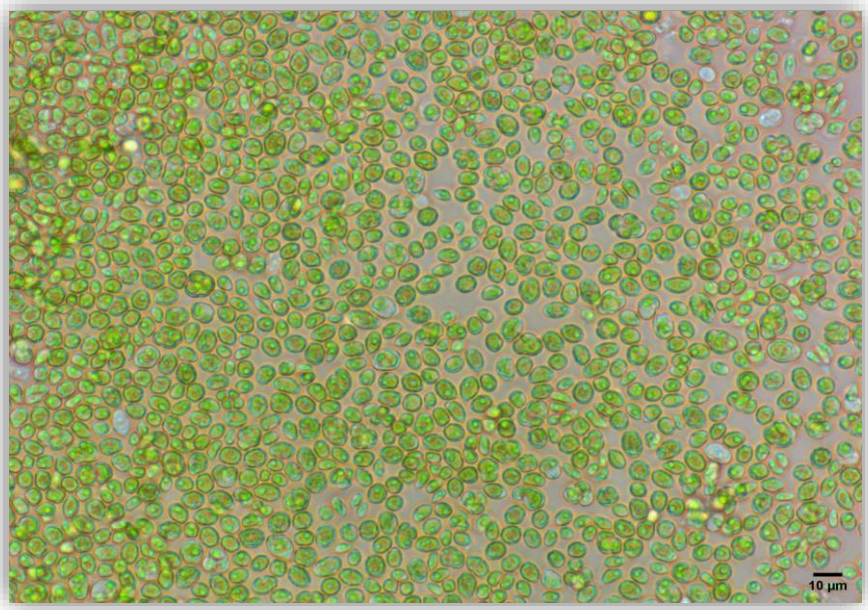

Figure 2.2: Light microscopic (40X) image of *Scenedesmus* sp.

2.3 Culturing and maintenance of *Scenedesmus* sp.

Axenic culture of *Scenedesmus* sp. was cultivated and preserved in Blue Green-11 media (Stanier et al., 1971), whose composition is described in Table 2.1. Seed culture was revived once a week and was grown in culture room (Figure 2.2) maintained at 28±5°C temperature. The light intensity was maintained at 3000±500 Lux, provided by white LED/fluorescent tubes with photoperiod of 12:12 hours of light and dark (L-D) cycle. Cultures were grown statically without CO_2 bubbling.

Two-stage cultivation methodology was adopted for performing all the experiments. Seed cells were inoculated in flasks containing unmodified culture media keeping OD 0.5 at 680 nm for all the experiments performed. This mother culture grown till 10^{th} day was used as seed culture/initial inoculum for experimental flasks containing modified media as per treatment plan. All the trials were executed in three replicates, were 250 mL flasks having 100 mL of cell culture.

Table 2.1: Blue Green 11 (BG-11) media composition (Stanier et al., 1975)

IUPAC	Chemical Formula	Concentration (gm/L)
Sodium nitrate	$NaNO_3$	1.5
Dipotassium hydrogen phosphate	K_2HPO_4	0.04
Magnesium sulfate hexahydrate	$MgSO_4.6H_2O$	0.075
Calcium chloride dihydrate	$CaCl_2.2H_2O$	0.036
Ammonium ferric citrate	$(NH_4)_5$ [Fe $(C_6H_4O_7)_2$]	0.006
2-hydroxypropane-1,2,3-tricarboxylic acid	$C_6H_8O_7$	0.006
Ethylenediaminetetraacetic acid disodium salt dihydrate	$C_{10}H_{18}N_2Na_2O_{10}$	0.001
Disodium carbonate	Na_2CO_3	0.02
Trace Elements (1 mL/Liter)		
Hydroperoxyboronic acid	H_3BO_4	2.86
Manganese (II) chloride tetrahydrate	$MnCl_2.4H_2O$	1.81
Sodium sulfate heptahydrate	$Na_2SO_3.7H_2O$	0.22
Disodium dioxide (dioxo) molybdenum dihydrate	$Na_2MoO_4.2H_2O$	0.39
Copper sulfate pentahydrate	$CuSO_4.5H_2O$	0.08
Cobalt (II) dinitrate hexahydrate	Co $(NO_3)_2.6H_2O$	0.05

2.4 Long term exposure to stress

2.4.1 Impact of different salts with varying concentrations on indigenously isolated microalgae, Scenedesmus sp.

Three different salts: NaCl (Sodium chloride), $MgCl_2.6H_2O$ (Magnesium chloride hexahydrate), and $CaCl_2.2H_2O$ (Calcium chloride dihydrate), were explored with varying concentrations of 0 mM, 30 mM, 50 mM, 70 mM, and 100 mM to target enhanced lipid accumulation in selected species. Varying saline conditions lead to high and low osmotic shock levels, which further aid in determining the algal response and the impact of salt supplementation on lipid

enhancement. The testing was performed till the cells reaches its late stationary phase.

2.4.2 Sodium chloride as lipid inducer under nutrients repleted/depleted conditions-Chronic exposure to understand long term effects

This part of study evaluates the combined effect of sodium chloride with varying nutrient (repleted/depleted) conditions on the physiological and biochemical composition of *Scenedesmus* sp. at varying NaCl (0, 10, 50, 100 and 200 mM), based on the previously obtained results was combined with $NaNO_3$ (Sodium nitrate) (0, 17.64 and 35.29 mM) and K_2HPO_4 (dipotassium hydrogen phosphate) (0, 0.22 and 5.74 mM) to obtain various combinations.

2.5 Short term exposure to stress

2.5.1 Effect of hydrogen peroxide and nutrients to understand growth behavior and FAME profile of the studied strain- Acute exposure for short term duration

During short term exposure conditions, the impact of H_2O_2 (Hydrogen peroxide) in the concentration range from 0-10 mM combined with $NaNO_3$ (0, 17.64, and 35.29 mM) and K_2HPO_4 (0, 0.22, and 5.74 mM) in different combinations was investigated. In two phase plans, the combined effect of H_2O_2, $NaNO_3$, and K_2HPO_4 on *Scenedesmus* sp. was studied to explore lipid and biomass accumulation. In first phase, algal cells were grown under modified media with nitrate and phosphate depleted/repleted conditions for 48 hrs and then H_2O_2 induction was done for 24 hours in second phase.

2.5.2 Multicomponent environment to evaluate biomass and lipid productivity of evaluated strain

Impact of multivariant treatment on examined strain was monitored in this part of study. While performing this experiment, NaCl (100 mM) and H_2O_2 (10 mM) combined with $NaNO_3$ (0, 17.64

and 35.29 mM) and K_2HPO_4 (0, 0.22 and 5.74 mM) in different combinations were examined for their influence on algal cells metabolism. H_2O_2 treatment was given in same manner in two phase plans as mentioned in the previous part.

2.6 Analytical methods

2.6.1 Growth rate and biomass production

2.6.1.1 Alliance flanked by OD at 680 nm and biomass in Scenedesmus sp. cells

A set of well-grown cultures (approximately OD_{680} = 1) were used to prepare serial dilutions of varying OD. Biomass was calculated from the slope equation obtained. Although dry cell weight (DCW; Biomass) was calculated from the correlation curve constructed between OD and biomass (mg/mL), the range of OD (0.2, 0.4, 0.6, 0.8 and 1) was taken and was harvested to obtain cell biomass discarding the supernatant. Pellet was rinsed 2-3 times with distilled water (dH_2O) followed by drying of cells via lyophilization. Once the constant weight is achieved, DCW obtained for each OD was measured in the weighing balance and was used to construct a standard calibration curve (Figure 2.2) between OD (X-axis) vs DCW (Y-axis) in mg/mL

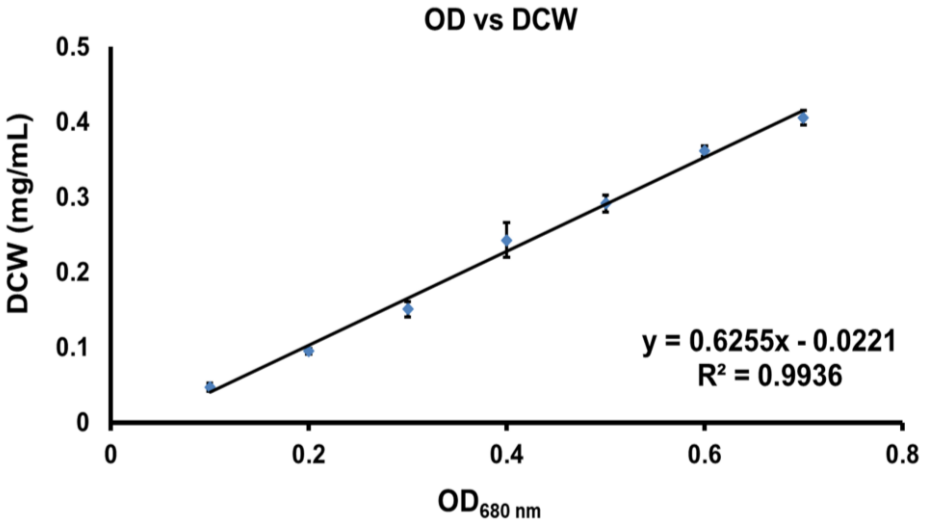

Figure 2.3: Linear correlation between optical density and dry cell weight (DCW) to allow the conversion of absorbance into biomass

The straight-line equation obtained was used to calculate dry cell weight or biomass for each experiment ($y = 0.6255x - 0.0221$). Growth of species was checked at regular interval by measuring the cell density at 680 nm (Hach spectrophotometer, DR6000). For the reading, a 2 mL sample was taken from each flask. Biomass productivity, growth rate, and doubling time (Levasseur et al., 1993; Srivastava and Goud, 2017) were calculated based on the formula described below:

$$\boldsymbol{Biomass\ Productivity}\left(\frac{\mu g}{\frac{mL}{d}}\right) = \frac{\boldsymbol{Final\ dry\ cell\ weight - Initial\ dry\ cell\ weight}}{\boldsymbol{Cultivation\ time}} \quad (1)$$

$$Specific\ grwoth\ rate\ (\mu) = \frac{\ln\left(\frac{X_2}{X_1}\right)}{(t_2 - t_1)} \quad (2)$$

Initial and final dry cell weights are represented by X1 and X2; similarly, t_1 and t_2 shows initial and final time interval. Doubling time (tg) was obtained from the following equation:

$$\boldsymbol{Doubling\ time}\ (\boldsymbol{tg}) = \frac{\mathbf{0.6931}}{\mu} \quad (3)$$

2.6.2 Chlorophyll estimation

Chlorophyll content was estimated at an interval of 5 days, i.e., at 0th day (0 hours), 5th day (120 hours), 10th day (240 hours), and 15th day (360 hours).

Chlorophyll estimation was done by following the method based on Arnon (1949) and Su et al. (2010), respectively. 5 mL culture taken from each flask and was harvested for 5 minutes at 5000 rpm using centrifuge. Pellet obtained was washed (2-3 times) with dH_2O discarding the supernatant. To the pellet obtained, 5 mL absolute ethanol (99.9%) was added and kept for 5 minutes incubation at 100°C. The sample was brought down to room temperature, and the supernatant was recorded at 663 and 645 nm using Hach spectrophotometer (DR6000) to quantify chlorophyll content

$$\boldsymbol{Chlorophyll\ 'a'}\left(\frac{\boldsymbol{g}}{\boldsymbol{L}}\right) = (\mathbf{0.0127} * \boldsymbol{OD_{663nm}}) - (\mathbf{0.00269} * \boldsymbol{OD_{645nm}}) \quad (4)$$

2.6.3 Total lipid estimation

Lipid quantitation was performed using Sulfo-Phospho Vanillin (SPV) method, which includes several analytical steps (Mishra et al., 2014). The explicit and rapid assessment of total lipids, even in a small amount of algal biomass, can be achieved with the aid of SPV method as compared to other conventional lipid estimation methodologies.

Phospho-vanillin (PV) reaction mixture was formulated by mixing vanillin (0.6 gm) of vanillin in 10 mL of ethanol, processed by 90 mL addition of dH_2O and 400 mL of orthophosphoric acid. Standard calibration curve (Figure 2.3) was prepared primarily, by taking varying concentrations (60, 120, 180, 240 and 300 µg) of glycerol triolate, a lipid standard. Curve was prepared by taking OD_{530} at y-axis and varying concentrations of the standard on x-axis. The lipid concentration in unknown algal samples was calculated by considering the slope equation (y = 0.0036x-0.0102, R^2= 0.995) derived from the standard curve.

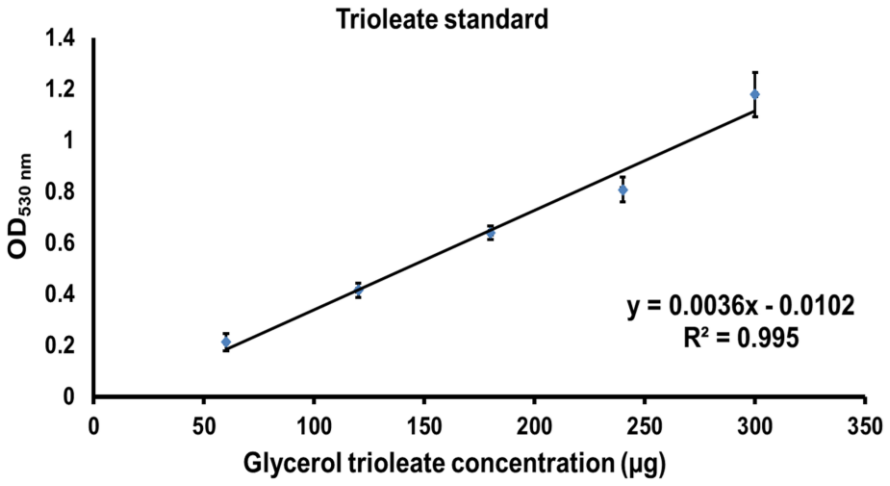

Figure 2.4: Linear correlation of glycerol trioleate (lipid standard) to allow the estimation of total lipids

For algal analysis, 1 mL sample centrifuged at 5000 rpm from each replica flask for 5 minutes. The pellet obtained was washed (2-3 times) with dH_2O, and 100 µL of dH_2O was added to form algal cell

suspension. Concentrated H_2SO_4 (2 mL) was blended, and the sample mixture kept at 100°C for 10 minutes. Once incubation period was over, the sample mixture was brought to room temperature, 5 mL of recently prepared PV reagent was added and mixed properly and kept for incubation in a shaker incubator at 200 rpm at 37°C for 15 minutes. The samples were recorded at a wavelength of 530 nm using multimode plate reader (SYNERGY H1 BioTek) to quantify total lipids.

2.6.4 Total carbohydrate estimation

The anthrone test was done to estimate the quantity of carbohydrate accumulated inside the algal cells (Joseph and Roe, 1955). Anthrone reagent was prepared carefully by the addition of thiourea (1 gm), and anthrone (100 mg) in the mixture of 75% concentrated sulphuric acid. Standard calibration curve (Figure 2.4) was prepared by taking varying concentrations (0, 10, 20, 30 and 40 µg/mL) of glucose, as carbohydrate standard. A graph was framed by taking OD_{620} at y-axis and varying concentrations of the standard at x-axis. The carbohydrate concentration in unknown algal samples was calculated by considering the slope equation derived from the standard curve.

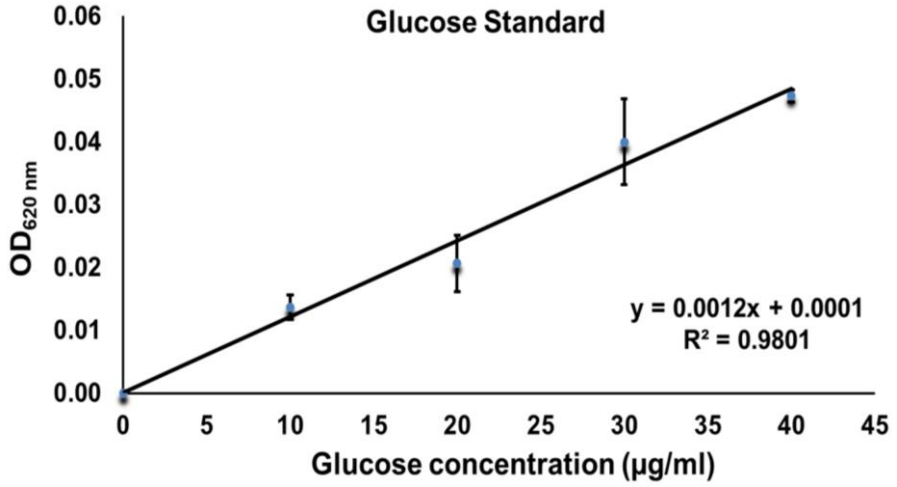

Figure 2.5: Linear correlation of glucose standard to allow the estimation of total carbohydrate

Sample (1 mL) was taken from each experimental flask and was subjected to centrifugation at 5000 rpm to obtain a cell pellet which was rinsed twice or thrice with dH_2O. The cell pellet was obtained was redissolved in 1 mL dH_2O, trailed by the addition of anthrone reagent (4 mL). The sample was mixed thoroughly and sat for 15 minutes at 100°C. Once the reaction mixture brought to ambient temperature, the absorbance of supernatant taken at a wavelength 620 nm using multimode microplate (SYNERGY H1 BioTek) reader.

2.6.5 Fatty acid methyl ester analysis

Fatty acid methyl esters (FAME) were the first fatty acid esters having a generic term for biodiesel. The transesterification reaction is carried out to quantify and identify the FAMEs. Until injecting the sample for gas chromatography (GC) analysis to evaluate the fatty acid composition, alcohol (methanol) is added to the lyophilized sample in the presence of a catalyst (acidic or basic). The FAME composition is highly influenced by various factors, such as diverse culture conditions, harvesting strategies, storage techniques and different lipid extraction methods. Ríos et al. (2013) method was followed to extract and quantify FAME content and evaluate its composition.

Dried biomass 20 mg was assessed and assorted with reaction mixture-I (4.5 mL), which included 10:1:1 v/v/v methanol, hydrochloric acid, and chloroform. Each sample replica vortexed thoroughly for 10 seconds and was kept at 90°C in the water bath for 120 minutes. After bringing the sample to an ambient temperature, 1.5 mL dH_2O, 3 mL reaction mixture-II [hexane: chloroform (4:1 v/v)] was further added to the tested sample and then vortexed for 10 seconds. The aliquots were kept at ambient temperature to distinguish the organic and aqueous phases, and the organic phase was used for gas chromatography with hexane and methyl nonadecanotae (C19:0) fatty acid as an internal norm in a 5:4:1 (v/v/v) ratio. For FAME profiling, an Agilent 7890B GC with a flame ionisation detector (FID) and a SelectTM Biodiesel CP9080 column (30m 0.32mm 0.25m) are used.

The carrier gas was helium (purity 99.99 percent) at a flow rate of 1.5 mL/min, and a sample volume of 2 µL was injected with a split ratio of 10:1. Shirazi et al. (2013) showed the temperature programmed that was used. Peaks were detected by comparing the results with reference (FAME mix C4:C24; Sigma Aldrich #18919-1AMP) (Figure 2.6). Individual fatty acid composition was calculated using the equations described below.:

$$\boldsymbol{FAME}\ \left(\frac{\boldsymbol{\mu g}}{\boldsymbol{mg}}\right) = \frac{(\boldsymbol{Internal\ Standard\ concentration} * \boldsymbol{Area\ of\ individaul\ fatty\ acid})}{(\boldsymbol{RRF} * \boldsymbol{Area\ of\ Internal\ Standard})} \Big/ \boldsymbol{Biomass\ (mg)} \qquad (5)$$

$$\boldsymbol{RRF} = \frac{(\boldsymbol{Area\ of\ individual\ FAME} * \boldsymbol{Concentration\ of\ Internal\ Standard})}{(\boldsymbol{Area\ of\ internal\ standard} * \boldsymbol{Concentration\ of\ individual\ FAME})} \qquad (6)$$

where IS stands for internal standards, RRF stands for relative response factor, and FA stands for fatty acid.

The overall FAME concentration was calculated by combining all of the distinct fatty acid methyl ester content, which was also used to determine the individual FAME percentage

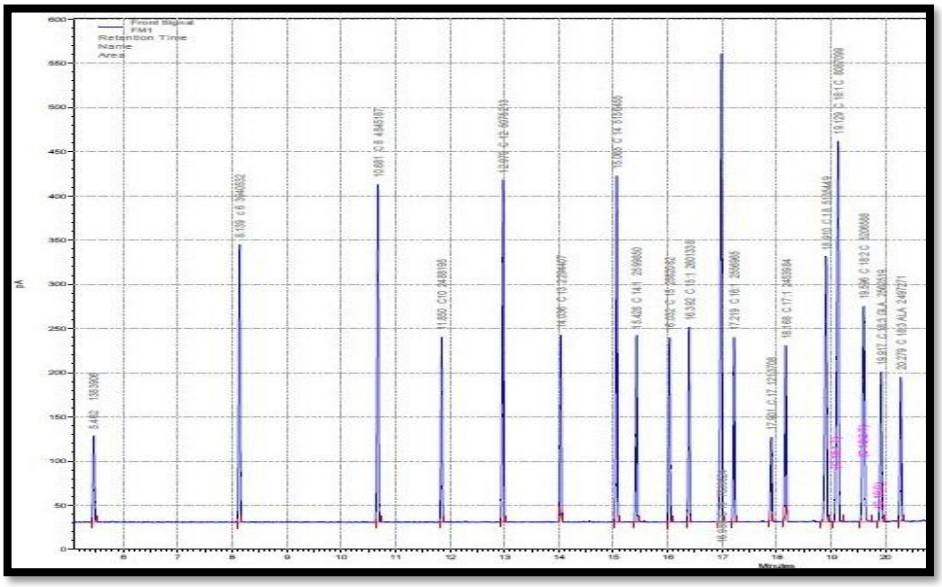

Figure 2.6: A chromatogram of FAME mix

2.6.6 Fourier-transform infrared (FTIR) spectroscopy analysis

FTIR spectroscopy is a rapid technique employed to identify different functional groups present in several biomolecules present in an algal cell (Sudhakar and Premalatha, 2015; Osundeko et al., 2014; Sigee et al., 2007). The structure, functional groups, and characteristics of different biomolecules present in an algal cell are altered significantly at fluctuating environmental exposure such as oxidative stress, pH, nutrient, temperature, and salinity so on. These molecular changes can be monitored eminently with the help of FTIR spectroscopy. It can, however, be used to monitor the effect on carbon allocation and flux (Mayers et al., 2013). This method has a number of advantages over conventional chemical methods, including increased speed, sensitivity, and accuracy (Wagner et al., 2010).

The FTIR study was done on lyophilized biomass. The ATR-FTIR from Perkin Elmer was used for the research. The transmission of biomolecules took place at a frequency of 400-4000 cm^{-1}. The collected spectral data was analysed using the Origin Pro 8.5 software, which applied second-order differentiation to obtain transmission percentage.

2.7 Algal cells imaging

2.7.1 Bright field microscopy

Bright-field microscopy is one of the fundamental visualization techniques. In bright-field microscopy, once the illuminating light transmits through the sample, a contrast is generated in the specimen's dense area after the absorption of light by the cells. Bright-field microscopy has drawbacks such as reduced contrast for low absorbing samples and reduced resolution due to out-of-focus material becoming blurry.

The purity of cells was checked regularly with the help of an Olympus (CKX53-SLP) microscope inbuilt with Magcam DC 5 (5.1MP, 1/2.5" CMOS SENSOR). 20 μL sample was placed over a

clean microscopic slide and covered with coverslip to visualize under the microscope (60X).

2.7.2 Scanning electron microscope

The scanning electron microscope (SEM), was used for examining solid material surfaces directly, uses a low-energy beam of directed electrons as an electron probe that is scanned repeatedly through the specimen.

The cells morphology was examined using a Field Emission Scanning Electron Microscope (FE-SEM, Supra55 Zeiss) after they had been exposed to different stress conditions. 1 mL of sample was centrifuged to pelletize the cell biomass and was rinsed two to three times to remove any remaining salts. After removing the supernatant, the cell biomass was used to prepare the samples. Following that, samples were fixed with 37 percent formaldehyde and then subjected to an ethanol gradient treatment (25, 50, 75, 90, and 95 percent ethanol), followed by 100 percent ethanol. After adding 100 percent absolute ethanol for overnight once they were left for 10 minutes at each gradient stage to extract moisture content and ensure full dehydration until imaging. Following that, a drop-cast method was used to load 20 µL of sample volume onto a thin, microscopic slide. After that, copper film was used to coat the samples before being loaded onto a sample holder for SEM imaging with stubs (Sarno et al., 2007).

2.7.3 Confocal microscopy

For lipid quantification, various screening methods have been developed, including gravimetric, high-pressure liquid chromatography (HPLC), solvent extraction, and gas-liquid chromatography (GLC). Using lipo-fluorescent dyes including Nile red (9-diethylamino-5-benzo [α] phenoxazinone), have attempted to establish quick in situ methods.

Confocal laser scanning microscopy was used to visualise neutral lipids (Olympus-IX83, Objective lens NA1.4, Laser-405, 488

and 559nm, software-FV10-ASW 4.2). 1 mL of culture mixed with 330 mL of dimethyl sulfoxide (25% (v/v), DMSO). 15 µL of Nile red (0.1 mg/mL) was added to the mixture, which was then stained for 10 minutes at 40°C (Zhang et al., 2016). The neutral lipids present in cells were then visualized using confocal microcopy at 60/100X.

2.8 Antioxidative defense mechanism analysis

The imbalance in metabolic function will generate free radicals, and activate antioxidant mechanism, which engulf free radicals. Increase in free radical production will be counteract by the various defense mechanism associated with the species. Free radicals are molecules are with an odd or unpaired electron in the outer shell of an atom that grips the oxygen electron, generating the most common biological free radical, reactive oxygen species (ROS). Hydrogen peroxide, superoxide anion, hydroxyl radical, and other compounds linked to a variety of metabolic process. Antioxidative enzymes such as glutathione peroxidase (GPX), superoxide dismutase (SOD), ascorbate peroxidase (APX), catalase (CAT), transferrin, and ferritin that catalyze the removal of ROS.

2.8.1 Reactive oxygen species quantification

ROS was computed in terms of H_2O_2 content in the cells. Biomass was centrifuged and was lysed in TCA, 0.1% (w/v). The reaction mixture was mixed thoroughly and centrifuge at 15,880 g for 10 minutes to obtain supernatant and was mixed with phosphate buffer (0.5 mL, 10 mM, pH 7.0). Subsequently, after that, 1 mL potassium iodide (1 M) was applied, and the absorbance at 390 nm was measured. H_2O_2 was calculated using a standard calibration curve (Figure 2.5) based on known H_2O_2 concentrations (Velikova et al., 2000).

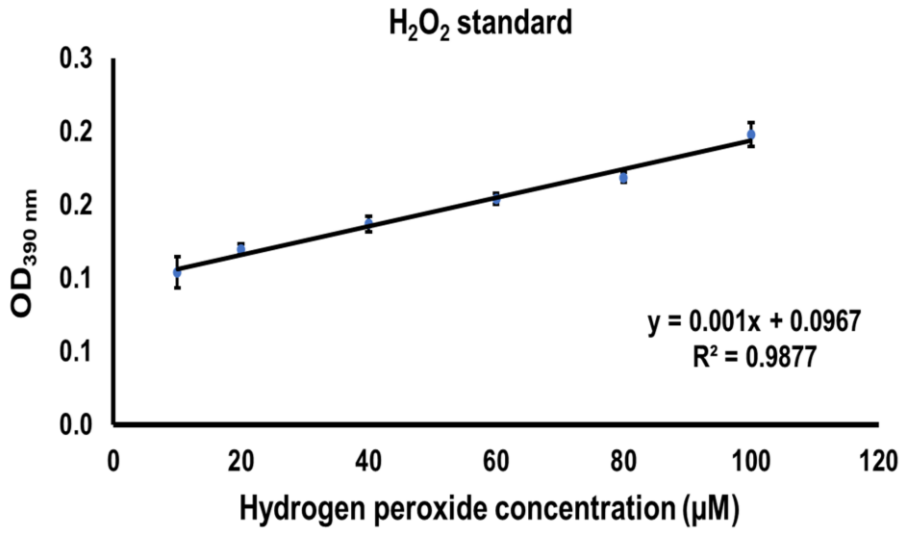

Figure 2.7: Linear correlation of hydrogen peroxide standard to allow the estimation of reactive oxygen species (ROS)

2.8.2 Enzymatic assays

Crude protein extract was prepared for each combination under consideration (Liu et al., 2018). The cell cultures were gathered by harvesting for 30 minutes at 4000 rpm. 1 mL phosphate buffer saline (PBS pH 7.2) was mixed with the pellet and was mixed thoroughly. Cell lysis was carried out with the help of bath probe sonicator (QSONICA Sonicators, US). Once sonication was done, centrifugation at 15,000 rpm for 15 minutes at 4˚C was performed to remove the cell debris (using Model 7000 Ultracentrifuge, Kubota Corporation, Japan). Supernatant obtained was used for protein estimation (Bradford, 1976) followed by enzyme (SOD and CAT) assay.

According to manufacturer, the colorimetric kit (Item No. 707002 Cayman 1180 E. Ellsworth Rd-Ann Arbor, MI-USA) was used to estimate catalase (CAT) activity using standard curve (Figure 2.6). At 25°C, catalase activity is equal to the amount of enzyme that produces 1.0 nmol of formaldehyde per minute. Superoxide dismutase (SOD) activity was also calculated based on the instructions given in the manufacturer's kit using standard curve (Figure 2.7) (Item No.

706002). The amount of enzyme needed to dismutate the superoxide radical by 50% is one unit of SOD action.

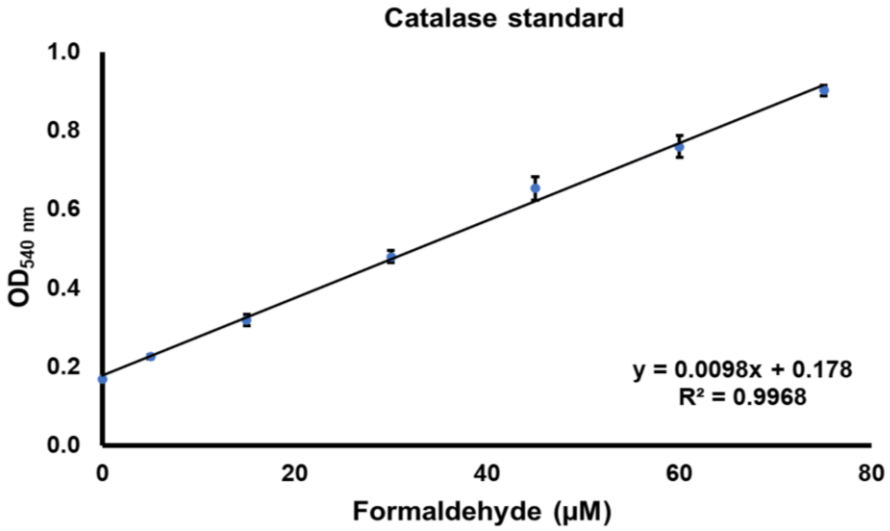

Figure 2.8: Linear correlation of formaldehyde (catalase) standard to allow the estimation of catalase activity.

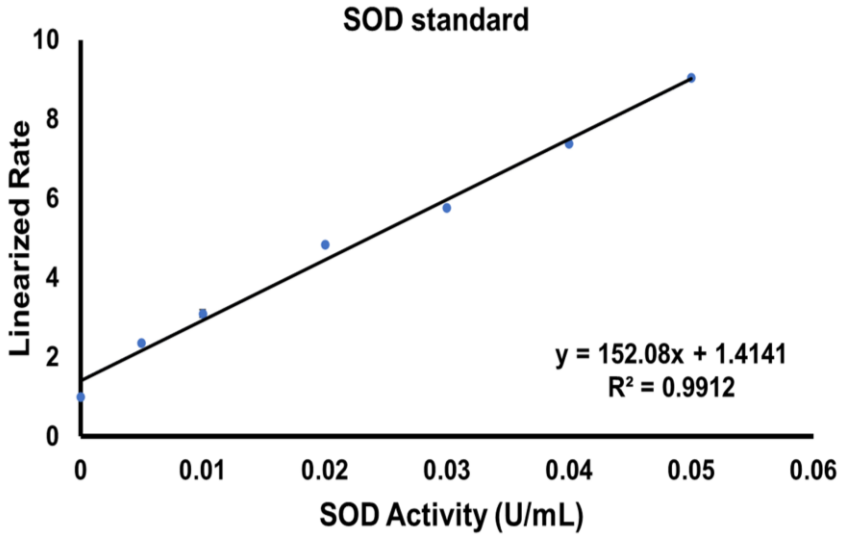

Figure 2.9: Linear correlation of superoxide dismutase standard to allow the estimation of SOD activity

2.9 Biodiesel properties

Fatty acids or algal lipids undergo transesterification reaction to produce biodiesel. Algae oil is a mixture of saturated, monounsaturated and polyunsaturated fatty acid. This fatty acid composition has an ultimate effect on biodiesel properties (Sharma et al., 2008). "Biofuels is a monoalkyl esters of long-chain fatty acids obtained from vegetable oils or animal fats, named B100," according to ASTM (ASTM D6751-08, 2008). The composition of FAME governs the physical and chemical properties of biodiesel.

FAME percentage obtained from FAME analysis is used for the estimation of biodiesel properties. Iodine value (IV), degree of unsaturation (DUm), cetane number (CN) are few parameters that give the reference of biodiesel quality (Knothe, 2005; Knothe, 2007).

Cetane number is calculated from the below equation (Mishra et al., 2016)

$$\boldsymbol{CN = 63.41 - (0.0728 * DU_m) + (0.03495 * SCSF) - (3.26 * 0.0001 * DU_m * SCSF)} \quad (7)$$

Where;

$$\boldsymbol{DU_m = (1 * MUFA, C_{n:1}, wt\%) + (2 * PUFA, C_{n:2}, wt\%) + (3 * PUFA, C_{n:3}, wt\%)} \quad (8)$$

$$\boldsymbol{SCSF = \left(\frac{1}{100}\right) \Sigma (M * wt\% \ of \ saturated \ methyl \ ester)} \quad (9)$$

CN= cetane number; SCSF= straight-chain saturation factor; Du_m= degree of unsaturation M= Molecular weight of individual fatty acid.

Iodine and saponification values are obtained from below equation (Krisnangkura,1986).

$$\boldsymbol{SV = \Sigma \left(\frac{(560 * N)}{M}\right)} \quad (10)$$

$$\boldsymbol{IV = \Sigma \frac{(254 * DN)}{M}} \quad (11)$$

N= percent of each fatty acid; D= number of bonds; M= molecular weight of individual fatty acid.

2.10 Principal Component Analysis

To reduce the complexity and dimensionality of data sets pertaining to the recovery of lipid and biomass parameters in different experimental conditions with various variants applied, principal component analysis (PCA) was carried out. With the aim of determining maximum variance in the obtained data, three dimension/principal components were selected, based on the Kaiser Concept (Eigenvectors having more than 1), and the main contributing factors were determined with respect to biomass parameters across different combinations. PCA was performed in R studio desktop version 4.0.0 by using R packages, ‘factoextra’ (Kassambara and Mundt, 2020), ‘FactoMineR’ (Lê S et al., 2008), ‘devtools’ (Wickham et al., 2019) and ‘ggbiplot’ (Vincent, 2011).

References

Armon, D. I. (1949). Copper enzymes in isolated chloroplast. Plant physiol, 24, 1-15.

Bradford M. M. (1976). A rapid and sensitive method for the quantitation of microgram quantities of protein utilizing the principle of protein-dye binding. Analytical Biochemistry, 72, 248–254.

Kassambara, A., & Mundt, F. (2017). Factoextra: extract and visualize the results of multivariate data analyses. R package version, 1(5), 337-354.

Knothe, G. (2007). Some aspects of biodiesel oxidative stability. Fuel Processing Technology, 88(7), 669-677.

Knothe, G., & Steidley, K. R. (2005). Kinematic viscosity of biodiesel fuel components and related compounds. Influence of compound structure and comparison to petrodiesel fuel components. Fuel, 84(9), 1059-1065.

Krisnangkura, K. (1986). A simple method for estimation of cetane index of vegetable oil methyl esters. Journal of the American Oil Chemists' Society, 63(4), 552-553.

Lê, S., Josse, J., & Mazet, F. (2008). Package ‘FactoMineR. J Stat Softw [Internet], 25(1), 1-18.

Levasseur, M., Thompson, PA., & Harrison, PJ. (1993). Physiological acclimation of marine phytoplankton to different nitrogen sources. Journal of Phycology, 29(5), 587-595.

Liu, Y., Wang, S., Wang, Z., Ye, N., Fang, H., & Wang, D. (2018). TiO_2, SiO_2 and ZrO_2 nanoparticles synergistically provoke cellular oxidative damage in freshwater microalgae. Nanomaterials, 8(2), 95.

Mayers, J. J., Flynn, K. J., & Shields, R. J. (2013). Rapid determination of bulk microalgal biochemical composition by Fourier-Transform Infrared spectroscopy. Bioresource Technology, 148, 215-220.

Mishra, S. K., Suh, W. I., Farooq, W., Moon, M., Shrivastav, A., Park, M. S., & Yang, J. W. (2014). Rapid quantification of microalgal lipids in aqueous medium by a simple colorimetric method. Bioresource Technology, 155, 330-333.

Mishra, S., Anand, K., & Mehta, P. S. (2016). Predicting the cetane number of biodiesel fuels from their fatty acid methyl ester composition. Energy & Fuels, 30(12), 10425-10434.

Osundeko, O., Dean, A. P., Davies, H., & Pittman, J. K. (2014). Acclimation of microalgae to wastewater environments involves increased oxidative stress tolerance activity. Plant and Cell Physiology, 55(10), 1848-1857.

Ríos, S. D., Castañeda, J., Torras, C., Farriol, X., & Salvadó, J. (2013). Lipid extraction methods from microalgal biomass harvested by two different paths: Screening studies toward biodiesel production. Bioresource Technology, 133, 378-388.

Roe, J. H. (1955). The determination of sugar in blood and spinal fluid with anthrone reagent. Journal of Biological Chemistry, 212, 335-343.

Sarno, D., Kooistra, W. H., Balzano, S., Hargraves, P. E., & Zingone, A. (2007). Diversity in the genus *Skeletonema* (Bacillariophyceae): III. Phylogenetic position and morphological variability of *Skeletonema costatum* and *Skeletonema grevillei*, with the description of *Skeletonema ardens* sp. NOV. 1. Journal of Phycology, 43(1), 156-170.

Sharma, Y. C., Singh, B., & Upadhyay, S. N. (2008). Advancements in development and characterization of biodiesel: a review. Fuel, 87(12), 2355-2373.

Shirazi, M. M. A., Kargari, A., Tabatabaei, M., Mostafaeid, B., Akia, M., Barkhi, M., & Shirazi, M. J. A. (2013). Acceleration of biodiesel–glycerol decantation through NaCl-assisted gravitational settling: a strategy to economize biodiesel production. Bioresource Technology, 134, 401-406.

Sigee, D. C., Bahrami, F., Estrada, B., Webster, R. E., & Dean, A. P. (2007). The influence of phosphorus availability on carbon allocation and P quota in *Scenedesmus subspicatus*: a synchrotron-based FTIR analysis. Phycologia, 46(5), 583-592.

Srivastava, G., & Goud, V. V. (2017). Salinity induced lipid production in microalgae and cluster analysis (ICCB 16-BR_047). Bioresource Technology, 242, 244-252.

Stanier, R. Y., Kunisawa, R., Mandel, M., & Cohen-Bazire, G. (1971). Purification and properties of unicellular blue-green algae (order Chroococcales). Bacteriological Reviews, 35(2), 171.

Su, S., Zhou, Y., Qin, J. G., Yao, W., & Ma, Z. (2010). Optimization of the method for chlorophyll extraction in aquatic plants. Journal of Freshwater Ecology, 25(4), 531-538.

Sudhakar, K., & Premalatha, M. (2015). Characterization of micro algal biomass through FTIR/TGA/CHN analysis: application to *Scenedesmus* sp. Energy Sources, Part A: Recovery, Utilization, and Environmental Effects, 37(21), 2330-2337.

Velikova, V., Yordanov, I., & Edreva, A. (2000). Oxidative stress and some antioxidant systems in acid rain-treated bean plants: protective role of exogenous polyamines. Plant Science, 151(1), 59-66.

Vincent, Q.V., (2011). GitHub - vqv/ggbiplot: A biplot based on ggplot2. https://github.com/vqv/ggbiplot. Accessed 23 Jul 2020.

Wickham, H., & Chang, W. (2019). devtools: Tools to make developing R packages easier, 2016. URL https://CRAN. R-project. org/package= devtools. R package version, 1(0), 103.

Zhang, Y., He, M., Zou, S., Fei, C., Yan, Y., Zheng, S., ... & Wang, C. (2016). Breeding of high biomass and lipid producing *Desmodesmus* sp. by Ethylmethane sulfonate-induced mutation. Bioresource Technology, 207, 268-275.

CHAPTER 3

Chapter 3

Impact of varying concentrations of different salts on growth profile and biochemical composition of *Scenedesmus* sp.

3.1 Introduction

Microalgae, when grown in different environmental perturbations, have shown the potential of accumulating a high amount of lipid. Algae can be cultivated in arid or marginal areas to produce higher aerial biomass compared to conventional energy crops (Davis et al., 2011). Though microalgae have been gaining impetous in the field of biofuels, yet certain difficulties pose a major obstacle enroute towards the commercialization of algal biofuels.

Salinity-induced stress is known to stimulate the increased accumulation of lipid content leading to the enhanced production of fatty acid methyl esters (FAME). It has been well established that algal biochemical composition can be controlled through defined cultivation conditions such as exposure to variable nutrients (nitrate, phosphate), different types of stress such as salinity induced osmotic stress, hydrogen peroxide (H_2O_2) induced oxidative stress, light, temperature, pH etc. (Pancha et al., 2015). However, these variable conditions have their own limitations and may result in low biomass productivity through stress behaviour. The two-stage cultivation has addressed this issue to some extent, in which algae are first cultivated in nutrient sufficient conditions and then transferred to nutrient-deprived conditions in the second stage (Sun et al., 2014).

Salinity stress has been found to enhance the lipid accumulation by extensively influencing several biochemical metabolic pathways associated with algal growth. Likewise, osmotic stress helps manipulate

the biochemical profile of algal strain for increased lipid production (Asulabh et al., 2012). However, under the supplementation of salt, both osmotic and ionic disquiet leads to reduced Na^+/H^+ antiporters activity affecting the tolerance capacity of photosynthetic machinery as well as oxygen-evolving machinery. It has been reported that the stress caused by salinity can lead to a rapid decline in the oxygen-evolving process of PSII and affects the transport of electrons, as revealed in a cyanobacterium, *Synechococcus* sp. PCC 7942. Exposure to high concentration of Na^+ leads to changes in physiological conditions of algae such as *Dunaliella salina* and *Chlorella* sp., which results in high accumulation of lipids for survival under stressed conditions that further persists until the arrival of favorable growth conditions. Though several species can survive in varying saline conditions, but *Dunaliella salina* has been explored the most due to its outstanding ability to tolerate a wide range of saline supplementation (Azachi et al., 2002).

The accumulation of lipid is a usual process that occurs inside algae cells when subjected to any kind of environmental stress, and thus cells get adapted to these changes by modifying their morphological and physiological pathways (Asulabh et al., 2012). Stress conditions like high salt concentration results in the increment of saturated fatty acid and decrement of polyunsaturated fatty acid content (Kan et al., 2012). Under high concentrations of salts, algal species produce specific metabolites leading to lipid accumulation, which ultimately protects them from stress imposed, enabling them to adapt to the surrounding osmotic environment (Rao et al., 2007). These qualities make them a suitable candidate to study the effect of salinity in context to biofuels production potential (Sharma et al., 2012). Salinity stress causes multiple effects such as physiological, biochemical, or morphological changes in the cells, resulting in the diversion of fatty acid metabolism towards the accumulation of lipid bodies inside cells (Kalita et al., 2011).

Certain cost-effective and rapid lipid detection techniques such as fluorescent staining, chromatographic and colorimetric analysis have

been explored substantially to detect biofuel precursors, specifically biodiesel precursor like lipid (Krank et al., 2007). Amongst these techniques, the fluorescent method involves the usage of nile red dye for tagging neutral lipid content inside the microalgae, which is further visualized as well as quantified with the help of confocal microscopy (Cooksey et al., 1987; Elsey et al., 2007), whereas the chromatographic technique is utilized for separation as well as quantification of algal lipid. However, both the methods have some drawbacks, such as the pre-requisite for the chromatography includes chemical/solvent extraction of metabolite, which is a time-consuming method, whereas confocal microscopy or fluorescent method cannot quantify the lipid to much extent as compared to the chromatography (Dean et al., 2010).

Besides the methodologies mentioned above for macromolecular quantification, a non-invasive technique known as Fourier Transform Infrared (FTIR) spectroscopy is used for the qualitative analysis of the algal cells. Several researchers have used FTIR to monitor the changes in metabolic pathways of algal species when exposed to nitrate or phosphate depleted conditions (Dean et al., 2008; Laurens and Wolfrum, 2011; Meng et al., 2014). FTIR spectroscopy is also applied for distinguishing various microalgal species based on their biochemical composition (Bounphanmy et al., 2010; Driver et al., 2015). Apart from these, FTIR spectroscopy had been successfully utilized as a technique to explore the properties of microalgae as bio-sorbent for heavy metal removal (Kiran et al., 2016). This technique is regarded as a physiological fingerprint technique for studying or identifying various types of chemical bonds present and their molecular structure in microalgae. FTIR spectroscopy is a fast technique for identifying functional groups (Sudhakar and Premalatha 2015; Osundeko et al., 2014; Sigee et al., 2007). Apart from the lipid estimation, growth of species, impact on molecular structure, and types of functional groups under varying environmental conditions such as nutrient variation, salinity stress, pH, temperature etc., can also be

monitored through FTIR spectroscopy. Besides these, it can also be used to investigate the impact of such conditions on the carbon allocation/flux (Mayers et al., 2013). The benefit of this aspect over the traditional chemical analyses involves less time for measurement, high sensitivity, and high consistency (Wagner et al., 2010).

This chapter enlightens the relation between osmotic stress provided and the FAME profile of microalgae. The optimization of each algal species under differently stressed culture conditions is required to systematically target enhancement of lipid content inside algal cells so as to process the cellular feedstock for generation of biofuel precursor (FAME). Therefore, this chapter represents a novel approach to discuss the outcomes of the induction of salt stress on lipid accumulation in microalgae, *Scenedesmus* sp. Detailed analysis is done to understand the impact of the addition of some important salts, namely magnesium chloride ($MgCl_2$), sodium chloride (NaCl) as well as calcium chloride ($CaCl_2$) for the generation of salinity stress inside microalgae, which may eventually lead to the augmented accumulation of cellular lipid bodies. In the present study, the effect of the salts in different concentrations were monitored. The parameters chosen to monitor the physiological, biochemical, and morphological changes of the algae include growth pattern, biomass accumulation, neutral lipids, and SEM (Scanning Electron Microscopy) analysis along with fatty acid profile and FTIR spectroscopy.

3.2 Materials and Methods

3.2.1 Experimental design

Once the seed culture of *Scenedesmus* sp. reached exponential phase, the culture with 0.5 (OD_{680}) as an initial cell density was inoculated in 100 mL modified BG-11 broth in 250 mL Erlenmeyer flasks. BG-11 media was amended by adding different concentrations (10, 30, 50, 70 and 100 mM) of sodium chloride (NaCl), magnesium chloride hexahydrate ($MgCl_2.6H_2O$) and calcium chloride dihydrate

($CaCl_2.2H_2O$) (Figure 3.1). Triplicity was maintained while conducting the experiment.

3.2.2 Microalgae growth and chlorophyll estimation

To study the growth kinetics of microalgae *Scenedesmus* sp. under treatment, the density of algal cells was recorded by a Hach spectrophotometer (DR6000) at 680 nm wavelength. The experiment was performed for up to 15 days, and the cell density was measured periodically at the time interval of 48 hours. Biomass productivity and growth rate (μ) were calculated as demonstrated by Levasseur et al. (1993) and Srivastava and Goud (2017), respectively, which has been described extensively in chapter 2.

The chlorophyll 'a' extracted in ethanol was quantified spectrophotometrically as per the method described by Su et al. (2010) and Arnon (1949).

3.2.3 Biochemical analysis

Anthrone and Sulfo-Phospho-Vanillin (SPV) methods were followed to quantify total lipids (Mishra et al., 2014) and carbohydrates (Joseph and Roe, 1955) present in the salt-induced algal cells, whose detailed protocol has been described in chapter 2.

3.2.4 Fourier Transform Infrared Spectroscopy (FTIR)

Analysis with the help of FTIR was carried out with lyophilized biomass. Transmission of biomolecules was observed in the range of 400-4000 cm^{-1}. The spectral data obtained was processed through Origin Pro 8.5 software by calculating a second derivative order of the results obtained.

3.2.5 Confocal and SEM imaging

Neutral lipids accumulated in algal cells were visualized on the 15^{th} day of the experiment using a confocal laser scanning microscope (Olympus) while following a modified version of the protocol

described by Zhang et al. (2016). Likewise, the morphology of treated algal cells was also observed under Field Emission Scanning Electron Microscope (FE-SEM) (Supra55 Zeiss) (Sarno et al., 2007).

3.2.6 GC analysis and estimation of biodiesel quality

Ríos et al. (2013) was followed for the characterization of FAME. Peaks were identified by running external standards (FAME mix C4:C24; Sigma Aldrich #18919-1AMP) under similar conditions. The FAME percentage obtained from FAME analysis was employed further for the estimation of biodiesel properties. Iodine value (IV), degree of unsaturation (DUm), cetane number (CN), etc., were specific parameters that can fetch us the reference of the quality of biodiesel (Knothe and Steidley, 2005; Knothe, 2007).

3.2.7 ROS and antioxidative enzymatic analysis

ROS was estimated in terms of H_2O_2 content in the cells on the 10^{th} day of the experiment by following the procedure demonstrated by Velikova et al. (2000). H_2O_2 was analyzed through a standard calibration curve prepared using a known concentration of H_2O_2 as depicted in a chapter 2.

The extraction and quantification of raw protein were carried out by following Liu et al. (2018) and Bradford (1976) assays, respectively. Enzymatic kits (SOD and CAT) were purchased from Cayman chemical (MI-USA), and analysis was performed as per the manufacturer's instruction.

3.2.8 PCA analysis

PCA was performed in R studio desktop version 4.0.0 by using R packages, 'factoextra' (Kassambara and Mundt, 2017), 'FactoMineR' (Lê S, 2008), 'devtools' (Wickham, 2019), and 'ggbiplot' (Vincent, 2011).

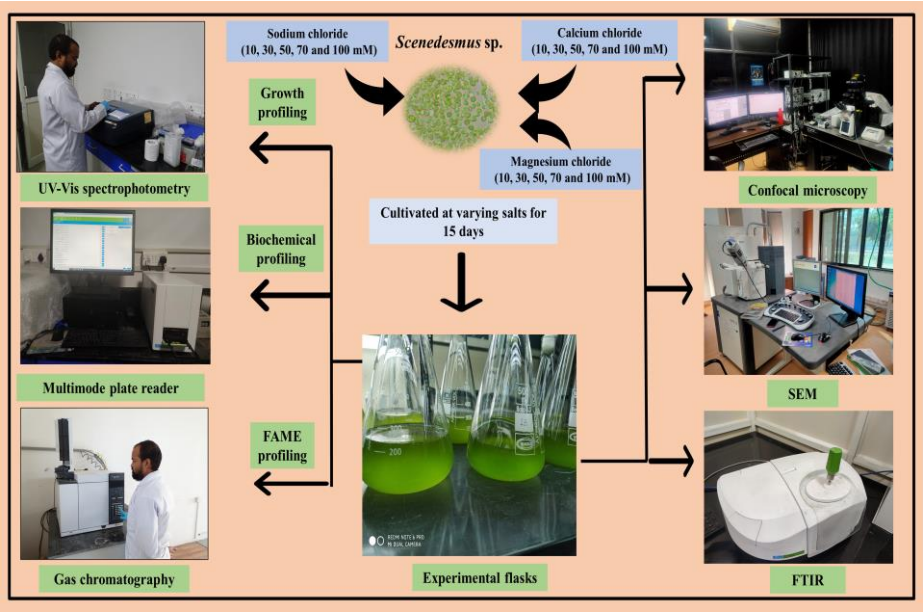

Figure 3.1: Graphical representation of salinity impact on *Scenedesmus* sp. along with output parameters

3.3 Results and Discussion

3.3.1 Microalgae growth profile under various salt treatments

Sodium chloride, calcium chloride, and magnesium chloride (NaCl, $CaCl_2$, $MgCl_2$) are explored as stress inducers for enhancing lipid content in the microalgae, *Scenedesmus* sp. The growth rate of cells cultivated in sodium chloride was found to be better than that of cells cultivated in magnesium chloride and calcium chloride. Figure 3.2 (A, B, and C) depicts the cell density of *Scenedesmus* sp. under different salt concentrations at varying time intervals. Biomass was calculated using a standard calibration curve constructed between optical/cell density and biomass (R^2 = 0.9936). The biomass content (Table 3.1) of cells cultivated in 10 mM of sodium chloride, calcium chloride, and magnesium chloride exposure was observed to be 1076.3±27.9 µg/mL, 924.3±13.2 µg/mL and 725.0±32.9 µg/mL, respectively on 15th day of the experiment. The biomass content was further observed to decrease upto 804.3±39.5 µg/mL, 598.0±11.8 µg/mL, and 485.3±13.6 µg/mL at 100 mM (Table 3.1) of sodium chloride, calcium chloride, and magnesium chloride exposure,

respectively. Additionally, the overall growth rate of cells treated with sodium chloride was not much affected as compared to other salt treated algal cells, explaining the adaptive response of sodium chloride. During exposure of algal cells to varying concentrations of sodium chloride, different processes occur inside the algal cell such as aggregation of osmo-protecting solutes (glycerol), recovery of turgor pressure, modulation of export and uptake of ions via the cell membrane. Osmoprotectants aid in balancing the external osmotic pressure generated by sodium chloride, which further prevents the loss of water and maintains cell turgor along with the activation of some stress-induced proteins that eventually leads to a steady-state growth (Allakhverdiev et al., 2000; Alkayal et al., 2010; Taleb et al., 2013). Inferences drawn from the results of this study conducted as well as from literature data, illustrate the species-specific salt tolerance potential algae. Many such reports such as *S. obliquus* found sensitive to NaCl concentrations equal to or more than 0.05 M (Zhang et al., 1997); NaCl more than 0.02 mM resulted in growth inhibition of *S. quadricauda* (Kirrolia et al., 2011); 0.1 M NaCl leading to higher biomass productivity of *S. almeriensis* (Benavente-Valdés et al., 2016). In our study, the growth of *Scenedesmus* sp. has not been much affected on altering the concentration of sodium chloride, while on the other hand, both magnesium chloride and calcium chloride showed lower growth kinetics as presented in Figure 3.2. The presence of the excessive salt concentration and the unfavourable culture conditions due to high salinity conditions (Vazquez-Duhalt and Arredondo-Vega, 1991) might be resulting in biomass reduction due to salinity induced osmotic stress (Mohan and Devi, 2014). Biomass, chlorophyll ‘a’, and specific growth rate (Table 3.1) of *Scenedesmus* sp. cultivated under varying levels (mM) of different salts, delineating that there is decrease in biomass and chlorophyll ‘a’ accumulation with increase in salt concentrations on 15^{th} day of experiment. Algal cells were not able to grow significantly even after 15 days, and the growth was reduced more in the case of magnesium chloride than calcium chloride. On the basis of growth profile, it can be portrayed that there was slow growth

of algal cells reflected through extended lag phase under the treatment of different salts, which further indicates that the cells have the ability to tolerate and survive these stress conditions by diverting the biochemical pathways towards the accumulation of cell storage molecules such as lipid and carbohydrate. Similarly, biomass productivity declined with rise in the salt concentration. On the 15^{th} day, sodium chloride (100 mM) showed the highest biomass productivity (33.3 µg/mL/d). However, for calcium chloride (19.4 µg/mL/d) and magnesium chloride (12.6 µg/mL/d) biomass productivity decreased by 41.4 and 62.1%, respectively as compared to that of sodium chloride. Furthermore, the comparative evaluation showed a limited effect on biomass productivity and specific growth rate in case of sodium chloride as compared to magnesium chloride and calcium chloride. Thus, *Scenedesmus* sp. was determined to be more adaptable to sodium chloride treatment as compared to magnesium chloride and calcium chloride.

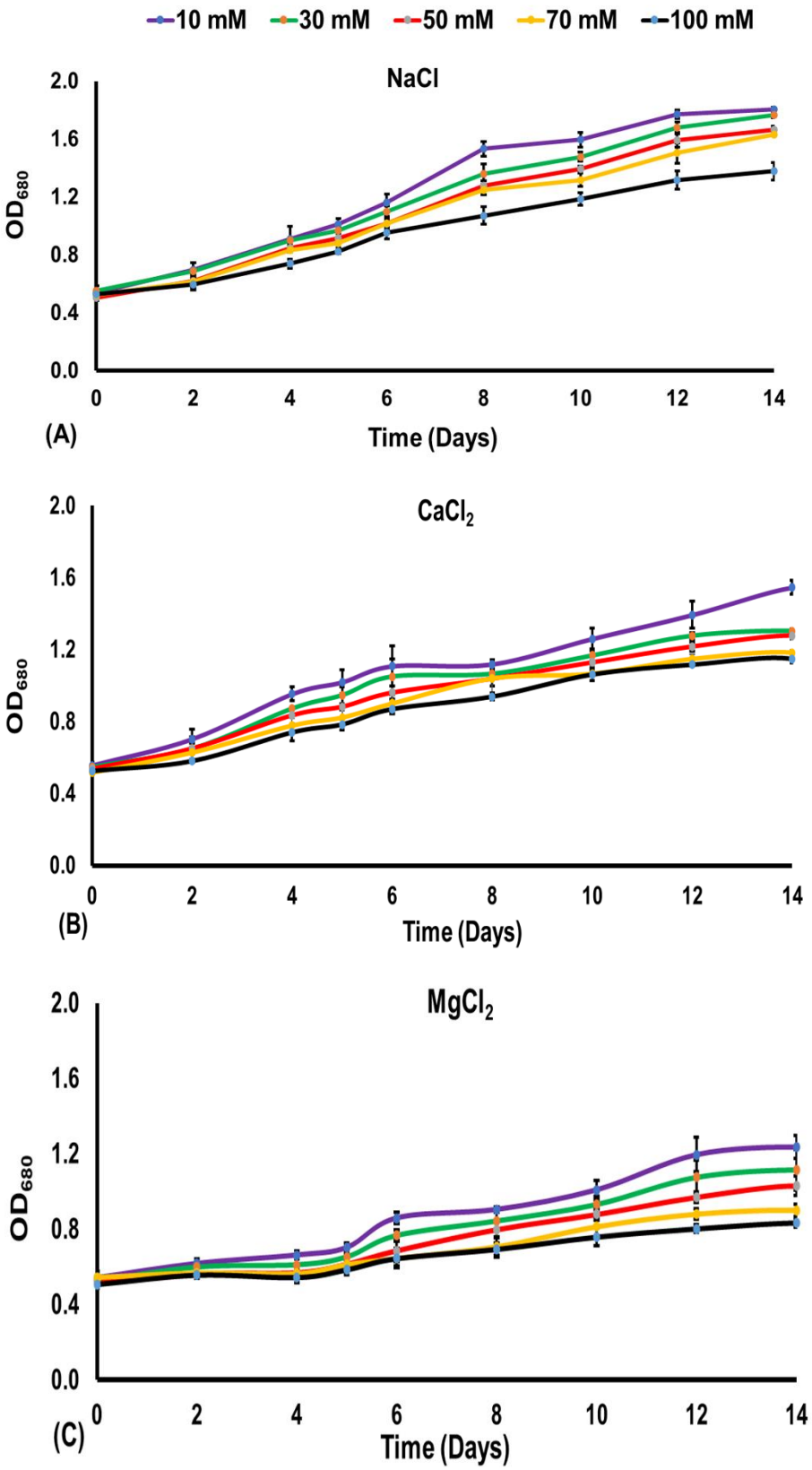

Figure 3.2: Cell density of *Scenedesmus* sp. under salinity exposure (A) NaCl (mM); (B) $CaCl_2$ (mM); (C) $MgCl_2$ (mM)

Table 3.1: Biomass, chlorophyll 'a' and specific growth rate of *Scenedesmus* sp. cultivated under varying levels (mM) of different salts, where sodium chloride, calcium chloride and magnesium chloride are represented with S, C and M, respectively

Salts (mM)	**Biomass Accumulation (µg/mL)**			**Chlorophyll Accumulation (µg/mL)**			**Specific Growth Rate (day^{-1})**
	5^{th} day	**10^{th} day**	**15^{th} day**	**5^{th} day**	**10^{th} day**	**15^{th} day**	**10^{th} day**
S_{10}	610.0±23.5	975.3±32.5	1076.3±27.9	10.7±1.0	15.7±0.5	20.5±1.3	0.10±0.01
S_{30}	581.9±12.0	902.3±20.2	1043.8±13.0	9.4±1.0	14.9±0.5	17.3±0.3	0.09±0.01
S_{50}	551.3±24.9	850.3±11.2	998.7±25.2	8.7±0.2	13.9±0.4	15.7±0.3	0.10±0.00
S_{70}	527.5±19.1	801.5±28.6	973.9±12.7	8.0±0.3	12.2±0.9	14.5±0.2	0.09±0.00
S_{100}	493.5±11.5	719.5±26.2	804.3±39.5	7.1±0.2	11.0±0.1	13.7±0.6	0.08±0.01
C_{10}	615.7±41.9	766.6±36.0	924.3±13.2	9.1±0.1	13.9±0.5	17.0±0.5	0.08±0.01
C_{30}	570.2±29.2	708.0±16.6	768.6±24.0	8.8±0.2	12.4±0.2	16.2±0.3	0.07±0.00
C_{50}	530.3±10.9	684.2±27.0	731.7±11.3	9.2±0.7	12.1±0.4	14.3±0.7	0.07±0.00
C_{70}	493.2±30.7	644.8±26.5	652.6±8.2	8.4±0.4	10.7±0.3	12.7±0.2	0.07±0.00
C_{100}	468.5±19.1	642.7±21.4	598.0±11.8	7.3±0.1	9.9±0.2	11.8±0.1	0.07±0.00
M_{10}	418.4±15.1	609.0±31.9	725.0±32.9	10.1±0.3	14.3±0.7	15.4±0.9	0.06±0.01
M_{30}	386.7±23.7	560.6±26.1	653.0±60.9	8.6±0.4	11.0±0.5	12.5±0.4	0.05±0.00
M_{50}	363.0±33.5	528.2±18.4	581.1±20.7	7.4±0.4	10.4±0.4	9.8±0.4	0.05±0.01
M_{70}	362.1±14.6	486.8±29.3	508.7±21.2	6.9±0.3	9.4±0.7	9.3±0.5	0.03±0.00
M_{100}	344.9±17.9	453.2±28.0	485.3±13.6	6.1±0.2	8.3±0.5	8.8±0.2	0.04±0.00

3.3.2 Effect of salt stress on chlorophyll content

Microalgae are rich source of pigments and the quantitative measurement of some pigments including chlorophyll and xanthophyll can be correlated with the stress behaviour of microalgae (Ahmad et al., 2013). The accumulation of chlorophyll has been deployed as an algal growth indicator. In the present study, chlorophyll 'a' concentration was estimated at a regular interval of 5 days up to 15^{th} day of the experiment. It was observed that chlorophyll content decreases with increase in salt concentration for all the salt treatments (Figure 3.3), similar to the trend of biomass content. Chlorophyll 'a' content (Table 3.1) observed at 10 mM of sodium chloride (20.5±1.3 µg/mL), calcium chloride (17.0±0.5 µg/mL) and magnesium chloride (15.4±0.9 µg/mL) were found to decrease further with increase in salt concentrations. Chlorophyll content decreases by 13.8 and 35.7 % for 100 mM calcium chloride (11.8±0.1 µg/mL) and magnesium chloride (8.8±0.2 µg/mL), respectively in comparison to 100 mM sodium chloride (13.7±0.6 µg/mL) on 15^{th} day analysis (Table 3.1). The reduced chlorophyll content in response to stress conditions was in line with earlier results obtained by different researchers (Hiremath and Mathad, 2010; Kirrolia et al., 2011). The depletion in chlorophyll accumulation can probably be related to the modifications occurring in the metabolic flux of microalgae due to the implementation of stress, which eventually affects the cell's physiology (Rai et al., 2015). During salinity stress, the rate of carbon dioxide uptake and nutrient utilization by algae is reduced owing to the slow rate of Nicotinamide Adenine Dinucleotide Phosphate (NADPH) formation. This phenomenon ultimately affects chlorophyll synthesis resulting in low chlorophyll content along with reduced biomass accumulation (Rai et al., 2015). Sodium ions (Na^+) play an important role in maintaining cellular osmolarity. However, if there is an imbalance in any of salt ion concentration then it may lead to stimulation of osmotic stress, and the cells metabolic pathway gets tweaked in order to survive in the adverse conditions leading to the production of ROS (Reactive Oxygen Species). However, the presence

of ROS may act as a retardation factor for cell growth due to the interference of ROS with cellular pathways, thus obliterating the production process of essential biomolecules responsible for the survival of cell. This hindrance culminates a hike in the production of antioxidant enzymes for the counterattack to the generated ROS (Mallick and Mohn, 2000).

An inhibitory effect of ionic stress due to accumulated salt ions seems to be the main reason behind the change in chlorophyll concentration. Reduction in chlorophyll accumulation and depletion in photosynthesis rate may be due to the induction of oxidative stress by exposure to salt treatment (Affenzeller et al., 2009). Photo-inhibition of cells due to salinity-induced oxidative stress contributes to the impeded cell growth rate (Yilancioglu et al., 2014). In accordance with the literature, it has been revealed that the production of neutral lipids has been involved substantially in scavenging the accumulated ROS (Pancha et al., 2015).

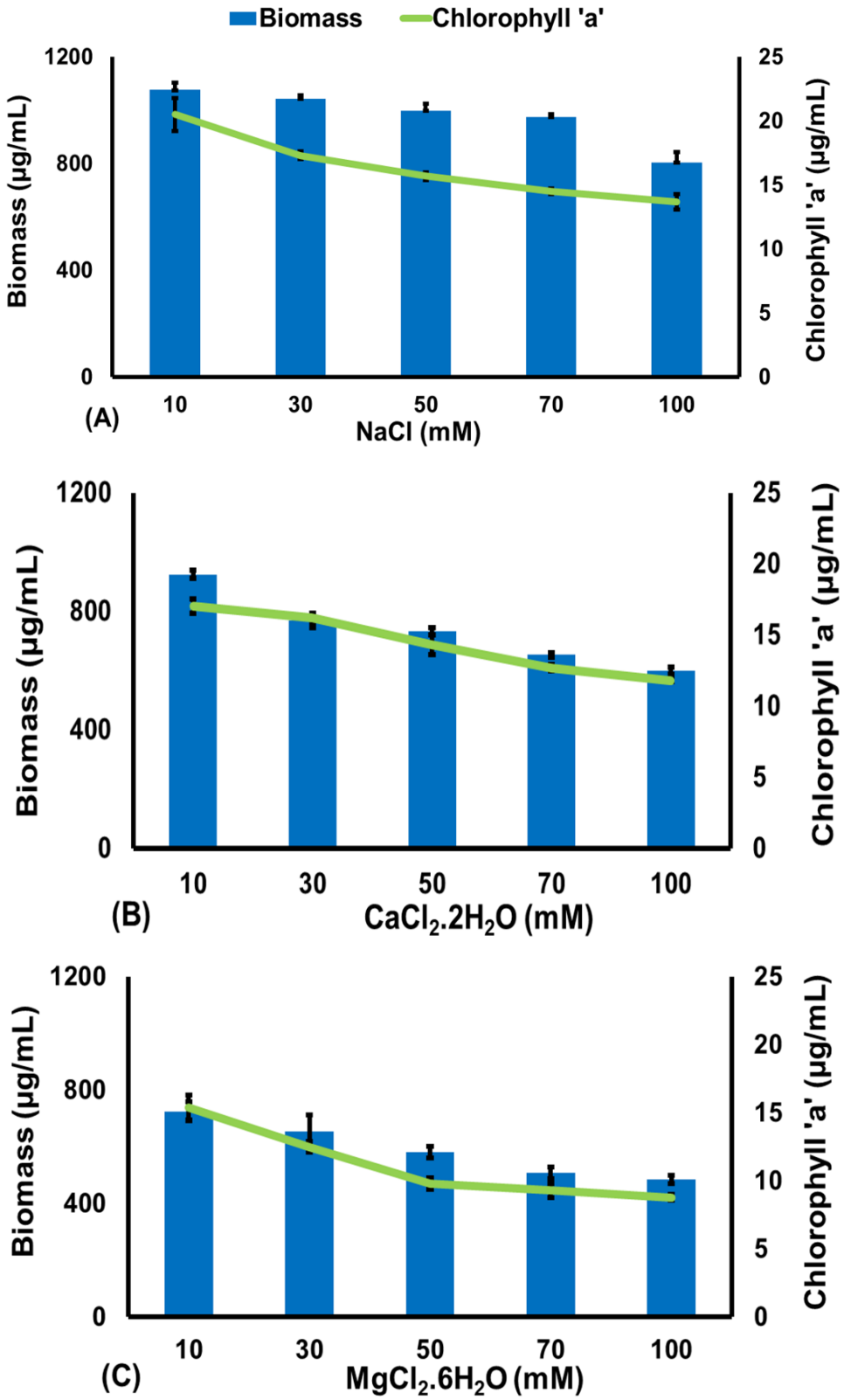

Figure 3.3: Biomass and Chlorophyll 'a' correlation of *Scenedesmus* sp. under salt exposure (A) NaCl (mM); (B) $CaCl_2$ (mM); (C) $MgCl_2$ (mM) on 15^{th} day

3.3.3 Total lipids

The lipid concentration of varying salt-treated algal cells was estimated and is reported in Table 3.2. Amongst various mono-component salts (sodium chloride, calcium chloride, and magnesium chloride), increase in concentration (0 to 100 mM) leads to an increase in lipid accumulation. Maximum lipid concentration was obtained for NaCl at 100 mM (197.6±4.9 µg/mg), which was followed by 70 mM of NaCl (159.1±6.4 µg/mg). However, under varying $MgCl_2$ levels, high amount of lipid was obtained at 70 mM (182.5±3.1 µg/mg) of salt, which was also a second highest accumulator of total lipids. NaCl showed maximum total lipid production followed by $MgCl_2$ and $CaCl_2$. As represented in Table 3.2, minimum lipid production was observed in $CaCl_2$ treated cells. NaCl plays an essential role in osmoregulation of algae under different environmental conditions and helps to regulate membrane potential. However, under high NaCl exposure, there is decrease in the level of electron transport occurring in the machinery of photosynthesis because of the breaking of 23 KDa polypeptide associated with photosystem II (Sudhir and Murthy 2004).

3.3.4 Total carbohydrate

Carbohydrate is the first molecule, which is synthesized under normal growth conditions. However, under different treatment strategies, the synthesis of carbohydrates depends upon the carbon flux and the amount of stress given to the sample. In the current study, the carbohydrate was found maximum for NaCl at 50 mM (509.4±9.3 µg/mg). It was noticed that with increment in the concentration of NaCl beyond 50 mM, there was no further significant increase in carbohydrate content, as evident in Table 3.2. However, an enhancement in lipid content was observed for higher NaCl concentrations, which clearly indicates that during stress conditions, carbon flux diverts from carbohydrate synthesis towards lipid synthesis and is used as an energy molecule during adverse conditions. Although in the case of $CaCl_2$, the amount of carbohydrate produced was almost

the same for varying concentrations (10, 30, and 50 mM), beyond which an increase in carbohydrate content was ascertained. In the case of $MgCl_2$, maximum carbohydrate was obtained at 100 mM (668.6±36.7 µg/mg), which was also found to be the highest carbohydrate accumulator. Sucrose is a low molecular weight carbohydrate produced under osmotic stress to protect cells from the hardness of salt. In general, lipids and carbohydrates allow species to adjust their growth and development in response to changing environmental conditions. However, the potential of accumulating carbohydrates has been a species-specific characteristic, such as *Dunaliella* sp. accumulate glycerol under salt stress produced through the catabolism of carbohydrates and this glycerol accumulation further results in the enhancement of lipid production (Shetty et al., 2019).

Table 3.2: Biochemical composition of *Scenedesmus* sp. cultivated under varying levels (mM) of different salts, where sodium chloride, calcium chloride and magnesium chloride are represented with S, C and M, respectively

Salts (mM)	Lipid Concentration (µg/mg)	Lipid Content (%)	Carbohydrate Concentration (µg/mg)	Carbohydrate Content (%)
S_{10}	105.8±6.1	10.5±0.6	234.4±6.8	23.4±0.6
S_{30}	102.9±5.8	10.2±0.5	353.6±15.1	35.3±1.5
S_{50}	130.0±2.6	13.0±0.2	509.5±9.3	50.9±0.9
S_{70}	159.1±6.4	15.9±0.6	446.5±13.8	44.6±1.3
S_{100}	197.6±4.9	19.7±0.4	470.3±23.8	47.0±2.3
C_{10}	73.5±2.7	7.3±0.2	367.1±20.6	36.1±2.0
C_{30}	96.5±1.5	9.6±0.1	366.3±30.8	36.6±3.0
C_{50}	119.1±2.3	11.9±0.2	309.0±7.4	30.9±0.7
C_{70}	109.5±7.0	10.9±0.7	469.1±13.9	46.9±1.3
C_{100}	134.5±8.1	13.4±0.8	473.0±10.2	47.3±1.0
M_{10}	124.5±8.0	12.4±0.8	533.6±12.1	53.3±1.2
M_{30}	127.3±3.0	12.7±0.3	526.6±17.5	52.6±1.7
M_{50}	103.2±4.4	10.3±0.4	512.6±51.4	51.2±5.1
M_{70}	182.5±3.1	18.2±0.3	464.4±20.9	46.4±2.0
M_{100}	179.8±19.7	17.9±1.9	668.7±36.7	66.8±3.6

3.3.5 Biomolecular insight study

Biomolecular transitions occurring inside *Scenedesmus* sp. treated with different concentrations of salt were analyzed on 15th day of experiment. The second-order derivative method was practiced as it helps in resolving the intersecting bands present in unprocessed spectra along with baseline errors, thus leading to the classification of minor and nearby absorption bands. Table 3.3 represents spectral peaks that

have been allocated to different functional groups belonging to different classes of macromolecules.

Table 3.3: Band assignments for infrared spectroscopy

Wavenumber (cm^{-1})	**Assignment**	**References**
~1075	υSi-O of silicate frustules	Giordano et al., 2001
~1200-900	υC-O of saccharides	Giordano et al., 2001
~1250-1230	υ_{as} P=O of phosphodiester groups of nucleic acid and phospholipids	Coates. 2000
~1398	δ_s CH_3 and δ_s CH_2 of proteins, and υ_s C-O of COO^- groups	Giordano et al., 2001
~1455	δ_{as} CH_3 and δ_{as} CH_2 of proteins	Giordano et al., 2001
~1540	δN-H of amides from proteins	Coates. 2000
~1650	υC=O of amides from proteins	Giordano et al., 2001
~1745	υC=O of ester groups, primarily from lipids and fatty acids	Giordano et al., 2001
3000-2800	υC-H of saturated CH	Coates. 2000

The stretches are mainly observed due to υ(CH_3) and υ(CH_2) corresponding to symmetrical and asymmetrical stretching movements of lipids from hydrocarbons. The presence of an intense band at ~1745 cm^{-1} corresponds to the presence of triacylglycerides (TAGs) related with υ (C=O) of ester groups mainly from lipids and fatty acids as shown in Figure 3.4A. Since the peak intensity corresponds to the concentration of TAGs present in the cells (Grace et al., 2020), the maximum TAG accumulation at 70 mM of NaCl was confirmed as depicted in Figure 3.4A, illustrating full carbon allocation or hydrocarbon stretch at 70 mM NaCl. Two characteristic bands of protein chains i.e., amide I and amide II were observed, one at ~1658 cm^{-1} υ (C=O) representing the stretching of an amide from protein and

second at ~1547 cm^{-1} showing δ (N-H) bending of amide from protein, respectively as delineated in Figure 3.4A. A similar pattern of stretches was observed by Stehfest et al. (2005) and Dean et al. (2010) in the microalgal species. Cells of *Scenedesmus* sp. treated with different concentrations of $CaCl_2$ showed maximum hydrocarbon stretches from lipids and TAGs at 30 mM, as shown in Figure 3.3B. In case of samples treated with various $MgCl_2$ concentrations, maximum stretching from lipids and neutral lipids was obtained at 50 mM concentration as shown in 3.4C.

Comparative lipid concentration was calculated by taking lipid (~1745 cm^{-1}) band to amide I (~1658 cm^{-1}) and amide II (~1547 cm^{-1}) ratio, and the samples treated with 70 mM concentration of NaCl showed maximum TAGs: Amide I and TAGs: Amide II ratio in comparison to other concentrations of the same salt used in this study as shown in Figure 3.5A. Although TAG: Amide I and TAG: Amide II ratio (Figure 3.5B) for calcium chloride was calculated to be maximum at 100 mM and 50 mM salt concentration, respectively. However, in case of $MgCl_2$, TAGs: Amide I and TAGs: Amide II ratio was found to be approximately equivalent (Figure 3.5C) for 10-, 30-, and 70 mM salt treatment, whereas least stretches were observed for 50 and 100 mM of $MgCl_2$.

Similarly, maximum hydrocarbon stretches (Figure 3.6A) and Hydrocarbon: Amide I (CH: AI) and Hydrocarbon: Amide II (CH: AII) (Figure 3.6A) ratio was observed in cells treated with 70 mM NaCl suggesting the superior potential of lipid production under the influence of 70 mM NaCl. On the other hand, maximum CH: AI and CH: AII ratio (Figure 3.7B) was found to be foremost in the case of 30 mM and 50 mM concentration of $CaCl_2$ as compared to other concentrations of the same salt. Similarly, CH: AI ratio was determined to be maximum in samples treated with 30 mM $MgCl_2$ (Figure 3.7C), and CH: AII ratio was found to be almost identical for all concentration of $MgCl_2$.

The results indicate that different salts have varying impacts on TAGs, hydrocarbons, and amide content of the cells as inferred from FTIR analysis. The detailed analysis of FTIR through second-order derivative helps us to understand the changes in the TAGs: Amide and CH: Amide ratio leading to the disclosure of different concentrations that can be used to enhance total lipid content of the cells. The results obtained are in line with earlier study done by Grace et al. (2020), where they have used different species and monitored their growth pattern for the accumulation of lipids as well as other compounds, leading to change in the intensity of TAGs at ~1745 cm^{-1}, affecting TAGs: Amide and CH: Amide ratios. Similar changes can be observed in our study as with varying concentration of different salts there is a change in stretching of the bands, altering TAGs: Amide and CH: Amide ratio. However, some reports are available showing changes in the lipid accumulation for different microalgae species with time depicted by changes in the stretches of hydrocarbons and TAGs at ~2800 cm^{-1} to ~3050 cm^{-1} and ~1745 cm^{-1}, respectively.

The changes observed in the relative content of TAGs: Amide ratio and CH: Amide ratio in the present study suggest that TAGs accumulation increases in the cells under stress and hydrocarbon and amide content decreases. This observation corresponds to the increase in lipid accumulation in *Scenedesmus* sp. under stress and a decrease in the protein and carbohydrate content accordingly. Hence, it can be validated that the cells of *Scenedesmus* sp. are channelizing the metabolism towards lipid accumulation under stress as evident from the FTIR analysis.

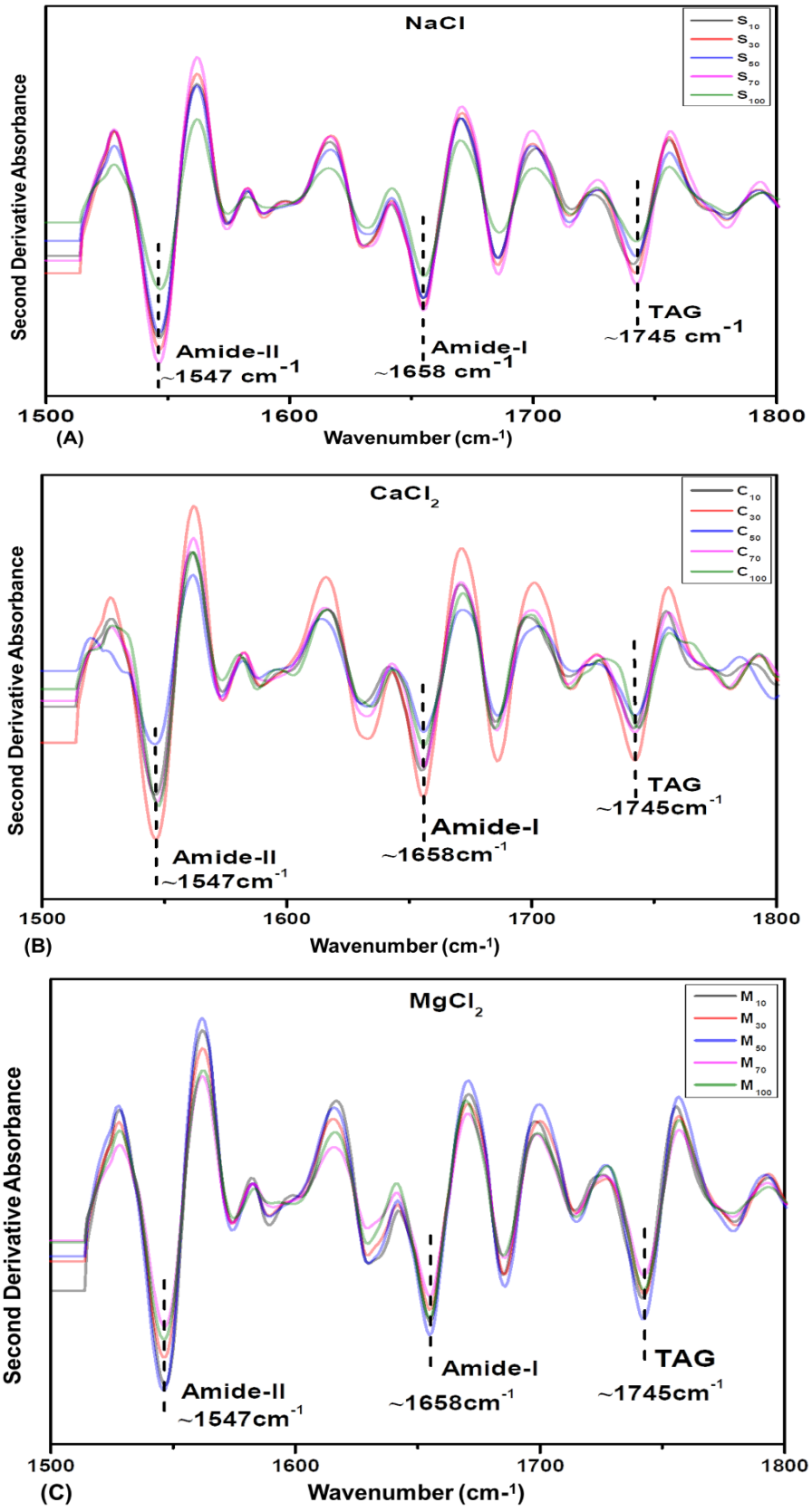

Figure 3.4: FTIR Spectra of *Scenedesmus* sp. under varying salt exposure (A) NaCl (B) $CaCl_2$ and (C) $MgCl_2$ at 1800-1500 cm^{-1}

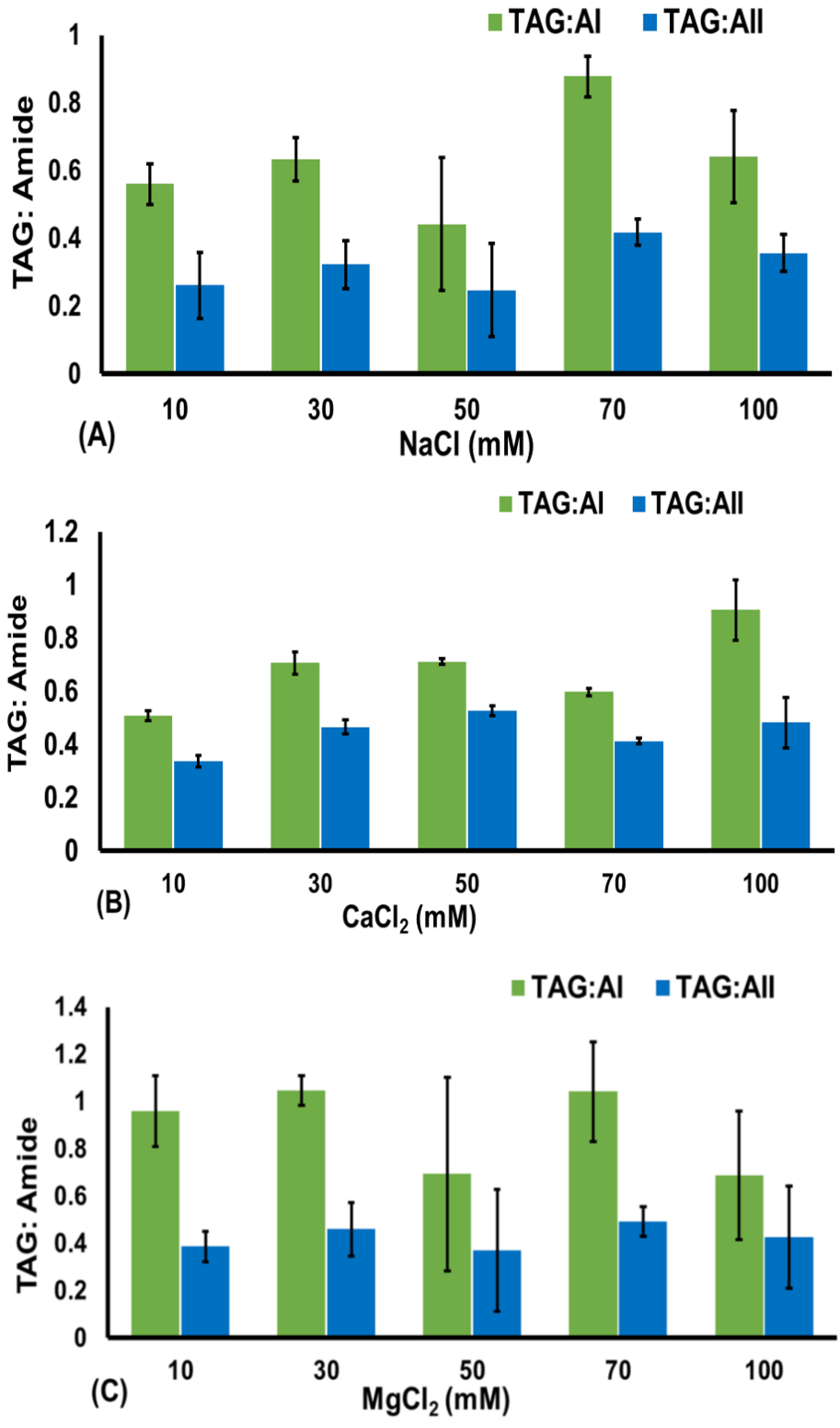

Figure 3.5: Relative content of (A) TAGs: Amide under varying concentrations of salt (# TAGs – Triacylglycerides; AI – Amide I; AII – Amide II)

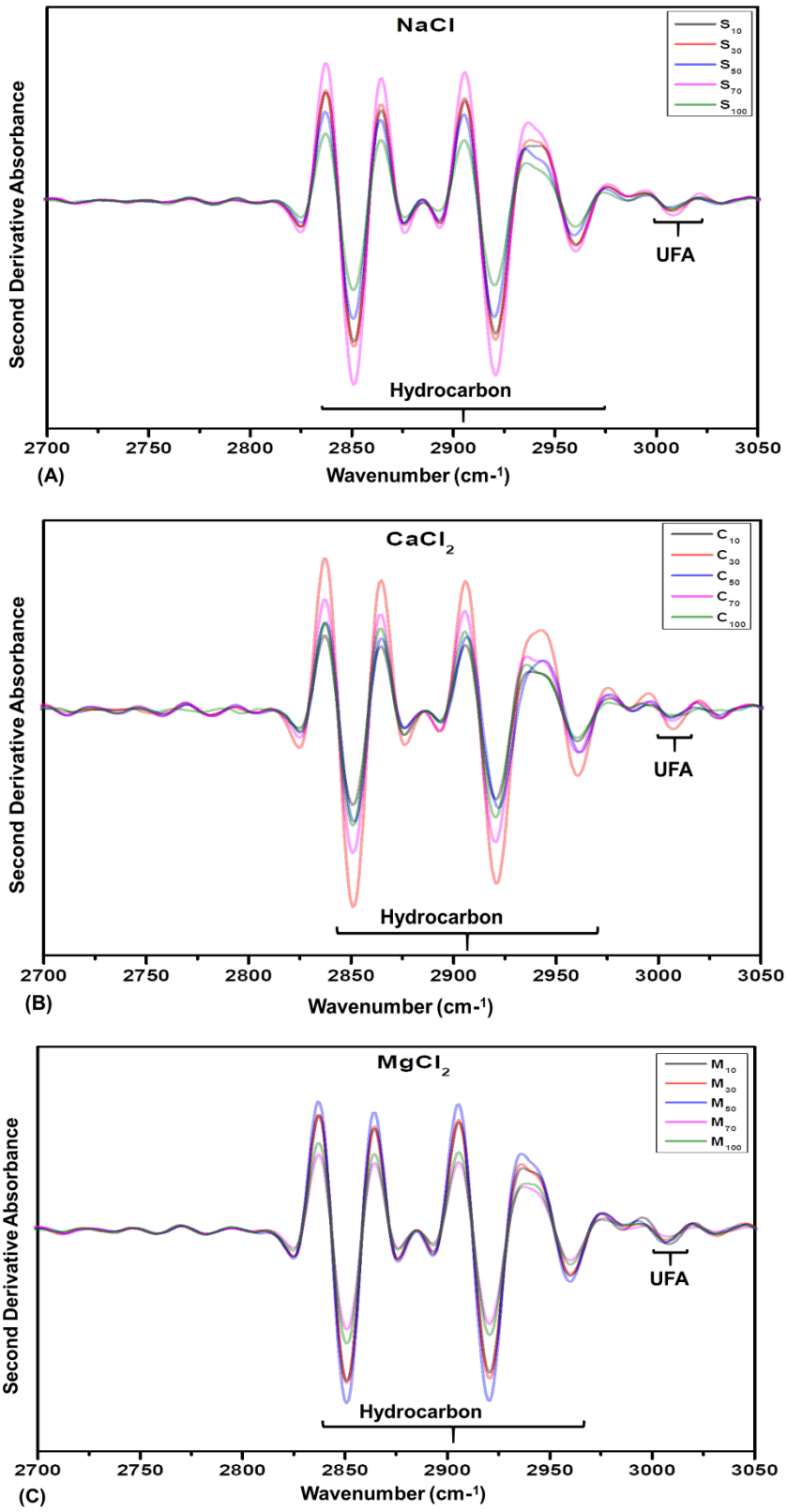

Figure 3.6: FTIR Spectra of *Scenedesmus* sp. under varying salt exposure (A) NaCl (B) $CaCl_2$ and (C) $MgCl_2$ on 15^{th} day at 3050-2700 cm^{-1} (# UFA = Unsaturated Fatty Acid)

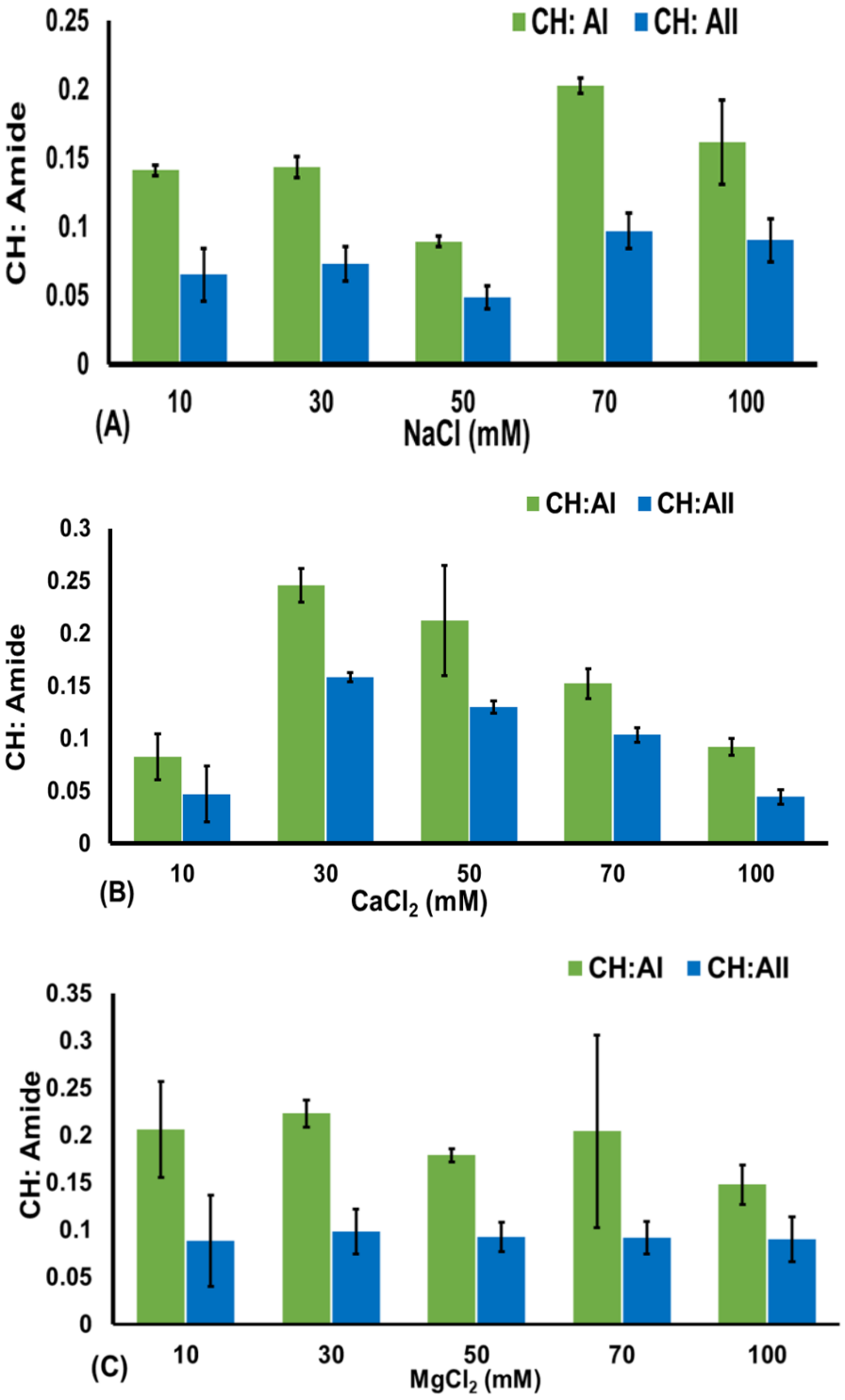

Figure 3.7: Relative content of CH: Amide under varying concentrations of salt (#CH – Hydrocarbon; AI – Amide I; AII – Amide II)

3.3.6 Confocal imaging under stress conditions

Lipid bodies (Neutral lipids) accumulated inside algal cells cultivated under salt treatment were visualized under confocal microscopy (Figure 3.8). High intensity of yellow color was observed in cells stained with Nile red, symbolizing the existence of neutral lipids inside the algal cell. Neutral lipid staining with lipophilic Nile red dye has been practiced from earlier times to identify intracellular neutral lipid bodies present in a given sample as it ought to be considered an excellent staining dye. It is a fluorescent lipophilic dye that intercalates with triacylglycerol (TAGs) specifically due to its lipophilic nature (Sitepu et al., 2012). The yellow fluorescence is formed on the interaction of neutral lipid with that of Nile red. From the confocal microscopy images, maximum neutral lipid bodies were visualized at 100 mM NaCl and $MgCl_2$ concentration compared to $CaC1_2$ exposure.

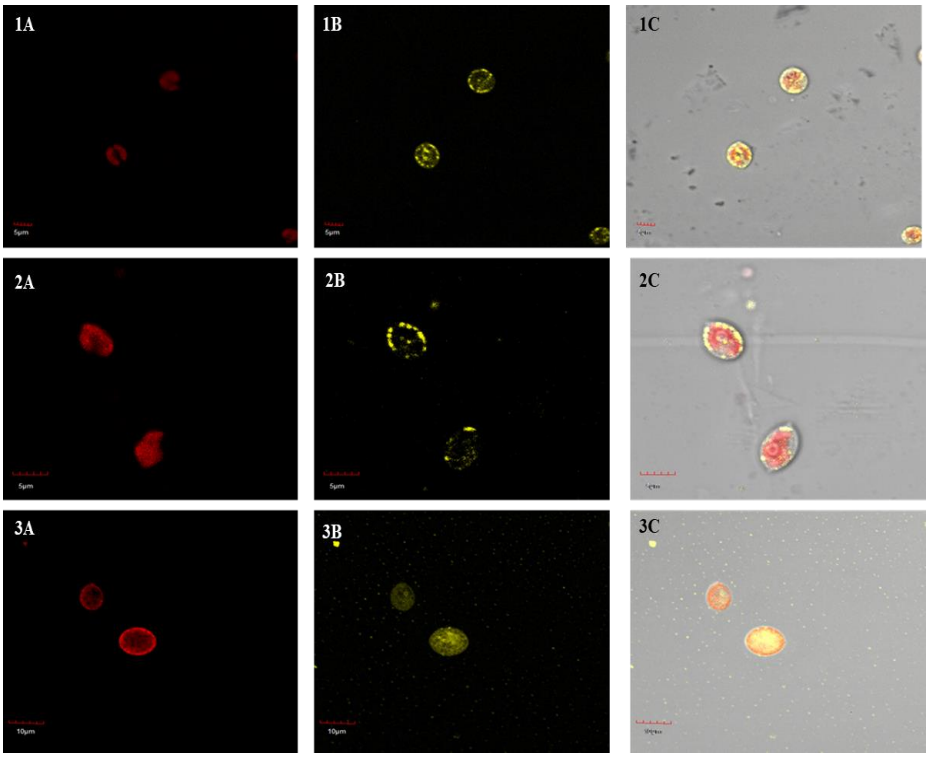

Figure 3.8: Neutral lipids of *Scenedesmus* sp. under confocal microscopy at 100 mM of (1) NaCl (2) $CaCl_2$ and (3) $MgCl_2$; A: Autofluorescence; B: Nile red-stained neutral lipid; C: Merged Image of A and B

3.3.7 Surface morphology through Scanning Electron Microscopy

SEM was performed to analyze morphological and topological changes occurring in the cells after exposure to salt stress, and images were taken at 3Kv EHT so that the cells do not get charred and images can be captured easily. As it is evident from the images shown in Figure 3.9, salt-treated samples of $MgCl_2$ and NaCl at 100 mM, the cells appear to be shrunken and pressed with irregular grooves and depressions on the surface. The appearance of cells suggest that the saline environment can cause changes in the morphology of algal cells, which eventually affects the cell functionality. The morphological variability in the cells can be observed in the SEM micrographs and can thus be utilized to explain the impact of treatment given to the cells, which is also reported in earlier studies (Sarno et al., 2007).

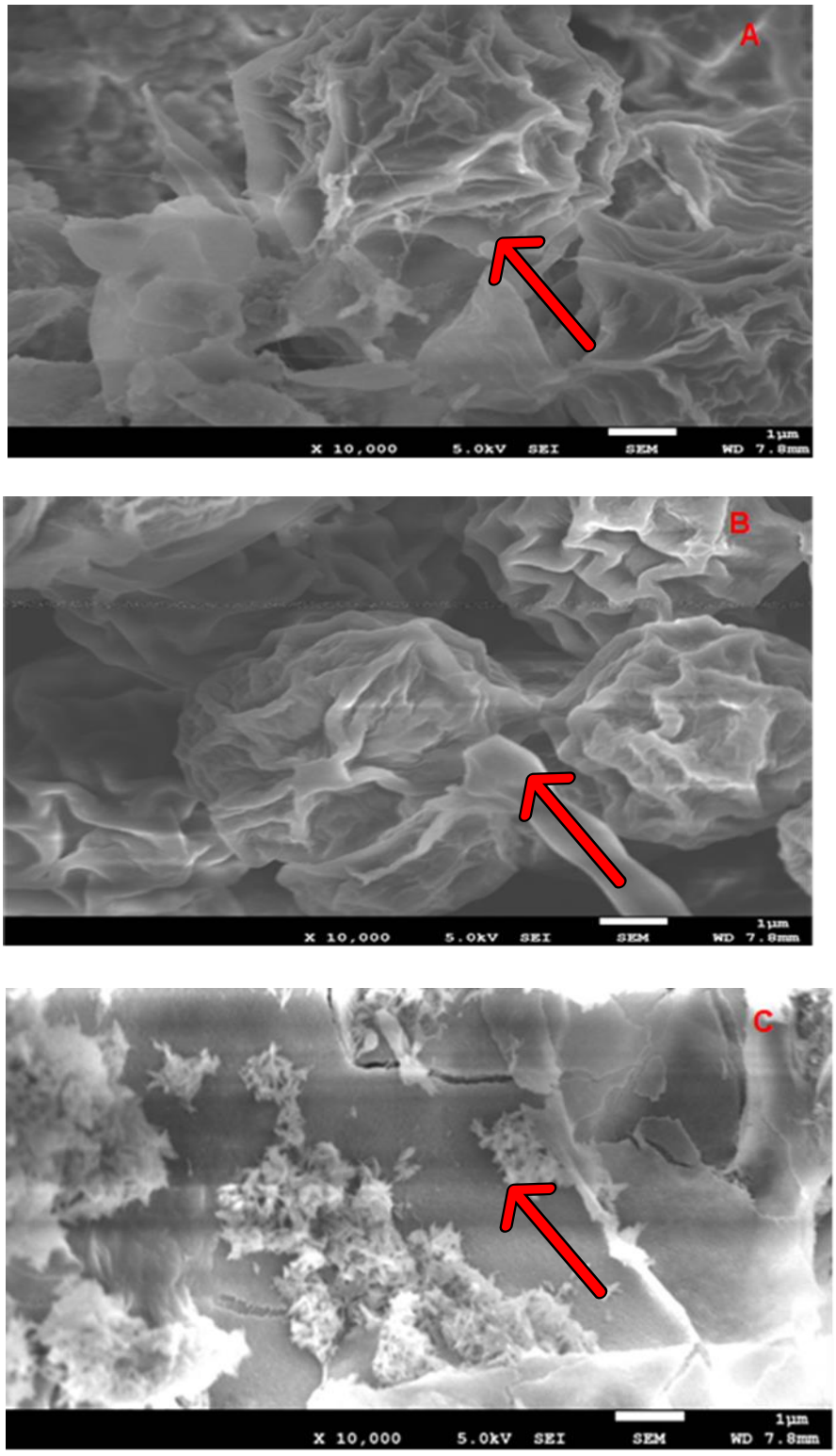

Figure 3.9: Scanning electron microscopy images of *Scenedesmus* sp. at 100 mM of (A) NaCl (B) $MgCl_2$ and (C) $CaCl_2$ on 15^{th} day

3.3.8 FAME profiling

Fatty acid profiling was done on 15th day of experiment to observe the influence of different salt treatments and their varying concentrations in the context to biodiesel properties. Under salt exposure, there is not only an increment in lipid content, but also a change in fatty acid profile. It was observed that under salinity stress, there is decline in polyunsaturated fatty acid content with an augmented saturated fatty acid percent as presented in Figure 3.10 (A, B, C). A high amount of saturated fatty acid suggests that there is less risk of combustion and ignition delay-related problems in the biodiesel produced (Benjumea et al., 2011).

The percentage of palmitic acid was higher under salt stress conditions and was found maximum in cells treated with 50 mM $MgCl_2$ (37.7%). Stearic acid percent was observed to be highest in cells exposed to 70 mM $CaCl_2$ (2.4%). Similarly, oleic acid and linoleic acid were the highest in cells treated with 100 mM NaCl (20.9%) and $CaCl_2$ (21.7%). In contrast, γ-linolenic acid showed an opposite trend with a decrease in treated samples, with maximum reduction observed in 100 mM NaCl (22.3%). Thus, there was decrease in polyunsaturated fatty acid content and an increase in saturated and monounsaturated fatty acid content when exposed to salt stress, which is important in context to biodiesel properties. Total FAME content was observed to be maximum for calcium chloride (44.1±5.8 µg/mg) at 100 mM (Figure 3.11), which was followed by sodium chloride at 100 mM (41.8±6.8 µg/mg).

During salt treatment, the concentration of ions in the media increases, which in turn allows the exchange of ions across the membrane affecting many other metabolic pathways. In the case of $CaCl_2$, there was an increase in Ca^{2+} ion concentration inside the cell, which further affected Na^{+} ion concentration, leading to the transportation of ions across the cells of a given species, and thus ultimately tweaks the fatty acid profile of microalgae along with its

quantity (Karimova et al., 2000). The involvement of Ca^{2+} ions in cell signalling can be

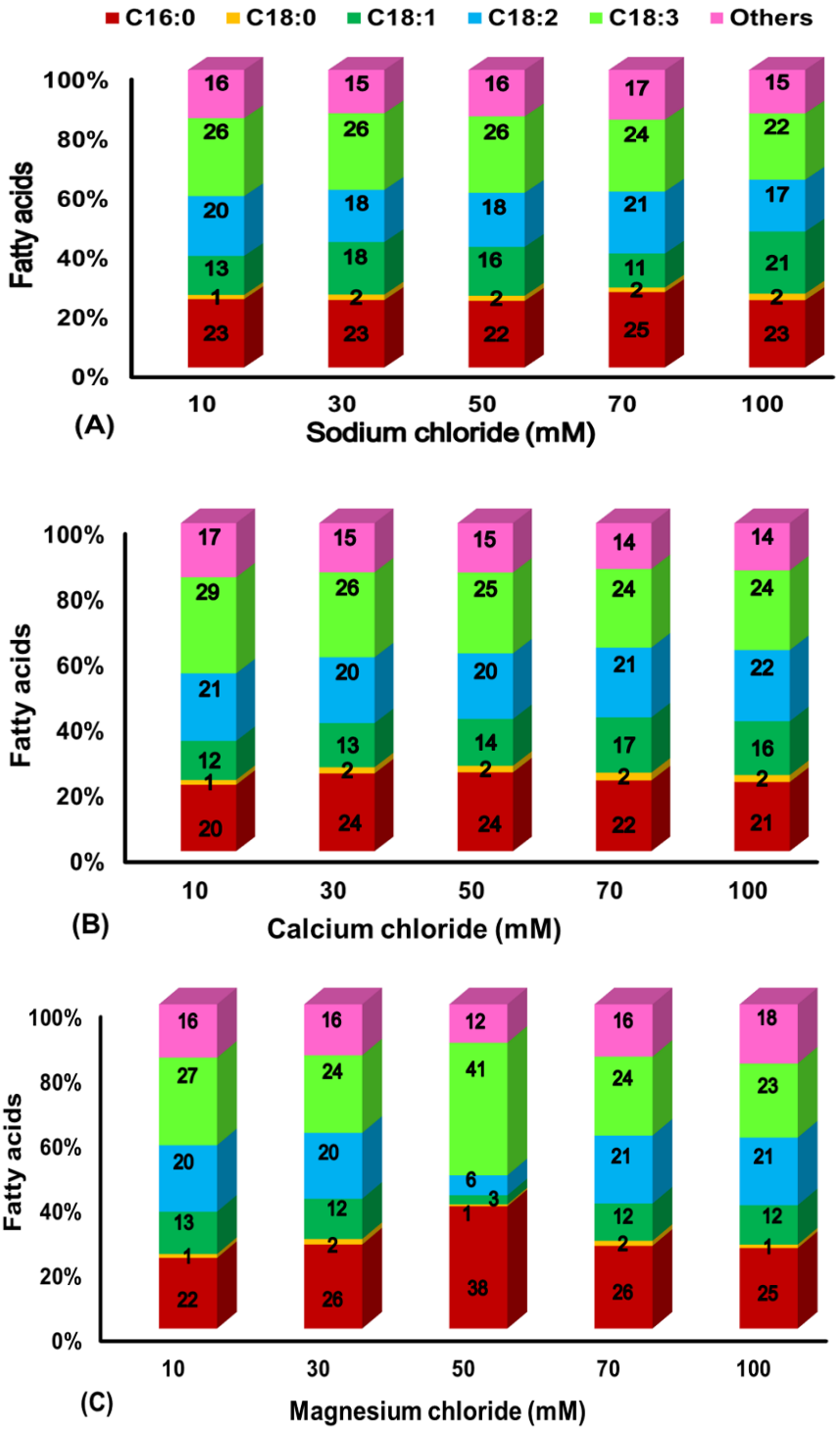

Figure 3.10: Fatty acid profile (percent) of *Scenedesmus* sp. cultivated under varying concentrations (mM) of different salts, (A) sodium chloride, (B) calcium chloride and (C) magnesium chloride

responsible for highest lipid accumulation inside cells exposed to $CaCl_2$ (Chen et al., 2014; Wheeler and Brownlee, 2008). Ca^{2+} ions being the designated signalling molecule is involved in different metabolic pathways occurring inside microalgae, such as light penetration, motor response, and circadian oscillations. These pathways further lead to a change in Na^+ and K^+ ions flux by stimulating high accumulation of K^+ ions inside the cells and expulsion of Na^+ out from the cells (Wheeler and Brownlee, 2008). Additionally, Ca^{2+}/H^+ pump is also maintained by the presence of Ca^{2+} ions, which enhances Ca^{2+} permeability across the cell's membrane (Campbell, 2014).

However, during diverse salinity stress, various metabolic pathways come into action to interact with different ion transporters so as to maintain homeostasis balance in the cytoplasm. Amongst these, the Salt Overly Sensitive (SOS) pathway is highly explored pathway consisting of SOS1, SOS2, and SOS3 as major proteins that maintains Na^+ ions concentration inside cells (Zhu, 2000). High concentration of Ca^{2+} inside cells has been reported to result in the activation of SOS3 and SOS2 protein. This SOS2 protein has been the most centric molecule and plays an essential role in blocking antiporter such as Na^+/H^+ present on the cell's plasma membrane and in the activation of Na^+/H^+ antiporter present on vacuole. Salinity stress also causes the release of certain reactive oxygen species (ROS) such as H_2O_2, OH^- and O_2^- which bind to DNA, protein, or any other biomolecule, thus initiating cell damage or programmed cell death (Zhu, 2000). Different enzymatic systems such as superoxide dismutase (SOD), catalase (CAT) etc. are engaged in scavenging ROS, while non-enzymatic systems such as proline, carotenoids etc., are also involved in the release of stress caused by different environmental perturbations (Zhu, 2016).

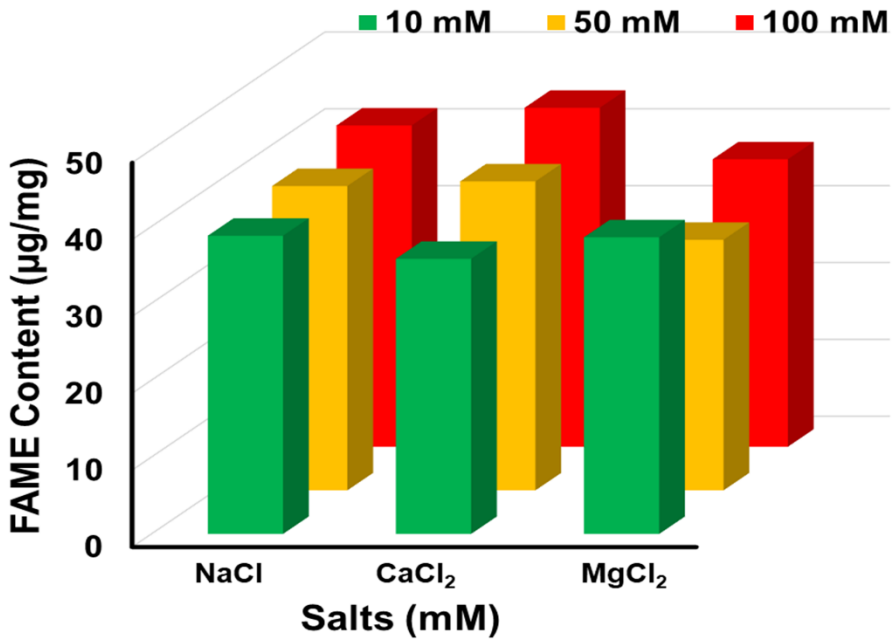

Figure 3.11: FAME yield of *Scenedesmus* sp. cultivated under varying concentrations (mM) of different salts, where sodium chloride, calcium chloride and magnesium chloride are represented with S, C and M, respectively

3.3.9 Biodiesel properties

The quality of biofuel was determined by calculating saponification value, cetane number, iodine value. These values were estimated from the percent of fatty acid methyl esters obtained. It was observed that the values were in accordance with the European standard (EN 14214) and American Society for Testing and Materials (ASTM) D6751. Cetane number (CN) obtained in our analysis was found 50.5, 49.7 and 50.0 at 100 mM of sodium chloride, calcium chloride and magnesium chloride, respectively. As per ASTM-D6751 and EN 14214, the minimum CN value is 47 and 51. Similarly Iodine value was obtained as 114.1 gI_2/100g; 123.6 gI_2/100g, 114.8 gI_2/100g; saponification value as 199.5, 199.0, 203.9; and degree of unsaturation as 28.2, 26.1, 31.3 for 100 mM of sodium chloride, calcium chloride and magnesium chloride, respectively.

3.3.10 ROS content and response of cellular antioxidants

Under the influence of different salt treatments provided, the ROS content of the *Scenedesmus* sp. was studied on the 10th day of experiment. ROS consists of peroxyl radicals (LOO·), superoxide anion (O_2^{-}), singlet oxygen ($O^{\cdot}$), lipid hydroperoxides (LOOH), hydrogen peroxide (H_2O_2), and hydroxyl radical (·OH). The levels of H_2O_2 (Figure 3.12) and antioxidant enzymes accumulated inside salt-treated algal cells have been represented in Table 3.4.

Table 3.4: Antioxidative enzyme analysis in *Scenedesmus* sp. exposed to various salts at 100 mM

Salts (mM)	**CAT (nmol/min/mL)**	**SOD (U/mL)**
S_{100}	27.1±1.0	28.2±0.1
C_{100}	112.4±2.0	34.0±0.1
M_{100}	77.6±1.1	31.8±0.3

In the present study, calcium chloride at 100 mM was found to generate maximum ROS (2213.1±75.4 µmolH_2O_2/g), revealing that cells are under maximal stress and this result was further supported by high levels of SOD (34.0±0.1 U/mL) and CAT (112.4±2.0 nmol/mL/min) activity at the same salt concentration. Therefore, *Scenedesmus* sp. was under maximum stress when exposed to the highest concentration of calcium chloride. The activity of SOD enzyme was estimated as it acts as the first line of defense and triggers the conversion of O_2^{-} to O_2, proceeding towards the production of H_2O_2. Apart from SOD, there are many other metabolic processes occurring in the tweaked culture environment that influence the cell growth and subsequently lead to the production of H_2O_2. CAT activity was also observed to reveal a similar pattern as that of SOD. Therefore, an enhancement in SOD, CAT, and H_2O_2 levels was observed to vary with deviating exposures or treatments, and thus general criteria cannot be

set for all the varied treatments. Every combination examined in this study with varying salt levels has different metabolic alterations leading to differences in H_2O_2, SOD, and CAT activities. Moreover, it was observed that increased ROS levels inhibit algal growth by damaging the cell, whereas increased ROS levels can lead to oxidative damage to cellular components and adversely affect cell growth, which eventually influences the FAME profile.

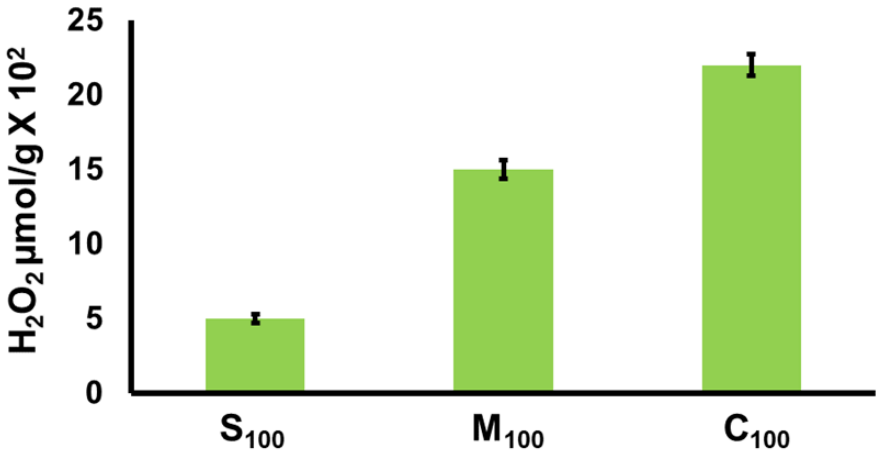

Figure 3.12: Reactive Oxygen species generation (H_2O_2) in *Scenedesmus* sp. exposed to varying salt treatment (15^{th} day)

3.3.11 Principal component analysis (PCA)

Principal component analysis of the biomass, chlorophyll, total lipid, total fatty acid content, and important fatty (C16:0, C18:0, C18:1, C18:2, C18:3 and C20:0) acid etc. verified a statistical distinction amongst three salts (NaCl, $CaCl_2$ and $MgCl_2$). The scree plot is (Figure 3.13A) used to govern the number of factors to retain in an examining factor analysis (FA) or principal components. The maximum variance is governed by first three (PC 1, PC 2 and PC 3) component contributing to 83.9% as presented in Table 3.5. There are 11 dimensions obtained, explaining 100% variance; based on Kaiser Concept. PCA biplot and variables (Figure 3.13B and 3.13C) shows how variables are correlated with one another and based on their directions away from the Principal Component (PC) origin, the influence on that Principal Component has also been presented. Beyond

three PCs, the variance reduced and contributed least in the overall variance.

The biplots in Figure 3.13B and 3.13C depict that some vectors' directions are away from the PC origin, showing more influence on that specific PC. The loading biplots indicate that C18:1, C18:2, and C18:0 is closely related to each other, mainly due to the salt treatment, and are negatively correlated with C18:3 and C16:0. In comparison, FAME was illustrated to have low or no correlation with lipids and carbohydrates but was found to be related to chlorophyll and biomass.

Table 3.5: Eigen analysis of the correlation matrix

Dimension	**Eigen value**	**Variance (%)**	**Cumulative variance (%)**
PC1	4.8	43.6	43.6
PC2	3.1	28.4	72.0
PC3	1.3	11.9	83.9
PC4	0.7	6.8	90.3
PC5	0.4	3.8	94.1
PC6	0.3	3.3	97.5
PC7	0.1	1.1	98.6
PC8	0.0	0.8	99.4
PC9	0.0	0.2	99.7
PC10	0.0	0.2	99.9
PC11	0.0	0.1	100

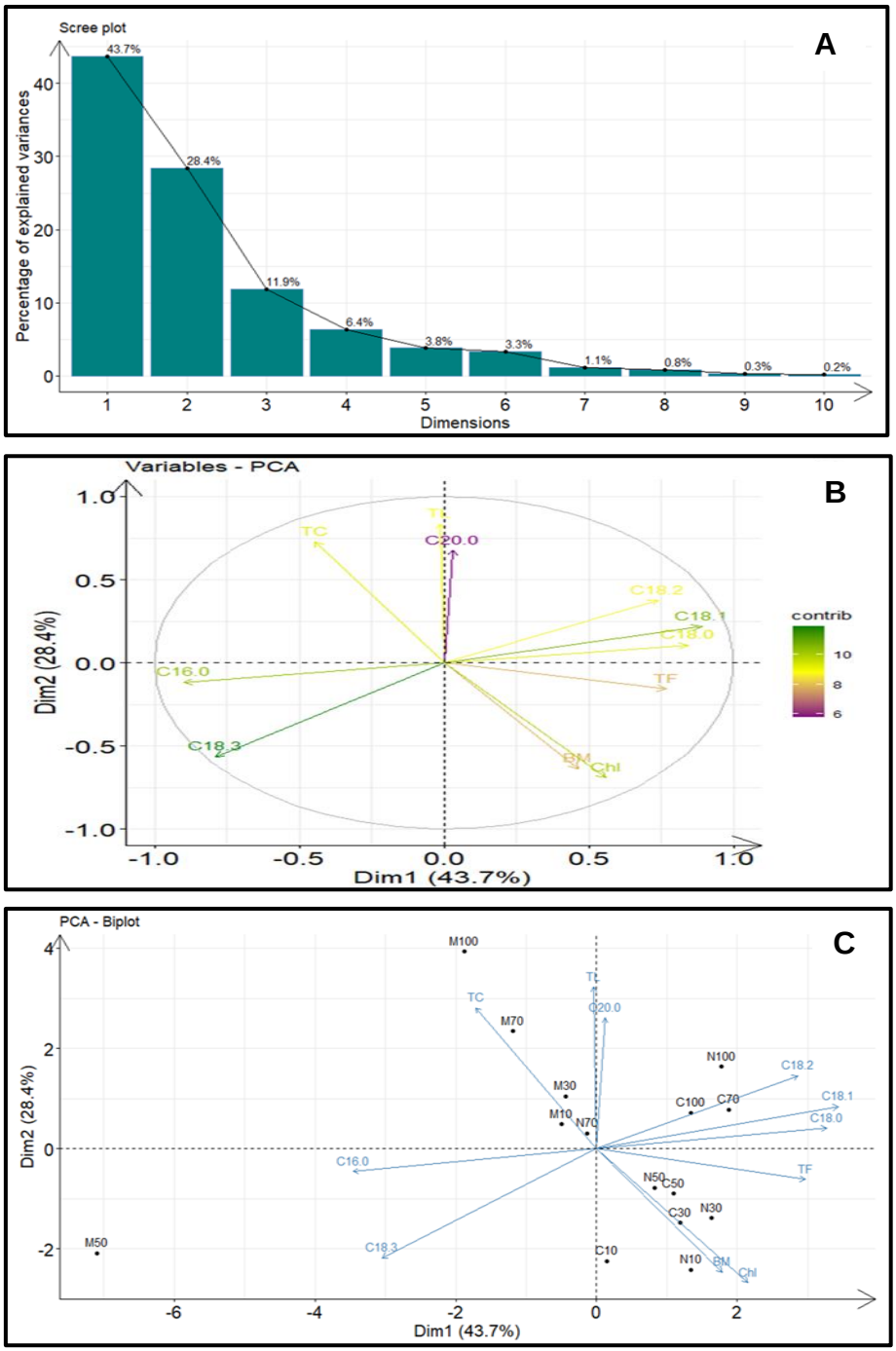

Figure 3.13: (A) Scree plot, a steep curve displays the magnitude of variation in each principal component captured from the data sets where first three PCs are explaining maximum variation (B) PCA variables plot (C) PCA Biplots

3.4. Conclusions

During the salt-induced stress exposure to algal cells, the experimental data revealed that there was a positive impact of salt-induced stress on biosynthesis of lipid in *Scenedesmus* sp. The algal growth rate and chlorophyll accumulation portrayed tolerance and adaptability of the species under observation in response to the salt environment. There was a significant increase in the percentage of saturated fatty acids like palmitic and stearic acid at 50 mM magnesium chloride and 70 mM calcium chloride. The algal cells cultivated in sodium chloride showed a better response in terms of biomass productivity and specific growth rate. The biomass productivity was computed to be highest at 100 mM sodium chloride exposure (33 µg/mL/d) followed by calcium chloride (19.5 µg/mL/d) and magnesium chloride (12.6 µg/mL/d). *Scenedesmus* sp. delineated better results under stress conditions in terms of lipid enhancement, and therefore it can be proposed as a preferable species for the production of biofuels. It was found that NaCl had greater impact on lipid accumulation as compared to that other salt. Therefore, in the next chapter NaCl was combined with nitrate and phosphate-two very critical nutrients for algal growth and lipid accumulation.

References

Affenzeller, M. J., Darehshouri, A., Andosch, A., Lütz, C., & Lütz-Meindl, U. (2009). Salt stress-induced cell death in the unicellular green alga *Micrasterias denticulata*. Journal of Experimental Botany, 60(3), 939-954.

Ahmad, P., Azooz, M. M., & Prasad, M. N. V. (2013). Salt stress in plants. Heidelberg: Springer.

Alkayal, F., Albion, R. L., Tillett, R. L., Hathwaik, L. T., Lemos, M. S., & Cushman, J. C. (2010). Expressed sequence tag (EST) profiling in hyper saline shocked *Dunaliella salina* reveals high expression of protein synthetic apparatus components. Plant Science, 179(5), 437-449.

Allakhverdiev, S. I., Sakamoto, A., Nishiyama, Y., Inaba, M., & Murata, N. (2000). Ionic and osmotic effects of NaCl-induced inactivation of photosystems I and II in *Synechococcus* sp. Plant Physiology, 123(3), 1047-1056.

Arnon, D. I. (1949). Copper enzymes in isolated chloroplasts. Polyphenoloxidase in *Beta vulgaris*. Plant Physiology, 24(1), 1.

Asulabh K, Supriya G, & Ramachandra T (2012). Effect of salinity concentrations on growth rate and lipid concentration in Microcystis sp., *Chlorococcum* sp. and *Chaetoceros* sp. National Conference on Conservation and Management of Wetland Ecosystems School of Environmental Sciences, Mahatma Gandhi University, Kottayam, Kerala.

Azachi, M., Sadka, A., Fisher, M., Goldshlag, P., Gokhman, I., & Zamir, A. (2002). Salt induction of fatty acid elongase and membrane lipid modifications in the extreme halotolerant alga *Dunaliella salina*. Plant Physiology, 129(3), 1320-1329.

Benavente-Valdés, J. R., Aguilar, C., Contreras-Esquivel, J. C., Méndez-Zavala, A., & Montañez, J. (2016). Strategies to enhance the

production of photosynthetic pigments and lipids in *chlorophycae* species. Biotechnology Reports, 10, 117-125.

Benjumea, P., Agudelo, J. R., & Agudelo, A. F. (2011). Effect of the degree of unsaturation of biodiesel fuels on engine performance, combustion characteristics, and emissions. Energy & Fuels, 25(1), 77-85.

Bounphanmy, S., Thammathaworn, S., Thanee, N., Pirapathrungsuriya, K., Beardall, J., McNaughton, D., & Heraud, P. (2010). Discrimination of cyanobacterial strains isolated from saline soils in Nakhon Ratchasima, Thailand using attenuated total reflectance FTIR spectroscopy. Journal of Biophotonics, 3(8-9), 534-541.

Bradford M. M. (1976). A rapid and sensitive method for the quantitation of microgram quantities of protein utilizing the principle of protein-dye binding. Analytical Biochemistry, 72, 248–254.

Campbell, A. K. (2014). Intracellular calcium. John Wiley & Sons.

Chen, H., Zhang, Y., He, C., & Wang, Q. (2014). Ca^{2+} signal transduction related to neutral lipid synthesis in an oil-producing green alga *Chlorella* sp. C2. Plant and Cell Physiology, 55(3), 634-644.

Coates, J. (2006). Interpretation of infrared spectra, a practical approach. Encyclopedia of analytical chemistry: applications, theory and instrumentation.

Cooksey, K. E., Guckert, J. B., Williams, S. A., & Callis, P. R. (1987). Fluorometric determination of the neutral lipid content of microalgal cells using Nile Red. Journal of Microbiological Methods, 6(6), 333-345.

Davis, R., Aden, A., & Pienkos, P. T. (2011). Techno-economic analysis of autotrophic microalgae for fuel production. Applied Energy, 88(10), 3524-3531.

Dean, A. P., Nicholson, J. M., & Sigee, D. C. (2008). Impact of phosphorus quota and growth phase on carbon allocation in

Chlamydomonas reinhardtii: an FTIR microspectroscopy study. European Journal of Phycology, 43(4), 345-354.

Dean, A. P., Sigee, D. C., Estrada, B., & Pittman, J. K. (2010). Using FTIR spectroscopy for rapid determination of lipid accumulation in response to nitrogen limitation in freshwater microalgae. Bioresource Technology, 101(12), 4499-4507.

Driver, T., Bajhaiya, A. K., Allwood, J. W., Goodacre, R., Pittman, J. K., & Dean, A. P. (2015). Metabolic responses of eukaryotic microalgae to environmental stress limit the ability of FT-IR spectroscopy for species identification. Algal Research, 11, 148-155.

Elsey, D., Jameson, D., Raleigh, B., & Cooney, M. J. (2007). Fluorescent measurement of microalgal neutral lipids. Journal of Microbiological Methods, 68(3), 639-642.

Giordano, M., Kansiz, M., Heraud, P., Beardall, J., Wood, B., & McNaughton, D. (2001). Fourier transform infrared spectroscopy as a novel tool to investigate changes in intracellular macromolecular pools in the marine microalga *Chaetoceros muellerii* (Bacillariophyceae). Journal of Phycology, 37(2), 271-279.

Grace, C. E. E., Lakshmi, P. K., Meenakshi, S., Vaidyanathan, S., Srisudha, S., & Mary, M. B. (2020). Biomolecular transitions and lipid accumulation in green microalgae monitored by FTIR and Raman analysis. Spectrochimica Acta Part A: Molecular and Biomolecular Spectroscopy, 224, 117382.

Hiremath, S., & Mathad, P. (2010). Impact of salinity on the physiological and biochemical traits of *Chlorella vulgaris* Beijerinck. Journal of Algal Biomass Utilization,1:51.

Kalita, N., Baruah, G., Goswami, R. C. D., Talukdar, J., & Kalita, M. C. (2011). *Ankistrodesmus falcatus*: a promising candidate for lipid production, its biochemical analysis and strategies to enhance lipid productivity. Journal of Microbiology and Biotechnology Research, 1(4), 148-157.

Kan, G., Shi, C., Wang, X., Xie, Q., Wang, M., Wang, X., & Miao, J. (2012). Acclimatory responses to high-salt stress in *Chlamydomonas* (Chlorophyta, Chlorophyceae) from Antarctica. Acta Oceanologica Sinica, 31(1), 116-124.

Karimova, F. G., Kortchouganova, E. E., Tarchevsky, I. A., & Iagoucheva, M. R. (2000). The oppositely directed Ca^{2+} and Na^{+} transmembrane transport in algal cells. Protoplasma, 213(1-2), 93-98.

Kassambara, A., & Mundt, F. (2017). Factoextra: extract and visualize the results of multivariate data analyses. R package version, 1(5), 337-354.

Kiran, B., Pathak, K., Kumar, R., Deshmukh, D., & Rani, N. (2016). Influence of varying nitrogen levels on lipid accumulation in *Chlorella* sp. International Journal of Environmental Science and Technology, 13(7), 1823-1832.

Kirrolia, A., Bishnoi, N. R., & Singh, N. (2011). Salinity as a factor affecting the physiological and biochemical traits of *Scenedesmus quadricauda*. Journal of Algal Biomass Utilization, 2(4), 28-34.

Knothe, G. (2007). Some aspects of biodiesel oxidative stability. Fuel Processing Technology, 88(7), 669-677.

Knothe, G., & Steidley, K. R. (2005). Kinematic viscosity of biodiesel fuel components and related compounds. Influence of compound structure and comparison to petrodiesel fuel components. Fuel, 84(9), 1059-1065.

Krank, J., Murphy, R. C., Barkley, R. M., Duchoslav, E., & McAnoy, A. (2007). Qualitative analysis and quantitative assessment of changes in neutral glycerol lipid molecular species within cells. Methods in Enzymology, 432, 1-20.

Laurens, L. M., & Wolfrum, E. J. (2011). Feasibility of spectroscopic characterization of algal lipids: chemometric correlation of NIR and FTIR spectra with exogenous lipids in algal biomass. Bioenergy Research, 4(1), 22-35.

Lê, S., Josse, J., & Mazet, F. (2008). Package 'FactoMineR. J Stat Softw [Internet], 25(1), 1-18.

Levasseur, M., Thompson, P. A., & Harrison, P. J. (1993). Physiological acclimation of marine phytoplankton to different nitrogen sources 1. Journal of Phycology, 29(5), 587-595.

Liu, Y., Wang, S., Wang, Z., Ye, N., Fang, H., & Wang, D. (2018). TiO_2, SiO_2 and ZrO_2 nanoparticles synergistically provoke cellular oxidative damage in freshwater microalgae. Nanomaterials, 8(2), 95.

Mallick, N., & Mohn, F. H. (2000). Reactive oxygen species: response of algal cells. Journal of Plant Physiology, 157(2), 183-193.

Mayers, J. J., Flynn, K. J., & Shields, R. J. (2013). Rapid determination of bulk microalgal biochemical composition by Fourier-Transform Infrared spectroscopy. Bioresource Technology, 148, 215-220.

Meng, Y., Yao, C., Xue, S., & Yang, H. (2014). Application of Fourier transform infrared (FT-IR) spectroscopy in determination of microalgal compositions. Bioresource Technology, 151, 347-354.

Mishra, S. K., Suh, W. I., Farooq, W., Moon, M., Shrivastav, A., Park, M. S., & Yang, J. W. (2014). Rapid quantification of microalgal lipids in aqueous medium by a simple colorimetric method. Bioresource Technology, 155, 330-333.

Mohan, S. V., & Devi, M. P. (2014). Salinity stress induced lipid synthesis to harness biodiesel during dual mode cultivation of mixotrophic microalgae. Bioresource Technology, 165, 288-294.

Osundeko, O., Dean, A. P., Davies, H., & Pittman, J. K. (2014). Acclimation of microalgae to wastewater environments involves increased oxidative stress tolerance activity. Plant and Cell Physiology, 55(10), 1848-1857.

Pancha, I., Chokshi, K., & Mishra, S. (2015). Enhanced biofuel production potential with nutritional stress amelioration through

optimization of carbon source and light intensity in *Scenedesmus* sp. CCNM 1077. Bioresource Technology, 179, 565-572.

Pancha, I., Chokshi, K., Maurya, R., Trivedi, K., Patidar, S. K., Ghosh, A., & Mishra, S. (2015). Salinity induced oxidative stress enhanced biofuel production potential of microalgae *Scenedesmus* sp. CCNM 1077. Bioresource Technology, 189, 341-348.

Rai, M. P., Gautom, T., & Sharma, N. (2015). Effect of salinity, pH, light intensity on growth and lipid production of microalgae for bioenergy application. OnLine Journal of Biological Sciences, 15(4), 260.

Rao, A. R., Dayananda, C., Sarada, R., Shamala, T. R., & Ravishankar, G. A. (2007). Effect of salinity on growth of green alga *Botryococcus braunii* and its constituents. Bioresource Technology, 98(3), 560-564.

Ríos, S. D., Castañeda, J., Torras, C., Farriol, X., & Salvadó, J. (2013). Lipid extraction methods from microalgal biomass harvested by two different paths: Screening studies toward biodiesel production. Bioresource Technology, 133, 378-388.

Roe, J. H. (1955). The determination of sugar in blood and spinal fluid with anthrone reagent. Journal of Biological Chemistry, 212, 335-343.

Sarno, D., Kooistra, W. H., Balzano, S., Hargraves, P. E., & Zingone, A. (2007). Diversity in the genus *Skeletonema* (Bacillariophyceae): III. Phylogenetic position and morphological variability of *Skeletonema costatum* and *Skeletonema grevillei*, with the description of S*keletonema ardens* sp. NOV. 1. Journal of Phycology, 43(1), 156-170.

Sharma, K. K., Schuhmann, H., & Schenk, P. M. (2012). High lipid induction in microalgae for biodiesel production. Energies, 5(5), 1532-1553.

Shetty, P., Gitau, M. M., & Maróti, G. (2019). Salinity stress responses and adaptation mechanisms in eukaryotic green microalgae. Cells, 8(12), 1657.

Sigee, D. C., Bahrami, F., Estrada, B., Webster, R. E., & Dean, A. P. (2007). The influence of phosphorus availability on carbon allocation and P quota in *Scenedesmus subspicatus*: a synchrotron-based FTIR analysis. Phycologia, 46(5), 583-592.

Sitepu, I. R., Ignatia, L., Franz, A. K., Wong, D. M., Faulina, S. A., Tsui, M., ... & Boundy-Mills, K. (2012). An improved high-throughput Nile red fluorescence assay for estimating intracellular lipids in a variety of yeast species. Journal of Microbiological Methods, 91(2), 321-328.

Srivastava, G., & Goud, V. V. (2017). Salinity induced lipid production in microalgae and cluster analysis (ICCB 16-BR_047). Bioresource Technology, 242, 244-252.

Stehfest, K., Toepel, J., & Wilhelm, C. (2005). The application of micro-FTIR spectroscopy to analyze nutrient stress-related changes in biomass composition of phytoplankton algae. Plant Physiology and Biochemistry, 43(7), 717-726.

Su, S., Zhou, Y., Qin, J. G., Yao, W., & Ma, Z. (2010). Optimization of the method for chlorophyll extraction in aquatic plants. Journal of Freshwater Ecology, 25(4), 531-538.

Sudhakar, K., & Premalatha, M. (2015). Characterization of micro algal biomass through FTIR/TGA/CHN analysis: application to *Scenedesmus* sp. Energy Sources, Part A: Recovery, Utilization, and Environmental Effects, 37(21), 2330-2337.

Sudhir, P., & Murthy, S. D. S. (2004). Effects of salt stress on basic processes of photosynthesis. Photosynthetica, 42(2), 481-486.

Sun, X., Cao, Y., Xu, H., Liu, Y., Sun, J., Qiao, D., & Cao, Y. (2014). Effect of nitrogen-starvation, light intensity and iron on triacylglyceride/carbohydrate production and fatty acid profile of

Neochloris oleoabundans HK-129 by a two-stage process. Bioresource Technology, 155, 204-212.

Talebi, A. F., Tabatabaei, M., Mohtashami, S. K., Tohidfar, M., & Moradi, F. (2013). Comparative salt stress study on intracellular ion concentration in marine and salt-adapted freshwater strains of microalgae. Notulae Scientia Biologicae, 5(3), 309-315.

Vazquez-Duhalt, R., & Arredondo-Vega, B. O. (1991). Haloadaptation of the green alga *Botryococcus braunii* (race A). Phytochemistry, 30(9), 2919-2925.

Velikova, V., Yordanov, I., & Edreva, A. (2000). Oxidative stress and some antioxidant systems in acid rain-treated bean plants: protective role of exogenous polyamines. Plant Science, 151(1), 59-66.

Vincent, Q.V., (2011). GitHub - vqv/ggbiplot: A biplot based on ggplot2. https://github.com/vqv/ggbiplot. Accessed 23 Jul 2020.

Wagner, H., Liu, Z., Langner, U., Stehfest, K., & Wilhelm, C. (2010). The use of FTIR spectroscopy to assess quantitative changes in the biochemical composition of microalgae. Journal of Biophotonics, 3(8-9), 557-566.

Wheeler, G. L., & Brownlee, C. (2008). Ca^{2+} signalling in plants and green algae–changing channels. Trends in Plant Science, 13(9), 506-514.

Wickham, H., & Chang, W. (2019). devtools: Tools to make developing R packages easier, 2016. URL https://CRAN. R-project. org/package= devtools. R package version, 1(0), 103.

Yilancioglu, K., Cokol, M., Pastirmaci, I., Erman, B., & Cetiner, S. (2014). Oxidative stress is a mediator for increased lipid accumulation in a newly isolated *Dunaliella salina* strain. PLoS One, 9(3), e91957.

Zhang, X., Luo, S., Yang, Q., Zhang, H., & Li, J. (1997). Accumulation of uranium at low concentration by the green alga *Scenedesmus obliquus* 34. Journal of Applied Phycology, 9(1), 65-71.

Zhang, Y., He, M., Zou, S., Fei, C., Yan, Y., Zheng, S., ... & Wang, C. (2016). Breeding of high biomass and lipid producing *Desmodesmus* sp. by Ethylmethane sulfonate-induced mutation. Bioresource Technology, 207, 268-275.

Zhu, J. K. (2000). Genetic analysis of plant salt tolerance using Arabidopsis. Plant Physiology, 124(3), 941-948.

Zhu, J. K. (2016). Abiotic stress signaling and responses in plants. Cell, 167(2), 313-324.

CHAPTER 4

Chapter 4

Efffect of sodium chloride under nutrients replete/deplete conditions

4.1 Introduction

Microalgae are highly explored to produce biofuels and make it economically feasible and environmentally sustainable. Enhanced lipid accumulation can be achieved by treating microalgae with various physical (such as pH, temperature, photoperiod, and light intensity) and chemical factors (such as nutrients variation, salinity, and oxidative agent treatment) (Chen et al., 2013; Singh et al., 2014).

Biochemical strategies are mainly concerned with nutrient variations (viz. nitrogen, phosphorus, iron and salt), whereas physical exposure includes temperature, pH, light intensity and photoperiod. All these treatments are known to directly affect the lipid content and biomass productivity of microalgae (Chu et al., 2013; Converti et al., 2009; Ji et al., 2013). Nitrogen being one such essential element is not only required for protein synthesis but is also involved in cell division and growth process of microalgae (Miller et al., 2010). Since, nitrogen assimilation is associated with carbon fixation and plays a vital role in the maintenance of metabolic balance, therefore, providing appropriate amount of nitrogen to the cells is of utmost importance (Adams et al., 2013). In the case of nitrogen deficiency, protein synthesis is severely affected, which ultimately declines the photosynthetic rate resulting in the diversion of metabolic flux towards lipid biosynthesis. Lipids are highly reduced molecules and act as source of energy for the survival of microalgae under unseasonal environment (Ho et al., 2014). Different microalgal species have been reported with high lipid content under nitrogen deprived conditions (Courchesne et al., 2009; Gao et al., 2013; Radakovits et al., 2010).

Along with the presence of nitrogen, phosphorus is also required for microalgal growth and plays a significant role in cell metabolism, survival and development (Ghosh et al., 2020). Phosphorus is also known to aid the maintenance of specific rate of photosynthesis and plays a key role in the functioning of signal transduction pathways (Sharma et al., 2012; Xin et al., 2010). During phosphorus deprivation, increased lipid content in microalgae e.g. *Pavlova lutheri*, *Chaetoceros* sp., *Phaeodactylum tricornutum*, and *Isochrysis galbana* has been reported (Sharma et al., 2012). Besides nitrogen and phosphorus, supplementation of varying salt concentration too plays an important role in diverting the carbon flux towards the synthesis of desired biomolecule. Mohan and Devi have also observed an increase in lipid accumulation under sodium chloride variation and found maximum lipid content at 1 g/L of NaCl (Mohan and Devi, 2014). It has also been observed that the presence of unfavourable environmental conditions leads to the displacement of electron from electron transport chain of different organelles such as mitochondria and plasma membrane of chloroplast that ultimately leads to the production of ROS (Alscher et al., 1997). Different kinds of oxidative stresses are known to initiate the excessive production of ROS, which can cause organelle dysfunction, mutagenesis, or changes in cell structure (Rezayian et al., 2019). However, these various types of oxidative stress positively affect the lipid accumulation potential of microalgae (Yilancioglu et al., 2014). Therefore, the combined effect of these factors has lots of significance for further enhancement of lipid production. Much work has been done to study the mutual effect of phosphorus, nitrogen and iron along with environmental stress, including photoperiod, pH, light intensity, and temperature etc. (Cao et al., 2014; Ji et al., 2013). *Chlorella minutissima* has shown enhanced lipid accumulation under combined exposure to sodium chloride, nitrogen and iron (Cao et al., 2014). However, there seems to be a lack of literature to show the combined effect of nitrogen, phosphorous, and sodium chloride in *Scenedesmus* sp. to the best of our knowledge.

This chapter focuses on the assessment of the synergistic/antagonistic effect of sodium chloride (NaCl), dipotassium hydrogen phosphate (K_2HPO_4), and sodium nitrate ($NaNO_3$) on lipid production efficiency and photosynthetic performance of *Scenedesmus* sp.

4.2 Materials and methods

4.2.1 Setup of microalgae experiment

Integrated effect of sodium chloride (0, 10, 50, 100, and 200 mM), sodium nitrate (0, 17.64, and 35.29 mM), and dipotassium hydrogen phosphate (0, 0.22, and 5.74 mM) were evaluated on algal growth and biochemical profile (Figure 4.1); where sodium chloride was represented as S_0, S_{10}, S_{50}, S_{100}, and $S_{200;}$ sodium nitrate as N_0, $N_{17.64}$, $N_{35.29}$ and dipotassium hydrogen phosphate as P_0, $P_{0.22}$, $P_{5.74}$. The combinations were chosen depending on low, high, and optimum values of different media components. The study was conducted in triplicates.

4.2.2 Growth kinetics and pigment quantification

The growth profile of microalgae was monitored at a regular interval of 48 hours by taking the optical density of cells at 680 nm. Biomass was measured using a standard calibration curve (as described in chapter 2) constructed between OD vs. DCW (R^2= 0.99). Biomass productivity (BP) was calculated on the 15^{th} day (Levasseur et al., 1993; Srivastava and Goud, 2017).

Chlorophyll content was computed at a regular interval of 5 days, and the experiment was continued till 15 days. Su et al. (2010) and Arnon (1949) method was followed for the estimation of chlorophyll ‘a’ content accumulated in treated algal cells. The detailed protocol has been described in chapter 2.

4.2.3 Determination of lipid and carbohydrate concentration

The protocols demonstrated by Mishra et al. (2016) and Roe et al. (1955) were followed for determining the total lipid and carbohydrate accumulation inside the treated algal cells, respectively.

4.2.4 Biomolecular transition study

Lyophilized dry biomass of algal cells subjected to various treatments was exploited for conducting FTIR analysis (Perkin Elmer spectrum two) in the range of 400-4000 cm^{-1} so as to study the pattern of multiple transitions occurring in between different biomolecules being produced in the stressed cells.

4.2.5 Microscopic analysis

In order to visualize the lipid droplets accumulated inside the stressed cells, a confocal laser scanning microscope was exploited, and sample preparation was done, as discussed previously in chapter 2.

The structural framework of cells under treatment was characterized using a field emission scanning electron microscope, and the samples were prepared by fixing the algal cells using formaldehyde (37%) (Sarno et al., 2007). The drop-cast method was used to load the sample (10 μL) onto a small slide, followed by copper coating to make the surface conducting and generate secondary electrons for depicting the cell's morphology.

4.2.6 FAME profiling and assessment of fuel properties

FAME profiling was performed through the direct transesterification method illustrated by Rios et al. (2013). Subsequently, biodiesel properties were also calculated empirically by taking into account the fatty acid percentage obtained from FAME analysis. The detailed protocol and equations have been discussed extensively in a chapter 2.

4.2.7 Assay of oxidative stress and ROS generation

On the 10th day of the experiment, ROS generated in the cells due to the exposure to stress has been analyzed by the procedure described in chapter 2 (Velikova et al., 2000).

Assays described by Liu et al. (2018) and Bradford, 1976 were followed for crude protein extraction and quantification, respectively. The instructions provided within the colorimetric kits (Item No. 707002 Cayman 1180 E. Ellsworth Rd-Ann Arbor, MI-USA and Item No. 706002) were followed for determining catalase (CAT) and superoxide dismutase (SOD) activity.

4.2.8 Data interpretation using R studio

PCA was executed with the help of R packages such as 'factoextra' (Kassambara and Mundt, 2020), 'FactoMineR' (Lê S, 2008), 'devtools' (Wickham, 2019), and 'ggbiplot' (Vincent, 2011) integrated into R studio desktop version 4.0.0.

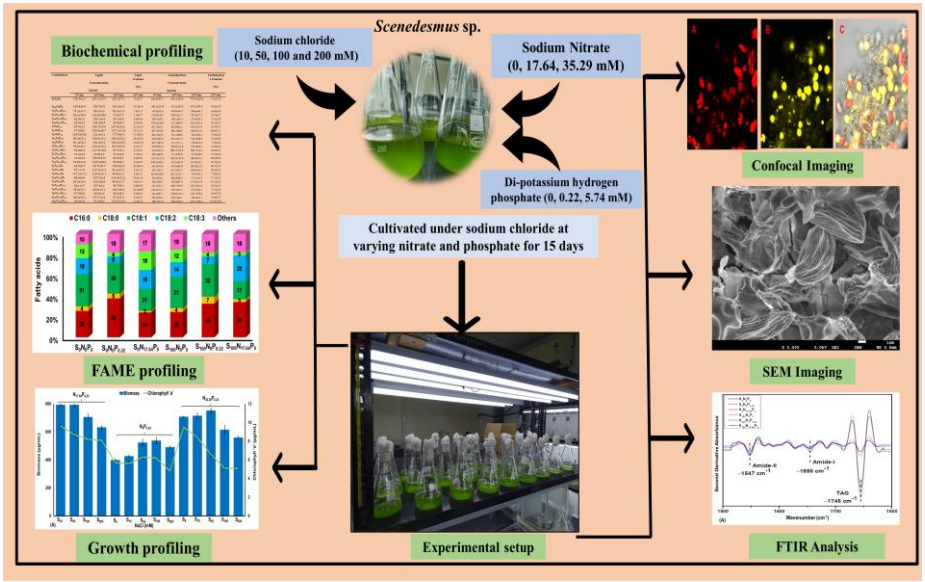

Figure 4.1: Systematic representation of experimental plan to understand the impact of sodium chloride under varying nutrients

4.3 Results and Discussion

4.3.1 Biomass accumulation in Scenedesmus sp. under sodium chloride, sodium nitrate and dipotassium hydrogen phosphate exposure

Biomass accumulation varied in different combinations. Amongst various combinations of SNP (salt, nitrate, and phosphate), the higher biomass productivity was obtained for modified media consisting of NaCl (10 mM), $NaNO_3$ (17.64 mM), and K_2HPO_4 (0.22 mM) ($S_{10}N_{17.64}P_{0.22}$, 32.1±0.5 µg/mL/d). The biomass productivity, though, was found to decrease with an increase in NaCl concentration. However, at $N_{35.29}P_{0.22}$ and $N_{17.64}P_0$ levels along with varying NaCl concentrations, biomass content was found to increase till 50 mM NaCl and further decreased with increasing salt concentrations. Similar trend was observed for $N_0P_{0.22}$ treatment with increasing biomass upto 100 mM salt concentration and subsequently decreased at 200 mM on 15^{th} day as shown in Figure 4.2A and 4.2B depicting the correlation between biomass and chlorophyll, where 4.2A represents treatment of varying sodium nitrate and sodium chloride at constant phosphate level and 4.2(B) represents the treatment of varying dipotassium hydrogen phosphate and sodium chloride at constant nitrate level. At $N_{17.64}P_{0.22}$ and $N_{17.64}P_{5.74}$, overall biomass was found to decrease with an increase in salt concentration till 200 mM, as observed in Table 4.1. Salt concentrations support species to stabilize under nutrient variant conditions but upto a specific concentration, beyond which it affects microalga growth. Chlorophyll 'a' (Figure 4.2A and 4.2B) content at $N_{17.64}P_{0.22}$, $N_{35.29}P_{0.22}$, and N_0P_0 decreased with an increase in salt concentration. However, at $N_0P_{0.22}$ and $N_{17.64}P_{5.74}$, not much distinct variation in chlorophyll content with varying salt concentration was observed. Many studies show the effect of both ionic as well as osmotic stress, which lead to reduction in the activity of Na^+/H^+ antiporters; thus, depicting the tolerance capacity of photosynthetic machinery as well as oxygen-evolving machinery (Srivastava and Goud, 2017). Therefore, it can be suggested that under saline conditions, there is decrease in biomass content.

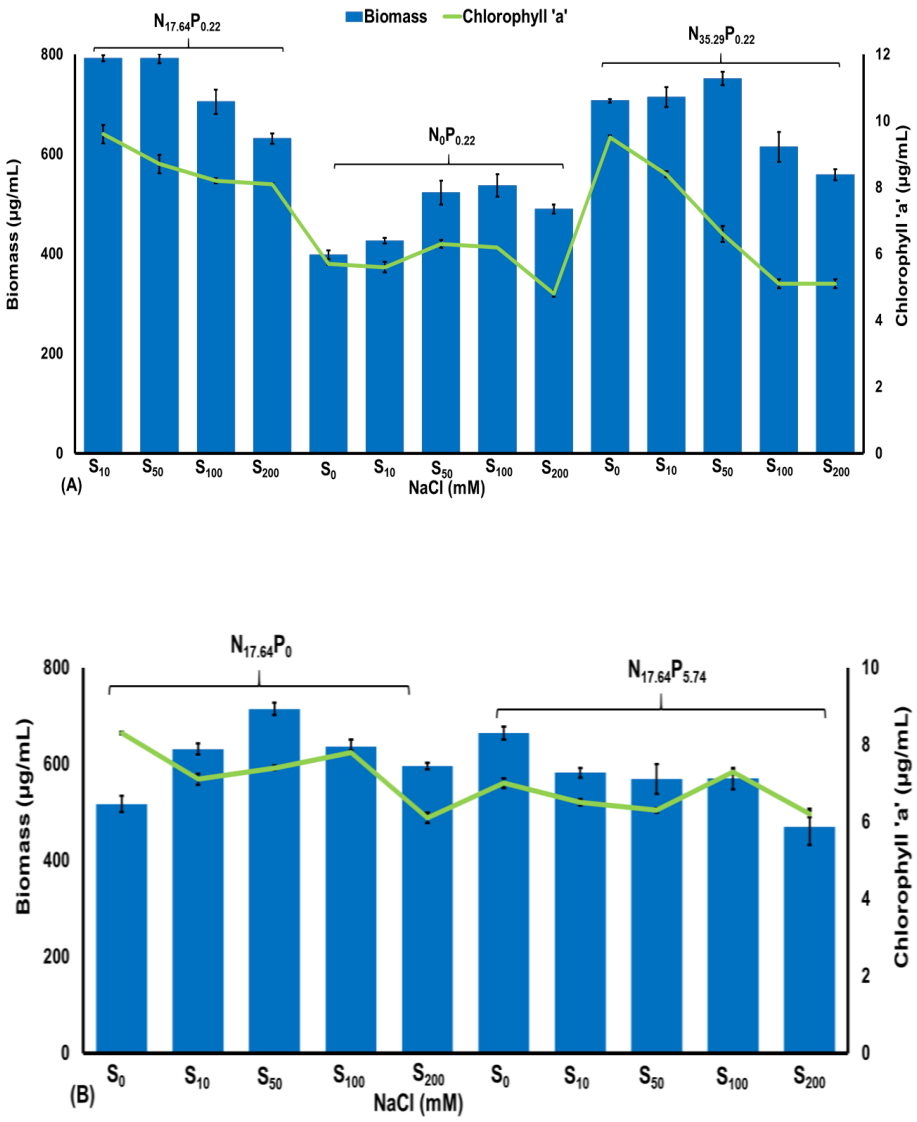

Figure 4.2: Relationship between biomass (15th day) and chlorophyll 'a' (15th day) in *Scenedesmus* sp. under exposure to (A) varying sodium nitrate and sodium chloride at constant phosphate level (B) varying dipotassium hydrogen phosphate and sodium chloride at constant nitrate level

Table 4.1: Biomass, chlorophyll 'a' and specific growth rate of *Scenedesmus* sp. exposed to sodium chloride under varying nutrient levels

Combinations	Biomass Accumulation (µg/mL)			Chlorophyll Accumulation (µg/mL)			Specific Growth Rate (day^{-1})
	5^{th} day	10^{th} day	15^{th} day	5^{th} day	10^{th} day	15^{th} day	10^{th} day
$S_0N_0P_0$	490.0±3.7	442.2±10.6	545.7±5.4	6.3±0.1	6.4±0.2	5.7±0.2	0.03±0.01
$S_{100}N_0P_0$	483.4±30.9	583.9±42.0	498.4±8.8	6.2±0.1	4.8±0.1	4.3±0.1	0.06±0.00
$S_{10}N_{17.64}P_{0.22}$	546.1±8.7	836.1±91.2	792.3±6.1	5.9±0.1	7.7±0.2	9.6±0.3	0.09±0.01
$S_{50}N_{17.64}P_{0.22}$	544.0±37.7	862.5±75.6	791.5±9.5	4.7±0.1	9.2±0.2	8.6±0.3	0.09±0.01
$S_{100}N_{17.64}P_{0.22}$	563.0±7.6	744.6±84.7	704.7±24.2	5.0±0.0	8.5±0.2	8.2±0.1	0.08±0.00
$S_{200}N_{17.64}P_{0.22}$	537.3±88.1	678.0±101.3	631.0±10.6	5.3±0.2	8.8±0.5	8.1±0.0	0.08±0.01
$S_0N_0P_{0.22}$	538.1±23.8	322.9±4.6	397.7±8.8	4.8±0.1	5.5±0.2	5.7±0.0	0.02±0.01
$S_{10}N_0P_{0.22}$	468.6±6.6	569.8±15.3	426.1±5.3	4.6±0.1	5.6±0.2	5.6±0.2	0.06±0.00
$S_{50}N_0P_{0.22}$	484.8±29.9	584.9±8.05	522.6±24.2	4.5±0.1	5.6±0.1	6.3±0.1	0.06±0.07
$S_{100}N_0P_{0.22}$	511.3±16.8	623.3±27.8	537.0±22.3	4.9±0.1	5.3±0.1	6.2±0.1	0.07±0.01
$S_{200}N_0P_{0.22}$	483.4±30.8	583.9±42.0	489.4±8.8	5.3±0.2	8.0±0.2	4.8±0.1	0.06±0.01
$S_0N_{35.29}P_{0.22}$	548.6±35.5	722.9±111.4	706.9±3.9	5.5±0.2	10.8±0.1	9.5±0.1	0.08±0.01
$S_{10}N_{35.29}P_{0.22}$	513.2±12.5	722.2±109.5	714.0±19.7	4.6±0.1	6.3±0.2	8.4±0.1	0.08±0.01
$S_{50}N_{35.29}P_{0.22}$	538.0±61.0	761.2±67.5	751.2±13.5	3.8±0.2	5.4±0.1	6.6±0.2	0.09±0.01
$S_{100}N_{35.29}P_{0.22}$	550.7±106.6	617.6±60.6	614.7±29.9	6.1±0.1	5.9±0.2	5.1±0.1	0.07±0.01
$S_{200}N_{35.29}P_{0.22}$	501.9±113.5	648.2±170.3	558.3±11.2	4.9±0.2	8.9±0.2	5.1±0.1	0.08±0.02
$S_0N_{17.64}P_0$	669.3±34.7	950.2±20.8	516.8±17.1	6.8±0.2	8.6±0.2	8.3±0.0	0.10±0.01
$S_{10}N_{17.64}P_0$	548.2±25.9	722.5±52.2	630.8±11.0	5.4±0.1	8.2±0.2	7.1±0.1	0.08±0.01
$S_{50}N_{17.64}P_0$	474.7±51.5	676.0±111.9	714.2±12.9	5.6±0.1	7.6±0.3	7.4±0.1	0.08±0.01
$S_{100}N_{17.64}P_0$	489.6±14.2	695.3±61.8	635.9±15.0	6.1±0.2	8.1±0.1	7.8±0.0	0.08±0.01
$S_{200}N_{17.64}P_0$	491.4±5.4	647.2±69.5	595.3±6.2	6.1±0.2	8.6±0.2	6.1±0.1	0.07±0.01
$S_0N_{17.64}P_{5.74}$	571.4±11.9	744.1±84.8	663.5±13.4	5.7±0.1	7.4±0.2	6.9±0.1	0.09±0.01
$S_{10}N_{17.64}P_{5.74}$	589.3±67.9	676.0±39.4	581.5±10.6	3.4±0.3	6.6±0.1	6.5±0.1	0.08±0.01
$S_{50}N_{17.64}P_{5.74}$	526.6±48.6	582.3±5.0	568.2±30.8	4.6±0.2	6.7±0.2	6.3±0.1	0.07±0.01
$S_{100}N_{17.64}P_{5.74}$	499.7±52.9	640.7±8.5	569.3±22.4	4.9±0.1	7.7±0.1	7.3±0.1	0.07±0.01
$S_{200}N_{17.64}P_{5.74}$	464.5±21.1	463.8±24.6	468.9±37.4	5.1±0.1	6.7±0.2	6.2±0.1	0.04±0.00

4.3.2 Biochemical composition analysis of Scenedesmus sp.

Total lipids (µg/mg) and carbohydrates (µg/mg) accumulated inside algal cells under combined treatment were analyzed at regular intervals i.e., 5^{th}, 10^{th}, and 15^{th} day based on algal growth cycle (Table 4.2). The highest total lipid accumulation was obtained for $S_{100}N_0P_{0.22}$ (385.4±34.2 µg/mg), which was followed by $S_{200}N_0P_{0.22}$ (356.2±16.5 µg/mg) and $S_0N_0P_{0.22}$ (253.8±24.2 µg/mg). Maximum lipid content (%) was found as 38.5%. The highest lipid productivity was observed for $S_{100}N_0P_{0.22}$ (5.9±0.2 µg/mL/d). In addition to the above combinations, $S_0N_0P_0$ (203.2±7.3 µg/mg) and $S_{100}N_0P_0$ (191.0±4.3 µg/mg) had also shown an increase in total lipid content. In a similar study, *S. obliquus* (HM103382) upon treatment with NaCl (100 mM) was reported to yield 21% lipid content (Salama et al., 2013). The results suggests that nitrate depleted conditions in addition to salinity stress led to higher lipid productivity. High sodium chloride concentration along with nitrogen deficiency played a major role in lipid accumulation inside cells but hindered biomass production. The observation was found in agreement with previous reports where nitrogen-starvation played a pivotal role in enriching the lipid content of algal cells (Converti et al., 2009) in the same way as sodium chloride supplementation has been reported. Maximum carbohydrate concentration was estimated for $S_{10}N_{35.29}P_{0.22}$ (966.7±21.0 µg/mg) with a carbohydrate productivity of 26.6±1.3 µg/mL/d.

Although different combinations showed varying chlorophyll content along with lipid accumulation but $S_{100}N_0P_{0.22}$ (Table 4.1) produced a considerable amount of chlorophyll content (6.2±0.08 µg/mL) with high lipid productivity (5.9±0.2 µg/mL/d). Thus, it is concluded that the combination $S_{100}N_0P_{0.22}$ can be trusted and exploited further for efficacious large-scale production of algal lipids, which are prime biodiesel precursor without compromising the biomass productivity.

Minimum chlorophyll was observed for $S_{100}N_0P_0$ (4.3±0.1 µg/mL), which was found to be the second highest producer of carbohydrates (876.17±30.46 µg/mg). On the other hand, dipotassium hydrogen phosphate supplementation under sodium nitrate deficiency yielded a high amount of storage energy compounds (lipids) without much decrease in the chlorophyll content. Therefore, the presence of nitrogen is a major factor supporting algal growth. Previous reports too suggested that conditions enhancing lipid accumulation without compromising biomass production can increase lipid productivity (Benvenuti et al., 2015).

Amongst all, few combinations such as $S_0N_0P_0$, $S_0N_0P_{0.22}$, $S_0N_{17.64}P_0$, $S_{100}N_0P_0$, $S_{100}N_0P_{0.22}$, and $S_{100}N_{17.64}P_0$ were selected for FTIR, gas chromatography, confocal and SEM imaging after considering lipid accumulation and growth profile data. It has been well established beforehand that under nitrogen-deficient conditions, the metabolic pathway of algae gets highly affected. Nitrogen has been considered one of the major constituents of proteins and nucleic acid synthesis (Adams et al., 2013; Cao et al., 2014). Under nitrogen deficiency, phosphorus acts as polyphosphate molecule that provides energy in a similar way as ATP for regulating metabolic pathways to utilize available carbon towards the synthesis of fatty acids (Chu et al., 2013; Miller et al., 2010). Besides nitrogen, phosphorus also plays a vital role in microalgal cultivation as it is involved in energy transfer, respiration, signal transduction, and photosynthesis during the cellular metabolic process (Grace et al., 2020; Sharma et al., 2012).

Table 4.2: Biochemical profiling of *Scenedesmus* sp. exposed to sodium chloride under varying nutrient levels

Combinations	Lipid Concentration (µg/mg)			Lipid Content (%)	Carbohydrate Concentration (µg/mg)			Carbohydrate Content (%)
	5th day	10th day	15th day	15th day	5th day	10th day	15th day	15th day
$S_0N_0P_0$	138.9±2.5	265.1±13.4	203.2±7.3	20.±0.7	600.9±40.3	498.2±20.6	734.6±20.6	73.4±2.0
$S_{100}N_0P_0$	129.8±4.9	185.7±5.0	191.0±4.3	19.1±0.4	560.2±23.9	715.5±20.0	876.1±30.4	87.6±3.0
$S_{10}N_{17.64}P_{0.22}$	75.2±32.7	86.1±4.2	76.3±13.3	7.6±1.3	530.9±33.6	679.6±49.3	566.6±46.1	56.6±4.6
$S_{50}N_{17.64}P_{0.22}$	61.1±38.8	122.0±16.0	73.4±7.7	7.3±0.7	574.9±130.7	628.3±32.7	587.3±27.2	58.7±2.7
$S_{100}N_{17.64}P_{0.22}$	62.9±3.2	104.1±9.6	90.1±6.6	9.0±0.6	588.4±50.2	598.1±61.0	533.6±39.2	53.3±3.9
$S_{200}N_{17.64}P_{0.22}$	34.0±9.3	105.4±4.4	85.8±8.0	8.5±0.8	479.2±139.6	557.3±64.4	652.5±25.4	65.2±2.5
$S_0N_0P_{0.22}$	85.4±2.0	226.7±25.0	253.8±24.2	25.3±2.4	617.3±43.1	902.8±62.2	405.2±31.9	40.5±3.1
$S_{10}N_0P_{0.22}$	97.8±9.0	109.9±26.7	147.1±11.8	14.7±1.1	807.4±70.8	882.2±98.6	806.0±11.0	80.6±1.1
$S_{50}N_0P_{0.22}$	104.5±10.6	123.4±4.1	177.0±6.4	17.7±0.6	601.2±24.9	722.3±69.0	740.3±26.3	70.4±2.6
$S_{100}N_0P_{0.22}$	99.0±20.2	149.9±11.2	385.4±34.2	38.5±3.4	458.2±87.8	944.5±27.3	343.5±48.9	34.3±4.8
$S_{200}N_0P_{0.22}$	91.4±18.1	182.4±9.4	356.2±16.5	35.6±1.6	642.7±82.6	531.5±77.2	776.9±42.0	77.6±4.2
$S_0N_{35.29}P_{0.22}$	56.6±18.1	116.4±12.1	66.1±15.0	6.1±1.5	576.0±24.6	780.0±114.0	558.2±26.2	55.8±2.6
$S_{10}N_{35.29}P_{0.22}$	52.8±8.5	117.9±19.6	67.7±9.3	6.7±0.9	434.9±32.4	869.7±134.6	966.7±21.0	96.6±2.1
$S_{50}N_{35.29}P_{0.22}$	51.4±4.2	94.9±3.6	57.3±2.8	5.7±0.2	703.3±99.9	575.3±50.8	725.3±46.8	72.5±4.6
$S_{100}N_{35.29}P_{0.22}$	41.0±2.6	158.0±15.5	90.5±8.1	9.0±0.8	554.7±115.0	926.5±113.9	684.9±54.5	68.4±5.4
$S_{200}N_{35.29}P_{0.22}$	55.6±12.0	119.7±26.6	85.9±8.1	8.5±0.8	679.7±164.1	562.1±95.9	817.0±24.5	81.7±2.4
$S_0N_{17.64}P_0$	62.0±6.5	50.7±16.7	108.8±2.8	10.8±0.2	545.9±14.6	444.9±63.8	681.8±15.0	68.1±1.5
$S_{10}N_{17.64}P_0$	87.1±7.6	137.5±13.2	82.2±15.3	8.2±1.5	541.3±37.4	832.0±20.7	694.9±23.4	69.4±2.3
$S_{50}N_{17.64}P_0$	147.2±17.5	110.3±11.1	90.9±12.1	9.0±1.2	833.6±168.4	824.5±131.7	779.3±30.3	77.9±3.0
$S_{100}N_{17.64}P_0$	88.6±9.8	147.3±2.9	129.9±13.2	12.9±1.3	414.0±50.3	892.8±88.3	577.5±34.3	57.7±3.4
$S_{200}N_{17.64}P_0$	93.5±15.0	110.2±6.6	99.9±13.7	9.9±1.3	592.3±29.7	520.8±67.4	671.0±25.8	67.1±2.5
$S_0N_{17.64}P_{5.74}$	92.1±4.7	90.7±4.2	80.7±9.4	8.0±0.9	515.1±21.2	680.7±40.9	387.5±41.6	38.7±4.1
$S_{10}N_{17.64}P_{5.74}$	59.0±15.1	68.0±15.1	105.1±8.2	10.5±0.8	526.5±121.1	508.4±24.5	551.1±26.7	55.1±2.6
$S_{50}N_{17.64}P_{5.74}$	67.9±9.0	49.4±3.6	86.5±8.2	8.6±0.8	544.2±67.5	739.6±133.5	654.7±76.8	65.4±7.6
$S_{100}N_{17.64}P_{5.74}$	40.4±16.2	55.7±12.6	63.3±3.4	6.3±0.3	303.0±28.3	846.5±80.7	439.1±33.1	43.9±3.3
$S_{200}N_{17.64}P_{5.74}$	28.8±4.6	53.3±6.0	110.7±13.4	11.0±1.3	488.5±52.9	668.6±46.8	659.1±108.0	65.9±10.8

4.3.3 Qualitative analysis of lipid accumulation through FTIR spectroscopy

In the present study, FTIR data helped in understanding the effect of treatments on the transitions of biomolecules of cells along with lipid accumulation. The presence of TAGs is evident from FTIR analysis in samples with combined stress at higher concentrations. The bands in Figure 4.3A observed at 1546 cm^{-1} and 1652 cm^{-1} indicate the presence of Amide-II, Amide-I bonds from proteins (IR), and cis υ(C=C) from unsaturated lipids, respectively. The intensity of both Amide-I and Amide-II recorded at 1546 cm^{-1} decreased in the absence of sodium nitrate supporting the requirement of nitrates for the growth of algae. The band observed at 1746 cm^{-1} (Figure 4.3A) indicated the presence of υ(C=O) stretches due to the presence of ester in the lipids and validates the presence of TAGs (Dean et al., 2010).

The band at ~1746 cm^{-1}, which occurred due to the presence of TAGs, has been studied as a measure of neutral lipid content and change in band intensity can help to understand the effect of different variables on neutral lipid content. Previous studies have reported that the accumulation of lipids in microalgae could be estimated through FTIR analysis (Grace et al., 2020). The band in the region, 3050 to 2700 cm^{-1} (Figure 4.3B), corresponding to υ(CH_3) and υ(CH_2), asymmetric and symmetric stretches of hydrocarbon were also recorded in the FTIR analysis of treated cells. The saturated lipids present at ~1445 cm^{-1} went low under nitrogen-deprived conditions, which suggests that nitrogen plays a significant role in the accumulation of lipids along with the osmotic stress imposed by NaCl. The present study is in line with the previously reported studies for lipid accumulation under osmotic stress and nutrition-deprived conditions (Cao et al., 2014). The current study depicts the usage of non-invasive techniques like FTIR for estimation of changes in the lipid and amide profile of cells, adequately paving way for futuristic tools of analysis, which can be performed more rapidly than the conventional colorimetric assays.

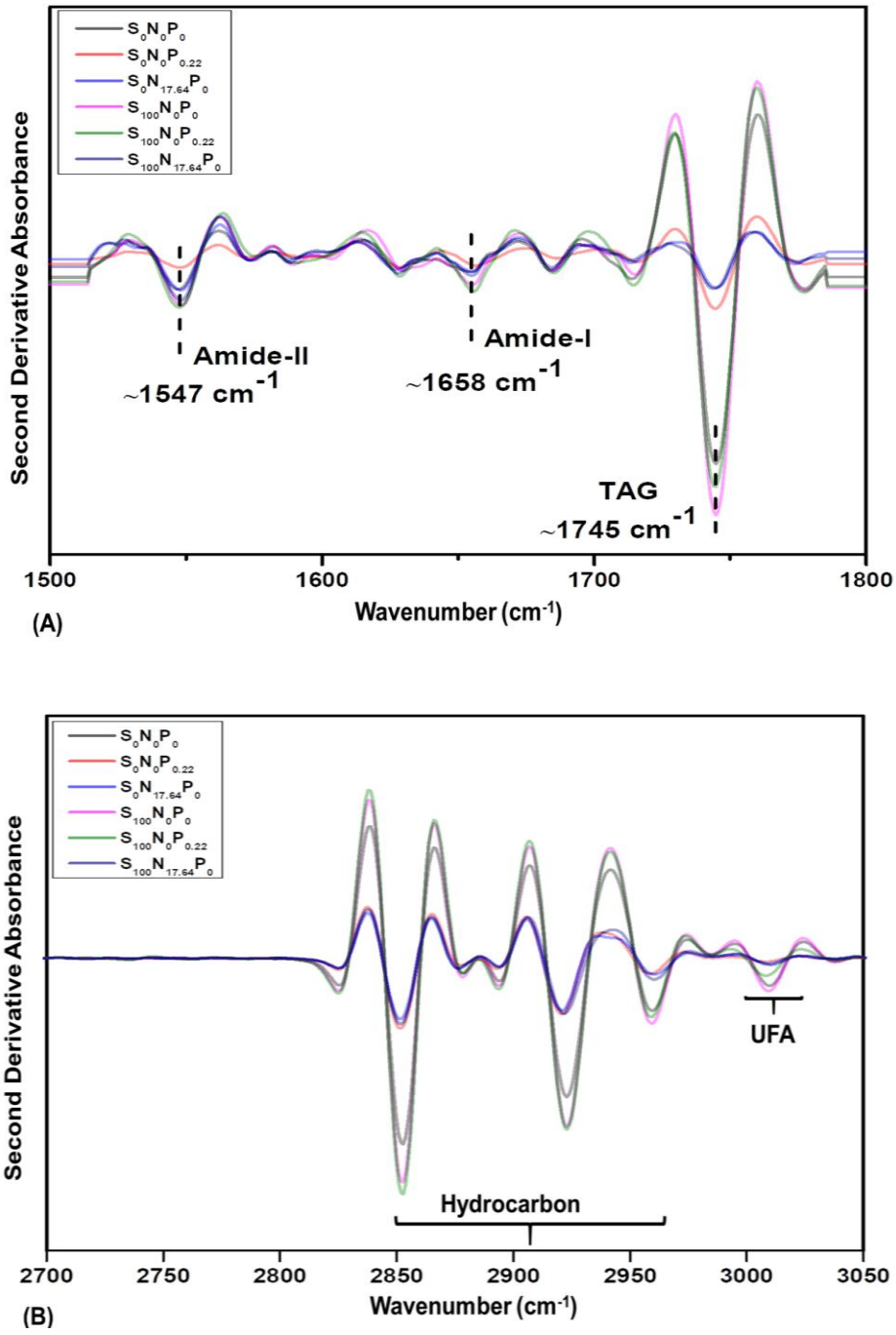

Figure 4.3 Second derivative spectra of lyophilized algal biomass recorded between (A) 1800-1500 cm^{-1} and (B) 3050-2700 cm^{-1} on 15^{th} day, after exposure to sodium chloride at varying nutrient levels (# TAGs: - Triacylglycerides; UFA: -Unsaturated Fatty Acid)

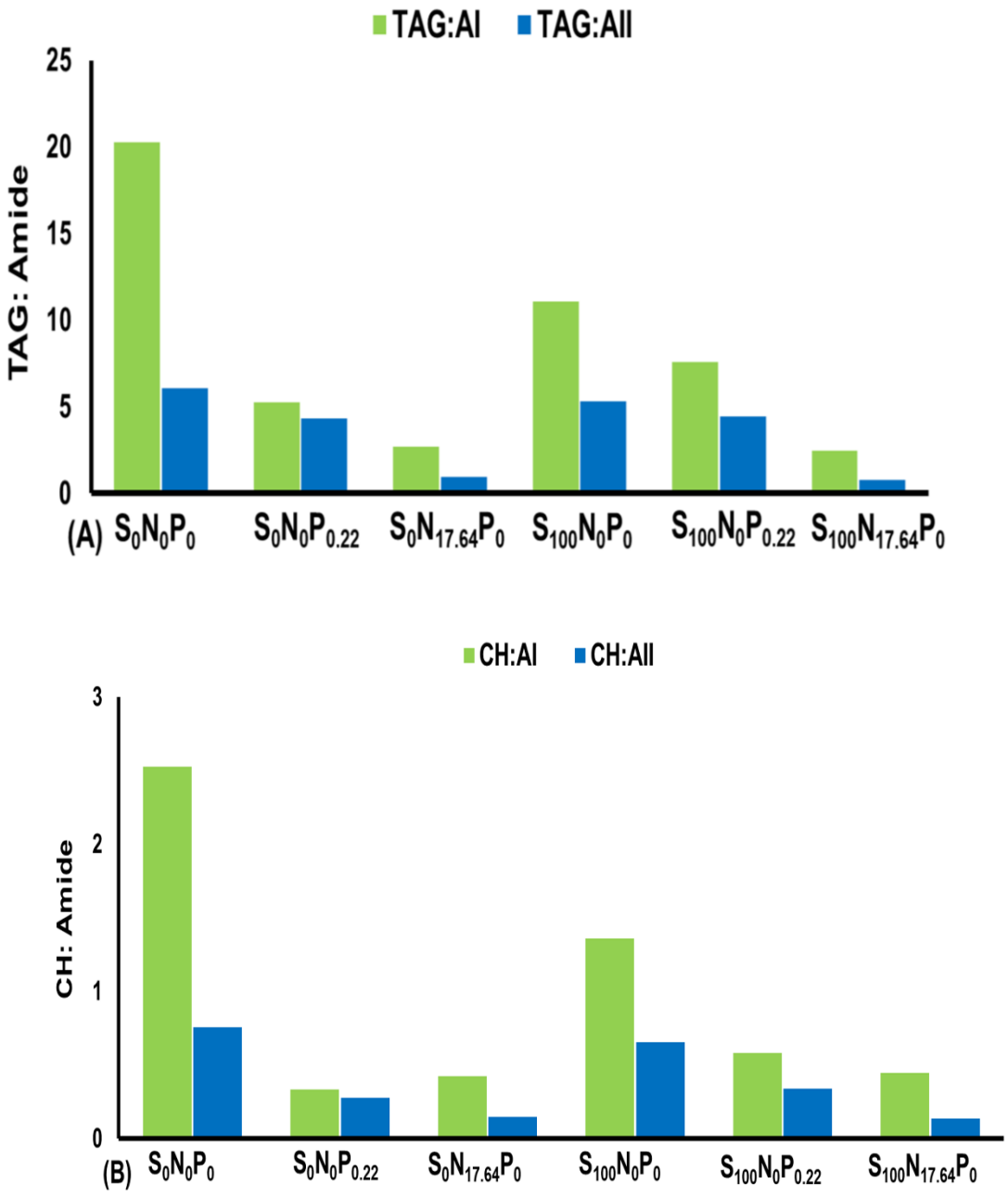

Figure 4.4: Relative content of (A) Triacylglycerides (TAGs) and (B) Hydrocarbons (CH) with respect to Amide-I (AI) and Amide-II (AII) of *Scenedesmus* sp. exposed to sodium chloride at varying nutrient levels

4.3.4 Visualization of neutral lipids inside cells through confocal microscopy

The samples subjected to FTIR analysis were also selected for visualization of neutral lipid bodies in confocal microscopy. The lipid droplets bound to Nile red were visualized on 15th day at $S_{100}N_0P_{0.22}$ as shown in Figure 4.5, where red color indicates autofluorescence and yellow color represents Nile red-stained neutral lipids.

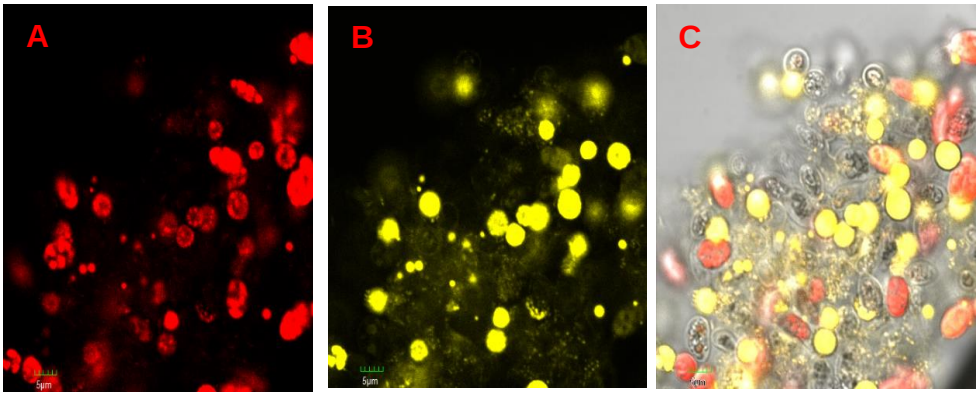

Figure 4.5: Neutral lipids under confocal microscopy at $S_{100}N_0P_{0.22}$ on 15th day, A: Autofluorescence; B: Nile red-stained neutral lipid; C: Merged image of A and B

4.3.5 Imaging morphological changes under stress through SEM

The samples which showed enhanced production of lipid bodies under combined stress (variations in concentrations of sodium nitrate, dipotassium hydrogen phosphate, and sodium chloride) were examined for any morphological changes under scanning electron microscopy. The morphology of cells under stress was found to be distorted owing to its shriveled appearance with asymmetrical grooves (Figure 4.6). The observation indicates that under stress conditions, the cells morphology changes and some of the cells may get completely distorted. As evident from Figure 5, cells appear to be diffused due to exposure to varying media composition. *Scenedesmus* sp. being a pleomorphic strain, alter its morphology, reproductive mode, and biological function under various environmental conditions, e.g., salinity, light intensity,

photoperiod duration, pH, and nutrient variation. These factors may influence the morphological expression in *Scenedesmus* species. These morphological changes can be attributed to the combined effect of different stress factors acting on algal cells. One possible reason for the presence of unicellular *Scenedesmus* sp. when cultivated in lab-scale can be high concentration of nitrate and phosphate present in the growth medium, which is, however, limited in natural conditions like oligotrophic lakes or other environmental conditions.

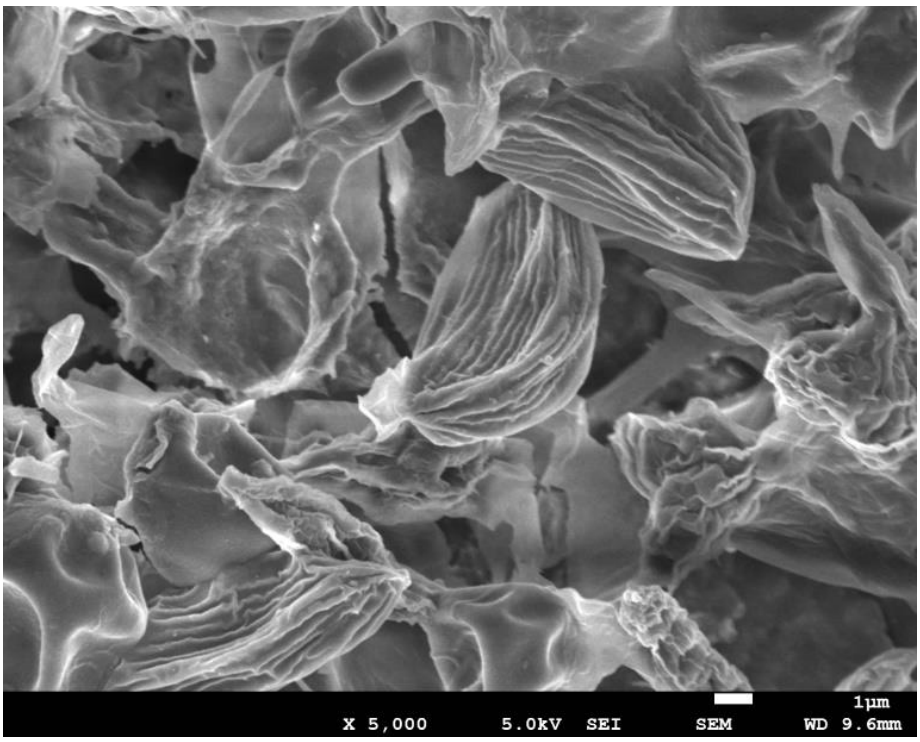

Figure 4.6: Scanning electron microscopy image of *Scenedesmus* sp. cultivated at $S_{100}N_0P_{0.22}$ on 15^{th} day

4.3.6 Quantification of total FAME content and FAME percent under multicomponent stress environment

Fatty acid profiling was done on 15th day for the selected combinations, which were also subjected to FTIR analysis, confocal and SEM imaging. The total fatty acid content was observed maximum for $S_{100}N_0P_0$ (168.4 µg/mg) and $S_{100}N_0P_{0.22}$ (90.41 µg/mg). Although total FAME produced by $S_{100}N_0P_{0.22}$ (90.41 µg/mg) was 1.86-folds less than $S_{100}N_0P_0$ but pertaining to total lipids and chlorophyll content, $S_{100}N_0P_{0.22}$ has cemented its place in current selection. For the commercialization of algal biofuels, both lipid and biomass equally play a major role. Figure 4.7 represents profile of five important fatty acids (in percent) which greatly impact biodiesel quality. It was observed from Figure 4.6 that C16:0 (palmitic acid) fatty acid was maximum for $S_0N_0P_{0.22}$ (38%) followed by $S_{100}N_{17.64}P_0$ (34%), and $S_{100}N_0P_{0.22}$ (33%).

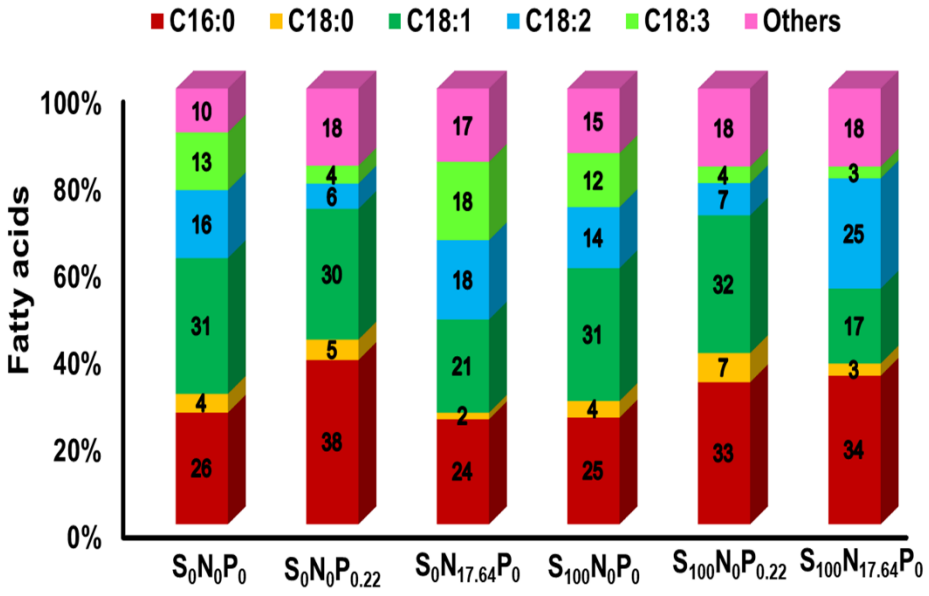

Figure 4.7: Fatty acid profile of *Scenedesmus* sp. exposed to sodium chloride at varying nutrient levels

Increased content of C16:0 fatty acid in *Scenedesmus* sp. under stress condition was observed because these fatty acid acts as stored energy under unfavorable environmental condition alongwith their

requirement for proper membrane function. Similarly, nitrogen-depleted condition resulted in biosynthesis of fatty acids because of declining growth rate. The presence of C18:1 (Oleic acid) fatty acid showed an interesting pattern as there was not much difference in the presence of nitrate. High salt (S_{100}) and low salt (S_0) having optimal nitrate ($N_{17.64}$) do not show much difference in C18:1 fatty acid synthesis; however, a significant difference was observed in both the concentrations of salt when nitrate was absent (N_0). Monounsaturated fatty acid (C18:1) was found to be maximum in $S_{100}N_0P_{0.22}$ (32%), followed by $S_0N_0P_0$ (31%) and $S_{100}N_0P_0$ (30.5%). The maximum amount of C18:2 (linoleic acid) was found for $S_{100}N_{17.64}P_0$ (25%), and varying content of C18:2 fatty acid in response to different treatments suggest that C18:2 is being synthesized due to changes taking place in photosynthetic activity under varying stress conditions. Likewise, previous reports also presented increment in saturated fatty acid under various nutrient stress (Talebi et al., 2013). The saturated fatty acids produced under varying nutrient supplementation was reported with an increment of 38.48 % in *Ankistrodesmus falcatus* KJ671624, when compared to BG11 medium as a control (Singh et al., 2015).

The quality of fuel was also estimated by calculating various properties such as cetane number (CN), iodine value (IV), and saponification value. Cetane number obtained at $S_0N_0P_0$, $S_0N_0P_{0.22}$, $S_0N_{17.64}P_0$, $S_{100}N_0P_0$, $S_{100}N_0P_{0.22}$ and $S_{100}N_{17.64}P_0$ varied between 51 - 55 and saponification value obtained is from 89 to 196 mgKOH/g oil. Iodine values found between 52 - 91 gI_2/100g for different combinations. The results obtained in this study are in accordance with the standards described by ASTM-D675 and EN 14214. The IV refers to biodiesel's ability to react close to ambient temperature with oxygen. The number and position of the double bonds in the alkyl esters' carbon chains depend on this characteristic, thus higher the IV (the iodine mass in grams absorbed by 100 g of a chemical substance), the greater the risk of oxidation, which results in the formation of deposits and degradation of the chemical substance. As per the standard, the

maximum IV value is 120 gI2/100 g, and our results lie in the range of standards.

4.3.7 Effect on antioxidant enzymes activity and reactive oxygen species (ROS) in Scenedesmus sp.

In many cellular metabolic processes, reactive oxygen species (ROS) are essential secondary messengers that can help to activate defense mechanisms and increase metabolite production in microalgae. Accumulation of ROS during stress is encountered by the internal defense system of cells, which include various types of antioxidative scavengers such as catalase (CAT), superoxide dismutase (SOD), ascorbate peroxidase (APX) etc. Besides that, few non-enzymatic antioxidant molecules include proline, polyphenol, flavonoids, pigments, etc. are also present in cells. Activities of these enzymes (Table 4.3) vary corresponding to ROS (Figure 4.8) level in cells indicating the strategy of cells to fight stress caused by unfavorable conditions. The huge variation for ROS species in terms of H_2O_2 radicals was observed and maximum found in case of $S_{100}N_0P_{0.22}$ (10854 μmolH_2O_2/g) followed by $S_{100}N_0P_0$ (7855 μmolH_2O_2/g). At N_0P_0 and $N_0P_{0.22,}$ a high H_2O_2 production confirms stress produced inside the cells in the absence or presence of salt. Superoxide dismutase (SOD) is the initial enzyme, which is activated during stress condition for encountering ROS species. These enzymes catalyze the formation of H_2O_2 and O_2 through the dismutation of $O_2^{\cdot-}$ in which the addition of hydrogen ions neutralizes superoxide radicals, thereby reducing the probability of $OH^{\cdot}$ production via Haber–Weiss-type reaction. SOD activity was found to be maximum for $S_0N_0P_{0.22}$ (43 U/mL).

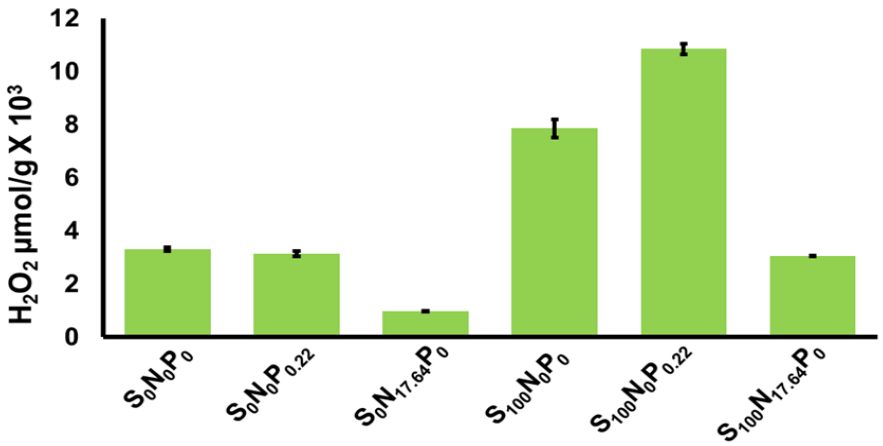

Figure 4.8: Reactive Oxygen species generation (H_2O_2) in *Scenedesmus* sp. exposed to various combination of nitrate, phosphate and sodium chloride (15^{th} day)

SOD enzyme analysis is followed by the estimation of catalase (CAT) enzyme activity which contains a porphyrin compound having heme in its active sites, that immediately dismutase H_2O_2 to H_2O and O_2. In CAT activity, maximum was observed for $S_{100}N_0P_0$ (128 nmol/mL/min). SOD activity cannot be directly linked to H_2O_2 levels, as many other metabolic reactions can produce H_2O_2 and other antioxidant enzymes also contribute towards H_2O_2 formation.

An Increase in the cytosolic ROS level under combined salinity and nutrients stress further confirmed ROS as an essential factor in lipid accumulation. A similar study was carried out by Pancha et al. (2015), where ROS level was reported to increase in coherence with lipid accumulation at 400 mM of NaCl stress in *Scenedesmus* sp. CCNM 1077. Zhao et al. (2019) carried out a similar study and observed that ROS level increases under Cd stress that eventually increases lipid accumulation. The current study shows the significance of ROS in context to enhancement of lipid accumulation under combined abiotic stress of sodium nitrate, dipotassium hydrogen phosphate, and sodium chloride.

Table 4.3: Effect of combined stress on enzymatic activities

Combinations	SOD (U/ml)	CAT (nmol/ml/min)
$S_0N_0P_0$	39±0.2	113±2.1
$S_0N_0P_{0.22}$	43±0.1	123±4.2
$S_0N_{17.64}P_0$	40±0.3	63±0.3
$S_{100}N_0P_0$	38±0.3	128±0.9
$S_{100}N_0P_{0.22}$	34±0.2	117±0.7
$S_{100}N_{17.64}P_0$	27±0.2	94±0.5

4.3.8 Principal component analysis (PCA)

PCA was performed to understand the treatment-variable relationship portrayed by *Scenedesmus* sp. under the exposure of combined stress. The amounts of biomass, chlorophyll, and total lipids produced under different sodium chloride concentrations at varying nitrate and phosphate levels were selected for principal component analysis (PCA). PC 1 (Figure 4.9A) showing flexibilities of 72%, supported by PC 2 (18.2%) and PC 3 (9.8%). PC 2 shows the extreme deviations of total lipids (Figure 4.9B). Biomass and chlorophyll were found to contribute equally in the variance as represented in Figure 4.9B.

Table 4.4: Eigen analysis of the correlation matrix

Dimension	Eigen value	Variance (%)	Cumulative variance (%)
PC1	2.1	72.0	72.0
PC2	0.5	18.1	90.2
PC3	0.2	9.7	100

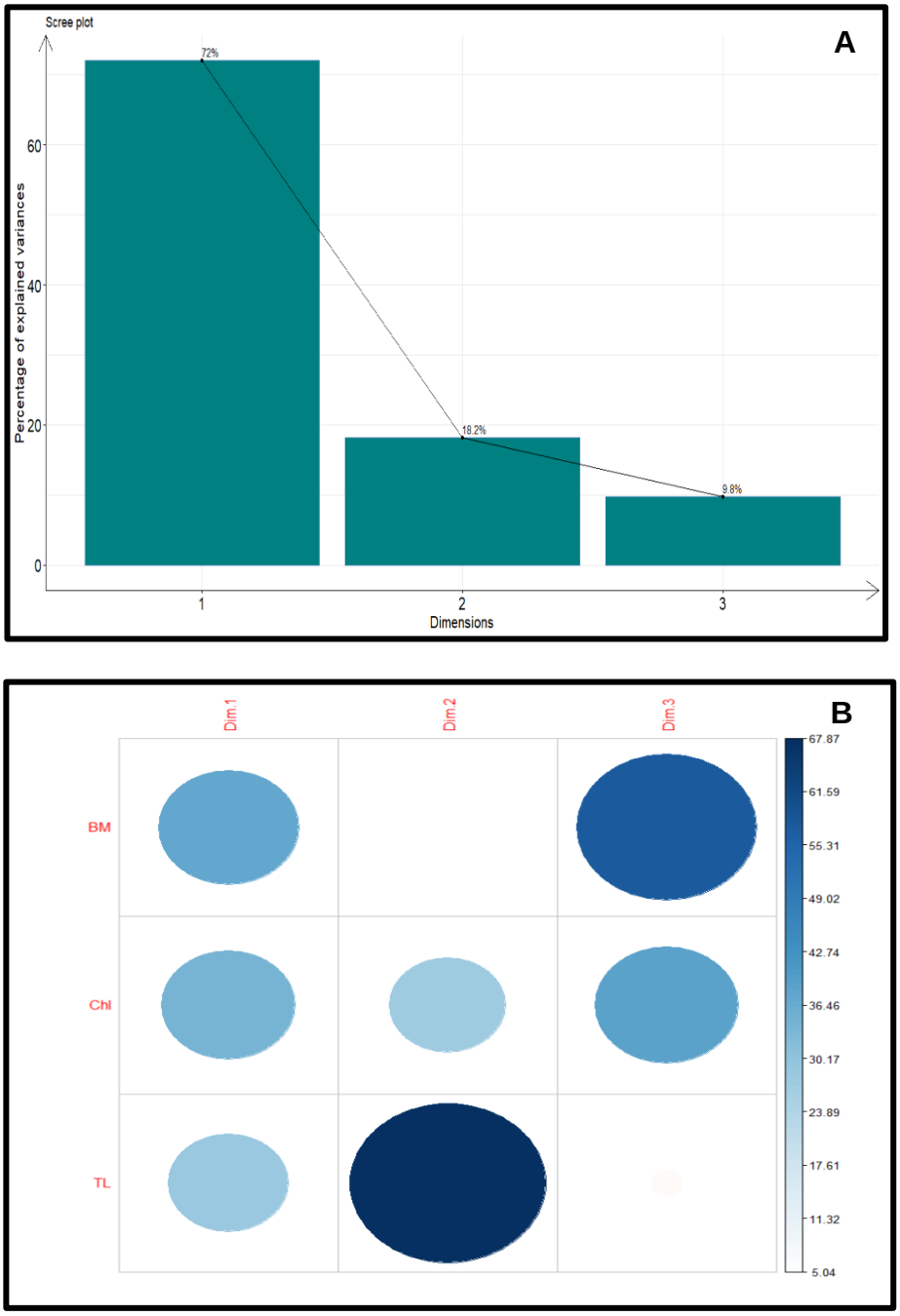

Figure 4.9: (A) Scree plot, a steep curve displays the magnitude of variation in each principal component captured from the data sets where first PC is explaining maximum variation (B) Individual contribution of different variables exposed to sodium chloride at varying nutrients levels, explaining the variation of about 72%

Eigen value of the first three PC are represented in Table 4.4 obtained at various combinations. Contribution of individual component from Figure 4.9B indicate $S_{200}N_0P_{0.22}$ and $S_{100}N_0P_{0.22}$ were

as the major contributor. Thus, it was clearly observed though Figure 4.10B, that salt treatment combined with nitrate depleted conditions affects the optimal production of lipid during various treatment conditions.

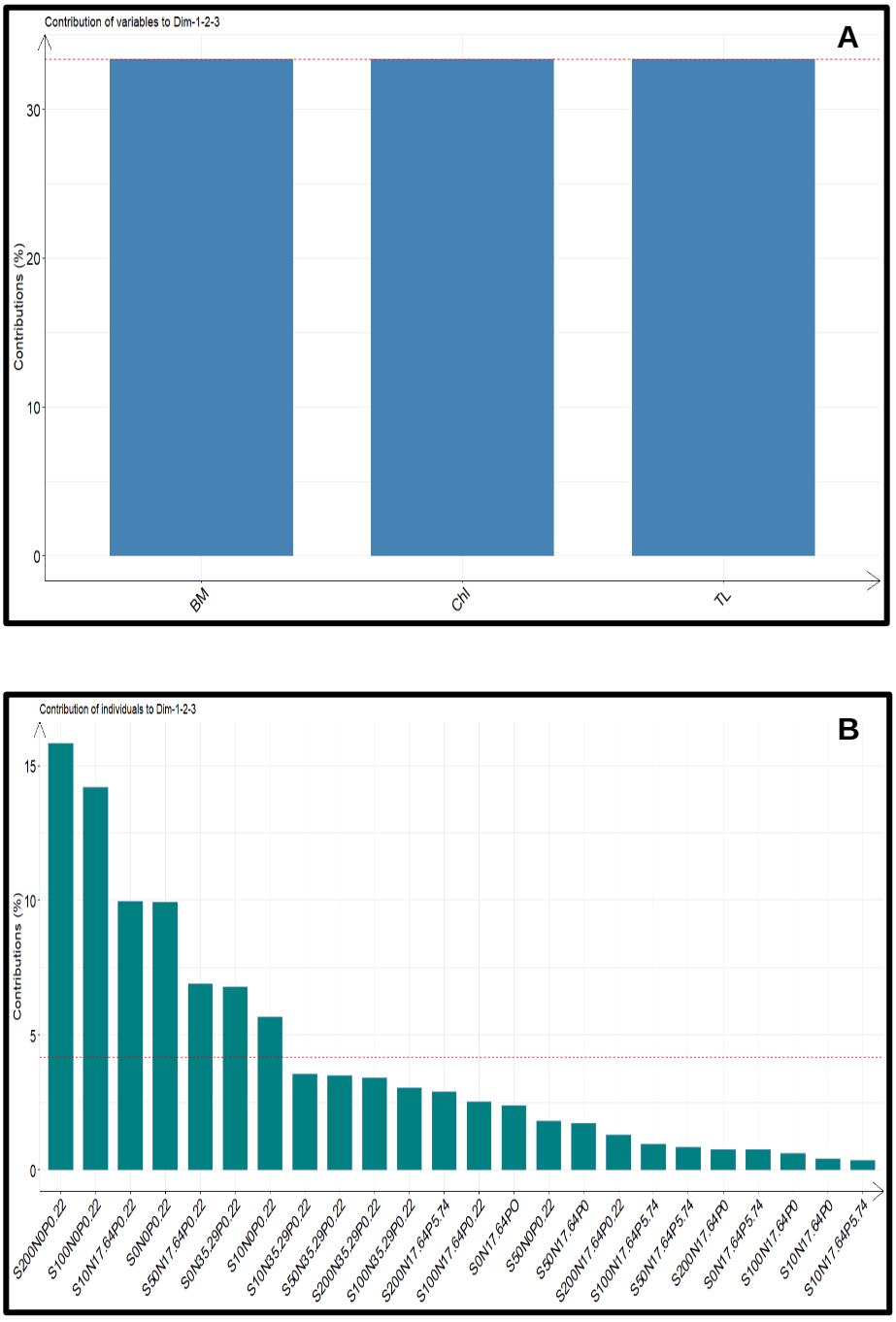

Figure 4.10: (A) Contribution of variables in first three dimensions, (B) Contribution of individual to various dimensions

4.4 Conclusions

The current study concludes that microalgal cells when exposed to varying combinations of stress factors results in the enhancement of lipid content inside algal cells. Total FAME content of $S_{100}N_0P_0$ (168 µg/mg) was found to be maximum amongst all the other combinations. Nevertheless, total lipids and lipid content were estimated to be maximum in $S_{100}N_0P_{0.22}$ (385.44±34.26 µg/mg, 38.5%) without even much influencing the growth of algae as illustrated in terms of chlorophyll. As lipid and biomass accumulation is taking longer time under these cultivation conditions, there is need to reduce this duration to target cost effectiveness. Therefore, it was planned to enhance the lipid accumulation along with biomass by giving a short-term treatment. In the next phase of study, two stage cultivation was performed where cells are cultivated at sodium chloride under varying exposure of nutrients for 48 hours and was followed by externally addition of hydrogen peroxide for 24 hours. It was observed from our study that the color cells changes from green to yellow after 72 hours which enables us to conclude the experiment at 72 hours.

References

Adams, C., Godfrey, V., Wahlen, B., Seefeldt, L., & Bugbee, B. (2013). Understanding precision nitrogen stress to optimize the growth and lipid content trade off in oleaginous green microalgae. Bioresource Technology, 131, 188-194.

Alscher, R. G., Donahue, J. L., & Cramer, C. L. (1997). Reactive oxygen species and antioxidants: relationships in green cells. Physiologia Plantarum, 100(2), 224-233.

Armon, D. I. (1949). Copper enzymes in isolated chloroplast. Plant Physiology, 24, 1-15.

Benvenuti, G., Bosma, R., Cuaresma, M., Janssen, M., Barbosa, M. J., & Wijffels, R. H. (2015). Selecting microalgae with high lipid productivity and photosynthetic activity under nitrogen starvation. Journal of Applied Phycology, 27(4), 1425-1431.

Cao, J., Yuan, H., Li, B., & Yang, J. (2014). Significance evaluation of the effects of environmental factors on the lipid accumulation of *Chlorella minutissima* UTEX 2341 under low-nutrition heterotrophic condition. Bioresource Technology, 152, 177-184.

Chen, C. Y., Chang, J. S., Chang, H. Y., Chen, T. Y., Wu, J. H., & Lee, W. L. (2013). Enhancing microalgal oil/lipid production from *Chlorella sorokiniana* CY1 using deep-sea water supplemented cultivation medium. Biochemical Engineering Journal, 77, 74-81.

Chu, F. F., Chu, P. N., Cai, P. J., Li, W. W., Lam, P. K., & Zeng, R. J. (2013). Phosphorus plays an important role in enhancing biodiesel productivity of *Chlorella vulgaris* under nitrogen deficiency. Bioresource Technology, 134, 341-346.

Converti, A., Casazza, A. A., Ortiz, E. Y., Perego, P., & Del Borghi, M. (2009). Effect of temperature and nitrogen concentration on the growth and lipid content of *Nannochloropsis oculata* and *Chlorella vulgaris* for biodiesel production. Chemical Engineering and Processing: Process Intensification, 48(6), 1146-1151.

Courchesne, N. M. D., Parisien, A., Wang, B., & Lan, C. Q. (2009). Enhancement of lipid production using biochemical, genetic and transcription factor engineering approaches. Journal of Biotechnology, 141(1-2), 31-41.

Dean, A. P., Sigee, D. C., Estrada, B., & Pittman, J. K. (2010). Using FTIR spectroscopy for rapid determination of lipid accumulation in response to nitrogen limitation in freshwater microalgae. Bioresource Technology, 101(12), 4499–4507.

Gao, Y., Yang, M., & Wang, C. (2013). Nutrient deprivation enhances lipid content in marine microalgae. Bioresource Technology, 147, 484-491.

Ghosh, A., Samadhiya, K., Kashyap, M., Anand, V., Sangwan, P., & Bala, K. (2020). The use of response surface methodology for improving fatty acid methyl ester profile of *Scenedesmus vacuolatus*. Environmental Science and Pollution Research, 27(22), 27457-27469.

Grace, C. E. E., Lakshmi, P. K., Meenakshi, S., Vaidyanathan, S., Srisudha, S., & Mary, M. B. (2020). Biomolecular transitions and lipid accumulation in green microalgae monitored by FTIR and Raman analysis. Spectrochimica Acta Part A: Molecular and Biomolecular Spectroscopy, 224, 117382.

Ho, S. H., Chan, M. C., Liu, C. C., Chen, C. Y., Lee, W. L., Lee, D. J., & Chang, J. S. (2014). Enhancing lutein productivity of an indigenous microalga *Scenedesmus obliquus* FSP-3 using light-related strategies. Bioresource Technology, 152, 275-282.

Ji, F., Hao, R., Liu, Y., Li, G., Zhou, Y., & Dong, R. (2013). Isolation of a novel microalgae strain *Desmodesmus* sp. and optimization of environmental factors for its biomass production. Bioresource Technology, 148, 249-254.

Kassambara, A., & Mundt, F. (2017). Factoextra: extract and visualize the results of multivariate data analyses. R package version, 1(5), 337-354.

Lê, S., Josse, J., & Mazet, F. (2008). Package 'FactoMineR. J Stat Softw [Internet], 25(1), 1-18.

Levasseur, M., Thompson, P. A., & Harrison, P. J. (1993). Physiological acclimation of marine phytoplankton to different nitrogen sources 1. Journal of Phycology, 29(5), 587-595.

Liu, Y., Wang, S., Wang, Z., Ye, N., Fang, H., & Wang, D. (2018). TiO_2, SiO_2 and ZrO_2 nanoparticles synergistically provoke cellular oxidative damage in freshwater microalgae. Nanomaterials, 8(2), 95.

Miller, R., Wu, G., Deshpande, R. R., Vieler, A., Gaertner, K., Li, X., ... & Benning, C. (2010). Changes in transcript abundance in *Chlamydomonas reinhardtii* following nitrogen deprivation predict diversion of metabolism. Plant Physiology, 154(4), 1737-1752.

Mishra, S. K., Suh, W. I., Farooq, W., Moon, M., Shrivastav, A., Park, M. S., & Yang, J. W. (2014). Rapid quantification of microalgal lipids in aqueous medium by a simple colorimetric method. Bioresource Technology, 155, 330-333.

Mohan, S. V., & Devi, M. P. (2014). Salinity stress induced lipid synthesis to harness biodiesel during dual mode cultivation of mixotrophic microalgae. Bioresource Technology, 165, 288-294.

Pancha, I., Chokshi, K., Maurya, R., Trivedi, K., Patidar, S. K., Ghosh, A., & Mishra, S. (2015). Salinity induced oxidative stress enhanced biofuel production potential of microalgae *Scenedesmus* sp. CCNM 1077. Bioresource Technology, 189, 341-348.

Radakovits, R., Jinkerson, R. E., Darzins, A., & Posewitz, M. C. (2010). Genetic engineering of algae for enhanced biofuel production. Eukaryotic Cell, 9(4), 486-501.

Rezayian, M., Niknam, V., & Ebrahimzadeh, H. (2019). Oxidative damage and antioxidative system in algae. Toxicology Reports, 6, 1309-1313.

Ríos, S. D., Castañeda, J., Torras, C., Farriol, X., & Salvadó, J. (2013). Lipid extraction methods from microalgal biomass harvested by two

different paths: Screening studies toward biodiesel production. Bioresource Technology, 133, 378-388.

Roe, J. H. (1955). The determination of sugar in blood and spinal fluid with anthrone reagent. Journal of Biological Chemistry, 212, 335-343.

Salama, E. S., Kim, H. C., Abou-Shanab, R. A., Ji, M. K., Oh, Y. K., Kim, S. H., & Jeon, B. H. (2013). Biomass, lipid content, and fatty acid composition of freshwater *Chlamydomonas mexicana* and *Scenedesmus obliquus* grown under salt stress. Bioprocess and Biosystems Engineering, 36(6), 827-833.

Sarno, D., Kooistra, W. H., Balzano, S., Hargraves, P. E., & Zingone, A. (2007). Diversity in the genus *Skeletonema* (Bacillariophyceae): III. Phylogenetic position and morphological variability of *Skeletonema costatum* and *Skeletonema grevillei*, with the description of *Skeletonema ardens* sp. NOV. 1. Journal of Phycology, 43(1), 156-170.

Sharma, K. K., Schuhmann, H., & Schenk, P. M. (2012). High lipid induction in microalgae for biodiesel production. Energies, 5(5), 1532-1553.

Singh, B., Guldhe, A., Rawat, I., & Bux, F. (2014). Towards a sustainable approach for development of biodiesel from plant and microalgae. Renewable and Sustainable Energy Rreviews, 29, 216-245.

Singh, P., Guldhe, A., Kumari, S., Rawat, I., & Bux, F. (2015). Investigation of combined effect of nitrogen, phosphorus and iron on lipid productivity of microalgae *Ankistrodesmus falcatus* KJ671624 using response surface methodology. Biochemical Engineering Journal, 94, 22-29.

Srivastava, G., & Goud, V. V. (2017). Salinity induced lipid production in microalgae and cluster analysis (ICCB 16-BR_047). Bioresource Technology, 242, 244-252.

Su, S., Zhou, Y., Qin, J. G., Yao, W., & Ma, Z. (2010). Optimization of the method for chlorophyll extraction in aquatic plants. Journal of Freshwater Ecology, 25(4), 531-538.

Talebi, A. F., Mohtashami, S. K., Tabatabaei, M., Tohidfar, M., Bagheri, A., Zeinalabedini, M., ... & Bakhtiari, S. (2013). Fatty acids profiling: a selective criterion for screening microalgae strains for biodiesel production. Algal Research, 2(3), 258-267.

Velikova, V., Yordanov, I., & Edreva, A. (2000). Oxidative stress and some antioxidant systems in acid rain-treated bean plants: protective role of exogenous polyamines. Plant Science, 151(1), 59-66.

Vincent, Q.V., (2011). GitHub - vqv/ggbiplot: A biplot based on ggplot2. https://github.com/vqv/ggbiplot. Accessed 23 Jul 2020.

Wickham, H., & Chang, W. (2019). devtools: Tools to make developing R packages easier, 2016. URL https://CRAN. R-project. org/package= devtools. R package version, 1(0), 103.

Xin, L., Hong-Ying, H., Ke, G., & Ying-Xue, S. (2010). Effects of different nitrogen and phosphorus concentrations on the growth, nutrient uptake, and lipid accumulation of a freshwater microalga *Scenedesmus* sp. Bioresource Technology, 101(14), 5494-5500.

Yilancioglu, K., Cokol, M., Pastirmaci, I., Erman, B., & Cetiner, S. (2014). Oxidative stress is a mediator for increased lipid accumulation in a newly isolated *Dunaliella salina* strain. PLoS One, 9(3), e91957.

Zhao, Y., Song, X., Yu, L., Han, B., Li, T., & Yu, X. (2019). Influence of cadmium stress on the lipid production and cadmium bioresorption by *Monoraphidium* sp. QLY-1. Energy Conversion and Management, 188, 76-85.

CHAPTER 5

Chapter 5

Algal behavior under hydrogen peroxide induction accompanied by nitrate and phosphate variation via two-stage cultivation

5.1 Introduction

The expeditious demand of non-renewable fuels with increasing world population has led to extensive reliance on fossil fuels causing its deterioration. These non-renewable sources of energy have various harmful effects like global warming. Microalgae are the rich source of neutral lipids (TAGs-triacylglycerides) and can act as potential feedstock for a renewable energy source.

The most common abiotic stress factors include nitrogen limitation/starvation, which is considered as an efficient treatment to enhance lipids inside algal cells. In addition to nitrogen stress, there are many other different kinds of abiotic stresses, for example, high or low light intensity, temperature variation or osmotic/oxidative stress such as salinity stress, etc. Under stress conditions, excess electrons are generated through the photosynthetic electron transport chain mechanism, which results in overproduction of reactive oxygen species (ROS) (Hu et al., 2008) and ultimately results in the induction of oxidative stress. These ROS can cause inhibition of photochemical reaction along with shattering the membrane proteins, lipids, and other biological molecules. Different studies have been carried out under several oxidative stress additions, showing enhanced lipid accumulation in microalgae. For example, *Dunaliella salina* showed elevated lipid accumulation levels in the cells at varying oxidative stress (Yilancioglu et al., 2014). Free radicals such as O_2^- (superoxide), H_2O_2 (hydrogen peroxide), or OH° (hydroxyl) radicals produced during

stress lead to reduced photosynthetic efficiency of the organism due to degradation of PS II complex, caused by thylakoids lipid peroxidation. Stress instigates the photosynthetic carbon channel of microalgae cells to synthesize compounds rich in energy, such as carbohydrates and lipids to be used by algae during adverse environmental conditions. Mostly, the up-surges of ROS is equivalent to the level of stress, which implies that higher is the stress given to organisms more significant is ROS accumulation.

In addition to the peroxidation effect of ROS, they also act as a signaling molecule in photosynthetic organisms. ROS along with some messenger molecule such as Ca^{2+}, generated during stress conditions, initiate phosphorylation cascade and target the significant gene, responsible for stress. Products of these gene expressions enable the species to survive under unfavorable conditions (Mahajan and Tuteja, 2005). Besides these, cells have inbuilt antioxidant defense systems to encounter these ROS, which includes antioxidative enzymes viz. catalase (CAT), ascorbate peroxidase (APX), and superoxide dismutase (SOD). Some non - enzymatic antioxidants, such as proline, polyphenols, etc., act as powerful scavengers of ROS to protect cells from oxidative damage (Zuppini et al., 2010). H_2O_2 is naturally synthesized ROS during cellular processes, which are being investigated for its role in high lipid accumulation in algae (Battah et al., 2015).

Beside mono-component stress, very few studies have been carried out where combined or synergistic effect of two or more component are viewed in terms of lipid enhancement in microalgae. For example, *Dunliella salina* cultivated in nutrient deprivation at high sodium chloride concentration resulted in the reduction of chlorophyll (Coesel et al., 2008). Another study revealed that H_2O_2 treatment might work by fetching the redox reaction, as part of procedure that changes the metabolism beyond biomass accumulation towards lipid synthesis during low nitrate environment. It was concluded that H_2O_2 may act as potent agent furnishing environmental nitrogen levels in *P. tricorutum,*

through post-translational protocol of nitrogen assimilation proteins (Rosenwasser et al., 2014).

In the present study, the effect of nutrient (sodium nitrate, dipotassium hydrogen phosphate) depleted and repleted conditions along with varying levels of hydrogen peroxide, provided in a phased manner was monitored to evaluate the effect on TAGs accumulation inside the microalgae, *Scenedesmus* sp. Biomass and chlorophyll content were recorded to study the impact of H_2O_2 on cell growth under varying nitrate and phosphate concentration during second phase cultivation. Besides biochemical analyses, stress-induced biomarkers like SOD, CAT, and H_2O_2 were also studied to understand the impact of reactive oxygen species. Additionally, biodiesel properties of selected samples based on nutrients repletion or depletion in combination with hydrogen peroxide were further investigated.

5.2 Materials and Methods

5.2.1 Experimental configuration to study the impact of integrated treatments

Algae cells were exposed to sodium nitrate ($NaNO_3$) (0, 17.64, and 35.29 mM designated as N_0, $N_{17.64,}$ and $N_{35.29}$, respectively), and dipotassium hydrogen phosphate (K_2HPO_4) (0, 0.22, and 5.74 mM designated as P_0, $P_{0.22,}$ and $P_{5.74}$, respectively) in various combinations for 48 hours in the first-stage cultivation. After 48 hours, different concentrations of hydrogen peroxide (H_2O_2) (0, 2, 4, 6, 8, and 10 mM represented as H_0, $H_{2,}$ $H_{4,}$ H_6, $H_{8,}$ and $H_{10,}$ respectively) was inducted into the nutrient varied algal cells for next 24 hours, following which all the analytical investigation and instrumental analysis were performed (Figure 5.1). All the experiments were performed in triplicates.

5.2.2 Assessment of growth and pigment in Scenedesmus sp.

After 24 hours of hydrogen peroxide exposure to nitrate/phosphate repleted and depleted algal cells, growth of

Scenedesmus sp. was assessed. The density of algal cells was examined by recording cell density at 680 nm. Chlorophyll 'a' was extracted, and its content was estimated by following Su et al., (2010) and Arnon, (1949) methods, respectively.

5.2.3 Extraction and quantification of lipids and carbohydrates

Sulfo-Phospho-Vanillin (SPV) method was followed for the quantification of total lipids accumulated inside the algal cell (Mishra et al., 2014), whereas carbohydrate was quantified using anthrone test as described by Roe (1955). Carbohydrate and lipid were quantified using a standard calibration (detailed in chapter 2) curve constructed by considering different concentrations of glucose and triolein as carbohydrate and lipid standard, respectively.

5.2.4 Spectroscopic insight into the algal composition

FTIR spectroscopy of dry algal biomass was performed in order to analyze different types of biomolecular transitions occurring within the algal cells due to different treatments conducted. The spectra were scrutinized in the limits of 400-4000 $cm^{-1,}$ and the same were refined using Origin Pro 8.5 software via the second-order differentiation method.

5.2.5 Nile lipid visualization and morphological analysis

The confocal laser scanning microscope (Multiphoton laser scanning microscope FV1200MPE, Olympus-IX83, Objective lens NA1.4, Laser-405, 488 and 559nm, software-FV10-ASW 4.2) and scanning electron microscope (FE-SEM) (Supra55 Zeiss) were employed explicitly for monitoring the neutral lipid bodies and the structural morphology of the algal cells under treatment, respectively (Sarno et al., 2007). The protocols followed for microscopy of algal cells have been described in detail in chapter 2.

5.2.6 Profiling fatty acid methyl ester (FAME) and biodiesel properties

For the assessment of fatty acid content, the triacylglycerides (TAG) were transesterified directly into FAME by emulating the protocol given by Ríos et al. (2013). Biodiesel properties were calculated with the help of the percentage of various fatty acids obtained from Gas Chromatography of derivatized dry algal cells.

5.2.7 Microplate assays for estimation of ROS levels and activities of enzymatic antioxidant scavengers

The Velikova et al., 2000 protocol was adopted for the evaluation of ROS accumulation symbolized by H_2O_2 production inside the algal cells. The colorimetric quantification was done by taking supernatant's absorbance at 390 nm (Velikova et al., 2000).

The antioxidative enzyme analysis was carried out 24 hours after hydrogen peroxide induction. Catalase (CAT) and superoxide dismutase (SOD) assay kits were purchased from Cayman chemical (MI-USA) and analyzed according to the manufacturer's instructions

5.2.8 Principal component assessment

R studio desktop version 4.0.0 with R packages, 'factoextra' (Kassambara and Mundt, 2020), 'FactoMineR' (Lê S, 2008), 'devtools' (Wickham, 2019), and 'ggbiplot' (Vincent, 2011) were exploited for principal component analysis (PCA).

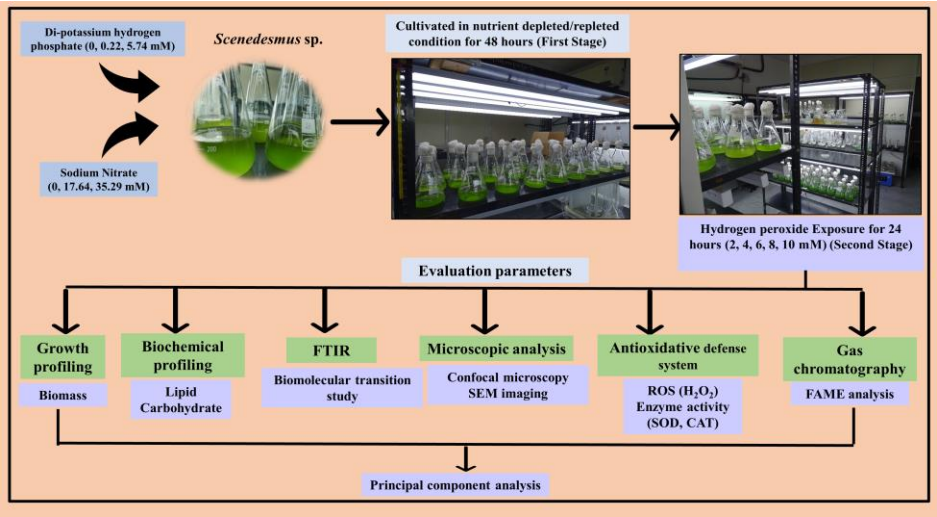

Figure 5.1: Systematic representation of impact of hydrogen peroxide under varying exposure of nutrients on *Scenedesmus* sp. and its analysis

5.3 Results and discussion

5.3.1 24 hours hydrogen peroxide exposure to *Scenedesmus* sp. growing in nutrient replete/deplete conditions

5.3.1.1 Biomass and chlorophyll content

It was determined that the hydrogen peroxide induction in the nutrient-treated algal cells for 24 hours led to a decline in cells' growth, as depicted in Figure 5.2. It was evident that the cell density of *Scenedesmus* sp. tends to decrease with an increase in hydrogen peroxide concentration. Biomass accumulation of *Scenedesmus* sp. exposed to hydrogen peroxide (second stage) under varying nitrate and phosphate levels (first stage) has been represented in Table 5.1.

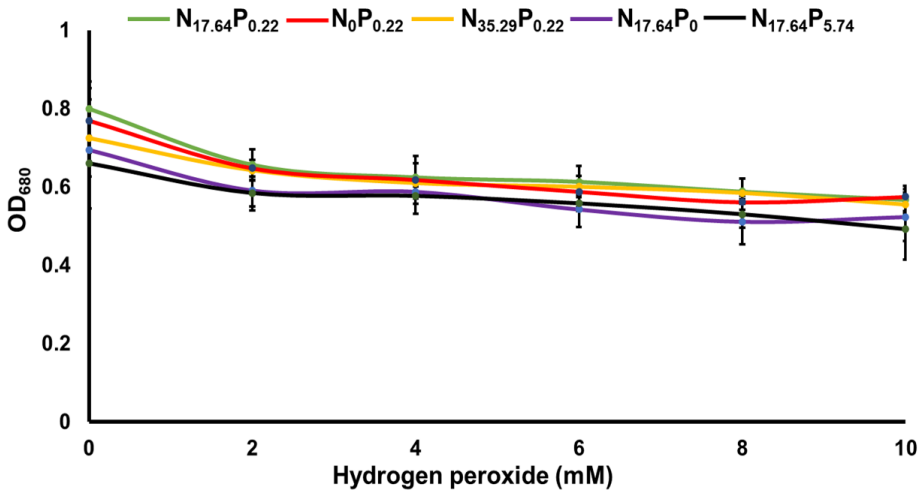

Figure 5.2: Cell density of *Scenedesmus* sp. exposed to hydrogen peroxide (second stage) at varying nutrients levels

All the combinations where nitrate and phosphate levels deviated from the normal value (N 17.64 mM and P 0.22 mM) displayed lower biomass accumulation. It has been a well-known fact that under stress conditions amount of biomass accumulation decreases. In Figure 5.3A, at $N_{17.64}P_{0.22}$, $N_0P_{0.22}$, and $N_{35.29}P_{0.22}$, that is, at varying sodium nitrate concentrations with constant phosphate level, biomass and chlorophyll were found to decrease gradually with an increase in hydrogen peroxide levels. A similar trend was observed for constant nitrate with varying phosphate concentrations (Figure 5.3B) i.e., biomass decreases with an increase in hydrogen peroxide. It was observed that at 17.64 mM, and 35.29 mM of nitrate exposure with fixed phosphate (0.22 mM), the amount of biomass produced is more than ($H_0N_{35.29}P_{0.22}$, 447.2±22.4 µg/mL; Table 5.1) nitrate-depleted condition. Furthermore, a linear decrease in biomass was observed after 24 hours hydrogen peroxide exposure. For phosphate, biomass accumulated at 0 mM was observed to be less than the amount of biomass accumulated under 5.29 mM, which was further decreasing linearly with increasing hydrogen peroxide exposure. Amongst all combinations of nitrate, phosphate, and hydrogen peroxide the lowest biomass was obtained for $H_{10}N_0P_0$ (286.9±12.0 µg/mL). Results obtained show that nitrate and phosphate play a vital role in cell growth and affect biomass accumulation. It was

also observed that an increase in the nitrate or phosphate level above optimum value does not have an impressive mark on the hike of biomass yield.

Similar results were obtained for chlorophyll ‘a’ as represented in Table 5.1, which suggests that the cell growth was halted at higher hydrogen peroxide concentration. The lowest chlorophyll content was obtained for $H_{10}N_0P_0$ (2.9±0.0 µg/mL), which confirms that hydrogen peroxide along with nitrate and phosphate have a crucial role in stress generation. Chlorophyll measurements are an essential parameter to observe the cell growth, and if cells experience stress, the chlorophyll level goes down, which is evident from the results obtained in the current study, as shown in Figures 5.3A and 5.3B. The decline in chlorophyll ‘a’ (Figure 5.3A and 5.3B) accumulation is an indicator of cells' growth pattern under the combined stress of nutrient deprivation and high hydrogen peroxide levels, which proved to be the critical players. Decrease in chlorophyll ‘a’ content depicts that hydrogen peroxide induces stress leading to decline in chlorophyll level even when the cells were provided with adequate nitrate and phosphate levels. However, the extent of stress generated by hydrogen peroxide increased when combined with nitrate and phosphate deprivation, leading to lower chlorophyll synthesis and lower cell growth.

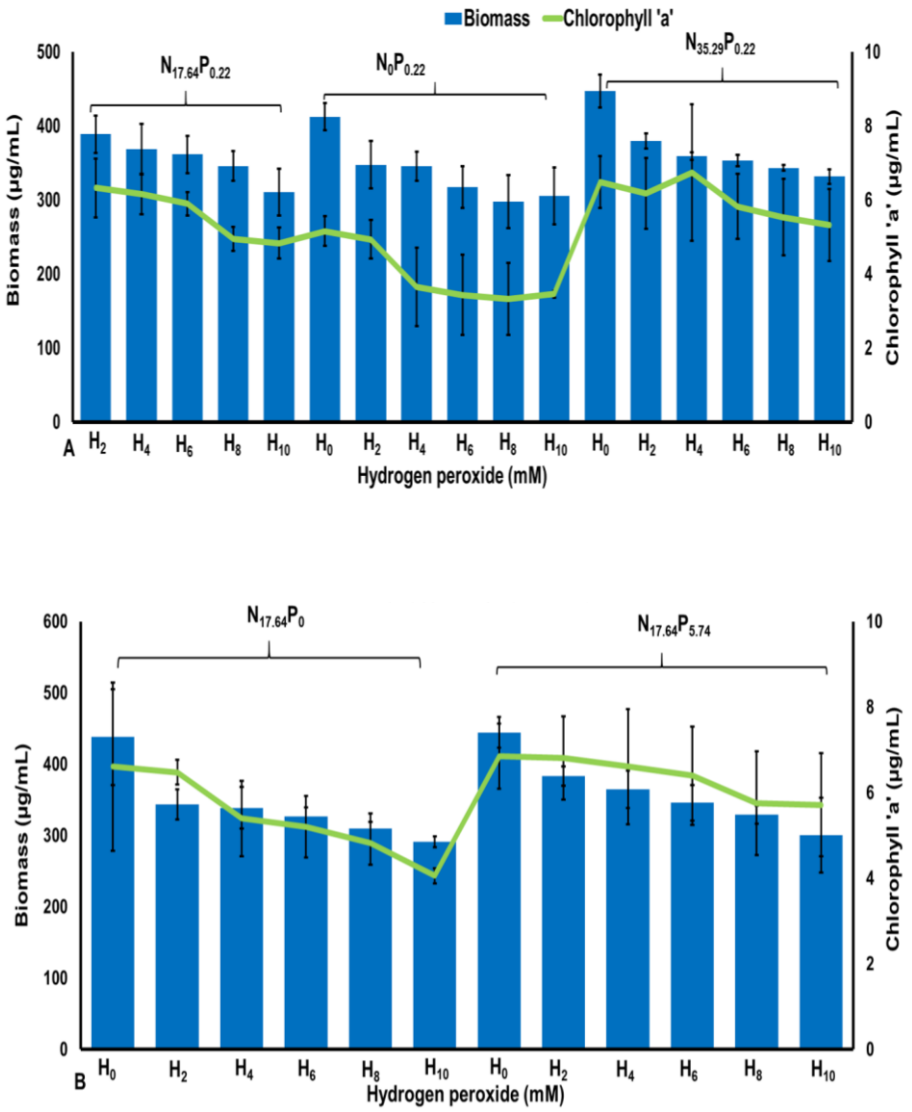

Figure 5.3: Relationship between biomass and chlorophyll ‘a’ in *Scenedesmus* sp. under exposure to (A) varying sodium nitrate and hydrogen peroxide at constant phosphate level (B) varying dipotassium hydrogen phosphate and hydrogen peroxide at constant nitrate level

Table 5.1: Biomass and chlorophyll 'a' profile of *Scenedesmus* sp. exposed to hydrogen peroxide (second stage) under varying nitrate and phosphate levels (first stage)

Combinations	Biomass Accumulation (µg/mL)	Chlorophyll Accumulation (µg/mL)
$H_0N_0P_0$	329.9±29.9	5.1±0.6
$H_{10}N_0P_0$	286.9±12.0	2.9±0.0
$H_2N_{17.64}P_{0.22}$	388.9±24.8	6.3±0.7
$H_4N_{17.64}P_{0.22}$	368.9±33.7	6.1±0.5
$H_6N_{17.64}P_{0.22}$	361.8±25.0	5.9±0.3
$H_8N_{17.64}P_{0.22}$	346.0±20.1	4.9±0.3
$H_{10}N_{17.64}P_{0.22}$	310.7±31.4	4.8±0.4
$H_0N_0P_{0.22}$	412.6±18.2	5.1±0.4
$H_2N_0P_{0.22}$	347.7±31.9	4.9±0.5
$H_4N_0P_{0.22}$	345.7±19.6	3.6±1.0
$H_6N_0P_{0.22}$	317.5±28.2	3.4±1.0
$H_8N_0P_{0.22}$	297.8±36.0	3.3±0.9
$H_{10}N_0P_{0.22}$	305.5±38.3	3.4±0.1
$H_0N_{35.29}P_{0.22}$	447.2±22.4	6.4±0.7
$H_2N_{35.29}P_{0.22}$	379.8±9.9	6.1±0.9
$H_4N_{35.29}P_{0.22}$	359.3±5.0	6.7±1.8
$H_6N_{35.29}P_{0.22}$	353.4±7.3	5.8±0.8
$H_8N_{35.29}P_{0.22}$	343.6±4.2	5.5±1.0
$H_{10}N_{35.29}P_{0.22}$	331.8±9.9	5.3±0.9
$H_0N_{17.64}P_0$	438.0±66.9	6.6±1.9
$H_2N_{17.64}P_0$	343.5±21.3	6.4±0.2
$H_4N_{17.64}P_0$	339.0±28.9	5.4±0.8
$H_6N_{17.64}P_0$	327.1±12.7	5.2±0.7
$H_8N_{17.64}P_0$	309.8±21.5	4.8±0.5
$H_{10}N_{17.64}P_0$	291.5±7.6	4.0±0.1
$H_0N_{17.64}P_{5.74}$	444.6±21.2	6.8±0.7
$H_2N_{17.64}P_{5.74}$	383.4±13.2	6.8±0.9
$H_4N_{17.64}P_{5.74}$	364.8±26.1	6.6±1.3
$H_6N_{17.64}P_{5.74}$	345.9±25.1	6.4±1.1
$H_8N_{17.64}P_{5.74}$	329.2±12.9	5.7±1.2
$H_{10}N_{17.64}P_{5.74}$	300.4±52.5	5.7±1.2

The above-discussed results suggest that both biomass and chlorophyll accumulation got hampered under the combined effect of nutrients and hydrogen peroxide variations. Our findings were also supported by earlier studies conducted by Barrington and Ghadouani, (2008) and Drábková et al., (2007), where hydrogen peroxide was stated as a reliable oxidizing agent, which can effectively inhibit the

growth of microalgae. The impact of hydrogen peroxide on growth of algae occurs after transformation into exceptionally sensitive hydroxyl radicals (ȮH), which triggers acute harm to DNA, RNA, membranes alongwith proteins (Halliwell and Gutteridge, 1984; Abo-Shady et al., 2008).

5.3.1.2 Lipid and carbohydrate accumulation after 24 hrs exposure to hydrogen peroxide

Lipid accumulation in microalgae is known to be enhance by growing algae under stress environments. Table 5.2 represents the amount of lipid and carbohydrate content obtained. The lipid accumulation, when analyzed after 72 hours, was found to be highest in the algal cells cultivated in $H_{10}N_0P_{0.22}$ media composition (156.6±24.3 µg/mg), followed by second highest and third highest lipid content in $H_0N_0P_0$ (145.2±33.3 µg/mg) and $H_{10}N_0P_0$ (139.8±38.1 µg/mg). It was observed that with an increase in hydrogen peroxide, the amount of lipid also increases. It was also marked that in the nitrate and phosphate deprived media, without the induction of H_2O_2, algal cells produced more lipid as compared to algal cells grown in H_2O_2 (10 mM) induced media. Different researchers have also stated that the nutrient diminution has been one of the significant factors for prompt and enhanced lipid production in microalgae (Chen et al., 2017; Ramya et al., 2017). Amongst various nutrients, nitrogen-hunger has also been believed to be an essential and practically achievable means to increase the lipid content, which can be reproduced in large-scale production (Ramya et al., 2017). Under optimal nutrient-growth conditions, microalgae produce significant quantities of biomass but with minimal lipid content, while growing microalgae under nutrient-starved environment encourage high amounts of lipids but with reduced biomass accumulation, which is evident from previous findings too (Tan et al., 2016). From Table 5.2, it can be observed that during 24 hours exposure to hydrogen peroxide, dipotassium hydrogen phosphate does not play a significant role in lipid accumulation as being played by sodium nitrate. Our findings were also found to be in line with previous

literature where noticeable changes in lipid accumulation were observed (Anto et al., 2019).

Table 5.2: Biochemical composition of *Scenedesmus* sp. exposed to hydrogen peroxide under varying nitrate and phosphate levels

Combinations	Lipid Concentration (µg/mg)	Lipid Content (%)	Carbohydrate Concentration (µg/mg)	Carbohydrate Content (%)
$H_0N_0P_0$	145.2±33.3	14.5±3.3	435.1±177.9	43.5±17.7
$H_{10}N_0P_0$	139.8±38.1	13.9±3.8	497.8±26.7	49.7±2.6
$H_2N_{17.64}P_{0.22}$	99.6±43.0	9.9±4.3	383.3±31.6	38.3±3.1
$H_4N_{17.64}P_{0.22}$	99.6±40.8	9.9±4.0	369.8±28.3	36.9±2.8
$H_6N_{17.64}P_{0.22}$	84.8±56.1	8.4±5.6	403.1±73.9	40.3±7.3
$H_8N_{17.64}P_{0.22}$	93.8±59.5	9.3±5.9	444.8±71.0	44.4±7.1
$H_{10}N_{17.64}P_{0.22}$	118.3±15.2	11.8±1.5	471.9±65.3	47.1±6.5
$H_0N_0P_{0.22}$	121.5±45.8	12.1±4.5	535.3±291.7	53.5±29.1
$H_2N_0P_{0.22}$	91.8±61.7	9.1±6.1	531.7±75.9	53.1±7.5
$H_4N_0P_{0.22}$	89.4±77.6	8.9±7.7	476.9±64.3	47.6±6.4
$H_6N_0P_{0.22}$	86.5±71.0	8.6±7.1	745.9±32.5	74.5±3.2
$H_8N_0P_{0.22}$	101.7±70.7	10.1±7.0	472.7±88.4	47.2±8.8
$H_{10}N_0P_{0.22}$	156.6±24.3	15.6±2.4	434.9±137.4	43.9±13.7
$H_0N_{35.29}P_{0.22}$	81.0±5.0	8.1±0.5	425.6±103.5	42.5±10.3
$H_2N_{35.29}P_{0.22}$	91.0±51.5	9.1±5.1	384.8±41.1	38.4±4.1
$H_4N_{35.29}P_{0.22}$	83.6±74.4	8.3±7.4	423.7±43.7	42.3±4.3
$H_6N_{35.29}P_{0.22}$	111.7±50.6	11.1±5.0	441.1±26.4	44.1±2.6
$H_8N_{35.29}P_{0.22}$	113.3±51.9	11.3±5.1	450.2±29.6	45.0±2.9
$H_{10}N_{35.29}P_{0.22}$	111.7±18.0	11.1±1.8	447.8±36.8	44.7±3.6
$H_0N_{17.64}P_0$	87.7±24.8	8.7±2.4	340.2±63.9	34.0±6.3
$H_2N_{17.64}P_0$	61.8±24.0	6.1±2.4	308.2±54.4	30.8±5.4
$H_4N_{17.64}P_0$	76.3±36.5	7.6±3.6	296.3±50.5	29.6±5.0
$H_6N_{17.64}P_0$	72.1±28.4	7.2±2.8	259.2±84.6	25.9±8.4
$H_8N_{17.64}P_0$	79.4±25.1	7.9±2.5	334.4±90.3	33.4±9.0
$H_{10}N_{17.64}P_0$	97.5±49.3	9.7±4.9	366.9±47.3	33.6±4.7
$H_0N_{17.64}P_{5.74}$	81.9±27.3	8.1±2.7	315.1±10.6	31.5±1.0
$H_2N_{17.64}P_{5.74}$	83.9±28.9	8.3±2.8	210.7±66.4	21.0±6.6
$H_4N_{17.64}P_{5.74}$	105.9±44.5	10.5±4.4	267.1±27.2	26.7±2.7
$H_6N_{17.64}P_{5.74}$	93.4±36.6	9.3±3.6	248.0±102.2	24.8±10.2
$H_8N_{17.64}P_{5.74}$	81.3±35.6	8.1±3.5	178.5±45.7	17.8±4.5
$H_{10}N_{17.64}P_{5.74}$	122.1±44.7	12.2±4.4	289.6±22.6	28.9±2.2

Under different culture treatments, the synthesis of carbohydrates has been reported to depend upon the carbon flux and the amount of stress given to the sample. Carbohydrate accumulation was investigated to increase with an increase in hydrogen peroxide

concentration. The maximum carbohydrate content (745.9±32.5 µg/mg) was obtained in algal cells grown in $H_6N_0P_{0.22}$ media composition. In the case of dipotassium hydrogen phosphate exposure, carbohydrates accumulation was found to be low at the highest phosphate level. Our results supported that of Liang et al. (2013), where dropping phosphorus concentration from 240 to 32 µM led to the reduction in amount of carbohydrate content from 25.2 to 22.5 %.

5.3.1.3 Qualitative analysis of lipid accumulation through FTIR spectroscopy

In the present study, FTIR data supported in comprehension of the effect of treatments on the transitions of biomolecules present inside the algal cells along with the lipid accumulation. FTIR data revealed the presence of TAGs in algal cells under hydrogen peroxide exposure at varying nutrient levels. Spectra obtained were refined through second derivative order as described in chapter 2. The band observed at 1746 cm^{-1} (Figure 5.4A) pointed towards the presence of υ (C=O) stretches owing to the presence of esters in the lipids and therefore signifies the presence of TAGs (Dean et al., 2010). The maximum stretches were observed at $H_{10}N_0P_{0.22}$ (Figure 5.4A), which was further supported through TAGs: Amide-I and Amide-II ratio (Figure 5.5A). The bands (Figure 5.4A) observed at 1546 cm^{-1} and 1652 cm^{-1} indicated the presence of Amide-II and Amide-I bonds from proteins (IR) and cis υ (C=C) from unsaturated lipids, respectively.

TAGs (~1746 cm^{-1}), which have been assigned as a portion of neutral lipid content and fluctuate in its intensity, can help in knowing the effect of different variables on neutral lipid content. The accumulation of lipids in microalgae can be estimated through FTIR analysis as reported by Grace et al. (2020). The band in the region 3050 to 2700 cm^{-1} (Figure 5.4B) corresponding to υ (CH3) and υ (CH2) asymmetric and symmetric stretches of hydrocarbon were also present. The current research was in line with the earlier reports, which stated

lipid accumulation under oxidative stress and nutrition deprived conditions (Cao et al., 2014).

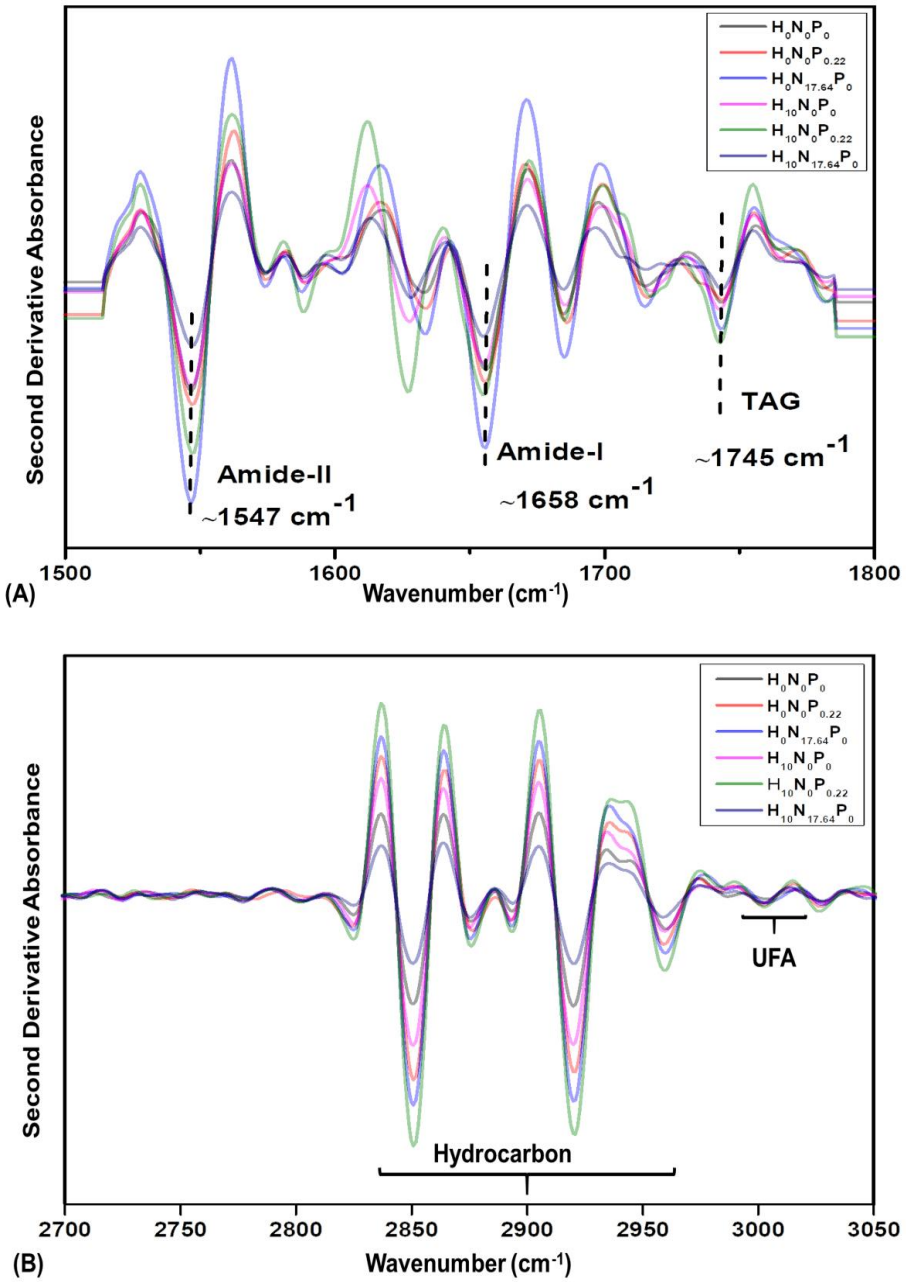

Figure 5.4: Second derivative spectra of lyophilized algal biomass between (A) 1800-1500 cm^{-1} and (B) 3050-2700 cm^{-1} (# TAGs - Triacylglycerides; UFA- Unsaturated Fatty Acid)

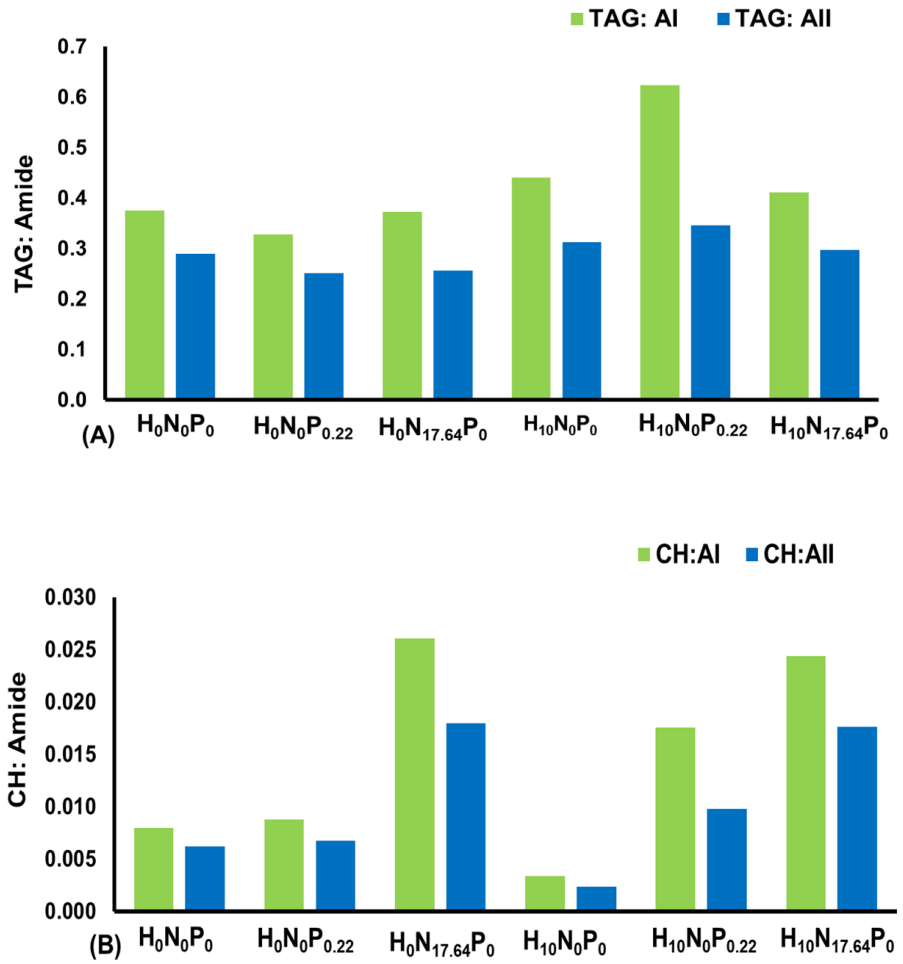

Figure 5.5: Relative content of (A) Triacylglycerides (TAGs) and (B) Hydrocarbons (CH) with respect to Amide I (AI) and Amide II (AII) of *Scenedesmus* sp.

5.3.1.4 Visualization of neutral lipids inside cells through confocal microscopy

Neutral lipids (TAGs) within algal cells were visualized under confocal microscopy. After 24 hours of hydrogen peroxide exposure, algal cells exposed to $H_{10}N_{17.64}P_0$, $H_0N_{17.64}P_0$, and $H_{10}N_0P_{0.22}$ were chosen for lipid bodies visualization, as illustrated in Figure 5.6; where A: Autofluorescence; B: Nile red-stained neutral lipid; and C: Merged image of A and B.

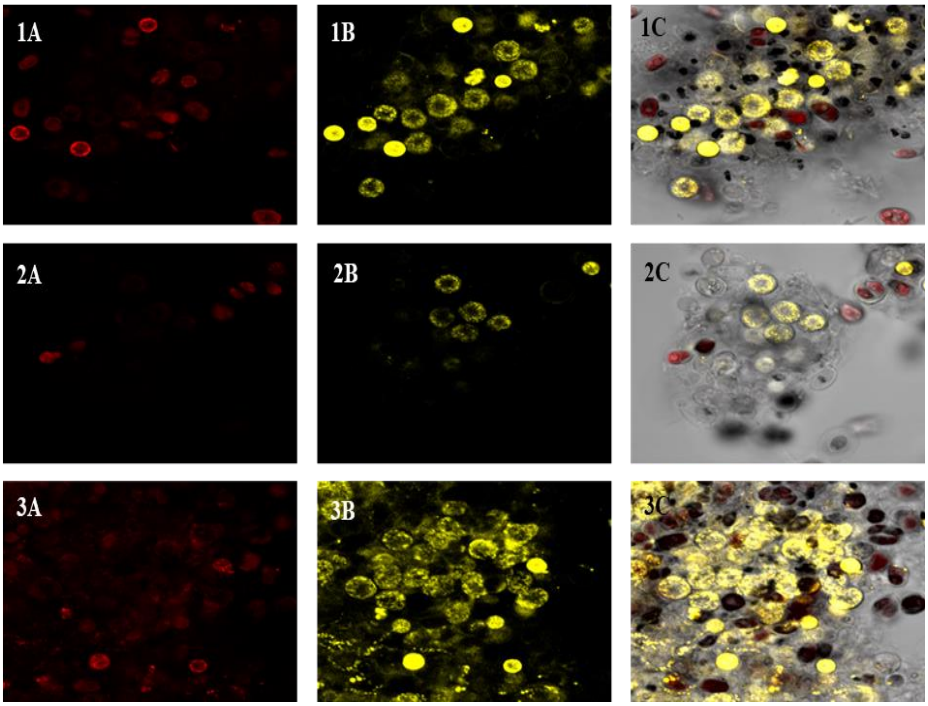

Figure 5.6: Neutral lipids under confocal microscopy at (1) $H_{10}N_{17.64}P_0$ (2) $H_0N_{17.64}P_0$ and (3) $H_{10}N_0P_{0.22}$, where A: Autofluorescence; B: Nile red-stained neutral lipid; and C: Merged image of A and B

5.3.1.5 Morphological changes under stress through scanning electron microscopy (SEM)

The same samples observed for lipid bodies under confocal microscopy were also examined through SEM to study the morphological changes occurring in the cells under combined oxidative and nutrient stress. The withered or dehydrated appearance of cells, depicted by the presence of uneven grooves (Figure 5.7) gave an indication that cells have been under stress conditions, which has led to morphological changes in cells along with the complete distortion of some cells. As evident from Figure 5.6, cells appear to be diffused due to stress. Thus, it can be suggested that under numerous environmental perturbations, *Scenedesmus* sp., survive by adapting itself in terms of physiological, morphological and regenerative functions.

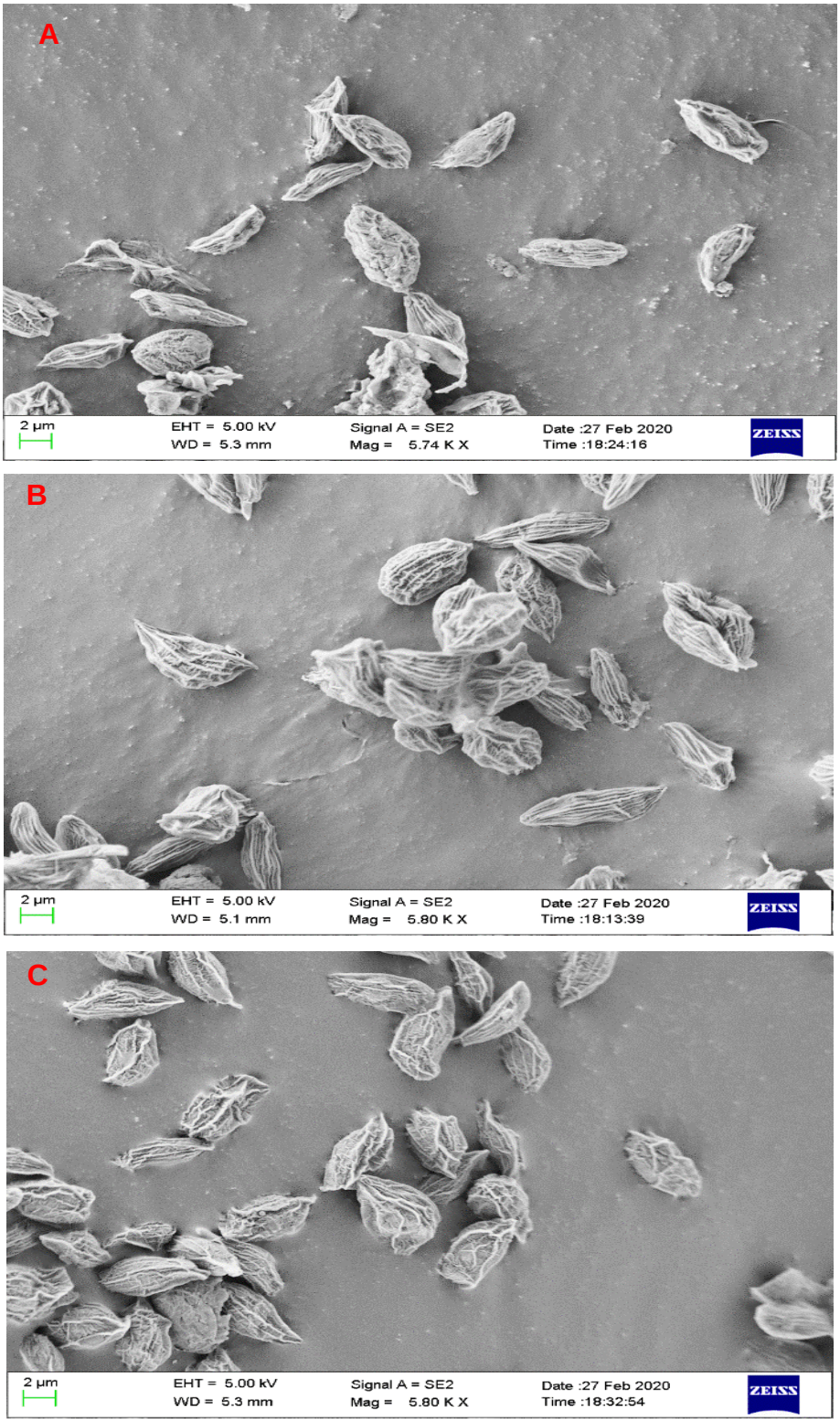

Figure 5.7: Scanning Electron Microscopy images of *Scenedesmus* sp. cells exposed to (A) $H_{10}N_{17.64}P_0$, (B) $H_0N_{17.64}P_0$ and (C) $H_{10}N_0P_{0.22}$

5.3.1.6 FAME profiling

The comparative percentage of fatty acids in *Scenedesmus* sp. exposed to the multicomponent environment of nitrate, phosphate, and hydrogen peroxide has been represented in Figure 5.8. The information gathered from Figure 5.8 indicates that oxidative stress induced by hydrogen peroxide causes tremendous deviations in the fatty acid symphony of *Scenedesmus* sp. Palmitic acid (C16:0) and oleic acid (C18:1n9c) were the dominant fatty acids observed in *Scenedesmus* sp. Furthermore, maximum C16:0 was obtained for $H_0N_0P_0$ (24%), closely followed by $H_{10}N_0P_0$ (23.2%) and $H_{10}N_0P_{0.22}$ (23.4%). Polyunsaturated fatty acid (PUFA) content was found to get decreased in the cells exposed to media deprived of sodium nitrate and dipotassium hydrogen phosphate under high hydrogen peroxide exposure. On the other hand, total FAME content obtained was maximum for $H_0N_{17.64}P_0$ (64.04 µg/mg), followed by $H_0N_0P_{0.22}$ (61.70 µg/mg). The accumulation of high neutral lipids or TAGs can be explained as cell's dynamic vibe for efficient energy storage in order to avoid oxidative cellular damage under ominous conditions (Miao and Wu, 2006).

Amongst various biodiesel properties-this study focused on empirically quantifying some important properties such as CN, IV, saponification value, and degree of unsaturation. Our results indicate that for all the combinations except $H_0N_{17.64}P_0$, CN values are in between 50 to 51 whereas for $H_0N_{17.64}P_0$, it is 53.5. The significance of cetane number (CN) lies in the perspective that it determines the fuel ignition delay time symbolizing the combustibility of biodiesel. (Knothe, 2005). According to European standards (EN 14214), 51 is the minimum cetane value, whereas according to standards given by the American Society for Testing and Materials (ASTM) D675, the minimum value for CN is 47.

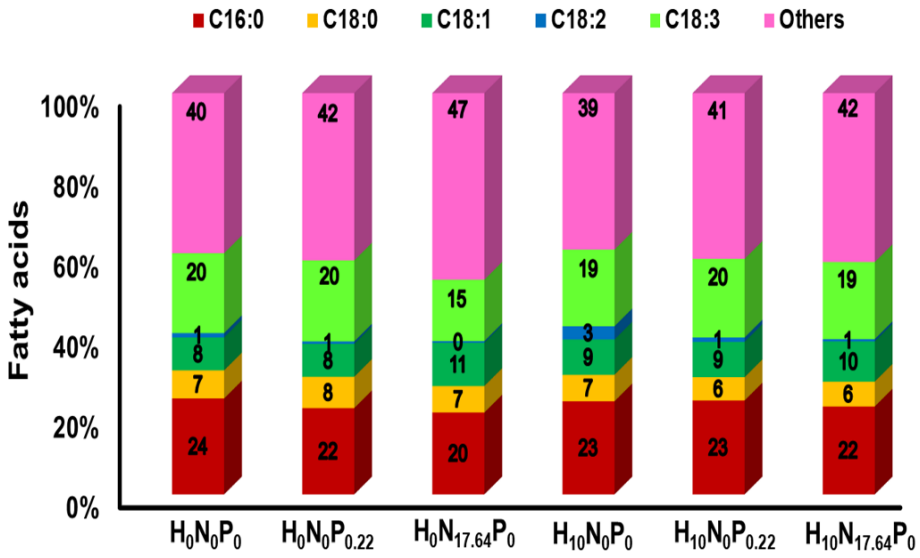

Figure 5.8: Fatty acid profile of *Scenedesmus* sp. exposed to hydrogen peroxide under varying nitrate and phosphate levels

On the other hand, the iodine value was found in the range of 60-70 gI_2/100g, which was lower than the value of sunflower oil (110–143 gI_2/100g) and soybean oil (120–141 gI_2/100g). However, for $H_0N_{17.64}P_0$, the iodine value was calculated to be 46.76 gI_2/100g, which was lower than that of palm oil (48-56 gI_2/100g), showing the least effect on oxidation. As per European standards, the maximum acceptable value for IV is 120 gI_2/100g. Since the iodine value was less than 120 gI_2/100g, which indicates that biodiesel obtained from *Scenedesmus* sp. is less susceptible to oxidation reaction. In support of this data, a high level of saturated fatty acids (SFA) was obtained in $H_0N_0P_0$ (61.2%). However, $H_{10}N_0P_{0.22}$ (60.1%) and $H_{10}N_{17.64}P_0$ (60.1%) were observed with a similar amount of SFA. Beside CN and IV value SV values obtained are also significant and lies in between 185-188 mg/KOH/goil, however, the saponification value of $H_0N_0P_{0.22}$ (88.5 mg/KOH/goil) was observed to be least. Therefore, as compared to ASTM-D675 or ES-14214 standards, the treatments mentioned above were observed to exhibit better values of biodiesel properties.

5.3.1.7 ROS content and response of cellular antioxidants

The effect of hydrogen peroxide on the oxidative defense system of *Scenedesmus* sp. was studied via estimating the concentration of ROS in addition to activities of antioxidant enzymes. Hydrogen peroxide (H_2O_2), peroxyl radicals (LOO·), superoxide anion (O_2^-), lipid hydroperoxides (LOOH), hydroxyl radical (·OH), and singlet oxygen ($O^{\cdot}$) are some of the reactive oxygen species generated in algal cells under stressed conditions (Zhang et al., 2017). The levels of H_2O_2 (Figure 5.9) and antioxidant enzyme system have been represented in Table 5.3.

Table 5.3: Antioxidative enzyme analysis in *Scenedesmus* sp. exposed to hydrogen peroxide under varying nitrate and phosphate levels

Samples	**SOD (U/ml)**	**CAT (nmol/ml/min)**
$H_0N_0P_0$	49.3±0.2	239.7±14.8
$H_0N_0P_{0.22}$	20.6±0.4	371.6±2.8
$H_0N_{17.64}P_0$	10.1±0.2	198.1±6.5
$H_{10}N_0P_0$	53.2±0.3	401.2±19.7
$H_{10}N_0P_{0.22}$	13.7±0.3	74.4±4.0
$H_{10}N_{17.64}P_0$	10.6±0.2	24.3±5.8

ROS was produced maximum at $H_{10}N_0P_0$, revealing that cells under this treatment experienced maximal stress, which was further supported by the highest levels of SOD and CAT activity. Therefore, the cells exposed to the maximum concentration of hydrogen peroxide under nitrate and phosphate deficient media ($H_{10}N_0P_0$) showed the highest level of stress. SOD acts as a primary obstruction to stress conditions by converting O_2^- to O_2 and thus initiates the production of H_2O_2. It was observed that the SOD activity of cells gets elevated due to stress imposed mainly due to nitrogen-deprived conditions, which was further enhanced with high H_2O_2 exposure. A similar trend was observed for CAT activity. This enhancement in SOD, CAT, and H_2O_2

levels was found to vary with exposure conditions, and therefore standard parameters cannot be set for varying treatments done. Every combination used in this study with varying levels of nitrate, phosphate, and H_2O_2 has different metabolic alterations leading to differences in activities of H_2O_2, SOD, and CAT. It has been observed that increased ROS levels lead to cells oxidative disruption, in turn hindering the algal growth, which eventually might affect the FAME profile, as explained in the next section.

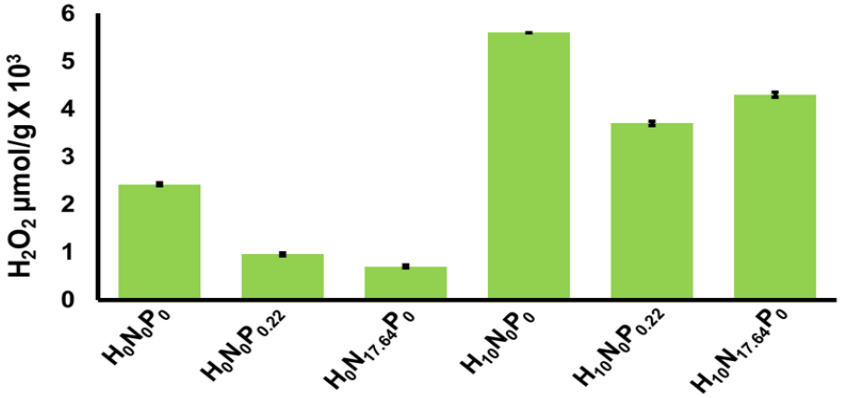

Figure 5.9: Reactive Oxygen species generation (H_2O_2) after exposure to varying levels of hydrogen peroxide, nitrate and phosphate

5.3.1.8 Principal component analysis (PCA)

PCA was executed to discern the treatment-variable relationship exhibited by the examined species. For the principal component analysis, the amounts of biomass, chlorophyll, total lipids, and total carbohydrate produced at different nitrate and phosphate levels under varying concentrations of hydrogen peroxide were taken into account.

Table 5.4: Eigen analysis of the correlation matrix.

Dimension	Eigen value	Variance (%)	Cumulative variance (%)
PC1	1.8	61.4	61.4
PC2	0.7	24.5	86.0
PC3	0.4	13.9	100

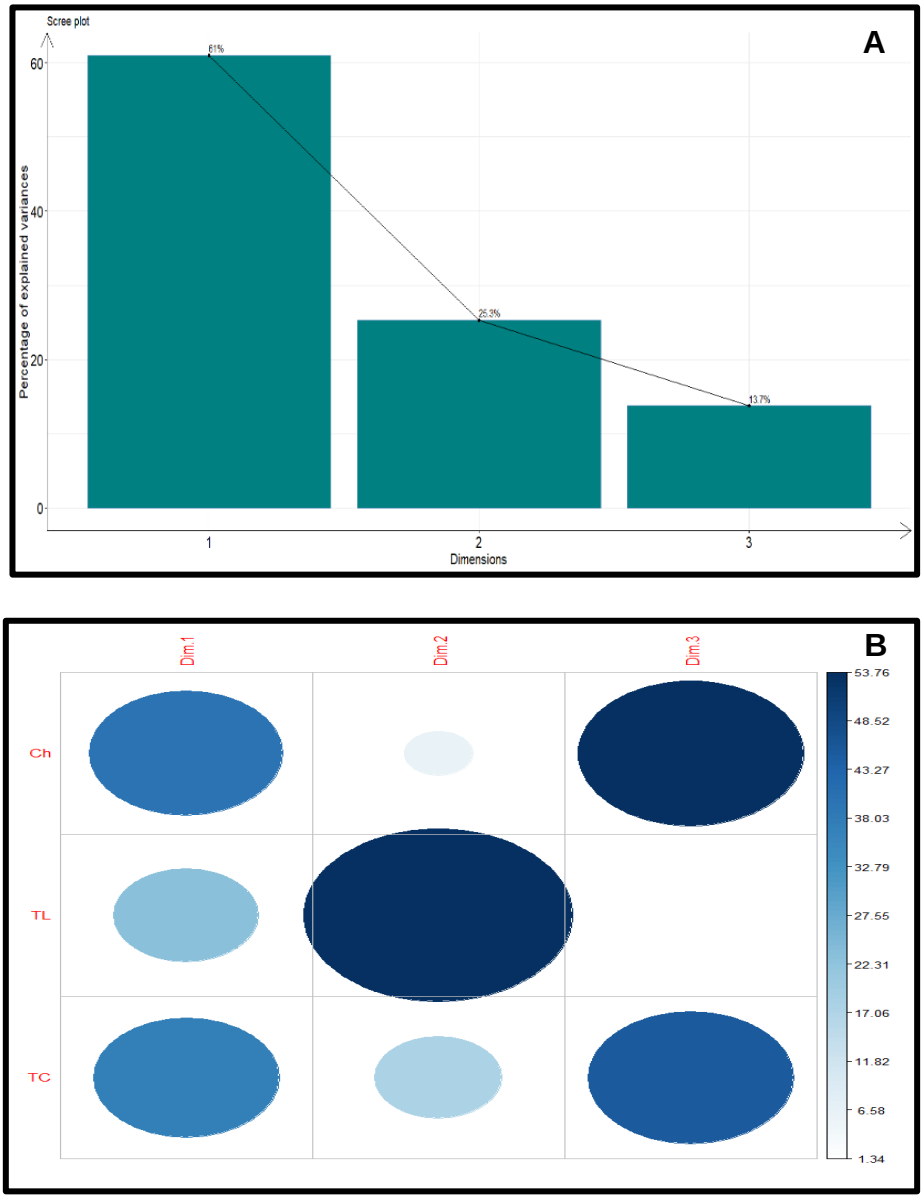

Figure 5.10: (A) Scree plot, a steep curve displays the magnitude of variation in each principal component captured from the data sets, where first PCs are explaining maximum variation (B) Individual contribution of different variables exposed to hydrogen peroxide at varying nutrients levels, explaining the variation of about 86 % variations

The scree plot (Figure 5.10A) depicted PC 1 with maximum variability (61%) and was followed by PC 2 (25.3%) and (13.7%). However, PC 2 represented the maximum contribution of total lipids

whereas PC 3 (Figure 5.10B) showed maximum contribution of chlorophyll followed by carbohydrates. Correlation matrix is represented in Table 5.4. Amongst various combinations $H_{10}N_0P_{0.22}$ and $H_6N_0P_{0.22}$ were observed to be the significant contributors to the variance, as shown in Figure 5.11(B).

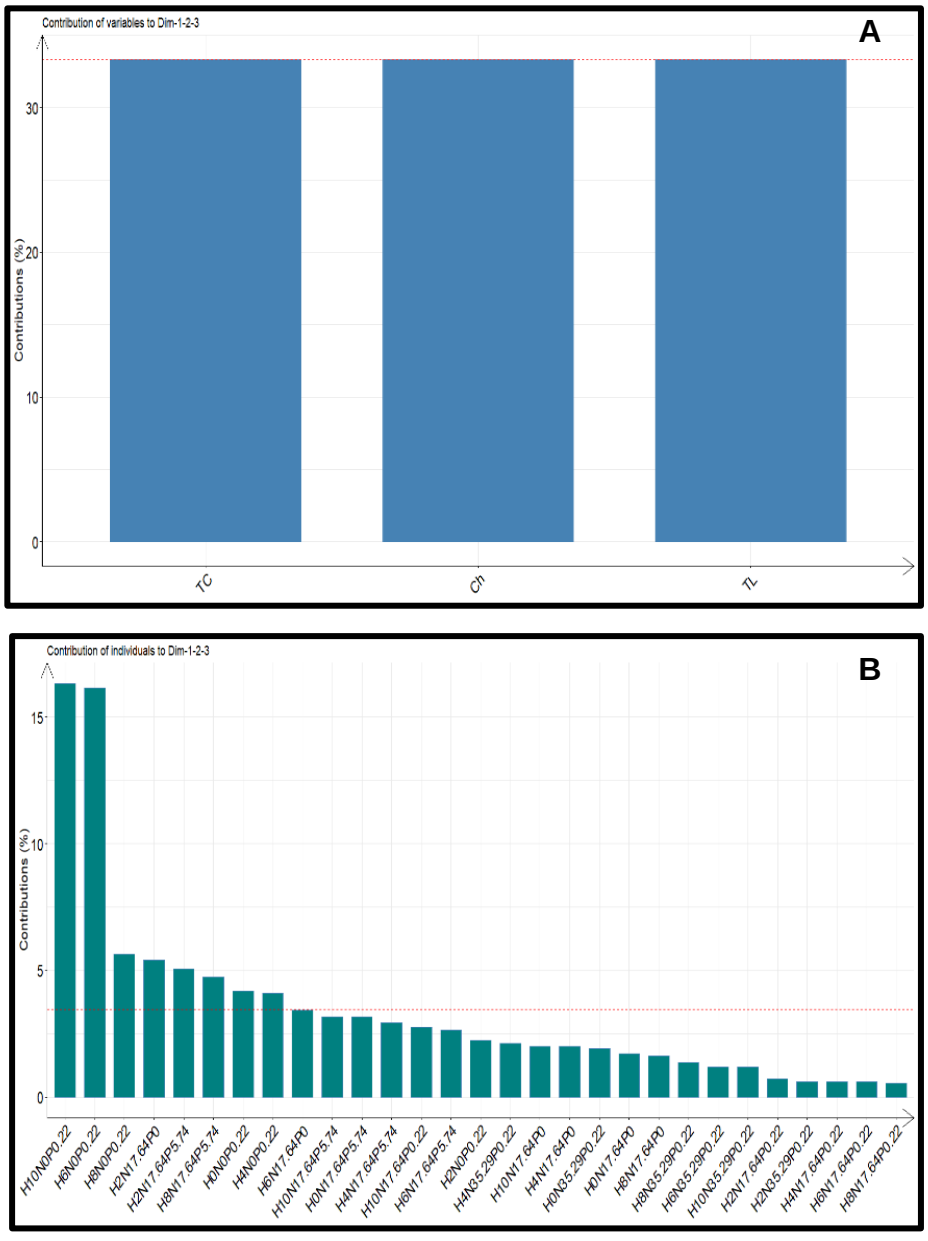

Figure 5.11: (A) Contribution of variables in first three dimensions, (B) Contribution of individual variable to various dimensions

5.4 Conclusions

Findings of the current study suggest hydrogen peroxide as an effective inducer of stress, which results into the enhancement of TAGs in *Scenedesmus* sp. Despite the algal growth inhibition due to application of various treatments, the percentage of C16:0 fatty acid content increased, and that of C18:3 fatty acid decreased concurrently. The results uncover the fact that under nitrogen ($H_{10}N_0P_{0.22}$) depleted culture conditions; the lipid production potential of unicellular green algal species increases explicitly. However, few studies have also revealed the physiological behavior of algae along with FAME content under the combined effect of nitrate, phosphate, and hydrogen peroxide. This study submits novel information endorsing the perspective of utilizing hydrogen peroxide under nutrient replete and depleted conditions and investigating the oxidative stress and FAME profile in context to biodiesel applications. As indicated by the analysis of biodiesel properties, the combined effect of nutrient deprivation and high hydrogen peroxide exposure has the potential to enhance the biodiesel quality making the commercialization more feasible. The same concentration of nitrate and phosphate from the previous chapter ($N_0P_{0.22}$) gave the maximum amount of lipid in combination with hydrogen peroxide.

However, lipid accumulation observed under long-term stress ($S_{100}N_0P_{0.22}$) was much higher as compared to the short-term stress ($H_{10}N_0P_{0.22}$). Since it was clear from previous chapter that the salt stress acted as a better stress inducer for lipid biosynthesis as compared to peroxide stress, therefore further investigation would be done to unravel the cumulative effect of hydrogen peroxide and sodium nitrate along with nitrate and phosphate variation on lipid accumulation potential of *Scenedesmus* sp.

References

Abo-Shady, A. M., El-Naggar, A. H., El-Sheekh, M. M., & Abomohra, A. E. F. (2008). Impact of UV-B radiation on antioxidant enzymes and protein electrophoretic pattern of the green alga *Chlorococcum* sp. Annals of Microbiology, 58(2), 195-201.

Anto, S., Pugazhendhi, A., & Mathimani, T. (2019). Lipid enhancement through nutrient starvation in *Chlorella* sp. and its fatty acid profiling for appropriate bioenergy feedstock. Biocatalysis and Agricultural Biotechnology, 20, 101179.

Arnon, D. I. (1949). Copper enzymes in isolated chloroplasts. Polyphenoloxidase in *Beta vulgaris*. Plant Physiology, 24(1), 1.

Barrington, D. J., & Ghadouani, A. (2008). Application of hydrogen peroxide for the removal of toxic cyanobacteria and other phytoplankton from wastewater. Environmental Science & Technology, 42(23), 8916-8921.

Battah, M., El-Ayoty, Y., Abomohra, A. E. F., Abd El-Ghany, S., & Esmael, A. (2015). Effect of Mn^{2+}, Co^{2+} and H_2O_2 on biomass and lipids of the green microalga *Chlorella vulgaris* as a potential candidate for biodiesel production. Annals of Microbiology, 65(1), 155-162.

Cao, J., Yuan, H., Li, B., & Yang, J. (2014). Significance evaluation of the effects of environmental factors on the lipid accumulation of *Chlorella minutissima* UTEX 2341 under low-nutrition heterotrophic condition. Bioresource Technology, 152, 177-184.

Chen, B., Wan, C., Mehmood, M. A., Chang, J. S., Bai, F., & Zhao, X. (2017). Manipulating environmental stresses and stress tolerance of microalgae for enhanced production of lipids and value-added products–a review. Bioresource Technology, 244, 1198-1206.

Coesel, S. N., Baumgartner, A. C., Teles, L. M., Ramos, A. A., Henriques, N. M., Cancela, L., & Varela, J. C. S. (2008). Nutrient limitation is the main regulatory factor for carotenoid accumulation

and for Psy and Pds steady state transcript levels in *Dunaliella salina* (Chlorophyta) exposed to high light and salt stress. Marine Biotechnology, 10(5), 602-611.

Dean, A. P., Sigee, D. C., Estrada, B., & Pittman, J. K. (2010). Using FTIR spectroscopy for rapid determination of lipid accumulation in response to nitrogen limitation in freshwater microalgae. Bioresource Technology, 101(12), 4499–4507.

Drábková, M., Admiraal, W., & Maršálek, B. (2007). Combined exposure to hydrogen peroxide and light selective effects on cyanobacteria, green algae, and diatoms. Environmental Science & Technology, 41(1), 309-314.

Grace, C. E. E., Lakshmi, P. K., Meenakshi, S., Vaidyanathan, S., Srisudha, S., & Mary, M. B. (2020). Biomolecular transitions and lipid accumulation in green microalgae monitored by FTIR and Raman analysis. Spectrochimica Acta Part A: Molecular and Biomolecular Spectroscopy, 224, 117382.

Halliwell, B., & Gutteridge, J. (1984). Oxygen toxicity, oxygen radicals, transition metals and disease. Biochemical Journal, 219(1), 1.

Hu, Q., Sommerfeld, M., Jarvis, E., Ghirardi, M., Posewitz, M., Seibert, M., & Darzins, A. (2008). Microalgal triacylglycerols as feedstocks for biofuel production: perspectives and advances. The Plant Journal: for Cell and Molecular Biology, 54(4), 621–639.

Kassambara, A., & Mundt, F. (2017). Factoextra: extract and visualize the results of multivariate data analyses. R package version, 1(5), 337-354.

Knothe, G. (2005). Dependence of biodiesel fuel properties on the structure of fatty acid alkyl esters. Fuel Processing Technology, 86(10), 1059-1070.

Lê, S., Josse, J., & Mazet, F. (2008). Package 'FactoMineR. J Stat Softw [Internet], 25(1), 1-18.

Liang, K., Zhang, Q., Gu, M., & Cong, W. (2013). Effect of phosphorus on lipid accumulation in freshwater microalga *Chlorella* sp. Journal of Applied Phycology, 25(1), 311-318.

Mahajan, S., & Tuteja, N. (2005). Cold, salinity and drought stresses: an overview. Archives of Biochemistry and Biophysics, 444(2), 139-158.

Miao, X., & Wu, Q. (2006). Biodiesel production from heterotrophic microalgal oil. Bioresource Technology, 97(6), 841-846.

Mishra, S. K., Suh, W. I., Farooq, W., Moon, M., Shrivastav, A., Park, M. S., & Yang, J. W. (2014). Rapid quantification of microalgal lipids in aqueous medium by a simple colorimetric method. Bioresource Technology, 155, 330-333.

Ramya, A. N., Ambily, P. S., Sujitha, B. S., Arumugam, M., & Maiti, K. K. (2017). Single cell lipid profiling of *Scenedesmus quadricauda* CASA-CC202 under nitrogen starved condition by surface enhanced Raman scattering (SERS) fingerprinting. Algal Research, 25, 200-206.

Ríos, S. D., Castañeda, J., Torras, C., Farriol, X., & Salvadó, J. (2013). Lipid extraction methods from microalgal biomass harvested by two different paths: Screening studies toward biodiesel production. Bioresource Technology, 133, 378-388.

Roe, J. H. (1955). The determination of sugar in blood and spinal fluid with anthrone reagent. Journal of Biological Chemistry, 212, 335-343.

Rosenwasser, S., van Creveld, S. G., Schatz, D., Malitsky, S., Tzfadia, O., Aharoni, A., ... & Vardi, A. (2014). Mapping the diatom redox-sensitive proteome provides insight into response to nitrogen stress in the marine environment. Proceedings of the National Academy of Sciences, 111(7), 2740-2745.

Sarno, D., Kooistra, W. H., Balzano, S., Hargraves, P. E., & Zingone, A. (2007). Diversity in the genus *Skeletonema* (Bacillariophyceae): III. Phylogenetic position and morphological variability of *Skeletonema costatum* and *Skeletonema grevillei*, with the description of

Skeletonema ardens sp. NOV. 1. Journal of Phycology, 43(1), 156-170.

Su, S., Zhou, Y., Qin, J. G., Yao, W., & Ma, Z. (2010). Optimization of the method for chlorophyll extraction in aquatic plants. Journal of Freshwater Ecology, 25(4), 531-538.

Tan, K. W. M., & Lee, Y. K. (2016). The dilemma for lipid productivity in green microalgae: importance of substrate provision in improving oil yield without sacrificing growth. Biotechnology for Biofuels, 9(1), 1-14.

Velikova, V., Yordanov, I., & Edreva, A. (2000). Oxidative stress and some antioxidant systems in acid rain-treated bean plants: protective role of exogenous polyamines. Plant Science, 151(1), 59-66.

Vincent, Q.V., (2011). GitHub - vqv/ggbiplot: A biplot based on ggplot2. https://github.com/vqv/ggbiplot. Accessed 23 Jul 2020.

Wickham, H., & Chang, W. (2019). devtools: Tools to make developing R packages easier, 2016. URL https://CRAN. R-project. org/package= devtools. R package version, 1(0), 103.

Yilancioglu, K., Cokol, M., Pastirmaci, I., Erman, B., & Cetiner, S. (2014). Oxidative stress is a mediator for increased lipid accumulation in a newly isolated *Dunaliella salina* strain. PLoS One, 9(3), e91957.

Zhang, J., Hao, H., Chen, M., Wang, H., Feng, Z., & Chen, H. (2017). Hydrogen-rich water alleviates the toxicities of different stresses to mycelial growth in *Hypsizygus marmoreus*. AMB Express, 7(1), 1-11.

Zuppini, A., Gerotto, C., & Baldan, B. (2010). Programmed cell death and adaptation: two different types of abiotic stress response in a unicellular chlorophyte. Plant and Cell Physiology, 51(6), 884-895.

CHAPTER 6

Chapter 6

Multicomponent exposure – Impact of hydrogen peroxide, sodium chloride, nitrate and phosphate on algal profile in two stage process

6.1 Introduction

Synergising the augmented algal biomass productivity and enhanced lipid concentration is the need of the hour to commercialise algal biofuels. All the perturbations explored to enhance lipids, are reported to minimise biomass productivity, implicating a slower growth rate and reduced oil yields due to curtailed photosynthetic proficiency. A recent two-staged microalgae cultivation methodology corresponding to the supplementation of growth media with high amount of nitrogen in the first stage followed by a nitrogen-deprived medium in the second stage is on the verge of replacing the intermediate nitrogen concentration supplementation method. In two-stage cultivation, several microalgal strains have exhibited the trend of high lipid content and insignificant biomass loss at the first stage, followed by a conjoint increment in both biomasses as well the lipid concentration in the second stage (Chen et al., 2011).

Furthermore, the induction of H_2O_2 for incrementing lipid synthesis has also been the topic of interest. H_2O_2 has been illustrated to impact the regulation of prime posttranslational proteins that are responsible for the accumulation of lipid and assimilation of nitrogen (Rosenwasser et al., 2014). However, the presence of high amount of hydrogen peroxide tend to enhance the ROS production, which eventually lead to lipid peroxidation and reduced lipid content (Zhang et al., 2017). Meanwhile, when synergistic effect of salt and hydrogen peroxide is considered, then it has been observed by the researchers that the lipid accumulation and biomass content in that condition has been

regulated by the involvement of ROS signalling as well as intracellular Ca^{2+} pathways. The crosstalk between these two pathways has been proven to take place by the modulation of expression level of MAPK and GSH content, while regulating the biosynthesis of lipid and growth of cell, simultaneously (Zhao et al., 2019). It has been reported further that the involvement of MAPK pathway in the production of algal lipids under the impact of abiotic stress, might be possible due to the augmented expression of MAPK pathway, after the induction of H_2O_2 in the salt-treated environment. Stress instigated activation of MAPK pathway can lead to the phosphorylation of proteins related to stress for the stimulation of cells response in opposition to stress, which might cause the production of various secondary metabolites (Sinha et al., 2011).

A growth media composition comprising of sodium nitrate ($NaNO_3$), dipotassium hydrogen phosphate (K_2HPO_4), and sodium chloride (NaCl) in different proportions were formulated in this study to obtain a modified culture medium for the growth of *Scenedesmus* sp. In this modified medium, cells were grown for 48 hours, followed by induction of hydrogen peroxide (H_2O_2) for 24 hours, intended to increase lipid accumulation and biomass simultaneously. This study significantly highlights the conjunct impact of multiple stress factors such as nutrient, salt, and hydrogen peroxide in varying concentrations, so as to accentuate both algal biomass and lipid profile.

6.2 Materials and Methods

6.2.1 Experimental methodology

Scenedesmus sp. was exposed for 48 hours to modified media (BG-11) composed of different concentrations of $NaNO_3$ (0, 17.64, and 35.2 9 mM; represented as N_0, $N_{17.64}$, and $N_{35.29}$), K_2HPO_4 (0, 0.22, and 5.74 mM designated as P_0, $P_{0.22}$, and $P_{5.74}$) and NaCl (0 and 100 mM represented as S_0 and S_{100}) in various combinations. Subsequently, after 48 hours, cells were exposed to H_2O_2 (0 and 10 mM designated as H_0 and H_{10}) for about 24 hours in the second phase, and eventually followed by

performing various biochemical analyses. All the analysis was done in triplicates (Figure 6.1).

6.2.2 Growth profile and chlorophyll estimation

The growth of algal cells exposed to hydrogen peroxide for the period of 24 hours preceded by the treatment of $NaNO_3$/K_2HPO_4/NaCl repleted and/ depleted conditions were investigated by recording the optical density (OD) at 680 nm using a Hach spectrophotometer and the amount of biomass was computed using a standard calibration curve plotted between OD vs. DCW (Dry cell weight) (R^2=0.99). Simultaneously, the chlorophyll accumulation was also monitored by taking the absorbance of the supernatant at 645 and 663 nm, followed by its computation as per the equation given in chapter 2 (Su et al., 2010; Arnon, 1949).

6.2.3 Lipid and carbohydrate estimation by SPV and anthrone assay

Colorimetric assays were adopted for the estimation of the lipid and carbohydrate content of the algae. Sulpho-Phospho-Vanillin (SPV) method described by Mishra et al., 2014 and Anthrone method illustrated by Roe et al., 1955 were utilized for colorimetric analysis of biochemical components such as lipid and carbohydrates. The content was further estimated empirically by considering a standard calibration curve (R^2 = 0.995).

6.2.4 FTIR micro-spectroscopy

The transition of biomolecules that have occurred inside the treated algal cells was studied by FTIR spectroscopy in the range of 400-4000 cm^{-1} while using dry biomass. The spectra obtained were processed by following the procedure discussed in chapter 2.

6.2.5 Observation of cell morphology

The morphological changes occurring due to multicomponent disquiet were visualized by the FE-SEM (Supra55 Zeiss) scanning

electron microscope, and the samples were prepared by fixing the algal cells in 37% formaldehyde (Sarno et al., 2007).

6.2.6 Examination of fatty acids (FA) composition along with the illustration of biodiesel properties

The characterization of fatty acid methyl ester (FAME) composition was carried out by Gas Chromatography while following the procedures described in detail in chapter 2. The fatty acid composition thus obtained was used for the calculation of biodiesel properties.

6.2.7 Colorimetric analysis of ROS levels and antioxidative enzymes

The H_2O_2 production representing the levels of ROS in treated algae was measured via colorimetric assay (Velikova et a. 2000). The results obtained were utilized further for the expression of H_2O_2 in terms of µmol H_2O_2/g, calculated through a standard calibration curve of known concentrations of H_2O_2.

Likewise, the activity of enzymes SOD and CAT were also estimated after 72 hours of an experiment by taking into account the crude protein extract of selected species. In order to accomplish the enzyme activity analysis of CAT and SOD, instructions given by respective enzyme analysis kits were followed.

6.2.8 Statistical Analysis using R studio

Principal component analysis (PCA) was carried out with the aim of determining the maximum variance in the obtained data. Three dimensions/principal components were selected, based on the Kaiser Concept (Eigenvectors having more than 1), and the main contributing factors were determined with respect to the biomass parameters across different H_2O_2 combinations. PCA was carried out in R studio desktop version 4.0.0 embedded with varying packages of R, including 'factoextra' (Kassambara and Mundt, 2020), 'FactoMineR' (Lê et al.,

2008), ‘devtools’ (Wickham, and Chang, 2019), and ‘ggbiplot’ (Vincent, 2011).

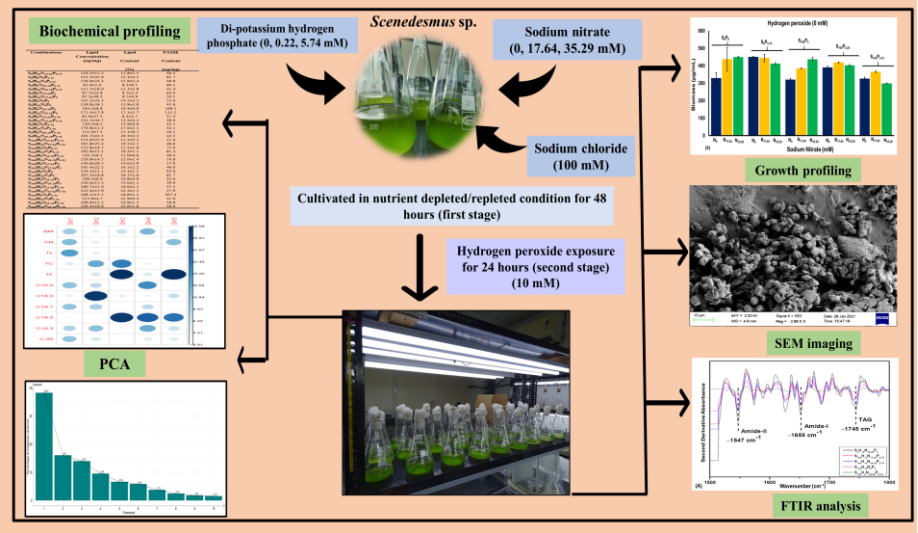

Figure 6.1: Multicomponent stress on *Scenedesmus* sp. and its analysis

6.3 Results and Discussion

6.3.1 Assessment of factors affecting biomass, chlorophyll and carbohydrate content

Microalgal development is reliant on a sufficient supply of macronutrients, primarily phosphorus and nitrogen, as well as other micronutrients including iron and manganese. Nitrogen and phosphorus are the main elements that make up the structure of biological macromolecules such as DNA, RNA, protein, and chlorophyll. As a result, stress caused by excessive nutrient uptake or deficiency has been shown to positively affect microalgal cellular physiology, which can negatively impact microalgal development (Benavente-Valdés et al., 2016; Ördög et al., 2012). *Scenedesmus* sp. can survive in a wide range of growth media composition, as shown in Figure 6.2A and 6.2B, which depicts the biomass accumulation under various combinations of nitrogen and phosphorus. Nutrient variation is further integrated with salinity and oxidative stress. For a better assessment of our results, we have grouped the experimentation into two parts.

The first part characterizes the impact of varying $NaNO_3$, K_2HPO_4 and NaCl concentrations on *Scenedesmus* sp. after 72 hours without exposure to H_2O_2 (0 mM). Thereby, the cell growth was discovered to be highest in $S_0H_0N_0P_{5.74}$ (451.0±3.0 µg/mL) followed by $S_0H_0N_{35.29}P_0$ (449.5±4.1 µg/mL) and $S_0H_0N_{17.64}P_{5.74}$ (444.6±21.2 µg/mL) (Figure 6.2A). It was observed that under oxidative stress, biomass symbolising growth declined because of critically affected metabolic activity, in response to numerous physiological and biological mechanisms relating to its growth.

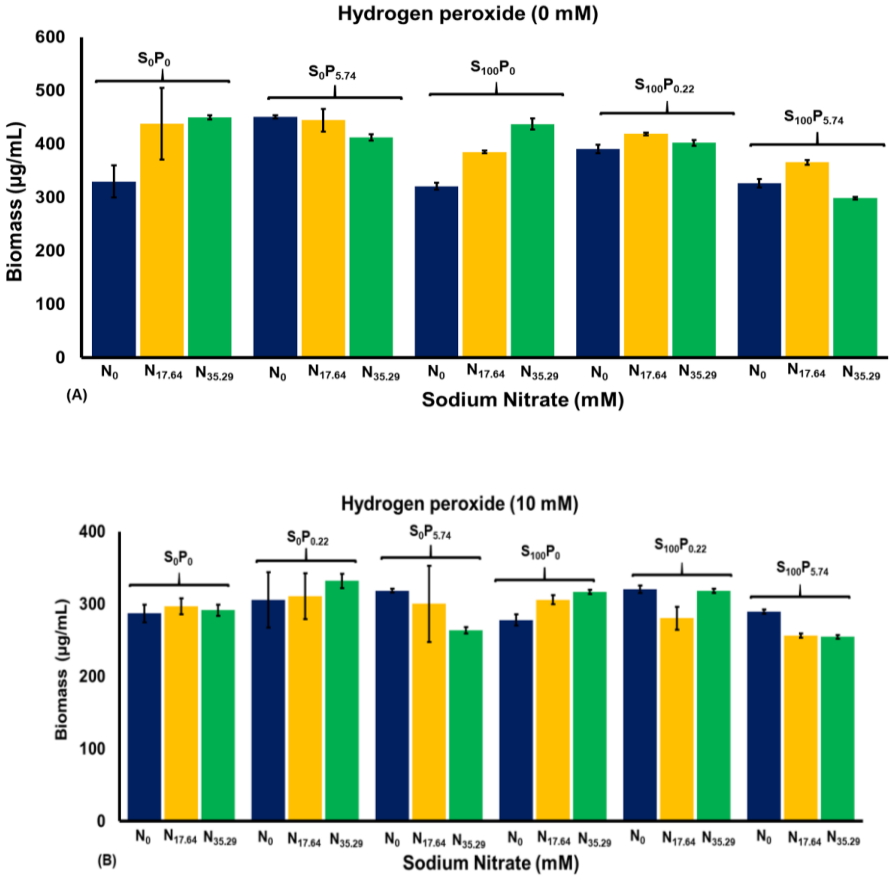

Figure 6.2: Biomass accumulation in *Scenedesmus* sp. under varying levels of salt, nitrate and phosphate (first stage) in the (A) absence and (B) presence of hydrogen peroxide (second stage)

In the second part (Figure 6.2B), the previous combinations cultivated for 48 hours with varying $NaNO_3$, K_2HPO_4 and NaCl were monitored after 24 hours exposure to varying H_2O_2 levels, which eventually led to the decrease in biomass (Figure 6.2B) by 1.4-fold

($S_0H_{10}N_0P_{5.74}$, 318.2±2.5 µg/mL); 1.5-fold ($S_0H_{10}N_{35.29}P_0$, 291.5±7.6 µg/mL), and 1.4-fold ($S_0H_{10}N_{17.64}P_{5.74}$, 300.4±52.5 µg/mL). The detailed accumulation of biomass at various combinations can be observed in Table 6.1. It was observed that when *Scenedesmus* sp. was cultivated in media composed of 10 mM H_2O_2 at all SNP (i.e., salt-nitrate-phosphate) combinations as well as in the presence of 100 mM NaCl at all HNP (i.e., hydrogen peroxide-nitrate-phosphate) combinations, exhibited a decrease in biomass and chlorophyll content after 72 hours of cultivation as compared to the media deprived of H_2O_2 and NaCl. While under maximal nutrient stress, the rapid consumption of nutrients by the growing algal cells results in nutrient deficiency in the culture conditions, which ultimately affects the growth of cells and biomass accumulation as a whole (Flynn, 1990; Wickham et al., 2019). An optimal ratio of nitrogen and phosphorous concentrations has been essential for the adequate growth and improved metabolism of algal cells. The organism's metabolic pathway gets affected by the stress-induced via nutrient starvation, which in turn leads to the neutral lipid and membrane lipid synthesis.

Chlorophyll ‘a’ (Table 6.1) content was observed following a similar trend as that of biomass accumulation. Maximum chlorophyll content (Figure 6.2A) was fetched for $S_0H_0N_{17.64}P_{5.74}$ (6.8±0.7 µg/mL) followed by $S_0H_0N_{17.64}P_0$ (6.6±1.7 µg/mL). Therefore, we can conclude that biomass accumulation and chlorophyll ‘a’ content seems directly synchronised to each other and to fetch higher chlorophyll ‘a’ content, biomass accumulation needs to be ameliorated. $S_{100}H_0N_{35.29}P_{0.22}$ (2.4±0.2 µg/mL) had the lowest chlorophyll ‘a', followed by $S_0H_0N_{35.29}P_{5.74}$ (2.7±0.5 µg/mL) and $S_{100}H_0N_{35.29}P_{5.74}$ (2.7±0.5 µg/mL).

In the second set (Figure 6.3B), chlorophyll ‘a’ content of the above-represented combinations was found to decrease further upon treatment with hydrogen peroxide. The decrease in chlorophyll ‘a’ content by 1.1-fold was observed for $S_0H_{10}N_{17.64}P_{5.74}$ (5.7±1.2 µg/mL), which further got reduced to 2-fold with the involvement of NaCl ($S_{100}H_{10}N_{17.64}P_{5.74}$, 3.4±0.2 µg/mL). A similar trend was observed when

cells were treated with $H_{10}N_{17.64}P_0$ in the absence of NaCl i.e., 1.6-fold decrease ($S_0H_{10}N_{17.64}P_0$, 4.0±0.1 µg/mL) and in the presence of NaCl, 3.0-fold ($S_{100}H_{10}N_{17.64}P_0$, 2.1±0.1 µg/mL) decrease was observed. Like biomass, chlorophyll 'a' content too decreased upon treatment with H_2O_2 at all varying combination of SNP (salt, nitrate and phosphate), and similarly, addition of NaCl (100 mM) at varying HNP (hydrogen peroxide, sodium nitrate and dipotassium hydrogen phosphate) too reduced the chlorophyll 'a' content. Thus, we can conclude that NaCl (100 mM) or H_2O_2 (10 mM) supplementation effectuates reduced biomass and chlorophyll accumulation under varying nitrogen and phosphorus combination.

Table 6.1: Biomass, chlorophyll ‘a’ and carbohydrates in *Scenedesmus* sp. exposed hydrogen peroxide (second stage) at varying nitrate, phosphate and sodium chloride treatment (first stage)

Combinations	Biomass Concentration (µg/mL)	Chlorophyll ‘a’ Concentration (µg/mL)	Carbohydrate Concentration (µg/mg)	Carbohydrate Content (%)
$S_0H_{10}N_{17.64}P_{0.22}$	310.7±31.4	3.7±0.7	471.9±65.3	47.1±6.5
$S_0H_0N_0P_{0.22}$	412.6±18.2	5.1±0.4	535.3±291.7	53.5±29.1
$S_0H_{10}N_0P_{0.22}$	305.5±38.3	3.4±0.1	434.9±137.4	43.4±13.7
$S_0H_0N_{35.29}P_{0.22}$	447.2±22.4	6.4±0.7	425.6±103.5	42.5±10.3
$S_0H_{10}N_{35.29}P_{0.22}$	331.8±9.9	5.3±0.9	447.8±36.8	44.7±3.6
$S_0H_0N_{17.64}P_0$	438.0±66.9	6.6±1.9	340.2±63.9	34.0±6.3
$S_0H_{10}N_{17.64}P_0$	296.9±11.2	4.0±0.1	366.9±47.3	36.6±4.7
$S_0H_0N_0P_0$	329.9±29.9	5.1±0.6	435.1±177.9	43.5±17.7
$S_0H_{10}N_0P_0$	288.9±12.0	2.9±0.0	497.8±26.7	49.7±2.6
$S_0H_0N_{35.29}P_0$	449.5±4.1	4.2±0.1	435.8±9.8	43.5±0.9
$S_0H_{10}N_{35.29}P_0$	291.5±7.6	3.1±0.1	398.8±21.5	39.8±2.1
$S_0H_0N_{17.64}P_{5.74}$	444.6±21.2	6.8±0.7	315.1±10.6	31.5±1.0
$S_0H_{10}N_{17.64}P_{5.74}$	300.4±52.5	5.7±1.2	289.6±22.6	28.9±2.2
$S_0H_0N_0P_{5.74}$	451.0±3.0	4.6±0.3	402.0±18.9	40.2±1.8
$S_0H_{10}N_0P_{5.74}$	318.2±2.5	4.1±0.2	373.3±34.5	37.3±3.4
$S_0H_0N_{35.29}P_{5.74}$	411.9±5.9	2.7±0.5	352.4±25.4	35.2±2.5
$S_0H_{10}N_{35.29}P_{5.74}$	263.7±4.0	2.6±0.3	470.5±27.8	47.0±2.7
$S_{100}H_0N_{17.64}P_{0.22}$	419.1±2.4	3.6±0.3	373.5±25.9	37.3±2.5
$S_{100}H_{10}N_{17.64}P_{0.22}$	280.4±16.1	3.4±0.2	448.8±32.6	44.8±3.2
$S_{100}H_0N_0P_{0.22}$	390.8±8.0	3.7±0.1	589.8±17.2	58.9±1.7
$S_{100}H_{10}N_0P_{0.22}$	320.2±4.9	2.6±0.2	515.3±37.5	51.5±3.7
$S_{100}H_0N_{35.29}P_{0.22}$	402.1±5.1	2.4±0.2	422.2±14.0	42.2±1.4
$S_{100}H_{10}N_{35.29}P_{0.22}$	318.5±2.9	2.2±0.1	443.3±23.0	44.3±2.3
$S_{100}H_0N_{17.64}P_0$	384.9±2.4	3.3±0.1	512.9±31.2	51.2±3.1
$S_{100}H_{10}N_{17.64}P_0$	288.5±4.9	2.1±0.1	437.8±27.6	43.7±2.7
$S_{100}H_0N_0P_0$	321.1±6.4	3.0±0.1	590.1±45.9	59.0±4.5
$S_{100}H_{10}N_0P_0$	278.1±8.0	2.0±0.1	540.4±24.1	54.0±2.4
$S_{100}H_0N_{35.29}P_0$	437.3±10.6	3.2±0.1	479.0±37.1	47.9±3.7
$S_{100}H_{10}N_{35.29}P_0$	316.7±3.1	2.2±0.1	448.8±35.2	44.8±3.5
$S_{100}H_0N_{17.64}P_{5.74}$	365.5±4.2	2.9±0.2	440.1±24.6	44.0±2.4
$S_{100}H_{10}N_{17.64}P_{5.74}$	256.3±3.1	2.4±0.3	425.9±26.6	42.5±2.6
$S_{100}H_0N_0P_{5.74}$	326.8±7.7	3.1±0.1	582.8±28.5	58.2±2.8
$S_{100}H_{10}N_0P_{5.74}$	289.4±2.8	2.4±0.3	511.0±7.0	51.1±0.7
$S_{100}H_0N_{35.29}P_{5.74}$	298.6±2.5	3.2±0.1	588.3±23.7	58.8±2.3
$S_{100}H_{10}N_{35.29}P_{5.74}$	254.6±2.6	2.7±0.1	468.7±31.9	46.8±3.1

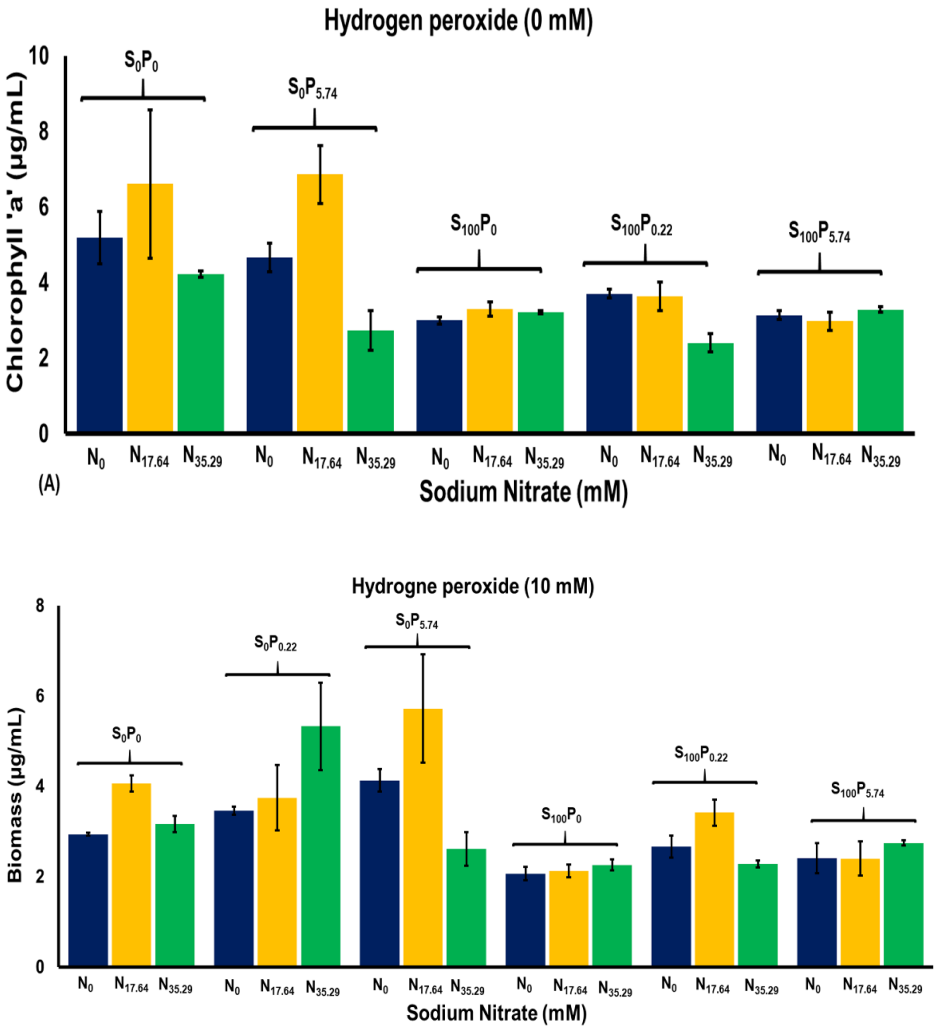

Figure 6.3: Chlorophyll accumulation in *Scenedesmus* sp. under varying levels of salt, nitrate and phosphate (first stage) in the (A) absence and (B) presence of hydrogen peroxide (second stage)

6.3.2 Total lipid and FAME content of Scenedesmus sp. under multi-component treatment

Salts play a crucial role in the growth of algal species, metabolism of fatty acid, and cell reproduction. Therefore, salinity exposure intertwined with nutrient stresses are amongst the highly adopted and economically feasible lipid enhancement strategies. Several studies are conducted on certain algal species to reduce the knowledge gap and understand the importance of salinity stress for an improved biochemical profile. Table 6.2 delineates the differential response of *Scenedesmus* sp. to the varying media composition in terms of lipid content and total FAME content.

It was interesting to observe that under higher concentration of NaCl, H_2O_2, $NaNO_3$ and K_2HPO_4, *Scenedesmus* sp. accumulated the highest amount of total lipids ($S_{100}H_{10}N_{35.29}P_{5.74}$, 226.4±16.6 µg/mg), whereas $S_{100}H_{10}N_{17.64}P_{5.74}$ (222.4±13.9 µg/mg) was identified as second-highest producer of total lipid. In the absence of $NaNO_3$, two combinations, $S_{100}H_{10}N_0P_{5.74}$ (213.9±4.7 µg/mg) and $S_{100}H_{10}N_0P_0$ (207.1±16.8 µg/mg), were fetched as the third and fourth level combinations for triggering lipid synthesis in *Scenedesmus* sp. Lipid accumulation was determined to increase with H_2O_2 (10 mM) addition at all varying SNP (salt-nitrate-phosphate) levels, and a similar trend was observed on the addition of NaCl (100 mM) at all levels of HNP. The cell membrane's structural composition has lipids as a prime component due to its storage property under nutritional shortage conditions. Under nutrient/salinity stress, the alternative metabolic pathways that fix inorganic carbon get activated to synthesise carbohydrates or lipids in microalgae (Deng et al., 2011; Pancha et al., 2014). These lipids are packed inside cell organelles in small quantities and utilised by the cell under an unfavourable environment for survival and other necessary metabolic processes (Courchesne et al., 2009). The genes that encode for enzymes involved in metabolic pathways (such as triacylglycerol biosynthesis by Kennedy pathway) of lipid synthesis show a higher range of transcription and becomes the basis for increased total lipid content (Deng et al., 2011; Weiss et al., 1960).

Table 6.2: Lipid and FAME content estimated in *Scenedesmus* sp. exposed hydrogen peroxide (second stage) at varying nitrate, phosphate and sodium chloride treatment (first stage)

Combinations	Lipid Concentration (µg/mg)	Lipid Content (%)	FAME Content (µg/mg)
$S_0H_{10}N_{17.64}P_{0.22}$	118.3±15.2	11.8±1.5	48.3
$S_0H_0N_0P_{0.22}$	121.5±45.8	12.1±4.5	61.7
$S_0H_{10}N_0P_{0.22}$	156.6±24.3	15.6±2.4	46.8
$S_0H_0N_{35.29}P_{0.22}$	81.0±5.0	8.1±0.5	60.2
$S_0H_{10}N_{35.29}P_{0.22}$	111.7±18.0	11.1±1.8	41.4
$S_0H_0N_{17.64}P_0$	87.7±24.8	8.7±2.4	64.0
$S_0H_{10}N_{17.64}P_0$	97.5±49.3	9.7±4.9	50.1
$S_0H_0N_0P_0$	145.2±33.3	14.5±3.3	55.6
$S_0H_{10}N_0P_0$	139.8±38.1	13.9±3.8	45.6
$S_0H_0N_{35.29}P_0$	104.5±8.8	10.4±0.8	166.1
$S_0H_{10}N_{35.29}P_0$	171.4±17.8	17.1±1.7	115.2
$S_0H_0N_{17.64}P_{5.74}$	81.9±27.3	8.1±2.7	37.4
$S_0H_{10}N_{17.64}P_{5.74}$	122.1±44.7	12.2±4.4	38.0
$S_0H_0N_0P_{5.74}$	139.4±6.2	13.9±0.6	42.5
$S_0H_{10}N_0P_{5.74}$	170.8±11.3	17.0±1.1	32.1
$S_0H_0N_{35.29}P_{5.74}$	111.0±7.3	11.1±0.7	56.1
$S_0H_{10}N_{35.29}P_{5.74}$	203.7±22.3	20.3±2.2	42.5
$S_{100}H_0N_{17.64}P_{0.22}$	113.6±25.0	11.3±2.5	51.6
$S_{100}H_{10}N_{17.64}P_{0.22}$	165.8±25.4	16.5±2.5	46.6
$S_{100}H_0N_0P_{0.22}$	155.8±16.7	15.5±1.6	75.9
$S_{100}H_{10}N_0P_{0.22}$	192.6±11.1	19.2±1.1	81.4
$S_{100}H_0N_{35.29}P_{0.22}$	120.5±8.3	12.0±0.8	49.4
$S_{100}H_{10}N_{35.29}P_{0.22}$	120.9±14.5	12.0±1.4	54.8
$S_{100}H_0N_{17.64}P_0$	140.6±28.5	14.0±2.8	57.8
$S_{100}H_{10}N_{17.64}P_0$	165.4±22.5	16.5±2.2	46.0
$S_{100}H_0N_0P_0$	144.3±11.1	14.4±1.1	63.0
$S_{100}H_{10}N_0P_0$	207.1±16.8	20.7±1.6	61.7
$S_{100}H_0N_{35.29}P_0$	108.3±8.0	10.8±0.8	32.6
$S_{100}H_{10}N_{35.29}P_0$	140.0±11.2	14.0±1.1	39.8
$S_{100}H_0N_{17.64}P_{5.74}$	180.7±21.0	18.0±2.1	47.3
$S_{100}H_{10}N_{17.64}P_{5.74}$	222.4±13.9	22.2±1.3	37.9
$S_{100}H_0N_0P_{5.74}$	166.1±11.5	16.6±1.1	207.4
$S_{100}H_{10}N_0P_{5.74}$	213.9±4.7	21.9±0.4	41.0
$S_{100}H_0N_{35.29}P_{5.74}$	169.6±11.2	16.9±1.1	38.8
$S_{100}H_{10}N_{35.29}P_{5.74}$	226.4±16.6	22.6±1.6	38.6

Photosystem II (PSII) is primarily impaired in green microalgae under nutrients/nitrogen stress conditions, which has a negative impact

on macromolecule synthesis, such as proteins involved in PSI and PSII. Besides this, such a starvation condition also crunches the production of photosynthetic pigments, such as carotenoids and chlorophyll (Berges et al., 1996). Actually, because of nitrogen deficiency, the flux of carbon that was set to be fixed photosynthetically is transformed to the lipid or carbohydrate synthesis metabolic pathway from that of protein synthesis metabolic pathway (Hu, 2004), resulting in the build-up of either carbohydrates or lipids. It was interesting to notice that the combination $S_{100}H_{10}N_{35.29}P_{5.74}$, (226.4±16.6 µg/mg) (Table 6.2) producing the maximum amount of total lipid, accumulate reduced carbohydrate content (468.7±31.9 µg/mg) (Table 6.1) in comparison to $S_{100}H_0N_0P_0$ (590.1±45.9 µg/mg) producing the maximum amount of carbohydrate. The same results were observed for the second-highest lipid producer, $S_{100}H_{10}N_{17.64}P_{5.74}$ (222.4±13.9 µg/mg), showing reduced-carbohydrate synthesis in comparison to the highest producer. The supplementation of NaCl (100 mM) at varying HNP levels also fetched significantly higher carbohydrate content. Therefore, we can culminate that lipid synthesis is preferably enhanced under multi-component stress conditions compared to other biochemical metabolites, such as carbohydrates, in *Scenedesmus* sp. The highest total FAME content (Table 6.2) was observed for $S_{100}H_0N_0P_{5.74}$ (207.4 µg/mg) and $S_0H_0N_{35.29}P_0$ (166.1 µg/mg) combinations, although the biomass content analysed for these combinations was not considerable, due to the absence of essential nutrient that is nitrate. However, the highest percentage of C16:0 (31.7%) and C18:3 (27.76%) (Table 3) was observed in the algal cells under $S_0H_{10}N_{35.29}P_0$ treatment, which was third-highest producer of total FAME (115.2 µg/mg).

6.3.3 Biomolecular insight study under 'Multi components' effect on Scenedesmus sp. *after 24hrs exposure to H_2O_2 on cells pre-cultvated in varying SNP for 48 hrs*

FTIR data delineates the accumulation of TAGs in the *Scenedesmus* sp. when exposed to varying nutrient levels along with hydrogen peroxide induction. The stretches depicted by the band

observed at 1746 cm^{-1} suggests the presence of TAGs in the cells exposed to multicomponent stress (Dean et al., 2010), and the maximum stretch was observed for $S_0H_{10}N_{35.29}P_0$ (Figure 6.4A), which was subsequently validated by TAGs: Amide I and TAGs: Amide II ratios (Figure 6.4A). The bands dedicated to protein and unsaturated lipids were spotted at 1546 cm^{-1} and 1652 cm^{-1}, respectively as shown in Figure 6.4A. Furthermore, the presence of TAGs, points towards the presence of neutral lipids and its strength varies as per the effect of various stress factors imposed on algal growth conditions. As reported by Grace et al. (2020), the aggregation of lipids in microalgae can be estimated via FTIR analysis. The band corresponding to the presence of υ (CH3) and υ (CH2) asymmetric and symmetric stretches of hydrocarbon were spotted in the region of 3050 to 2700 cm^{-1} (Figure 6.4B), respectively. The FTIR results obtained in the present study were in agreement with the previous studies performed, suggesting the accumulation of lipid under nutrient-depletion and oxidative stress exposure (Cao et al., 2014). Hence, in comparison to conventional colorimetric analysis, the practice of FTIR spectroscopy for investigating the deviations occurring in lipid and amide profile in response to different environmental conditions paved the way for non-invasive, innovative assessment techniques.

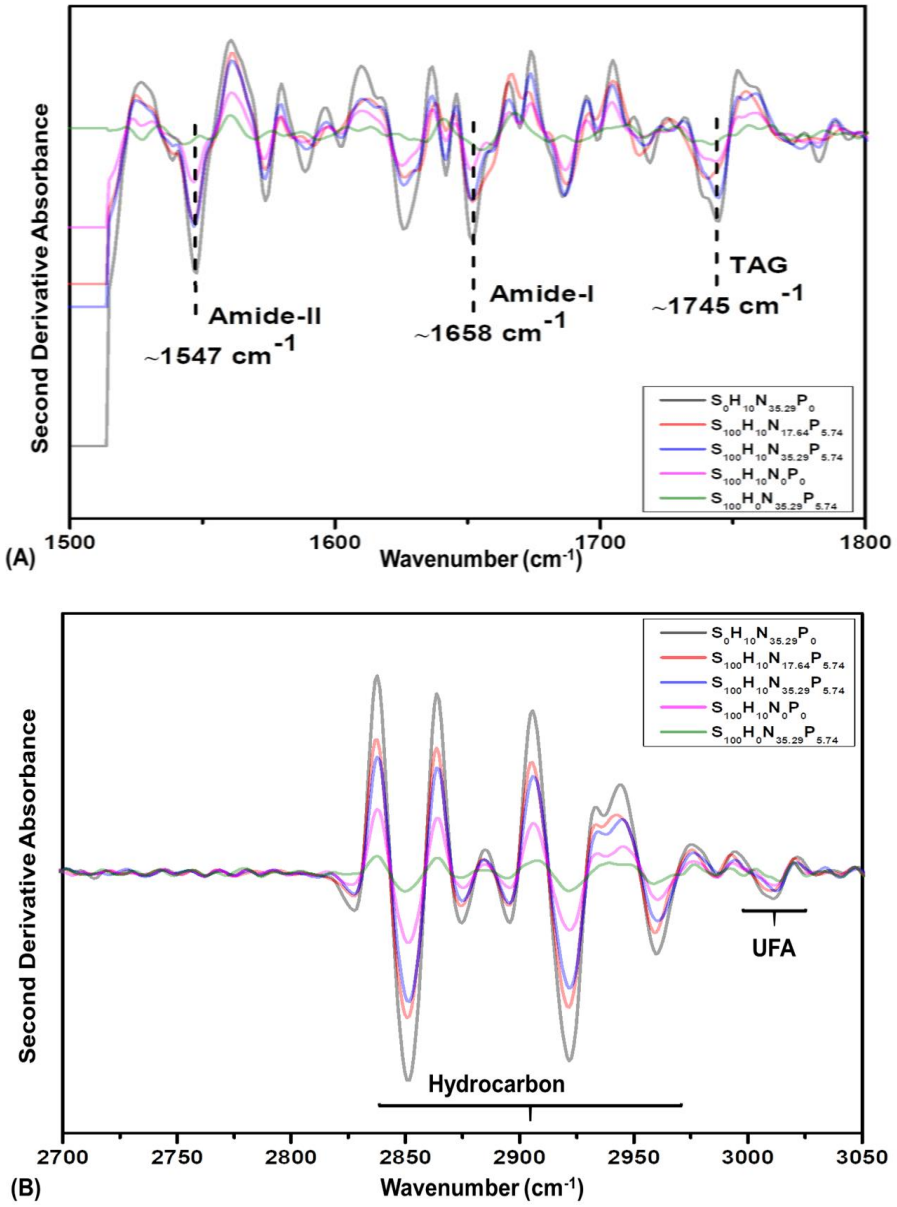

Figure 6.4: Second derivative spectra of lyophilized algal biomass between (A) 1800-1500 cm^{-1} and (B) 3050-2700 cm^{-1}

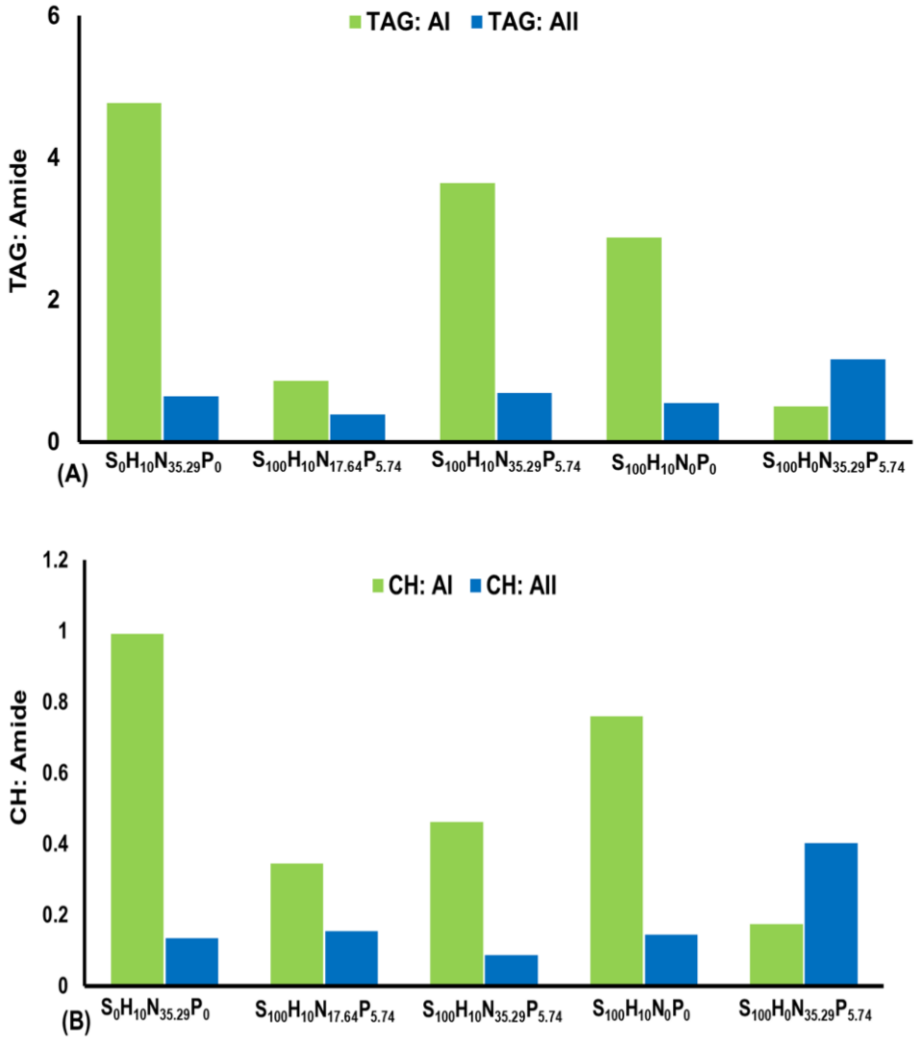

Figure 6.5: Relative content of (A) TAGs (Triacylglycerides) and (B) CH (Hydrocarbons) with respect to Amide I (AI) and Amide II (AII) of *Scenedesmus* sp.

6.3.4 Morphological changes under stress through scanning electron microscopy (SEM)

The imaging of morphological modifications that occurred on the cell surface via SEM illustrates that the cells are shrunk along with shifting of chambers in *Scenedesmus* sp. (Figure 6.6), implying the deformations and distortions that happened under the imposition of multi-component stress. SEM imaging results help in elucidating that the *Scenedesmus* sp. not only undergoes metabolic deviations but also get affected in morphology when exposed to stressed conditions.

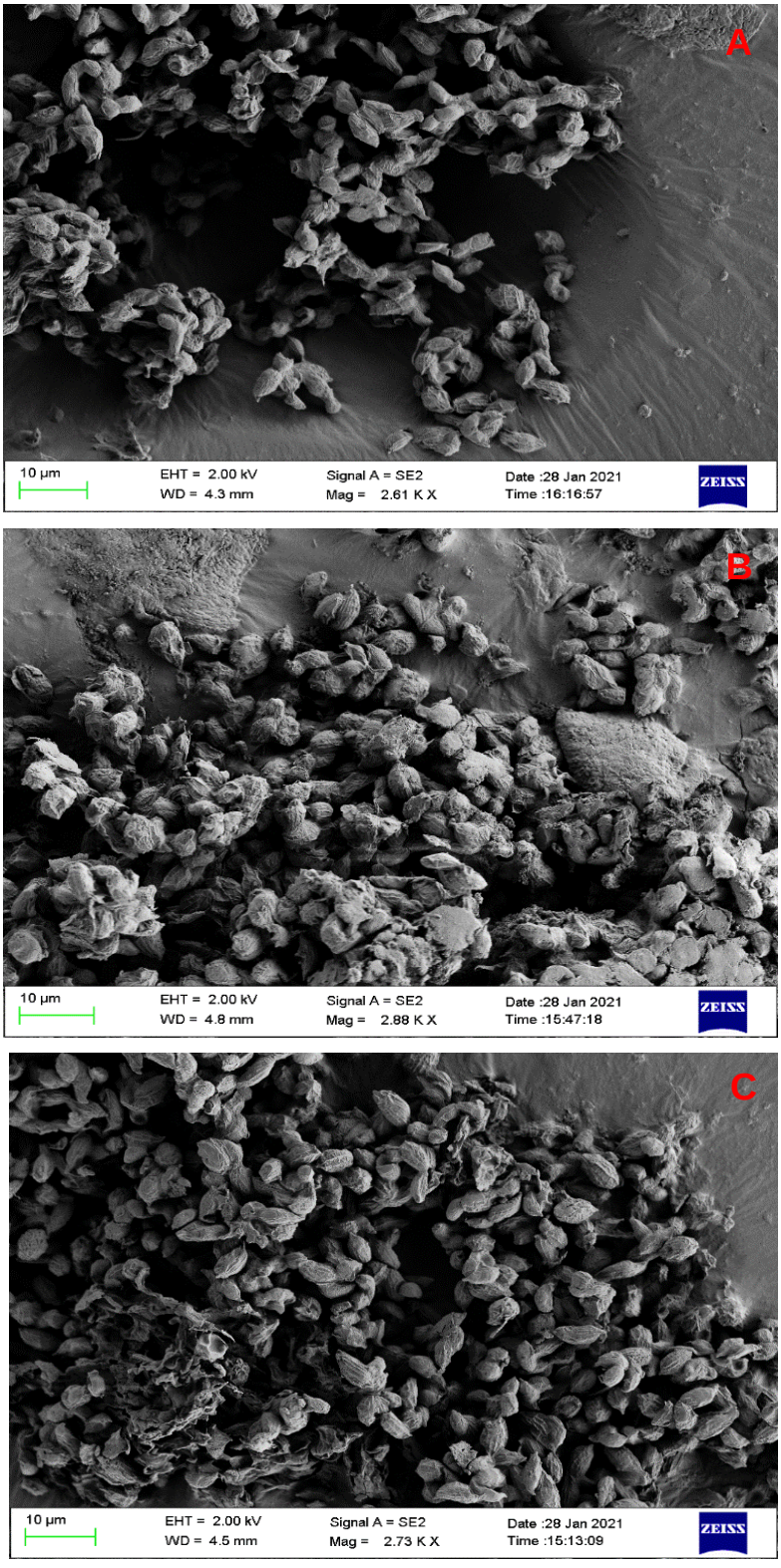

Figure 6.6: Scanning Electron Microscopy image of *Scenedesmus* sp. at (A) $S_{100}H_{10}N_0P_0$, (B) $S_{100}H_{10}N_{17.64}P_{5.74}$ and (C) $S_0H_{10}N_{35.29}P_0$

6.3.5 Multi components' effect on the profile of fatty acid methyl ester (%) and biodiesel properties

In algae, the fatty acids are present in the form of TAGs during unfavorable culture conditions; therefore, the estimation of fatty acid composition is of utmost importance. The percentage of various fatty acids determined via FAME profiling has been represented in Figure 6.7. The maximum amount of palmitic acid was obtained for $S_0H_{10}N_{35.29}P_0$ (31.7%). Although total FAME content was obtained highest for $S_{100}H_0N_0P_{5.74}$ (207.4 µg/mg) and $S_0H_0N_{35.29}P_0$ (166.1 µg/mg) combinations, biomass accumulation data implicates the fact that due to the absence of nitrogen in the previous combination, biomass was not accreted significantly. It was established that the presence of nitrate is critically essential compared to the presence of phosphate in the context of FAME yield. $S_0H_{10}N_{35.29}P_0$ combination fetched us the highest C16:0 (31.8%) and C18:3 (27.7%) fatty acids and became the third-highest producer of total FAME. $S_{100}H_0N_{17.64}P_0$ also yielded a considerable amount of FAME and was thus established as an optimum producer of both lipid and biomass.

The biodiesel combustion quality depends on CN, which specifies the fuel ignition time. This is inversely proportional to the length of the unbranched chain of fatty acids. As per the results obtained, cetane values lie between 53 and 56, which very well fits in the range of standards prescribed by the American standard - ASTM D675 (minimum 47) as well as the European standard - EN 14214 (minimum 51). Cetane number for $S_{100}H_{10}N_{35.29}P_{5.74}$, $S_{100}H_{10}N_{17.64}P_{5.74}$, $S_{100}H_{10}N_0P_{5.74}$ and $S_0H_{10}N_{35.29}P_0$ are 50.7, 50.0, 50.3, 49.9, respectively. Whereas Iodine value (IV) for same combinations is 68.5, 77.8, 75.4 and 85.5 $gI_2/100g$, respectively which is the next significant parameter that describes biodiesel/fuel's oxidation stability. FAME profile of microalgae is also known to be composed of polyunsaturated fatty acids (PUFAs) such as C18:2 and C18:3 abundantly. These unsaturated fatty acids are more susceptible to undergo oxidation during fuel storage and can hamper the acceptability of algal biodiesel for commercialization. Due to the

presence of excessive unsaturated fatty acids, algal biodiesel combustion leads to a higher rate of nitrate and nitrite emission into the environment (Chen et al., 2018; Ramos et al., 2009).

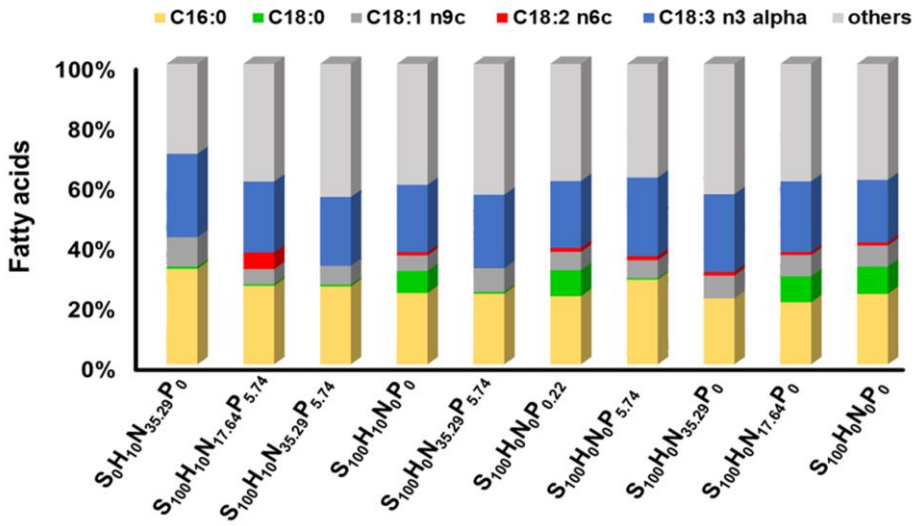

Figure 6.7: Fatty acid profile in *Scenedesmus* sp. exposed to hydrogen peroxide (second stage) at varying nitrate, phosphate and sodium chloride treatment (first stage)

6.3.6 ROS content and response of cellular antioxidants

The results obtained in terms of H_2O_2 (Figure 6.8), and SOD and CAT for some specific treatment combinations are represented in Table 6.3. After analysis, it was found that $S_{100}H_{10}N_{17.64}P_{5.74}$ generated maximum ROS (3306.0 µmolH_2O_2/g), revealing that cells were under maximal stress, that was further supported by high levels of SOD (24.6 U/mL) and CAT (102.5 nmol/mL/min) activity for the same treatment. Therefore, *Scenedesmus* sp. in the presence of maximum concentration of sodium chloride and hydrogen peroxide experienced the highest stress level. However, with the change in composition of culture broth, such as the supplementation of varying combinations of nitrate, phosphate, hydrogen peroxide, and sodium chloride, the production of enzymes under study changes, and thus specific standards cannot be set for a particular species. The increased stress exposure validated by the enzymatic study further points out to unfavourable cell environment,

which hinders the growth of the cell or might cause oxidative damage to cellular components, subsequently influencing the biochemical composition of cell.

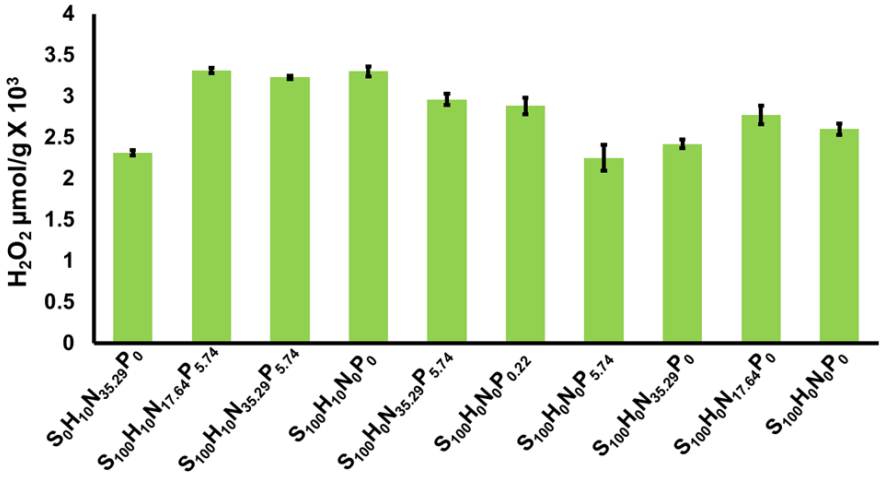

Figure 6.8: Reactive Oxygen species generation (H_2O_2) in *Scenedesmus* sp. exposed to hydrogen peroxide (second stage) at varying levels of nitrate, phosphate and sodium chloride (first stage)

Table 6.3: Enzymatic analysis in *Scenedesmus* sp. exposed to hydrogen peroxide (second stage) at varying nitrate, phosphate and sodium chloride treatment (first stage)

Combinations	SOD (U/mL)	CAT (nmol/mL/min)
$S_0H_{10}N_{35.29}P_0$	13.3±0.1	81.3±0.3
$S_{100}H_{10}N_{17.64}P_{5.74}$	24.6±0.1	102.5±1.5
$S_{100}H_{10}N_{35.29}P_{5.74}$	21.8±0.1	98.3±0.5
$S_{100}H_{10}N_0P_0$	21.1±1.4	95.2±1.5
$S_{100}H_0N_{35.29}P_{5.74}$	12.5±0.1	83.2±2.3
$S_{100}H_0N_0P_{0.22}$	13.9±0.1	87.0±0.3
$S_{100}H_0N_0P_{5.74}$	12.6±0.1	91.4±5.9
$S_{100}H_0N_{35.29}P_0$	16.2±0.1	87.7±1.6
$S_{100}H_0N_{17.64}P_0$	16.3±0.1	82.2±1.0
$S_{100}H_0N_0P_0$	10.6±0.5	79.7±3.6

6.3.7 Principal Component Analysis

The PCA analysis results presented in Figure 6.9A, 6.9B, and 6.9C indicates the contribution of variables and treatment in explaining the variance. Figure 6.10A, 6.10B, and 6.10C show the biplots of variables indicating how variables are correlated with each another and based on their directions, variables away from the Principal Component (PC) origin mark up the influence on that Principal Component. The bars presented in Figure 6.9A (Scree plot) indicate the percentage of explained variance captured in different dimensions (principal components). There are 11 dimensions obtained, explaining 100% variance; however, based on Kaiser Concept (Eigen values more than 1) first three dimensions or principal components were found explaining up to 69.5% (Table 6.4) variance (Figure 6.9A). Beyond three PCs, the variance percentage reduced and contributed least to the variance. Based on three PCs, the contribution of the amendments via salt treatment and the studied variables are shown in Figures 6.9B and 6.9C. The response above the dotted line indicates the main contributors in this study. Out of 35 with and without H_2O_2 combinations used, 10 combinations contributed (from 4 to 11%) maximally and influenced the biofuel parameters. $S_0H_{10}N_{35.29}P_0$ combination was found to contribute positively, followed by $S_0H_0N_{17.64}P_0$ and $S_{100}H_0N_{17.64}P_{5.74}$, which influenced the biofuel parameters such total lipid, total carbohydrate, C18:0, C16:0 chlorophyll and so on, whereas C20:0 was found to be least influenced by multi-component stress (Figure 6.9B).

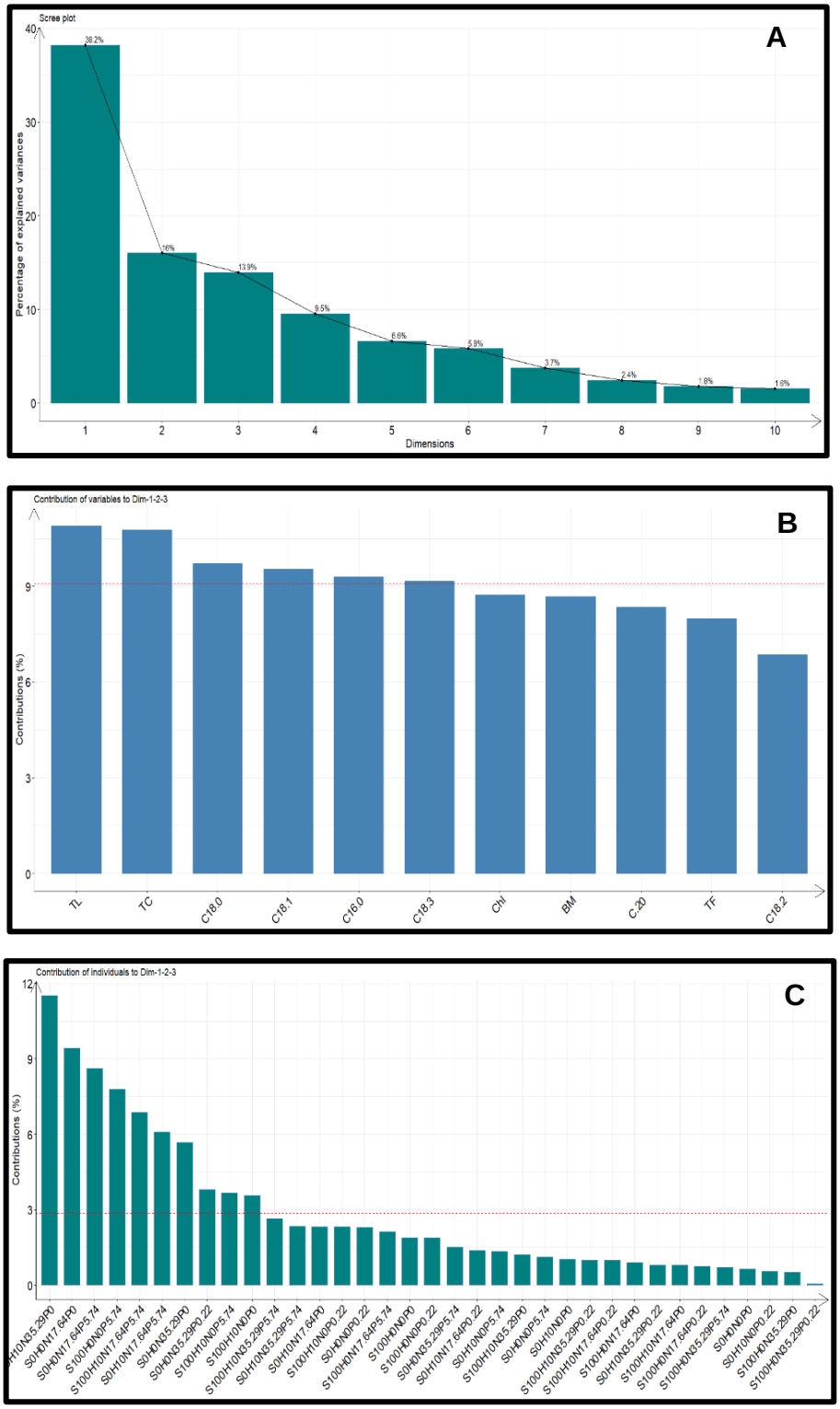

Figure 6.9: (A) Scree plot, a steep curve displays the magnitude of variation in each principal component captured from the data sets where first three PCs are explaining maximum variation. B and C are the contribution of variables (H_2O_2 combination) and individual explaining 68.1% variations

The biplots in Figure 6.10 depict that some vector directions are away from PC origin, showing more influence on that specific PC. The loading biplots (PCA 1 and 2 in Figures 6.10A and 6.10B) indicate that C18:1, chlorophyll, and biomass were closely related to each other due to the H_2O_2 treatment and were negatively correlated with C18:2, which showed lower yields, possibly due to the absence of H_2O_2. In comparison, FAME has low or no correlation with lipids and carbohydrates but was found to be related to C18:3 and C16:0. The variable biplot (Figure 6.10B) further explained the variable's contribution to H_2O_2 treatment, where carbohydrates and C18:2 showed least contribution. The eclipse Biplot (Figure 6.10C) explained that there was a clear-cut separation of eclipse of variables with respect to the treatments. However, H_2O_2 presence contributed to the maximum variance indicating their role in the enhanced recovery of biofuel parameters.

Table 6.4: Eigen analysis of the correlation matrix

Dimension	**Eigen value**	**Variance (%)**	**Cumulative variance (%)**
PC1	3.7	37.4	37.4
PC2	1.6	16.8	54.2
PC3	1.5	15.3	69.5
PC4	1.0	10.2	79.7
PC5	0.7	7.1	86.9
PC6	0.4	4.1	91.1
PC7	0.3	3.4	94.5
PC8	0.2	2.1	96.6
PC9	0.1	1.8	98.5
PC10	0.1	1.4	100

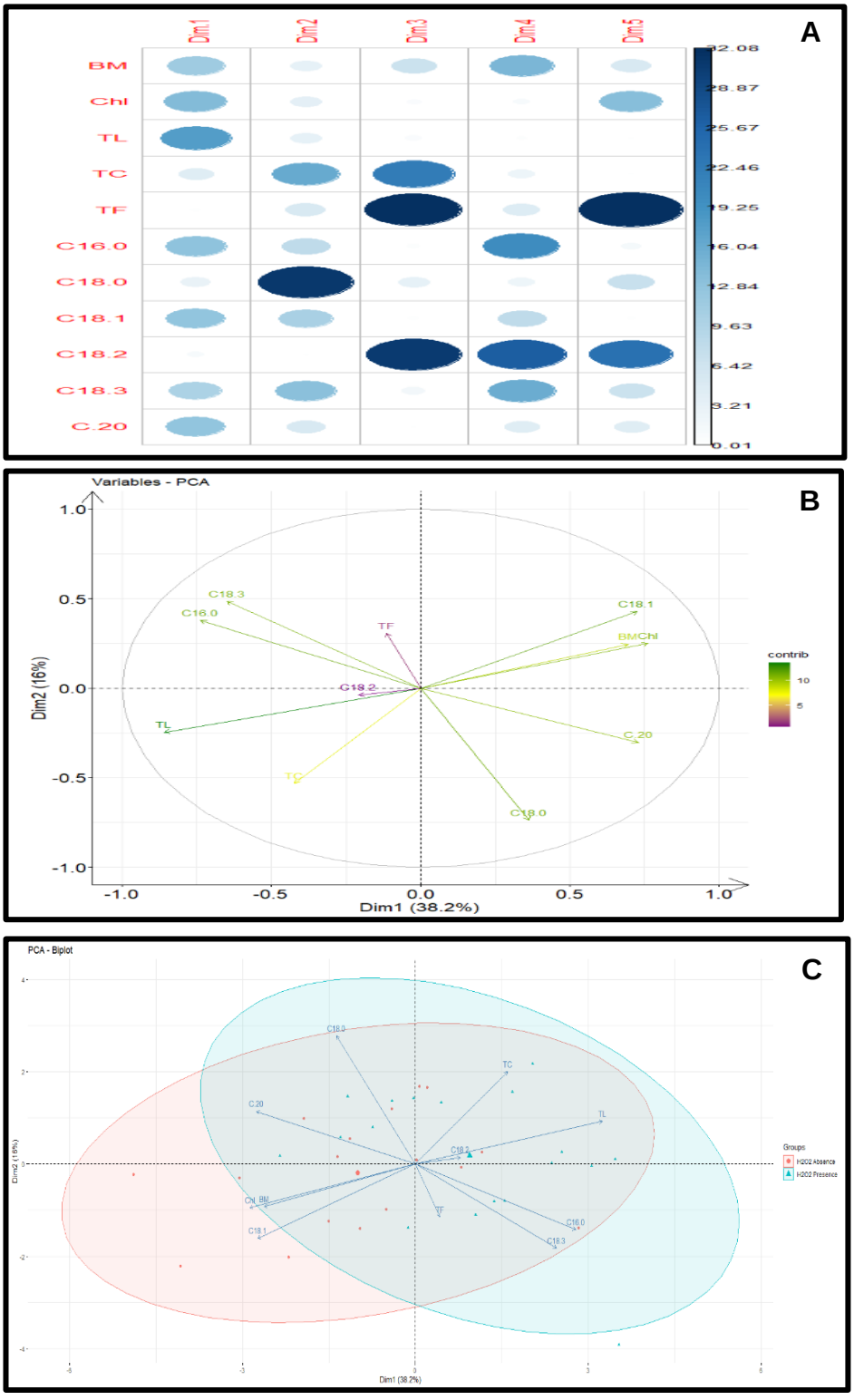

Figure 6.10: (A) Contribution of variables across various dimension (B) PCA variable shows loading of lipid biomass and associated parameters (variables or vectors) across the different combinations (C) Eclipse Biplot shows the variables separated in two groups

6.4 Conclusions

In a nutshell, $S_0H_{10}N_{35.29}P_0$ was determined as the best media composition for treating *Scenedesmus* sp. in order to produce a high amount of lipid, FAME, C16:0 fatty acid, and biomass concurrently. $S_{100}H_0N_{17.64}P_0$ also yielded a considerable amount of FAME, being the optimum producer of biomass and lipid. Microalgal strain under examination exhibited varying growth characteristics such as total lipids, carbohydrates, and fatty acid methyl ester profiles under deviating culture conditions. The algal cells were grown in tweaked stressful conditions and were established to procure higher total lipid yield and enriched fatty acid composition. Therefore, algae-derived oil can be considered for augmenting biofuel production, and *Scenedesmus* sp. can be explored and exploited further for large-scale production of biofuel precursors, paving the way for feasible commercial biodiesel.

References

Arnon, D. I. (1949). Copper enzymes in isolated chloroplasts. Polyphenoloxidase in *Beta vulgaris*. Plant Physiology, 24(1), 1.

Benavente-Valdés, J. R., Aguilar, C., Contreras-Esquivel, J. C., Méndez-Zavala, A., & Montañez, J. (2016). Strategies to enhance the production of photosynthetic pigments and lipids in *chlorophycae* species. Biotechnology Reports, 10, 117-125.

Berges, J. A., Charlebois, D. O., Mauzerall, D. C., & Falkowski, P. G. (1996). Differential effects of nitrogen limitation on photosynthetic efficiency of photosystems I and II in microalgae. Plant Physiology, 110(2), 689-696.

Cao, J., Yuan, H., Li, B., & Yang, J. (2014). Significance evaluation of the effects of environmental factors on the lipid accumulation of *Chlorella minutissima* UTEX 2341 under low-nutrition heterotrophic condition. Bioresource Technology, 152, 177-184.

Chen, H., Wang, J., Zheng, Y., Zhan, J., He, C., & Wang, Q. (2018). Algal biofuel production coupled bioremediation of biomass power plant wastes based on *Chlorella* sp. C2 cultivation. Applied Energy, 211, 296-305.

Chen, M., Tang, H., Ma, H., Holland, T. C., Ng, K. S., & Salley, S. O. (2011). Effect of nutrients on growth and lipid accumulation in the green algae *Dunaliella tertiolecta*. Bioresource Technology, 102(2), 1649-1655.

Courchesne, N. M. D., Parisien, A., Wang, B., & Lan, C. Q. (2009). Enhancement of lipid production using biochemical, genetic and transcription factor engineering approaches. Journal of Biotechnology, 141(1-2), 31-41.

Dean, A. P., Sigee, D. C., Estrada, B., & Pittman, J. K. (2010). Using FTIR spectroscopy for rapid determination of lipid accumulation in

response to nitrogen limitation in freshwater microalgae. Bioresource Technology, 101(12), 4499–4507.

Deng, X., Fei, X., & Li, Y. (2011). The effects of nutritional restriction on neutral lipid accumulation in *Chlamydomonas* and *Chlorella*. African Journal of Microbiology Research, 5(3), 260-270.

Flynn, K. J. (1990). The determination of nitrogen status in microalgae. Marine ecology progress series. Oldendorf, 61(3), 297-307.

Grace, C. E. E., Lakshmi, P. K., Meenakshi, S., Vaidyanathan, S., Srisudha, S., & Mary, M. B. (2020). Biomolecular transitions and lipid accumulation in green microalgae monitored by FTIR and Raman analysis. Spectrochimica Acta Part A: Molecular and Biomolecular Spectroscopy, 224, 117382.

Hu, Q. (2004). Environmental effects on cell composition. Blackwell Science Ltd.: Oxford, UK, 1, 83-93.

Kassambara, A., & Mundt, F. (2017). Factoextra: extract and visualize the results of multivariate data analyses. R package version, 1(5), 337-354.

Knothe, G., & Steidley, K. R. (2005). Kinematic viscosity of biodiesel fuel components and related compounds. Influence of compound structure and comparison to petrodiesel fuel components. Fuel, 84(9), 1059-1065.

Lê, S., Josse, J., & Mazet, F. (2008). Package 'FactoMineR. J Stat Softw [Internet], 25(1), 1-18.

Mishra, S. K., Suh, W. I., Farooq, W., Moon, M., Shrivastav, A., Park, M. S., & Yang, J. W. (2014). Rapid quantification of microalgal lipids in aqueous medium by a simple colorimetric method. Bioresource Technology, 155, 330-333.

Ördög, V., Stirk, W. A., Bálint, P., van Staden, J., & Lovász, C. (2012). Changes in lipid, protein and pigment concentrations in nitrogen-stressed *Chlorella minutissima* cultures. Journal of Applied Phycology, 24(4), 907-914.

Pancha, I., Chokshi, K., George, B., Ghosh, T., Paliwal, C., Maurya, R., & Mishra, S. (2014). Nitrogen stress triggered biochemical and morphological changes in the microalgae *Scenedesmus* sp. CCNM 1077. Bioresource Technology, 156, 146-154.

Ramos, M. J., Fernández, C. M., Casas, A., Rodríguez, L., & Pérez, Á. (2009). Influence of fatty acid composition of raw materials on biodiesel properties. Bioresource Technology, 100(1), 261-268.

Roe, J. H. (1955). The determination of sugar in blood and spinal fluid with anthrone reagent. Journal of Biological Chemistry, 212, 335-343.

Rosenwasser, S., van Creveld, S. G., Schatz, D., Malitsky, S., Tzfadia, O., Aharoni, A., ... & Vardi, A. (2014). Mapping the diatom redox-sensitive proteome provides insight into response to nitrogen stress in the marine environment. Proceedings of the National Academy of Sciences, 111(7), 2740-2745.

Sarno, D., Kooistra, W. H., Balzano, S., Hargraves, P. E., & Zingone, A. (2007). Diversity in the genus *Skeletonema* (Bacillariophyceae): III. Phylogenetic position and morphological variability of *Skeletonema costatum* and *Skeletonema grevillei*, with the description of *Skeletonema ardens* sp. NOV. 1. Journal of Phycology, 43(1), 156-170.

Sinha, A. K., Jaggi, M., Raghuram, B., & Tuteja, N. (2011). Mitogen-activated protein kinase signaling in plants under abiotic stress. Plant Signaling & Behavior, 6(2), 196-203.

Su, S., Zhou, Y., Qin, J. G., Yao, W., & Ma, Z. (2010). Optimization of the method for chlorophyll extraction in aquatic plants. Journal of Freshwater Ecology, 25(4), 531-538.

Velikova, V., Yordanov, I., & Edreva, A. (2000). Oxidative stress and some antioxidant systems in acid rain-treated bean plants: protective role of exogenous polyamines. Plant Science, 151(1), 59-66.

Vincent, Q.V., (2011). GitHub - vqv/ggbiplot: A biplot based on ggplot2.

Weiss, S. B., Kennedy, E. P., & Kiyasu, J. Y. (1960). The enzymatic synthesis of triglycerides. Journal of Biological Chemistry, 235(1), 40-44.

Wickham, H., & Chang, W. (2019). devtools: Tools to make developing R packages easier, 2016. URL https://CRAN. R-project. org/package= devtools. R package version, 1(0), 103.

Zhang, J., Hao, H., Chen, M., Wang, H., Feng, Z., & Chen, H. (2017). Hydrogen-rich water alleviates the toxicities of different stresses to mycelial growth in *Hypsizygus marmoreus*. AMB Express, 7(1), 1-11.

Zhao, Y., Wang, H. P., Han, B., & Yu, X. (2019). Coupling of abiotic stresses and phytohormones for the production of lipids and high-value by-products by microalgae: A review. Bioresource Technology, 274, 549-556.

CHAPTER 7

Chapter 7

Conclusions and scope for future work

Scenedesmus sp. has been recognized as a decent contender for biodiesel production and other delicate compounds or metabolites. High lipid content and statistic reveals that *Scenedesmus* sp. can sustain a wide range of environmental conditions such as saline environment, brackish water. As part of initial characterization, *Scenedesmus* sp. was screened and selected from 12 different species based on growth profile and lipid accumulation.

In the present work, the impact of various abiotic stress condition such as salinity stress (Chapter 3), salinity combined nutrient stress (Chapter 4), peroxide stress (Chapter 5) and multicomponent (salt, nutrient, and peroxide) stress was monitored to support the profitable growth of examined species with enhanced lipid production. This means that a suitable combination of modified media can be varied in a fully quantitative way in future work, which will lead to further insights into large scale production.

Chapter 3: ***Impact of varying concentrations of different salts on growth profile and biochemical composition of Scenedesmus sp .***

The impact of three different salts (NaCl, $MgCl_2$ and $CaCl_2$) with varying concentration on the examined species was monitored. The biomass content was observed to decrease with an increase in the concentration till 100 mM at all studied time points. Sodium chloride at 100 mM (804.3±39.5 µg/mL) showed less impact on biomass in comparison to $MgCl_2$ (485.3±13.6 µg/mL) and $CaCl_2$ (598.8±11.8 µg/mL). Total lipid accumulation in the case of NaCl at 100 mM (197.6±4.9 µg/mg) is better in comparison to $MgCl_2$ (179.8±19.7 µg/mg) and $CaCl_2$ (134.5±8.1 µg/mg). Maximum FAME content is found at 30 mM and 70 mM of $CaCl_2$, but biomass accumulation is

quite low at these concentrations, whereas $NaCl_{100}$ does not show much adverse impact on biomass and is also able to accumulate a considerable amount of FAME (37.09 µg/mg).

Chapter 4: ***Effect of sodium chloride under nutrients replete/deplete condition***

From the previous study, it was found that NaCl as salt had more significant impact on lipid accumulation as compared to other studied salts. Therefore, to investigate the impact of NaCl further, it was (NaCl) was combined with two very critical nutrients for algal growth and lipid accumulation.

At $N_{17.64}P_{0.22}$ and $N_{17.64}P_{5.74}$ treatment, overall biomass was observed to decrease with increasing NaCl concentration (10, 50, 100, 200 mM) on 15th day. At $N_{35.29}P_{0.22}$ and $N_{17.64}P_0$ treatment along with varying NaCl concentrations, biomass content was found to increase till 50 mM NaCl and further decreased with increasing salt concentrations, whereas the same trend was observed for $N_0P_{0.22}$ treatment, but the biomass content was found to increase upto 100 mM salt concentration and subsequently decreased at 200 mM on 15th day. It was observed on the 15th day that the algal cells cultivated in nitrogen deprived media, supplemented with S_{100} (sodium chloride, 100 mM) and $P_{0.22}$, accumulated maximum total lipid concentration ($S_{100}N_0P_{0.22}$, 385.4±34.26 µg/mg) and 38.5% lipid content. However, under minimal NaCl concentration ($S_{10}N_{17.64}P_{0.22}$), the lipid content was observed as 7.6%. Although, *Scenedesmus* sp. when cultivated in nitrate and phosphate deprived media, supplemented with NaCl ($S_{100}N_0P_0$, 191.0±4.3 µg/mg) and without ($S_0N_0P_0$, 203.2±7.3 µg/mg) NaCl exhibited reduced total lipid accumulation in the presence of salt concentration. Maximum neutal lipids or FAME content is found at $S_{100}N_0P_0$ (168.4 µg/mg), which is followed by $S_0N_0P_0$ (151.5 µg/mg) and $S_{100}N_0P_{0.22}$ (90.4 µg/mg). Oleic (C18:0) and steric (C18:1), when analyzed on the 15th day were maximum at $S_{100}N_0P_{0.22}$ media composition.

Chapter 5: ***Algal behavior under hydrogen peroxide induction accompanied by nitrate and phosphate variation via two-stage cultivation***

In this part of the experiment, it was planned to enhance the lipid accumulation by externally applying hydrogen peroxide and was performed till 72 hours because after that change in colour of cells from green to yellow was observed indicating decline of cells growth or cell are in death phase after 72 hours, which enable us to conclude the experiment at 72 hours.

Scenedesmus sp. when subjected to synergized varying nitrate and phosphate concentrations (N_0P_0, $N_{17.64}P_{0.22}$, $N_0P_{0.22}$, $N_{35.29}P_{0.22}$, $N_{17.64}P_0$ and $N_{17.64}P_{5.74}$) for 48 hours and after that the induction of different H_2O_2 concentrations for 24 hours exhibited a decrease in biomass and chlorophyll content with an increase in H_2O_2 concentrations (0, 2, 4, 6, 8 and 10 mM). The lipid accumulation, when analyzed after 72 hours, was found to be highest in the algal cells cultivated in $H_{10}N_0P_{0.22}$ media composition (156.62±24.30 µg/mg), followed by second highest and third highest lipid content in $H_0N_0P_0$ (145.20±33.36 µg/mg) and $H_{10}N_0P_0$ (139.85±38.12 µg/mg).

Chapter 6: ***Multicomponent exposure – Impact of hydrogen peroxide, sodium chloride, nitrate and phosphate on algal profile in two stage process***

The same concentration of nitrate and phosphate from chapter 4 and 5 ($N_0P_{0.22}$) gave maximum lipid concentration in combination with H_2O_2. However, the lipid accumulation observed under long term stress ($S_{100}N_0P_{0.22}$) was much higher as compared to short term stress ($H_{10}N_0P_{0.22}$). Since it was clear from the previous study that the salt stress acted as a better stress inducer for lipid biosynthesis as compared to peroxide stress, therefore to further investigate, the cumulative effect of both these stress inducer on lipid accumulation in *Scenedesmus* sp. was evaluated alongwith nitrate and phosphate variation.

It was observed that when *Scenedesmus* sp. was cultivated in media composed of 10 mM H_2O_2 at all SNP combinations as well as in the presence of 100 mM NaCl at all HNP combinations exhibited a decrease in biomass and chlorophyll content after 72 hours of exposure as compared to the media deprived of H_2O_2 and NaCl.

The highest lipid content estimated after 72 hours of cultivation (first stage - SNP for 48 hrs and second stage - addition of Hydrogen peroxide for 24 hrs) was observed in $S_{100}H_{10}N_{35.29}P_{5.74}$ (226.49±16.61 µg/mg), followed by $S_{100}H_{10}N_{17.64}P_{5.74}$ (222.43±13.97 µg/mg) and $S_{100}H_{10}N_0P_{5.74}$ (213.90±4.78 µg/mg). It was also observed that when *Scenedesmus* sp. was cultivated in media composed of 10 mM H_2O_2 at all SNP combinations as well as in the presence of 100 mM NaCl at all HNP combinations exhibited high lipid accumulation as compared to algal cells cultivated in the media deprived of H_2O_2 and NaCl. The highest carbohydrate content estimated was observed for $S_{100}H_0N_0P_0$, $S_{100}H_0N_0P_{0.22}$ and $S_{100}H_0N_{35.29}P_{5.74}$ combinations. Carbohydrate content was also found to increase after the addition of 100 mM NaCl at varying combinations of HNP.

Highest total FAME content was observed for $S_{100}H_0N_0P_{5.74}$ and $S_0H_0N_{35.29}P_0$ combinations, although the biomass content analyzed for these combinations was not good due to the absence of an essential nutrient, i.e. nitrate. However, highest C16:0 (31.7%) and C18:3 (27.76%) percentage were observed in the algal cells under $S_0H_{10}N_{35.29}P_0$ treatment, which was the third highest producer of total FAME. In a nutshell, it can be concluded that either the presence of H_2O_2 or that of NaCl produces a considerable amount of stress onto the algal cells, leading to the accumulation of high FAME content. The importance of the presence of nitrate in comparison to that of phosphate can also be summarized from the results obtained.

Overall conclusions

- After long term exposure, the total lipid content was observed as 18.4 and 38.5% at $S_{100}N_{17.64}P_{0.22}$ and $S_{100}N_0P_{0.22}$, along with biomass accumulation of 804.3 and 537.0. μg/mL, respectively. Total lipid content increased by 572 % with a decrease of 40 % biomass accumulation at $S_{100}N_0P_{0.22}$ in comparison to the least performer ($S_{50}N_{35.29}P_{0.22}$).
- After short term exposure, the optimum total lipid content was found as 15.6, 19.2 and 22.6 % at $S_0H_{10}N_0P_{0.22}$, $S_{100}H_{10}N_0P_{0.22}$, and $S_{100}H_{10}N_{35.29}P_{5.74}$ alongwith biomass accumulation of 305, 320, and 254 μg/mL, respectively. This study showed increase in total lipid content by 266 % alongwith 35 % decrease in biomass production at $S_{100}H_{10}N_{35.29}P_{5.74}$ in comparison to least accumulator ($H_2N_{17.64}P_0$).

It is concluded that, after long-term exposure to varying salts, NaCl at 100 mM ($S_{100}N_{17.64}P_{0.22}$) significantly enhanced lipid content which is further enhanced ($S_{100}N_0P_{0.22}$) at 100 mM NaCl in the absence of nitrate (N_0) with optimal phosphate ($P_{0.22}$) concentration. However, under short-term exposure increase in lipid accumulation was monitored but less than long term exposure. Therefore, all the strategies adopted to enhance the lipid accumulation in the algal cells acknowledge the appreciable potential of *Scenedesmus* sp., which needs to be explored and exploited further for sustainable large-scale lipid production.

Future directions

In recent time, there has been rise in the energy demand due to the ever increasing population and this has resulted in fuel shortage. Therefore, the recent focus has shifted towards biofuels which can replace fossil fuels. Algal biofuel processes has several advantages like low land requirement and high oil content with high productivity. However, there are few bottlenecks in term of commericalization of algae based biofuel such as low biomass production, lipid content etc. Sustainable nutrient sources include many organic fertilizers, which seem to be cost effective option. Additionally, agricultural runoff water, and wastewater from various domestic/industrial outlets, which also contains high levels of nitrates and phosphates can be optimized/explored for a sustainable and upscale production of algal biomass. Even results from current study can provide baseline information for combined evaluation of lipid enhancement and cost effective options in future. Seasonal variations in the industry-based wastewater need to be taken care off. Similarly, the exact concentration of organic fertilizers being used can differ from species to species. Therefore, it's necessary to keep all the parameters under check. So, in order to address these issues, optimization is needed for different species and conditions. It would be interesting to work on these aspects (sustainable nutrient sources) in future for making the process of algal production more viable with simultaneous increase in lipids. In addition harvesting of biomass which needs high energy inputs, enhancing lipids without much compromising biomass etc. are demand of the day. For an economic process development, a cost-effective and energy efficient harvesting methods are required with low energy input. Producing low-cost microalgal biofuels require better biomass harvesting methods, high biomass production with high oil productivity through genetic modification, which will be the future directions. Therefore, use of the standard algal harvesting technique, biorefinery concept, advances in photobioreactor design

and other downstream technologies will further reduce the cost of algal biofuel production, and make it a competitive resource in near future.

CURRICULUM VITAE

Dr. Vishal Anand
Algal EcoTechnology & Sustainability, BSBE, IIT Indore
Email: vishalnnd7@gmail.com
Contact No: +91-8103319951; 9608660767

Area of Interest

Experimental Biofuels and Bioenergy: Algal Biorefinery; Metabolomics, CO_2 sequestration; Wastewater treatment; Bioremediation

Academic Qualification

Degree/Certificate	Borad/University	Passing Year	Grad/Marks
PhD	IIT Indore	2021	Defended
M. Tech (Biotechnology)	BIT Mesra	2015	8.07/10
B. Tech (Biotechnology)	Anna University	2012	7.60/10
12^{th}	C.B.S.E.	2006	67.8%
10^{th}	C.B.S.E.	2004	77.8%

Ph.D. Thesis: Stress-Induced Lipid Enhancement in Microalgae-*Scenedesmus* sp.

Hands on experiences:

1. Sample Preparation: Triacylglycerides, Lipid, Carbohydrate, Protein, Native Enzymes
2. Characterization Techniques: Spectrophotometers (fluorescence measurement, UV-vis absorptions measurement, FTIR), Chromatography analysis (gas chromatography and mass spectroscopy), Molecular biology techniques (NATIVE PAGE and SDS PAGE), Microscopy techniques (Scanning electron microscope, confocal microscope, compound microscopy)
3. Data Analysis: Excel, GraphPad prism, Origin 8.5, Principal component analysis using R studio

UGC Project Fellow: Proteomic analysis and lipid profiling of *Chlamydomonas reinhardtii* and its relevance towards bio-fuel production**. (From 04-07-2015 to 26-04-2016)**

M. Tech. Thesis: Optimization of L-Glutaminase Production and Extraction by Aqueous Two-Phase System.

List of Publications

1. **Anand, V**; Kashyap, M; Mahaveer, P. S; & Kiran, B. (2021). Impact of hydrogen peroxide on microalgae cultivated in varying salt-nitrate-phosphate conditions. Journal of Environmental Chemical Engineering, 105814.
2. Kashyap, M., Samadhiya, K., Ghosh, A., **Anand, V**., Lee, H., Sawamoto, N., Ogura, A., Ohshita, Y., Shirage, P.M., Bala, K.* (2021). Synthesis, characterization, and application of intracellular Ag/AgCl nanohybrids biosynthesized in *Scenedesmus* sp. as neutral lipid inducer and antibacterial agent. Environmental Research, 111499.
3. **Anand, V**., Kashyap, M., Samadhiya, K., Ghosh, A., & Kiran, B. (2021). Strategy for lipid production in *Scenedesmus* sp. by multiple stresses induction. Biomass Conversion and Biorefinery, 1-11. https://doi.org/10.1007/s13399-021-01392-2.
4. Kashyap, M., **Anand,** V., Ghosh, A., & Bala, K.* (2021). Superintending *Scenedesmus* and *Chlorella* sp. with lead and cobalt tolerance governed via stress biomarkers. Journal of Water Supply. https://doi.org/10.2166/ws.2021.065.
5. Ghosh, A., Sangtani, R., **Anand, V**., Kashyap, M., & Bala, K.* (2021). Synergistic dynamics of critical cofactors effectuates fuel relevant metabolic profile of *Scenedesmus* sp.: Targeting cleaner energy production. Journal of Cleaner Production, 297, 126640. https://doi.org/10.1016/j.jclepro.2021.126640.
6. **Anand, V**., Kashyap, M., Ghosh, A., & Kiran, B. (2020) Spectroscopic insights exploring triacylglyceride accumulation in *Scenedesmus* sp. via biomolecular transitions. Bioresource technology report, 12, 100593. https://doi.org/10.1016/j.biteb.2020.100593.
7. **Anand, V**., Kashyap, M., Samadhiya, K., Ghosh, A., & Kiran, B. (2019). Salinity driven stress to enhance lipid production in *Scenedesmus vacuolatus*: A biodiesel trigger?. Biomass and Bioenergy, 127, 105252. https://doi.org/10.1016/j.biombioe.2019.05.021.
8. **Anand, V**., Kashyap, M., Samadhiya, K., & Kiran, B. (2019). Strategies to unlock lipid production improvement in algae. International journal of environmental science and technology, 16(3), 1829-1838. https://doi.org/10.1007/s13762-018-2098-8.
9. Kashyap, M., Samadhiya, K., Ghosh, A., **Anand, V**., Shirage, P. M., & Bala, K. (2019). Screening of microalgae for biosynthesis and optimization of Ag/AgCl nano hybrids having antibacterial effect. RSC advances, 9(44), 25583-25591. DOI: 10.1039/C9RA04451E.
10. Ghosh, A., Samadhiya, K., Kashyap, M., **Anand, V**., Sangwan, P., & Bala, K., 2019. The use of Response Surface Methodology for improving fatty acid methyl ester profile of *Scenedesmus vacuolatus*, Environmental Science and Pollution Research. 27(22), 27457-27469. https://doi.org/10.1007/s11356-019-07115-5.
11. **Anand, V**.; Singh, P; Banerjee, C; & Shukla P. (2017). Proteomic approaches in microalgae:

perspectives and applications. 3 Biotech, 7:197. https://doi.org/10.1007/s13205-017-0831-5.

12. **Anand, V**., Kumar, R., & Kiran, B*. (2017) Potential of biofuel production from algae cultivated in wastewater, In Press: Proceedings of National Conference on Climate Change, Resource Conservation and Sustainability Strategies held on 16th – 17th March 2017 at GGS IPU, Delhi.
13. **Anand, V**., Ghosh, A., Shingdilwar, S., Kumar, R., & Kiran, B*. (2017). Fame production and fatty acid profiling of microalgae for biodiesel production. Phycologia, 56(4), 8.
14. **Anand, V**., & Kiran, B*. (2017). Comparison of direct and indirect transesterification for fame profiling in *Chlorococcum* sp. Phycologia, 56(4), 8.
15. **Anand. V**., Perween. Q., Sinha. R., Singh. H., & Jha. S. (2015). Screening of L- glutaminase Producer and Optimization of Production Process by Taguchi Orthogonal Array. Int. J. Pharma. Clinical Res. 7(4): 246-251.
16. Perween. Q., **Anand. V**., Singh. H., & Jha. S. (2015). Enhanced Recovery of L- glutaminase by The Optimization of A Three-phase Partitioning System Using The Taguchi Doe Methodology. Int. J. Pharma. Clinical Res. 7(3): 216-220.

Conference /Workshop Attended

1. International conference on Emerging Areas in Biosciences and Biomedical Technologies (eBBT2), IIT Indore, January 7-9, 2020 (Participation)
2. International conference on Emerging Areas in Biosciences and Biomedical Technologies, IIT Indore, January 5-6, 2018 (Poster Presentation)
3. International Conference on Bioscience Research for Nutritional Security, Environmental Conservation & Human Health in Rural India; IINRG, Ranchi, December 22-24, 2014. (Poster Presentation)
4. National Conference on Empowering Mankind with Microbial Technologies (AMI-EMMT-2014), Tamil Nadu Agriculture University, Coimbatore, November 12-14, 2014. (Poster Presentation)
5. National Workshop on Immunoinformatics, Karpaga Vinayaga College of Engineering and Technology, Chennai, 21st September 2011. (Participation)
6. International Conference on Biomedical Instrumentation, Engineering and Environmental Management, Karpaga Vinayaga College of Engineering and Technology, Chennai, 22-23rd July 2011. (Participation)
7. National Conference on Recent Biotechnological Perspectives in Human Diseases and Therapeutics, Bharath University, Chennai, 4th March 2011. (Oral Presentation)
8. National Level Technical Symposium on Bioinformatics, Sastra University, Chennai, 23-

24th October 2010. (Participation)

9. National Level Workshop on Application of perl scripting and Bioinformatics Tools and Techniques for Biological Database, Karpaga Vinayaga College of Engineering and Technology, Chennai, 4-6th October 2010. (Participation)
10. Attended a short-term training course on Advanced Research Techniques on Genomics Proteomics and Bioinformatics (ARTGPB-2017) at National Facility for Marine Cyanobacteria, (NFMC), Tiruchirappall, November 7-21, 2017.

References

PhD Thesis Supervisor **Dr. Kiran Bala** Associate Professor Department of Biosciences & Biomedical Engineering, Indian Institute of Technology, Indore P.O. Simrol M.P. - 453552 Tel: +91-731-2438700 ext: 585 E-mail: kiranb@iiti.ac.in	**Research Collaborator** **Dr. Parasharam M. Shirage** Associate Professor and Ramanujan Fellow Discipline of Metallurgy Engineering and Materials Science and Discipline of Physics, Indian Institute of Technology (IIT) Indore, P.O Simrol, Khandwa Road Indore, M.P.- 453552 Phone: +91-787-52222-331 Email: pmshirage@iiti.ac.in
M. Tech Thesis Supervisor **Dr. Hare Ram Singh** Assistant Professor Department of Bio-Engineering BIT- Mesra, Ranchi Jharkhand-835 215 Phone: 9430220114 E-mail: hrsingh@bitmesra.ac.in	

Vishal Anand